

# Effect of Seismic Wave Incoherence on Foundation and Building Response

1013504

**DRAFT** Final Report, October 2006

Cosponsor  
U.S. Department of Energy  
Office of Nuclear Energy Sciences  
and Technology  
19901 Germantown Road, NE-20  
Germantown, MD, 20874-1290

EPRI Project Managers  
R. Kassawara and L. Sandell

ELECTRIC POWER RESEARCH INSTITUTE  
3420 Hillview Avenue, Palo Alto, California 94304-1395 • PO Box 10412, Palo Alto, California 94303-0813 • USA  
800.313.3774 • 650.855.2121 • [askepri@epri.com](mailto:askepri@epri.com) • [www.epri.com](http://www.epri.com)

**DISCLAIMER OF WARRANTIES AND LIMITATION OF LIABILITIES**

THIS DOCUMENT WAS PREPARED BY THE ORGANIZATION(S) NAMED BELOW AS AN ACCOUNT OF WORK SPONSORED OR COSPONSORED BY THE ELECTRIC POWER RESEARCH INSTITUTE, INC. (EPRI). NEITHER EPRI, ANY MEMBER OF EPRI, ANY COSPONSOR, THE ORGANIZATION(S) BELOW, NOR ANY PERSON ACTING ON BEHALF OF ANY OF THEM:

(A) MAKES ANY WARRANTY OR REPRESENTATION WHATSOEVER, EXPRESS OR IMPLIED, (I) WITH RESPECT TO THE USE OF ANY INFORMATION, APPARATUS, METHOD, PROCESS, OR SIMILAR ITEM DISCLOSED IN THIS DOCUMENT, INCLUDING MERCHANTABILITY AND FITNESS FOR A PARTICULAR PURPOSE, OR (II) THAT SUCH USE DOES NOT INFRINGE ON OR INTERFERE WITH PRIVATELY OWNED RIGHTS, INCLUDING ANY PARTY'S INTELLECTUAL PROPERTY, OR (III) THAT THIS DOCUMENT IS SUITABLE TO ANY PARTICULAR USER'S CIRCUMSTANCE; OR

(B) ASSUMES RESPONSIBILITY FOR ANY DAMAGES OR OTHER LIABILITY WHATSOEVER (INCLUDING ANY CONSEQUENTIAL DAMAGES, EVEN IF EPRI OR ANY EPRI REPRESENTATIVE HAS BEEN ADVISED OF THE POSSIBILITY OF SUCH DAMAGES) RESULTING FROM YOUR SELECTION OR USE OF THIS DOCUMENT OR ANY INFORMATION, APPARATUS, METHOD, PROCESS, OR SIMILAR ITEM DISCLOSED IN THIS DOCUMENT.

ORGANIZATION(S) THAT PREPARED THIS DOCUMENT

**ARES Corporation, Inc.**

**NOTE**

For further information about EPRI, call the EPRI Customer Assistance Center at 800.313.3774 or e-mail [askepri@epri.com](mailto:askepri@epri.com).

Electric Power Research Institute and EPRI are registered service marks of the Electric Power Research Institute, Inc.

Copyright © 2006 Electric Power Research Institute, Inc. All rights reserved.

## CITATIONS

---

This report was prepared by

ARES Corporation, Inc.  
5 Hutton Centre Drive  
Suite 610  
Santa Ana, CA 92707

Principal Investigators  
S. Short  
G. Hardy  
K. Merz

James J. Johnson and Associates  
7 Essex Court  
Alamo, CA 94507

Principal Investigator  
J. Johnson

This document describes research sponsored by the Electric Power Research Institute (EPRI) and the U.S. Department of Energy under Award No. (DE-FC07-04ID14533). Any opinions, findings, and conclusions or recommendations expressed in this material are those of the author(s) and do not necessarily reflect the views of the U.S. Department of Energy.

This publication is a corporate document that should be cited in the literature in the following manner:

*Effect of Seismic Wave Incoherence on Foundation and Building Response*. EPRI, Palo Alto, CA and the U.S. Department of Energy: 2006 1013504.



## PRODUCT DESCRIPTION

---

Task S2.1 of the New Plant Seismic Issues Resolution Program—a joint effort of EPRI and the Department of Energy (DOE)—entails a research program into the effect of seismic wave incoherence on foundation and building response. The task's objective is to systematically study seismic wave incoherence effects on structures/foundations similar to those being considered for advanced reactor designs. Seismic wave incoherence occurs because of the horizontal spatial variation of both horizontal and vertical ground motion. The phenomenon of seismic wave incoherence has been recognized for many years, but the lack of extensive recorded data prevented its incorporation into the dynamic analysis of nuclear power plant (NPP) structures. Based on newly developed coherency functions, seismic response has been evaluated in this study using the soil-structure interaction (SSI) computer program CLASSI, combined with random vibration theory. Seismic response is evaluated for rigid, massless foundations and for example structural models on foundation mats that behave rigidly.

### **Results and Findings**

Seismic analyses incorporating ground motion incoherence demonstrate a significant reduction in high-frequency seismic response as measured by in-structure response spectra. The computed incoherency transfer functions depend on the foundation area and are independent of site soil conditions. However, the resulting spectral reductions strongly depend on site soil conditions. The effect of seismic wave incoherence is primarily a high-frequency phenomenon. Hence, the observed reductions in foundation response spectra are much less for soil sites since the soil site-specific ground motion is not rich in the high-frequency portion of the spectra.

### **Challenges and Objectives**

This project's overall objective is to systematically study seismic wave incoherence effects on structures/foundations similar to those being considered for advanced reactor designs. To fulfill that objective, a program was developed to demonstrate the appropriate analysis techniques to evaluate the incoherency effects on structure and foundation seismic responses. These analytic methods were further validated with different computer programs and approaches to ensure the results from these studies were accurate and defensible. The end result was that two independent direct approaches using the CLASSI and SASSI computer programs are available to account for incoherency effects as well as a simplified approach which allows for the scaling of the free-field input to account for incoherency effects.

In EPRI NP-6041 (EPRI, 1991), American Society of Civil Engineers (ASCE) Standard 4 (ASCE, 2000), and DOE Standard-1020 (U.S. DOE, 2002), recommendations for response spectrum reduction factors to account for incoherency effects were developed as a function of the foundation plan dimension and frequency. Since the original publication of these

recommendations, several studies have indicated that these initial recommendations are likely conservative. Task S2.1 validates the premise that the published spectral reductions may be overly conservative (too small) in certain cases and, further, this study provides recommendations for a more realistic characterization of incoherency effects. Equally important, the task demonstrates that spectral reduction is not the proper way to characterize seismic wave incoherence effects because spectral reductions are highly dependent on the shape of ground response spectra.

### **Applications, Values, and Use**

The methods and procedures to incorporate incoherence effects described in this report constitute a viable approach for the documentation of the site-specific seismic response to support utility's ESP or COL applications. The primary value of these methods is that they present a more realistic quantification of the seismic response to the structures and equipment in the high-frequency portion of the response spectrum.

### **EPRI Perspective**

EPRI has an industry-wide perspective and a mandate to address technical issues related to the safe design and efficient operation of nuclear facilities. The methods and procedures described in this report contribute to stabilizing seismic safety review for new nuclear power units and to providing a more accurate approach for the treatment of the seismic ground motion incoherency phenomena.

### **Approach**

Based on the state-of-the-art coherency functions developed by Dr. N. Abrahamson, seismic response has been evaluated using the soil-structure interaction computer program CLASSI, combined with random vibration theory. Seismic response was evaluated for example rigid, massless foundations and for example structural models on rigid foundation mats. The basic relationship between motion in the free-field and motion on the rigid massless foundation is developed based on random vibration theory. The relationship between free-field ground motion at discretized points on the foundation is described by the cross power spectral density functions, normalized by the power spectral density (PSD) function of the free-field ground motion. The resulting PSDs of the motion of the rigid, massless foundation are used to define ITFs. ITFs, when applied to the free-field ground motion, take into account the effects of incoherence on the foundation input motion and permit the evaluation of structure and foundation seismic response directly using the CLASSI family of SSI analysis programs.

### **Keywords**

Eastern U.S. earthquakes  
Ground motions  
In-structure seismic response  
High-frequency effects  
Seismic wave incoherence  
Random vibrations  
Soil-structure interactions  
Ground motion incoherence

## ABSTRACT

---

Task S2.1 of the EPRI/DOE New Plant Seismic Issues Resolution Program results are presented herein. The objective of this task was to systematically study seismic wave incoherence effects on structures/foundations similar to those being considered for Advanced Reactor designs. In support of that objective, a set of key project subtasks were developed as follows:

- Demonstrate the process for directly analyzing the foundation/structural seismic responses with appropriate consideration of ground motion incoherence effects incorporated into a soil-structure interaction computer program (identified as the *direct approach*)
- Benchmark the direct approach analytical methods (random vibration theory approach and the eigen function decomposition approach) and programs (CLASSI and SASSI) to verify the accuracy of the results
- Conduct sensitivity studies on the key foundation and structure characteristics in order to understand the general effects of incoherence on representative nuclear structures
- Examine the feasibility of a *simplified* (alternate) *method* to scale the free-field input motion to account for the incoherency effects

Current probabilistic seismic hazard assessments (PSHAs) for sites in the Central and Eastern United States (CEUS) result in site-specific response spectra that contain high spectral amplitudes in the frequency range above 10 Hz. These uniform hazard spectra (UHS) do not represent the recorded ground motion of a single earthquake. Nevertheless, their characteristics are representative of recorded earthquake ground motions on stiff rock sites and, therefore, form the ground motion basis for this study. These results of current PSHAs provide motivation for this study, i.e., to realistically address the effect of incoherence of ground motion on structure response.

Observations of recorded earthquake ground motions over the last three decades have demonstrated that motions recorded on foundations of structures differ from those measured in the adjacent free-field. This difference is due to interaction of the foundation/structure system with the underlying soil or rock. Generally, the motion measured on the foundation is less than the motion recorded in the free-field, especially at high-frequencies. Two aspects of this soil-structure interaction contribute to these observations: kinematic and inertial interaction. Kinematic interaction is due to the spatial variation of the free-field ground motion over the portion of the foundation/structure system abutting the soil or rock. For nuclear power plant

structures, which have large and stiff foundation mats, the amplitudes of high-frequency seismic response of the foundation mat are expected to be significantly less than those in the free-field due to horizontal spatial variation of ground motion including incoherence. This study evaluates the response of nuclear power plant structures and foundations subjected to free-field ground motion with strong high-frequency characteristics.

The phenomenon of seismic wave incoherence has been recognized for many years, but the lack of an adequately large set of recorded data prevented quantification of the phenomenon and the development of approaches for the incorporation of the effect into the dynamic analysis of NPP structures. Abrahamson, in a separate study referenced herein, presents a state-of-the-art representation of the coherency function based on a large number of densely spaced ground motion recordings. Coherency functions define the relationships between ground motion at separate locations as a function of the separation distance between the locations and the frequency of the ground motion. Coherency of motion decreases significantly with increasing frequency and increasing distance between points of interest. For example, at a frequency of 20 Hz, the coherency of horizontal ground motion at two points 5 meters apart is on average, about 0.35, which is a measure of the degree to which the motions at the two points are out of phase (i.e., they are not coherent). At points greater than 5 meters apart the coherency decreases. Hence, the foundation/structure subjected to this wave field is not significantly excited by coherent motion at 20 Hz, and therefore, has significantly lower response. The coherency functions developed in this study accounts for this effect of incoherence at all frequencies of interest and all discretized points on the foundation.

Seismic response was evaluated for rigid, massless foundations and for example structural models on rigid foundation mats. The basic relationship between motion in the free-field and motion on the rigid massless foundation is developed based on random vibration theory. The starting points are the coherency functions developed by Dr. Abrahamson (Abrahamson, 2005, 2006). Coherency functions define the relationships between ground motion at separate locations as a function of two parameters (1) the separation distance between the locations and (2) the frequency of the ground motion. These coherency functions, combined with concepts of random vibration theory, were incorporated into the CLASSI system of SSI analysis programs. The next step is defining the relationship between free-field ground motion at discretized points on the foundation. The relationship is described by the cross power spectral density functions, normalized by the power spectral density (PSD) function of the free-field ground motion. The resulting PSDs of the motion of the rigid, massless foundation are used to define incoherency transfer functions (ITFs). The ITFs are equivalent to scattering functions in CLASSI nomenclature, i.e., frequency-dependent, complex-valued functions. The ITFs, when applied to the free-field ground motion, take into account the effects of incoherence on the foundation input motion. These scattering functions permit the evaluation of structure and foundation seismic response directly using the CLASSI family of SSI analysis programs. In general, each component of horizontal ground motion induces a horizontal translation and a companion torsional component. The vertical component of ground motion induces a vertical translation of the foundation and companion rocking components about the horizontal axes. The translational ITFs are principally a function of foundation area. The rotational ITFs are a function of foundation area and foundation shape.

Similarly, scaling functions based on the ITFs may be applied to modify the free-field ground motion. These scaling functions are applied to the amplitude of the Fourier transform of the free-field motion. This modified ground motion may be used in standard seismic response analyses as an alternate means of including the effects of seismic wave incoherence. In either case, the effects of incoherence on NPP structures/foundations are accounted for as a function of relevant parameters such as foundation area, foundation shape, structural characteristics, and free-field ground motion.

The direct approach for incorporation of the ITFs into the SSI analysis was validated during this study by an independent comparison with different methodology and software. The random vibration approach used herein with CLASSI produced excellent agreement with an eigen function decomposition approach used herein with SASSI.

The conclusions of this study are:

- Soil-structure interaction (SSI) analysis is important to calculating seismic response to structures mounted on rock sites and subjected to high-frequency ground motion. SSI produces significant reductions in high-frequency response for these conditions.
- Consideration of incoherence is important for the proper evaluation of the response of large base mat structures to high-frequency ground motions (primarily greater than 10 Hz). Realistically accounting for ground motion incoherence on the seismic response of nuclear power plant structures is significant and should be properly incorporated into seismic design analyses.
- Generally, for the rock site and corresponding high-frequency free-field ground motion considered in this study, incoherent earthquake ground motion results in calculated in-structure response spectra which demonstrate minimal effects below 10 Hz. In frequency ranges above 10 Hz increased conservatism in the coherent spectra exists and the ratio of coherent response spectra to incoherent response spectra varies from about 1 to greater than 2.
- The effects of incoherence are three-dimensional. Induced torsion couples response in the two horizontal directions. Induced rocking couples horizontal and vertical response, i.e., incoherent vertical ground motion induces horizontal response in the structure. Incoherency-induced rocking and torsion are shown to be important to in-structure response depending on the structure and its dynamic characteristics.
- A valid direct approach for accurately incorporating incoherency effects has been studied and recommendations for its implementation have been provided in this report:
  - The direct approach utilized in the majority of these studies incorporates the Abrahamson coherency functions directly into the CLASSI soil-structure interaction program.
  - For the purpose of benchmarking the CLASSI direct incoherency approach, the SASSI method by Bechtel and the ACS SASSI method by ARES have also been validated to treat the effects of incoherence on structures.
- Another valid, but conservative approach for incorporating incoherency effects has been studied, and recommendations for its implementation have been provided in this report. The

simplified approach applies a modified form of the Incoherency Transfer Function (ITFs) to the free-field ground motion and allows for the performance of the SSI analysis for the resulting modified ground motion assuming coherent input motions.

- Regarding the simplified approach, a recommendation has been provided for a simplified approach which will provide insight into the effects of incoherence on foundation and structure response. The simplified approach recommended in Chapter 5 is applicable to rock sites and the corresponding free-field ground motion with significant high-frequency content. The concept of the simplified approach has been validated herein. However, its generalization to foundation/structure systems of all types will require additional sensitivity studies to be performed. These sensitivity studies would include variations in structure and foundation conditions and ground motion characteristics. This simplified approach is necessarily conservative due to its goal of being generically applicable to as broad a range of structures and foundations as possible and due to the incoherency-induced rotations that exist for some structure/foundation configurations.
- The CLASSI analyses performed in this study rely on the assumption that the foundation of the structure behaves rigidly when subjected to earthquake ground motion. The behavior of a foundation is dependent on the effective stiffness, which is a function of the foundation itself and the stiffening due to the interconnecting structural elements anchored to the foundation. The results of this study are applicable to typical nuclear power plant structures whose foundations are significantly stiffened by inter-connecting structural systems.
- The combined effects of spatial variation of ground motion with depth in the rock/soil and the effect of incoherence of ground motion for structures with embedded foundations and partially embedded walls is judged to be analyzable by considering the effects simultaneously or by separation of the two effects and superimposing the results. A sensitivity study was performed to evaluate the effects of incoherence on surface/embedded foundation/structure systems. A representative reactor containment/internal structure, supported on the rock site profile and subjected to the companion high-frequency ground motion was analyzed. Surface founded coherent and incoherent responses were calculated and the effects of incoherence quantified. The same structure was analyzed for an embedment ratio of 0.5. Coherent and incoherent responses were calculated. The effects of incoherence were isolated from the other aspects of SSI. In general terms, the results demonstrate that the effects of incoherence and embedment are separable. In addition, the effects of embedment on response for coherent and incoherent ground motions were demonstrated to significantly reduce response. The ACS-SASSI program was used.
- Computer programs that model flexible foundations and embedment, such as SASSI (when modified to treat the phenomena of incoherency), can effectively analyze soil-structure systems including those effects.
- For realistic, but simplified, foundation shapes studied herein, the most important parameter was found to be foundation area. Foundation shape (square vs. rectangle vs. circle) and site soil conditions were found to have minimal effect on the translational component ITFs. Foundation shape does have a significant effect on induced rotational ITFs.

In summary, seismic analyses incorporating soil-structure interaction and ground motion incoherence demonstrate a significant reduction in high-frequency seismic response as measured

by in-structure response spectra. The computed incoherency transfer functions depend on the foundation area and are independent of site soil conditions. However, the resulting spectral reductions strongly depend on the site-specific free-field spectrum shape and the associated site soil conditions. The effect of seismic wave incoherence is primarily a high-frequency phenomenon. Hence, the observed reductions in foundation response spectra are much less for soil sites since the soil site-specific ground motion is generally deficient in the high-frequency range. The project effectively demonstrated the validity of using SSI codes modified to incorporate incoherency effects as a method for deriving structural responses for nuclear structures. The CLASSI program approach was validated using a series of benchmark problems with the SASSI code. A variety of sensitivity studies were completed which resulted in key insights as to the effects that foundation size, shape and soil properties have on the results. The project studied the options available to generate a simplified approach toward incorporation of incoherence effects that eliminates the need to perform a specific SSI analysis which incorporates the incoherence effect. A recommendation for this simplified approach has been provided based on the studies performed on the three example structures. The benefits of utilizing this simplified approach are that it is easier to implement and does not require the use of a modified version of a SSI computer program. The trade-off for that simplification is that the method is more conservative than the direct approach and may not provide the degree of realistic response desired by a specific new plant application.



## **ACKNOWLEDGEMENTS**

---

EPRI wishes to acknowledge the members of the Technical Review and Advisory Group (TRAG) for their support of this research project:

Robert Kennedy (Chair)	RPK Structural Consulting
Orhan Gurbuz	Consultant
Don Moore	Southern Nuclear
John Richards	Duke Power
Carl Stepp	Earthquake Hazards Solutions

EPRI wishes to acknowledge Farhang Ostadan at Bechtel Engineering for his support of this project in providing SASSI results for the Benchmark problem in Appendix C of this report.



# CONTENTS

---

<b>1 INTRODUCTION AND BACKGROUND .....</b>	<b>1-1</b>
Seismic Wave Incoherence.....	1-1
Consideration of Incoherence at Diablo Canyon.....	1-3
Project Sub-Tasks.....	1-3
Contents of the Report .....	1-5
<b>2 STUDY INPUT PARAMETERS.....</b>	<b>2-1</b>
Coherency Function.....	2-1
Site Parameters and Input Ground Motion.....	2-4
Foundation Parameters.....	2-10
Structure Properties .....	2-11
<b>3 TECHNICAL APPROACH.....</b>	<b>3-1</b>
General .....	3-1
Procedure to Evaluate the Incoherency Transfer Function (ITF).....	3-1
Procedure to Evaluate the Rigid Massless Foundation Incoherent Response Spectra .....	3-5
Procedure to Evaluate the Foundation and Structure Incoherent Response Spectra by Random Vibration Theory.....	3-6
Procedure to Evaluate the Foundation and Structure Incoherent Response Spectra by CLASSI.....	3-8
<b>4 RIGID, MASSLESS FOUNDATION RESPONSE .....</b>	<b>4-1</b>
General .....	4-1
Wave Passage Effects .....	4-1
Incoherency Transfer Function.....	4-4
Spectral Corrections.....	4-7
Rotations Induced by Incoherence.....	4-12
<b>5 SSI AND STRUCTURE RESPONSE .....</b>	<b>5-1</b>
General .....	5-1

SSI and Incoherence – Direct Method .....	5-2
Foundation Response .....	5-3
Auxiliary and Shield Building (ASB).....	5-5
Steel Containment Vessel (SCV) .....	5-6
Containment Internal Structure (CIS) .....	5-6
Summary of Direct Method Results.....	5-7
SSI and Incoherence – Scaling Input Fourier Amplitude (Simplified Method).....	5-26
Summary of Simplified Method Results.....	5-31
Effect of Embedment and Incoherence .....	5-52
Effect of SSI on High-Frequency Seismic Response .....	5-53
<b>6 SUMMARY, CONCLUSIONS AND RECOMMENDATIONS.....</b>	<b>6-1</b>
SUMMARY .....	6-1
Tasks Performed and Approach.....	6-1
Incoherency Transfer Function.....	6-2
Impact on Response Spectra Due to Incoherence Effects.....	6-3
Foundation response .....	6-3
Structure response .....	6-5
Benchmark Comparison.....	6-8
APPLICATIONS .....	6-8
CONCLUSIONS .....	6-10
<b>7 REFERENCES .....</b>	<b>7-1</b>
<b>A COMMENTS AND RESPONSES TO NRC REQUESTS FOR ADDITIONAL INFORMATION (RAIs) .....</b>	<b>A-1</b>
<b>B VALIDATION OF INCOHERENCY EFFECTS THROUGH RECORDED EVENTS .....</b>	<b>B-1</b>
B.1 Technical Literature on Validation of Incoherency Effects .....	B-1
B.2 Diablo Canyon Earthquakes .....	B-6
B.3 Measured Response of the Perry Nuclear Power Plant during the Northeastern Ohio Earthquake of January 31, 1986.....	B-10
B.4 Conclusions Regarding the Validation of incoherency Effects Through Recorded Events.....	B-18
B.5 References .....	B-19
<b>C BENCHMARK PROBLEM COMPARISON .....</b>	<b>C-1</b>

Rigid, Massless Foundation .....	C-2
SSI and Incoherency .....	C-5
<b>D UNCERTAINTY EFFECTS ON INCOHERENCY FUNCTIONS .....</b>	<b>D-1</b>
Background .....	D-1
Objective of Sensitivity Study on Coherency Uncertainty .....	D-2
Assumptions .....	D-2
Approach .....	D-2
Results .....	D-3
References .....	D-3
<b>E EFFECT OF EMBEDMENT AND INCOHERENCE .....</b>	<b>1</b>
E.1 Sensitivity Study Model .....	2
E.2 Soil-Structure Interaction Analyses .....	5
E.3 Conclusions .....	21
E.4 References .....	22



## LIST OF FIGURES

Figure 2-1 Coherency Function for Horizontal Ground Motion .....	2-2
Figure 2-2 Coherency Function for Vertical Ground Motion .....	2-3
Figure 2-3 Rock and Soil Site Profile Shear Wave Velocities vs. Depth.....	2-5
Figure 2-4 Rock and Soil Site Profiles Within 500 Feet of the Ground Surface.....	2-6
Figure 2-5 Site-Specific Response Spectra for Rock Site at Ground Surface (Depth 0-ft).....	2-8
Figure 2-6 Site-Specific Response Spectra for Soil Site at Ground Surface (Depth 0-ft).....	2-9
Figure 2-7 Computed and Target Response Spectra for Rock Site.....	2-10
Figure 2-8 Advanced Reactor Structure Stick Model .....	2-13
Figure 2-9 Advanced Reactor Structure Stick Model with Outriggers and Offset Mass Centers.....	2-14
Figure 2-10 Mode 1–ASB Fundamental Mode, Y-Direction, $f = 3.0$ Hz .....	2-19
Figure 2-11 Mode 6–SCV Fundamental Mode, Y-Direction, $f = 6.1$ Hz .....	2-20
Figure 2-12 Mode 1–CIS Fundamental Mode, Y-Direction, $f = 12.0$ Hz .....	2-21
Figure 4-1 Effect of Wave Passage on Incoherency Transfer Function for Horizontal Motion .....	4-2
Figure 4-2 Effect of Wave Passage on Foundation Horizontal Response Spectra.....	4-3
Figure 4-3 Effect of Wave Passage on Incoherency Transfer Function for Vertical Motion.....	4-3
Figure 4-4 Effect of Wave Passage on Foundation Vertical Response Spectra.....	4-4
Figure 4-5 Horizontal Motion Incoherency Transfer Function – Effect of Foundation Shape .....	4-5
Figure 4-6 Vertical Motion Incoherency Transfer Function – Effect of Foundation Shape.....	4-6
Figure 4-7 Horizontal Motion Incoherency Transfer Function – Effect of Foundation Area .....	4-6
Figure 4-8 Vertical Motion Incoherency Transfer Function – Effect of Foundation Area .....	4-7
Figure 4-9 Horizontal Motion Foundation Response Spectra, Rock Site.....	4-10
Figure 4-10 Vertical Motion Foundation Response Spectra, Rock Site .....	4-10
Figure 4-11 Horizontal Motion Foundation Response Spectra, Soil Site .....	4-11
Figure 4-12 Vertical Motion Foundation Response Spectra, Soil Site .....	4-11
Figure 4-13 Torsion Induced by Incoherent Horizontal Input, Square Foundation .....	4-13
Figure 4-14 Rocking Induced by Incoherent Vertical Input, Square Foundation .....	4-13
Figure 4-15 H1 Torsion Induced by Incoherent Horizontal Input, Rectangle Foundation .....	4-14
Figure 4-16 H2 Torsion Induced by Incoherent Horizontal Input, Rectangle Foundation .....	4-14
Figure 4-17 Rocking Induced by Incoherent Vertical Input, Rectangle Foundation .....	4-15

Figure 4-18 Response Spectra Including Torsion, Square Foundation, Rock Site..... 4-16

Figure 4-19 Response Spectra Including Torsion, Square Foundation, Soil Site..... 4-17

Figure 4-20 Response Spectra Including Rocking, Square Foundation, Rock Site..... 4-17

Figure 4-21 Response Spectra Including Rocking, Square Foundation, Soil Site..... 4-18

Figure 4-22 Response Spectra Including Torsion, Rectangle Foundation, Rock Site ..... 4-18

Figure 4-23 Response Spectra Including Torsion, Rectangle Foundation, Soil Site ..... 4-19

Figure 4-24 Response Spectra Including Rocking, Rectangle Foundation, Rock Site ..... 4-19

Figure 4-25 Response Spectra Including Rocking, Rectangle Foundation, Soil Site ..... 4-20

Figure 5-1 Locations on the AP1000-Based Stick Model Where In-Structure Response Spectra are Computed ..... 5-4

Figure 5-2 Foundation Response Spectra – X Direction –SSI Coherent, SSI Incoherent, SSI Incoherent with No Rotations (Node 1) ..... 5-8

Figure 5-3 Foundation Response Spectra – Y Direction –SSI Coherent, SSI Incoherent, SSI Incoherent with No Rotations (Node 1) ..... 5-8

Figure 5-4 Foundation Response Spectra – Z Direction –SSI Coherent, SSI Incoherent, SSI Incoherent with No Rotations (Node 1) ..... 5-9

Figure 5-5 Top of Shield Building Response Spectra – X Direction –SSI Coherent, SSI Incoherent, SSI Incoherent with No Rotations (Node 310) ..... 5-9

Figure 5-6 Top of Shield Building Response Spectra – Y Direction –SSI Coherent, SSI Incoherent, SSI Incoherent with No Rotations (Node 310) ..... 5-10

Figure 5-7 Top of Shield Building Response Spectra – Z Direction –SSI Coherent, SSI Incoherent, SSI Incoherent with No Rotations (Node 310) ..... 5-10

Figure 5-8 Top of Auxiliary Building Response Spectra – X Direction –SSI Coherent, SSI Incoherent, SSI Incoherent with No Rotations (Node 120mc)..... 5-11

Figure 5-9 Top of Auxiliary Building Response Spectra – Y Direction –SSI Coherent, SSI Incoherent, SSI Incoherent with No Rotations (Node 120mc)..... 5-11

Figure 5-10 Top of Auxiliary Building Response Spectra – Z Direction –SSI Coherent, SSI Incoherent, SSI Incoherent with No Rotations (Node 120) ..... 5-12

Figure 5-11 Low on ASB Response Spectra – X Direction – SSI Coherent, SSI Incoherent, SSI Incoherent with No Rotations (Node 80mc)..... 5-12

Figure 5-12 Low on ASB Response Spectra – Y Direction – SSI Coherent, SSI Incoherent, SSI Incoherent with No Rotations (Node 80mc)..... 5-13

Figure 5-13 Low on ASB Response Spectra – Z Direction – SSI Coherent, SSI Incoherent, SSI Incoherent with No Rotations (Node 80) ..... 5-13

Figure 5-14 Shield Building Outrigger Response Spectra – X Direction – SSI Coherent, SSI Incoherent, SSI Incoherent with No Rotations (Node 310out) ..... 5-14

Figure 5-15 Shield Building Outrigger Response Spectra – Y Direction – SSI Coherent, SSI Incoherent, SSI Incoherent with No Rotations (Node 310out) ..... 5-14

Figure 5-16 Shield Building Outrigger Response Spectra – Z Direction – SSI Coherent, SSI Incoherent, SSI Incoherent with No Rotations (Node 310out) ..... 5-15

Figure 5-17 Auxiliary Building Outrigger Response Spectra – X Direction – SSI Coherent, SSI Incoherent, SSI Incoherent with No Rotations (Node 120out)..... 5-15

Figure 5-18 Auxiliary Building Outrigger Response Spectra – Y Direction – SSI Coherent, SSI Incoherent, SSI Incoherent with No Rotations (Node 120out)..... 5-16

Figure 5-19 Auxiliary Building Outrigger Response Spectra – Z Direction – SSI Coherent, SSI Incoherent, SSI Incoherent with No Rotations (Node 120out)..... 5-16

Figure 5-20 Top of SCV Response Spectra – X Direction –SSI Coherent, SSI Incoherent, SSI Incoherent with No Rotations (Node 417) ..... 5-17

Figure 5-21 Top of SCV Response Spectra – Y Direction –SSI Coherent, SSI Incoherent, SSI Incoherent with No Rotations (Node 417) ..... 5-17

Figure 5-22 Top of SCV Response Spectra – Z Direction –SSI Coherent, SSI Incoherent, SSI Incoherent with No Rotations (Node 417) ..... 5-18

Figure 5-23 Low on SCV Response Spectra – X Direction – SSI Coherent, SSI Incoherent, SSI Incoherent with No Rotations (Node 406) ..... 5-18

Figure 5-24 Low on SCV Response Spectra – Y Direction – SSI Coherent, SSI Incoherent, SSI Incoherent with No Rotations (Node 406) ..... 5-19

Figure 5-25 Low on SCV Response Spectra – Z Direction – SSI Coherent, SSI Incoherent, SSI Incoherent with No Rotations (Node 406) ..... 5-19

Figure 5-26 SCV Outrigger Response Spectra – X Direction – SSI Coherent, SSI Incoherent, SSI Incoherent with No Rotations (Node 417out) ..... 5-20

Figure 5-27 SCV Outrigger Response Spectra – Y Direction – SSI Coherent, SSI Incoherent, SSI Incoherent with No Rotations (Node 417out) ..... 5-20

Figure 5-28 SCV Outrigger Response Spectra – Z Direction – SSI Coherent, SSI Incoherent, SSI Incoherent with No Rotations (Node 417out) ..... 5-21

Figure 5-29 Top of CIS Response Spectra – X Direction –SSI Coherent, SSI Incoherent, SSI Incoherent with No Rotations (Node 538mc) ..... 5-21

Figure 5-30 Top of CIS Response Spectra – Y Direction –SSI Coherent, SSI Incoherent, SSI Incoherent with No Rotations (Node 538mc) ..... 5-22

Figure 5-31 Top of CIS Response Spectra – Z Direction –SSI Coherent, SSI Incoherent, SSI Incoherent with No Rotations (Node 538) ..... 5-22

Figure 5-32 Low on CIS Response Spectra – X Direction –SSI Coherent, SSI Incoherent, SSI Incoherent with No Rotations (Node 535mc)..... 5-23

Figure 5-33 Low on CIS Response Spectra – Y Direction –SSI Coherent, SSI Incoherent, SSI Incoherent with No Rotations (Node 535mc)..... 5-23

Figure 5-34 Low on CIS Response Spectra – Z Direction –SSI Coherent, SSI Incoherent, SSI Incoherent with No Rotations (Node 535) ..... 5-24

Figure 5-35 CIS Outrigger Response Spectra – X Direction – SSI Coherent, SSI Incoherent, SSI Incoherent with No Rotations (Node 538out) ..... 5-24

Figure 5-36 CIS Outrigger Response Spectra – Y Direction – SSI Coherent, SSI Incoherent, SSI Incoherent with No Rotations (Node 538out) ..... 5-25

Figure 5-37 CIS Outrigger Response Spectra – Z Direction – SSI Coherent, SSI Incoherent, SSI Incoherent with No Rotations (Node 538out) ..... 5-25

Figure 5-38 Horizontal Incoherency Transfer Function Used for Simplified Approach ..... 5-26

Figure 5-39 Vertical Incoherency Transfer Function Used for Simplified Approach ..... 5-27

Figure 5-40 Foundation Response Spectra – X Direction –SSI Incoherent, SSI Incoherent with No Rotations, SSI Incoherent by ITF Scaling (Node 1) ..... 5-28

Figure 5-41 Top of Shield Building Response Spectra – X Direction – SSI Incoherent, SSI Incoherent with No Rotations, SSI Incoherent by ITF Scaling (Node 310)..... 5-28

Figure 5-42 Top of SCV Response Spectra – X Direction – SSI Incoherent, SSI Incoherent with No Rotations, SSI Incoherent by ITF Scaling (Node 417) ..... 5-29

Figure 5-43 Top of CIS Response Spectra – X Direction – SSI Incoherent, SSI Incoherent with No Rotations, SSI Incoherent by ITF Scaling (Node 538mc)..... 5-29

Figure 5-44 Foundation Response Spectra – X Direction – SSI Coherent, SSI Incoherent, SSI Incoherent by Modified ITF, SSI Incoherent by Modified and Scaled ITF (Node 1)..... 5-34

Figure 5-45 Foundation Response Spectra – Y Direction – SSI Coherent, SSI Incoherent, SSI Incoherent by Modified ITF, SSI Incoherent by Modified and Scaled ITF (Node 1)..... 5-34

Figure 5-46 Foundation Response Spectra – Z Direction – SSI Coherent, SSI Incoherent, SSI Incoherent by Modified ITF, SSI Incoherent by Modified and Scaled ITF (Node 1)..... 5-35

Figure 5-47 Top of Shield Building Response Spectra – X Direction – SSI Coherent, SSI Incoherent, SSI Incoherent by Modified ITF, SSI Incoherent by Modified and Scaled ITF (Node 310)..... 5-35

Figure 5-48 Top of Shield Building Response Spectra – Y Direction – SSI Coherent, SSI Incoherent, SSI Incoherent by Modified ITF, SSI Incoherent by Modified and Scaled ITF (Node 310)..... 5-36

Figure 5-49 Top of Shield Building Response Spectra – Z Direction – SSI Coherent, SSI Incoherent, SSI Incoherent by Modified ITF, SSI Incoherent by Modified and Scaled ITF (Node 310)..... 5-36

Figure 5-50 Top of Auxiliary Building Response Spectra – X Direction – SSI Coherent, SSI Incoherent, SSI Incoherent by Modified ITF, SSI Incoherent by Modified and Scaled ITF (Node 120mc)..... 5-37

Figure 5-51 Top of Auxiliary Building Response Spectra – Y Direction – SSI Coherent, SSI Incoherent, SSI Incoherent by Modified ITF, SSI Incoherent by Modified and Scaled ITF (Node 120mc)..... 5-37

Figure 5-52 Top of Auxiliary Building Response Spectra – Z Direction – SSI Coherent, SSI Incoherent, SSI Incoherent by Modified ITF, SSI Incoherent by Modified and Scaled ITF (Node 120)..... 5-38

Figure 5-53 Low on ASB Response Spectra – X Direction – SSI Coherent, SSI Incoherent, SSI Incoherent by Modified ITF, SSI Incoherent by Modified and Scaled ITF (Node 80mc)..... 5-38

Figure 5-54 Low on ASB Response Spectra – Y Direction – SSI Coherent, SSI Incoherent, SSI Incoherent by Modified ITF, SSI Incoherent by Modified and Scaled ITF (Node 80mc)..... 5-39

Figure 5-55 Low on ASB Response Spectra – Z Direction – SSI Coherent, SSI Incoherent, SSI Incoherent by Modified ITF, SSI Incoherent by Modified and Scaled ITF (Node 80)..... 5-39

Figure 5-56 Shield Building Outrigger Response Spectra – X Direction – SSI Coherent, SSI Incoherent, SSI Incoherent by Modified ITF, SSI Incoherent by Modified and Scaled ITF (Node 310out)..... 5-40

Figure 5-57 Shield Building Outrigger Response Spectra – Y Direction – SSI Coherent, SSI Incoherent, SSI Incoherent by Modified ITF, SSI Incoherent by Modified and Scaled ITF (Node 310out)..... 5-40

Figure 5-58 Shield Building Outrigger Response Spectra – Z Direction – SSI Coherent, SSI Incoherent, SSI Incoherent by Modified ITF, SSI Incoherent by Modified and Scaled ITF (Node 310out)..... 5-41

Figure 5-59 Auxiliary Building Outrigger Response Spectra – X Direction – SSI Coherent, SSI Incoherent, SSI Incoherent by Modified ITF, SSI Incoherent by Modified and Scaled ITF (Node 120out) ..... 5-41

Figure 5-60 Auxiliary Building Outrigger Response Spectra – Y Direction – SSI Coherent, SSI Incoherent, SSI Incoherent by Modified ITF, SSI Incoherent by Modified and Scaled ITF (Node 120out) ..... 5-42

Figure 5-61 Auxiliary Building Outrigger Response Spectra – Z Direction – SSI Coherent, SSI Incoherent, SSI Incoherent by Modified ITF, SSI Incoherent by Modified and Scaled ITF (Node 120out) ..... 5-42

Figure 5-62 Top of SCV Response Spectra – X Direction – SSI Coherent, SSI Incoherent, SSI Incoherent by Modified ITF, SSI Incoherent by Modified and Scaled ITF (Node 417)..... 5-43

Figure 5-63 Top of SCV Response Spectra – Y Direction – SSI Coherent, SSI Incoherent, SSI Incoherent by Modified ITF, SSI Incoherent by Modified and Scaled ITF (Node 417)..... 5-43

Figure 5-64 Top of SCV Response Spectra – Z Direction – SSI Coherent, SSI Incoherent, SSI Incoherent by Modified ITF, SSI Incoherent by Modified and Scaled ITF (Node 417)..... 5-44

Figure 5-65 Low on SCV Response Spectra – X Direction – SSI Coherent, SSI Incoherent, SSI Incoherent by Modified ITF, SSI Incoherent by Modified and Scaled ITF (Node 406)..... 5-44

Figure 5-66 Low on SCV Response Spectra – Y Direction – SSI Coherent, SSI Incoherent, SSI Incoherent by Modified ITF, SSI Incoherent by Modified and Scaled ITF (Node 406)..... 5-45

Figure 5-67 Low on SCV Response Spectra – Z Direction – SSI Coherent, SSI Incoherent, SSI Incoherent by Modified ITF, SSI Incoherent by Modified and Scaled ITF (Node 406)..... 5-45

Figure 5-68 SCV Outrigger Response Spectra – X Direction – SSI Coherent, SSI Incoherent, SSI Incoherent by Modified ITF, SSI Incoherent by Modified and Scaled ITF (Node 417out)..... 5-46

Figure 5-69 SCV Outrigger Response Spectra – Y Direction – SSI Coherent, SSI Incoherent, SSI Incoherent by Modified ITF, SSI Incoherent by Modified and Scaled ITF (Node 417out)..... 5-46

Figure 5-70 SCV Outrigger Response Spectra – Z Direction – SSI Coherent, SSI Incoherent, SSI Incoherent by Modified ITF, SSI Incoherent by Modified and Scaled ITF (Node 417out)..... 5-47

Figure 5-71 Top of CIS Response Spectra – X Direction – SSI Coherent, SSI Incoherent, SSI Incoherent by Modified ITF, SSI Incoherent by Modified and Scaled ITF (Node 538mc) ..... 5-47

Figure 5-72 Top of CIS Response Spectra – Y Direction – SSI Coherent, SSI Incoherent, SSI Incoherent by Modified ITF, SSI Incoherent by Modified and Scaled ITF (Node 538mc) ..... 5-48

Figure 5-73 Top of CIS Response Spectra – Z Direction – SSI Coherent, SSI Incoherent, SSI Incoherent by Modified ITF, SSI Incoherent by Modified and Scaled ITF (Node 538) ..... 5-48

Figure 5-74 Low on CIS Response Spectra – X Direction – SSI Coherent, SSI Incoherent, SSI Incoherent by Modified ITF, SSI Incoherent by Modified and Scaled ITF (Node 535mc) ..... 5-49

Figure 5-75 Low on CIS Response Spectra – Y Direction – SSI Coherent, SSI Incoherent, SSI Incoherent by Modified ITF, SSI Incoherent by Modified and Scaled ITF (Node 535mc) ..... 5-49

Figure 5-76 Low on CIS Response Spectra – Z Direction – SSI Coherent, SSI Incoherent, SSI Incoherent by Modified ITF, SSI Incoherent by Modified and Scaled ITF (Node 535) ..... 5-50

Figure 5-77 CIS Outtrigger Response Spectra – X Direction – SSI Coherent, SSI Incoherent, SSI Incoherent by Modified ITF, SSI Incoherent by Modified and Scaled ITF (Node 538out) ..... 5-50

Figure 5-78 CIS Outtrigger Response Spectra – Y Direction – SSI Coherent, SSI Incoherent, SSI Incoherent by Modified ITF, SSI Incoherent by Modified and Scaled ITF (Node 538out) ..... 5-51

Figure 5-79 CIS Outtrigger Response Spectra – Z Direction – SSI Coherent, SSI Incoherent, SSI Incoherent by Modified ITF, SSI Incoherent by Modified and Scaled ITF (Node 538out) ..... 5-51

Figure 5-80 Foundation Response Spectra – X Direction – SSI Coherent, SSI Incoherent, Fixed-Base (Node 1) ..... 5-54

Figure 5-81 Foundation Response Spectra – Z Direction – SSI Coherent, SSI Incoherent, Fixed-Base (Node 1) ..... 5-54

Figure 5-82 Top of Shield Building Response Spectra – X Direction – SSI Coherent, SSI Incoherent, Fixed-Base (Node 310) ..... 5-55

Figure 5-83 Top of Shield Building Response Spectra – Z Direction – SSI Coherent, SSI Incoherent, Fixed-Base (Node 310) ..... 5-55

Figure 5-84 Top of Auxiliary Building Response Spectra – X Direction – SSI Coherent, SSI Incoherent, Fixed-Base (Node 120mc) ..... 5-56

Figure 5-85 Top of Auxiliary Building Response Spectra – Z Direction – SSI Coherent, SSI Incoherent, Fixed-Base (Node 120) ..... 5-56

Figure 5-86 Top of SCV Response Spectra – X Direction – SSI Coherent, SSI Incoherent, Fixed-Base (Node 417) ..... 5-57

Figure 5-87 Top of SCV Response Spectra – Z Direction – SSI Coherent, SSI Incoherent, Fixed-Base (Node 417) ..... 5-57

Figure 5-88 Top of CIS Response Spectra – X Direction – SSI Coherent, SSI Incoherent, Fixed-Base (Node 538mc) ..... 5-58

Figure 5-89 Top of CIS Response Spectra – Z Direction – SSI Coherent, SSI Incoherent, Fixed-Base (Node 538) ..... 5-58

## LIST OF TABLES

<u>Table 2-1 Coherency Function Coefficients .....</u>	<u>2-2</u>
<u>Table 2-2 Layers and Properties for the Rock Site (EQ Strain) .....</u>	<u>2-6</u>
<u>Table 2-3 Layers and Properties for the Soil Site (EQ Strain) .....</u>	<u>2-7</u>
<u>Table 2-4 Nodes and Mass Properties for Structural Model .....</u>	<u>2-15</u>
<u>Table 2-5 Element Properties for Structural Model .....</u>	<u>2-17</u>
<u>Table 3-1 Procedure to Evaluate Incoherency Transfer Function .....</u>	<u>3-4</u>
<u>Table 3-2 Procedure to Evaluate the Rigid Massless Foundation Incoherent Response Spectra .....</u>	<u>3-6</u>
<u>Table 3-3 Procedure to Evaluate the Foundation and Structure Incoherent Response Spectra by CLASSI .....</u>	<u>3-10</u>
<u>Table 4-1 Spectral Corrections for Horizontal Motion .....</u>	<u>4-9</u>
<u>Table 4-2 Spectral Corrections for Vertical Motion .....</u>	<u>4-9</u>
<u>Table 5-1 Comparison of Incoherent Direct and Incoherent Simplified Spectra .....</u>	<u>5-32</u>

**Deleted:** Table 2-1 Coherency Function Coefficients . 2-2¶  
Table 2-2 Layers and Properties for the Rock Site (EQ Strain) . 2-6¶  
Table 2-3 Layers and Properties for the Soil Site (EQ Strain) . 2-7¶  
Table 2-4 Nodes and Mass Properties for Structural Model . 2-15¶  
Table 2-5 Element Properties for Structural Model . 2-17¶  
Table 3-1 Procedure to Evaluate Incoherency Transfer Function . 3-4¶  
Table 3-2 Procedure to Evaluate the Rigid Massless Foundation Incoherent Response Spectra . 3-6¶  
Table 3-3 Procedure to Evaluate the Foundation and Structure Incoherent Response Spectra by CLASSI . 3-10¶  
Table 4-1 Spectral Corrections for Horizontal Motion . 4-9¶  
Table 4-2 Spectral Corrections for Vertical Motion . 4-9¶  
Table 5-1 Comparison of Incoherent Direct and Incoherent Simplified Spectra . 5-32¶



# 1

## INTRODUCTION AND BACKGROUND

---

Task S2.1 of the EPRI/DOE New Plant Seismic Issues Resolution Program entails a research program into the effect of seismic wave incoherence on foundation and building response. The scope of work associated with Task S2.1 has been conducted with results presented herein. The objective of this task is to systematically study seismic wave incoherence effects on structures/foundations similar to those being considered for Advanced Reactor designs. In support of that objective, a set of key project tasks were developed:

- Demonstrate the process for directly analyzing the foundation/structural seismic responses with appropriate consideration of ground motion incoherence effects incorporated into a soil-structure interaction computer program (identified as the *direct approach*)
- Benchmark the direct approach analytical methods (random vibration theory approach and the eigen function decomposition approach) and programs (CLASSI and SASSI) to verify the accuracy of the results
- Conduct sensitivity studies on the key foundation and structure characteristics in order to understand the general effects of incoherence on representative nuclear structures
- Examine the feasibility of a *simplified* (alternate) *method* to scale the free-field input motion to account for the incoherency effects

### Seismic Wave Incoherence

Task S2.1 of the EPRI/DOE New Plant Seismic Issues Resolution Program entails a research program into the effect of seismic wave incoherence on foundation and building response. The scope of work associated with Task S2.1 has been conducted with results presented herein. The objective of this task is to systematically study seismic wave incoherence effects on structures/foundations similar to those being considered for Advanced Reactor designs. Seismic wave incoherence consists of spatial variation of both horizontal and vertical ground motion. Two sources of incoherence or horizontal spatial variation of ground motion are:

- a. Local wave scattering: Spatial variation from scattering of waves due to the heterogeneous nature of the soil or rock along the propagation paths of the incident wave fields.
- b. Wave passage effects: Systematic spatial variation due to difference in arrival times of seismic waves across a foundation due to inclined waves.

This study considers both of these phenomena, but the final results are based on local wave scattering.

Observations of recorded earthquake ground motions over the last three decades have demonstrated that motions recorded on foundations of structures differ from those measured in the adjacent free-field. This difference is due to interaction of the foundation/structure system with the underlying soil or rock. Generally, the motion measured on the foundation is less than the motion recorded in the free-field, especially at high-frequencies. Chang et al. (1986) and Johnson (2003) summarize many of the efforts to document these phenomena.

Seismic wave incoherence has been recognized as a phenomenon of particular interest to structures of large plan dimensions and for structures with multiple supports and large distances between supports, e.g., bridges. As reported by Chang et al. (1986), the horizontal variation of ground motion was observed many years ago, but only verified through very limited recorded data. The lack of extensive recorded data prevented the incorporation of the effect into the dynamic analysis of structures with large foundations, such as nuclear power plant structures.

Motions recorded by dense arrays of instruments have shown that the coherency of motions decreases with increasing spatial separation of recording points and with increasing frequency. Dr. Norm Abrahamson has developed a state-of-the-art representation of the coherency function based on the most applicable data available (Abrahamson, 2005, 2006). The coherency function is the relationship between ground motion at separate locations as a function of the separation distance between the locations and the frequency of the ground motion. The resulting coherency functions are employed in this task to demonstrate the effects of seismic wave incoherency on the seismic response of structures and their foundations.

Two aspects of this soil-structure interaction contribute to the observations of foundation motion being less than the free-field: kinematic and inertial interaction. Kinematic interaction is due to the spatial variation of the free-field ground motion over the portion of the foundation/structure system abutting the soil or rock. For nuclear power plant structures, which have large and stiff foundation mats, the amplitudes of high-frequency seismic response of the foundation mat are expected to be significantly less than those in the free-field due to horizontal spatial variation of ground motion including incoherence. The effective input motion to a large rigid foundation is the result of the averaging and summation of this incoherent ground motion. This phenomenon has been referred to as the base averaging effect by some authors. This study evaluates the response of nuclear power plant structures and foundations subjected to free-field ground motion with strong high-frequency characteristics.

In NUREG/CR-3805 (Chang et al., 1986), recommendations for modifications to response spectra were developed as a function of the foundation plan dimension and frequency. These recommendations were incorporated into EPRI NP-6041 (EPRI, 1991), ASCE Standard 4 (ASCE, 2000), and DOE Standard-1020 (U.S. DOE, 2002) and termed "reduction factors." Task S2.1 demonstrates that the published spectral reductions may be overly conservative in certain cases but, most importantly, demonstrates that spectral reduction is not the proper way to characterize the effects of seismic wave incoherence because the spectral reductions are highly dependent on the shape of the ground response spectra. By this task, the effects of incoherency are treated directly in the soil-structure interaction analysis or by modifying the Fourier amplitude of the free-field ground motion instead of spectral modifications. Incoherency

corrections in spectra are then evaluated after seismic wave incoherence is introduced into the seismic analysis.

## **Consideration of Incoherence at Diablo Canyon**

Seismic wave incoherence was considered in support of the Long Term Seismic Program (LTSP) in the late 1980s. For that study, site-specific spatial incoherence functions were developed from low amplitude motions. This site-specific representation of incoherence was determined by recordings on a dense array of motions from small earthquakes, dynamite explosions in boreholes, and air gun shots fired at sea. The results of the analyses performed demonstrated that seismic wave incoherence generally results in reductions in the soil/structure seismic response. The Nuclear Regulatory Commission (NRC) addressed the LTSP soil-structure interaction (SSI) analyses including incoherency in Safety Evaluation Report, NUREG-0675, Supplement No. 34 (Rood, 1991). In this report, it is noted that the SSI analysis provides acceptable Diablo Canyon plant seismic responses.

In the early 1990's, the LTSP seismic SSI analyses were repeated incorporating coherency functions based on recordings from the instrumentation array in Lotung, Taiwan. These recordings are from earthquakes with a range of magnitudes and distances from the Lotung Array. The Lotung recorded data showed greater incoherency in the free-field ground motion than previously assumed. When applying these new data to the Diablo Canyon structures, the re-analyses demonstrated greater reductions in foundation and structure response than previously predicted from the site-specific measurements of small earthquakes and explosions. The Lotung array, along with extensive other recorded data (Abrahamson 2005, 2006), forms the basis for the coherency functions used herein.

Earthquake motion has been measured in the free-field and on the containment foundation for the Diablo Canyon plant in the past few years. The magnitude 3.4 Deer Canyon Earthquake that occurred October 18, 2003 provides an opportunity to compare calculated and measured incoherency effects. Calculations simulating incoherent Deer Canyon foundation motion for the Diablo Canyon foundation footprint and soil conditions are compared to measured foundation and free-field Deer Canyon earthquake motion in Appendix B.

## **Project Sub-Tasks**

Based on the coherency functions recently developed by Dr. Abrahamson (Abrahamson, 2005, 2006), seismic response has been evaluated using the soil-structure interaction computer program CLASSI (Wong and Luco, 1980), combined with random vibration theory. Seismic response is evaluated for rigid, massless foundations and for example structural models on rigid foundation mats. The basic relationship between motion in the free-field and motion on the rigid massless foundation is developed in Section 3 based on random vibration theory. The relationship between free-field ground motion at discretized points on the foundation is described by the cross power spectral density functions, normalized by the power spectral density (PSD) function of the free-field ground motion. Incoherency transfer functions (ITFs) are directly developed from the resulting PSDs of the motion of the rigid, massless foundation. ITFs are equivalent to scattering

functions in CLASSI nomenclature, i.e., frequency-dependent, complex-valued functions when applied to the free-field ground motion take into account the effects of incoherence on the foundation input motion. These scattering functions permit the evaluation of structure and foundation seismic response directly using the CLASSI family of SSI analysis programs. This approach for incorporating incoherency effects is referred to as the “direct approach” within this study.

Similarly, scaling functions based on the ITFs, may be applied to modify the free-field ground motion. These scaling functions are applied to the amplitude of the Fourier transform of the free-field motion. This modified free-field ground motion may be used in standard seismic response analyses as an alternate means of including the effects of seismic wave incoherence. This approach is building specific and is referred to as the “simplified approach” within this study.

In either case, the effects of incoherence on NPP structures/foundations are accounted for as a function of relevant parameters such as foundation area, foundation shape, structural characteristics, and free-field ground motion.

Project sub-tasks to accomplish the work described above include:

- a. Define cases to be analyzed including site conditions, foundation characteristics, and structural characteristics.
- b. Develop the ground motion input to be considered including response spectra and time histories. Establish methods of computation of power spectral density functions (PSDs) from response spectra and, conversely, response spectra from PSDs.
- c. Establish coherency functions for horizontal and vertical ground motions as a function of separation distance and frequency, including the phenomena of local wave scattering and wave passage.
- d. Derive the approach to incorporating the coherency functions into the CLASSI family of programs. The approach is based on random vibration theory. The response of a rigid, massless foundation is derived from input motion defined by the PSD of the free-field ground motion and the calculated cross power spectral density matrix of foundation response. Incoherency transfer functions are derived from the diagonal elements of the cross power spectral density matrix.
- e. Conduct parametric studies of the rigid, massless foundation to determine incoherency transfer functions and foundation response spectra. Comparison of foundation and free-field response spectra demonstrate the effect of SSI and incoherence on foundation response.
- f. Benchmark the computed incoherency transfer functions and modified spectra for a specific case by comparing CLASSI results to those obtained using SASSI. For this benchmarking purpose, the effect of incoherent ground motion has been evaluated by:
  - Two different SSI computer programs; CLASSI and SASSI (two different versions of SASSI were used – Bechtel and ACS).
  - Two different algorithms; CLASSI-stochastic method and SASSI-eigen decomposition method.

- Two different analytical approaches; random vibration theory (RVT) by CLASSI, and time history dynamic analyses by SASSI.
- Two different organizations conducting the analyses; CLASSI by the ARES team, and SASSI by the ARES team and the Bechtel Corp.

This important sub-task served to benchmark the results by an independent comparison based on different methodology and software. Documentation of these benchmark studies are contained in Appendix C of this report.

- g. Conduct SSI analyses of an example structure incorporating seismic wave incoherence by the direct approach of the CLASSI family of programs. Quantify the effect on in-structure response spectra of SSI vs. fixed-base conditions and the additional effect of incoherence of ground motions.
- h. Investigate the feasibility of a *simplified* (alternate) *method* to modeling the effects of seismic wave incoherence. The *simplified method* is based on developing a function derived from the incoherency transfer function that is applied to the amplitude of the Fourier Transform of the free-field ground motion. The end result being a modified free-field ground motion that incorporates the effects of incoherency and can be used in standard SSI analysis programs assuming coherent input motion.
- i. Document all work in a final report.

## **Contents of the Report**

Chapter 2 defines the input parameters for this study: ground motion coherency functions, rock and soil site conditions and the corresponding free-field ground motions, and structure/foundation parameters for the sensitivity studies performed. Chapter 3 presents the derivation of the CLASSI/random vibration approach. Chapter 4 focuses on the responses of rigid, massless foundations, i.e., the kinematic interaction effects due to Incoherency. The responses of the rigid, massless foundation are the derived Incoherency Transfer Functions. These ITFs are used to calculate the SSI response of soil-structure system. Chapter 5 investigates the effects of incoherency of ground motion on the response of the representative structure described in Chapter 2. Chapter 5, also, presents the “simplified approach” – it’s derivation and application to the representative structure. Chapter 6 summarizes the results and presents conclusions of the present study.

There are five appendices to this report. Appendix A contains the complete set of 53 NRC Requests for Additional Information (RAIs) relative to the EPRI technical update report on this project (Short et al., 2005) that were sent to the Nuclear Energy Institute (NEI) on June 1, 2006. Appendix A also contains the industry responses to these RAIs. Appendix B contains the results of a study on the merits of using incoherence effects from recorded seismic events as the basis for validating the project results. Appendix C contains the results from the benchmark studies that compare the results of applying two different analytical formulations (CLASSI and SASSI) to the problem of incoherency of ground motions. The results verify the approaches. Appendix D presents the results of a sensitivity study investigating the effect of uncertainties in the coherency functions on the incoherency transfer functions. Appendix E presents the results of a sensitivity study on the subject of embedment.



# 2

## STUDY INPUT PARAMETERS

---

### Coherency Function

For this project, Dr. Abrahamson developed a coherency function (Abrahamson, 2005, 2006) that describes the relationship between ground motion at separate locations as a function of the separation distance and the frequency of the ground motion. This coherency function is expressed by the following equation:

$$\gamma_{PW} = \left[ 1 + \left( \frac{f \operatorname{Tanh}(a_3 \xi)}{a_1 f_c} \right)^{n_1} \right]^{-1/2} \left[ 1 + \left( \frac{f \operatorname{Tanh}(a_3 \xi)}{a_2 f_c} \right)^{n_2} \right]^{-1/2} \quad (\text{Equation 2-1})$$

$$\gamma = |\gamma_{PW}| \left[ \cos(2\pi f \xi_R s) + i \sin(2\pi f \xi_R s) \right] = |\gamma_{PW}| e^{i 2\pi f \xi_R s} \quad (\text{Equation 2-2})$$

Where  $\gamma_{PW}$  is the plane wave coherency representing random horizontal spatial variation of ground motion and  $\gamma$  is coherency including both local wave scattering and wave passage effects. Equation 2-2 can be used with vertically inclined waves to capture the systematic phase shifts due to an inclined wave (wave passage effects). The parameter  $f$  is ground motion frequency,  $\xi$  is the separation distance between locations in meters, and  $s$  is the slowness in seconds/meter. The reciprocal of  $s$  is the apparent wave velocity accounting for wave passage effects. Note that  $\xi_R$  is the separation distance in the radial direction in meters for which the median value is estimated as:

$$\xi_R = \frac{\xi}{\sqrt{2}} \quad (\text{Equation 2-3})$$

Coefficients to be used in Equation 2-1 for horizontal and vertical ground motion are presented in Table 2-1.

Deleted: SSI and Structure Response

Deleted: SSI and Structure Response

Deleted: SSI and Structure Response

Table 2-1  
Coherency Function Coefficients

Coefficient	Horizontal Ground Motion	Vertical Ground Motion
$a_1$	1.647	3.15
$a_2$	1.01	1.0
$a_3$	0.4	0.4
$n_1$	7.02	4.95
$n_2$	$5.1-0.51\ln(\xi+10)$	1.68
$f_c$	$1.886+2.221\ln(4000/(\xi+1)+1.5)$	$\text{Exp}(2.43-0.025 \ln(\xi+1)-0.048 (\ln(\xi+1))^2)$

The coherency function is plotted as a function of frequency for a number of separation distances in Figures 2-1 and 2-2 for horizontal and vertical ground motion, respectively. These figures show plane wave coherency (random spatial variation of ground motion) per Equation 2-1.

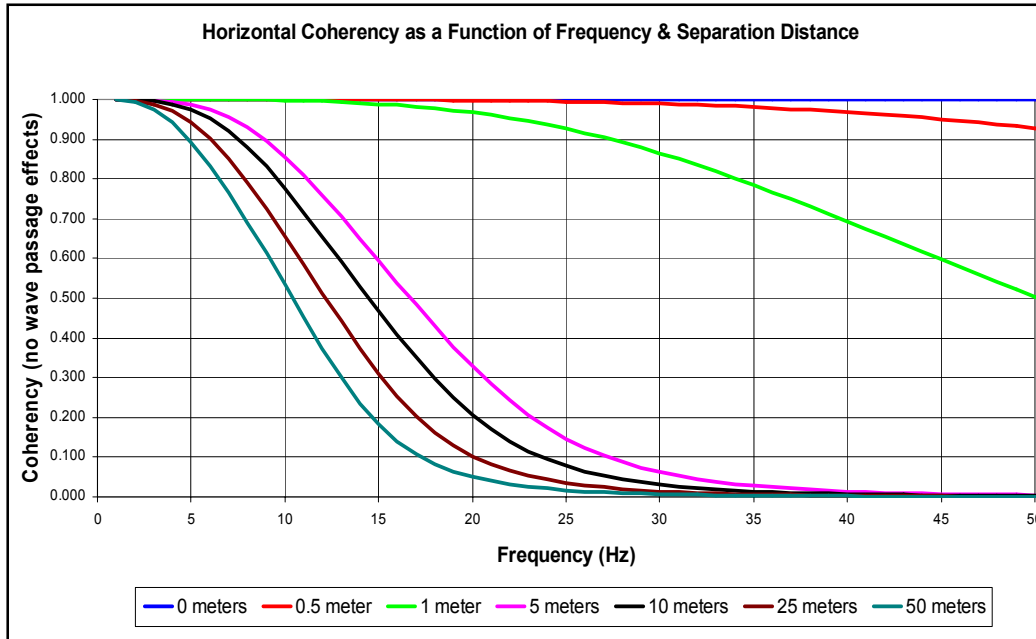


Figure 2-1  
Coherency Function for Horizontal Ground Motion

Deleted: SSI and Structure Response

Deleted: SSI and Structure Response

Deleted: SSI and Structure Response

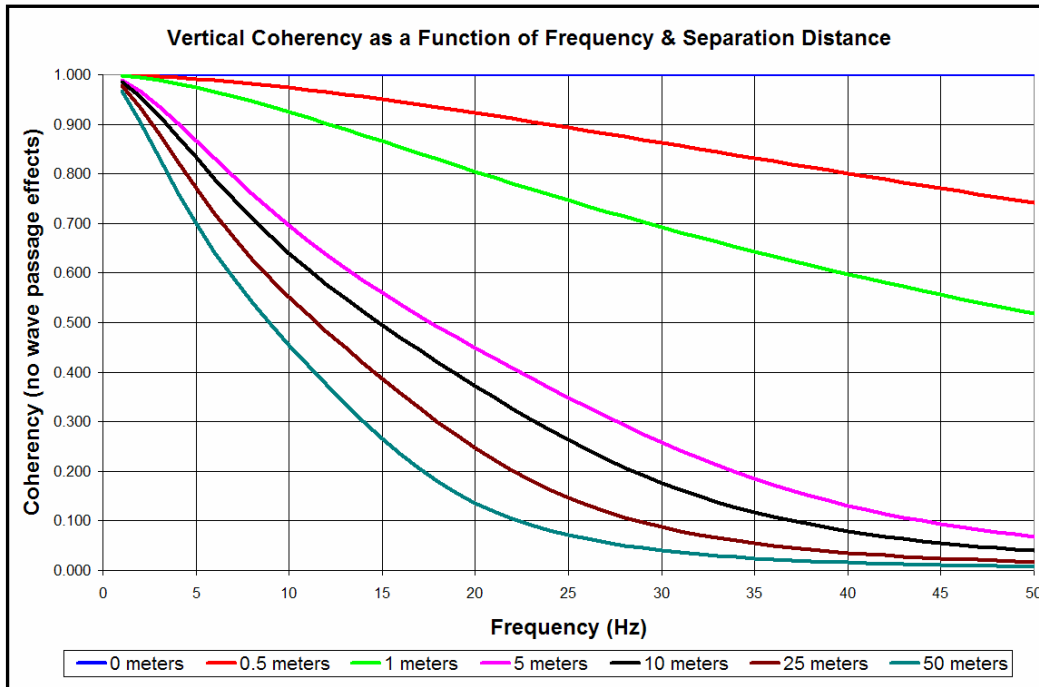


Figure 2-2  
Coherency Function for Vertical Ground Motion

The coherency functions presented above have been developed from all available and applicable recorded ground motion from dense instrument arrays. Data is from a variety of site conditions and earthquake magnitudes. In the development of these functions, Dr. Abrahamson has reached the following conclusions (Abrahamson, 2005, 2006):

- Coherency functions are appropriate for all frequencies (including those above 20 Hz). Ground motion data analyzed to develop the coherency functions have frequency content of 20 Hz and less. It is logical that the trends observed should extrapolate to higher frequencies.
- Coherency does not vary as a function of site shear wave velocity, but is strongly affected by topography. Data with strong topographic effects were not included for development of the coherency function.
- Coherency does not vary as a function of earthquake magnitude. This is true for magnitudes of interest that are greater than magnitude 4.5 to 5.0.
- Each component of earthquake input can be treated as uncorrelated. The coherency of cross-components is near zero.

For the design of NPP structures, mean input ground motion is the goal. As a result, the goal is to use mean coherency. The functions of equations 2-1 and 2-2, and Table 2-1 model median

coherency. Median coherency is slightly larger (only a few percent difference) than mean coherency.

**Deleted:**  
*SSI and Structure Response*

**Deleted:**  
*SSI and Structure Response*

**Deleted:**  
*SSI and Structure Response*  
*SSI and Structure Response*

## Site Parameters and Input Ground Motion

Site soil profiles have been selected that are representative of sites in the Central and Eastern United States. Site-specific response spectra compatible with each of the sites have been developed and used in this study. Shear wave velocities as a function of depth beneath the free-field ground surface are shown in Figure 2-3. The site profiles shown in the figure extend down to the Central and Eastern United States (CEUS) generic rock that has shear wave velocity of about 9200 fps (McCann, 2004).

For the foundation areas considered for this incoherence study, it is sufficient to define the site profile to a depth of about 300 feet beneath the foundation. The soil and rock shear wave velocities to a depth of 500 feet are illustrated in Figure 2-4.

The soil layers and properties shown in Tables 2-2 and 2-3 have been used for the evaluation of coherency effects in this study. These properties were taken from information provided within the advanced reactor submittals (North Anna and Clinton ESP submittals contained on NRC web site). For the soil case, high strain properties were calculated as noted below, consistent with the approach outlined within the soil site submittals for advanced reactors.

For CLASSI modeling purposes, the rock site is represented by nine layers extending down to 130-ft below the surface, and then a half-space of bedrock at a shear wave velocity of 9200 fps. Rock is assumed to have the low strain shear modulus (shear wave velocity) and no variation of damping at earthquake strain levels (i.e., linear elastic behavior). A damping ratio of 0.02 is assumed, which corresponds to about 0.001% shear strain.

**Deleted:**  
SSI and Structure Response

**Deleted:**  
SSI and Structure Response

**Deleted:**  
SSI and Structure Response  
SSI and Structure Response

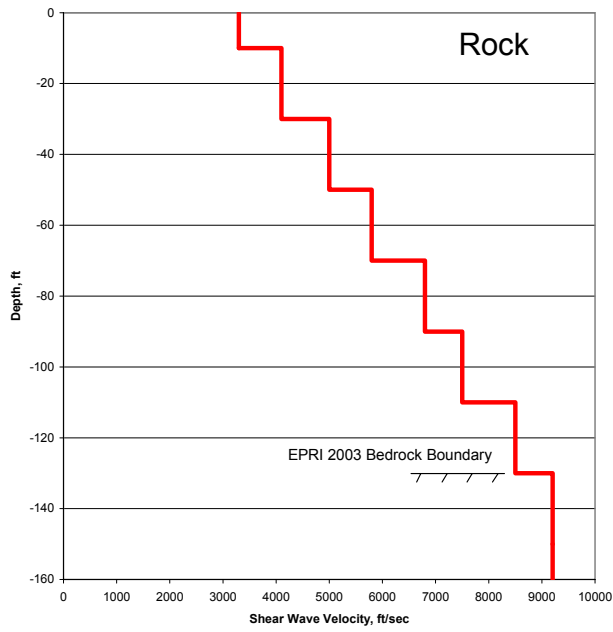
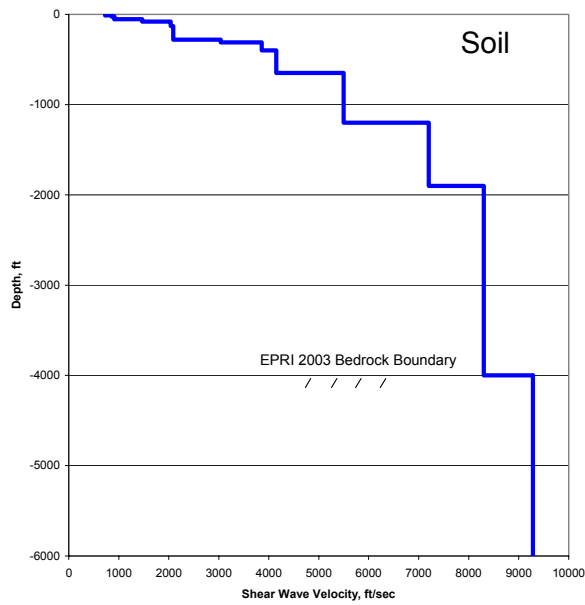
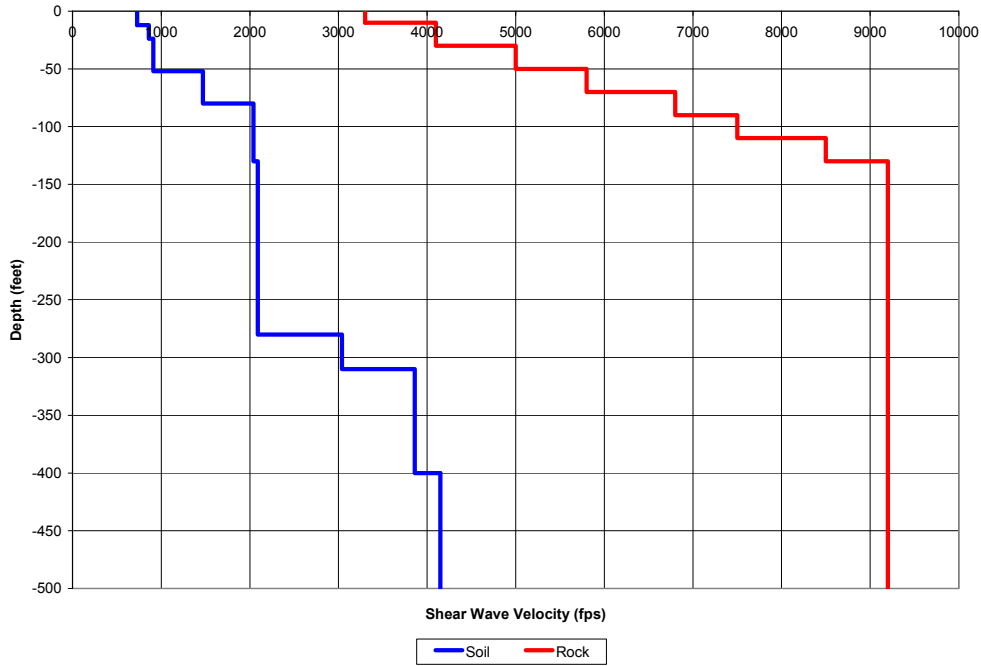


**Figure 2-3**  
**Rock and Soil Site Profile Shear Wave Velocities vs. Depth**



Deleted: SSI and Structure Response

Deleted: SSI and Structure Response

Deleted: SSI and Structure Response

**Figure 2-4**  
**Rock and Soil Site Profiles Within 500 Feet of the Ground Surface**

**Table 2-2**  
**Layers and Properties for the Rock Site (EQ Strain)**

Layer	Shear Wave Velocity (fps)	Weight Density (pcf)	Poisson's Ratio	Damping (fraction)	Thickness (ft)	Layer Top Depth (ft)
1	3300	160	0.33	0.02	5	0
2	3300	160	0.33	0.02	5	5
3	4100	160	0.33	0.02	10	10
4	4100	160	0.33	0.02	10	20
5	5000	160	0.33	0.02	20	30
6	5800	160	0.33	0.02	20	50
7	6800	160	0.33	0.02	20	70
8	7500	160	0.33	0.02	20	90
9	8500	160	0.33	0.02	20	110
10	9200	160	0.33	0.02	Half-space	130

**Deleted:**  
*SSI and Structure Response*

**Deleted:**  
*SSI and Structure Response*

**Deleted:**  
*SSI and Structure Response*  
*SSI and Structure Response*

The soil site is represented by 11 layers extending down to 400-ft below the surface, and then a half-space of bedrock at a shear wave velocity of 4150 fps. Soil shear modulus (shear wave velocity) and damping have been determined using EPRI degradation and damping curves (EPRI 1993 Guidelines for Determining Design Basis Ground Motion) as a function of earthquake strain level and depth. An earthquake strain level of  $10^{-2}\%$  has been assumed for this example study. It should be noted that for a design type application, the properties should be correlated with the site strain levels generated from a SHAKE analysis or another similar analytical technique.

**Table 2-3**  
**Layers and Properties for the Soil Site (EQ Strain)**

Layer	Shear Wave Velocity (fps)	Weight Density (pcf)	Poisson's Ratio	Damping (fraction)	Thickness (ft)	Layer Top Depth (ft)
1	730	131	0.46	0.05	6	0
2	730	131	0.46	0.05	6	6
3	860	131	0.46	0.05	12	12
4	910	131	0.46	0.034	12	24
5	910	131	0.46	0.034	16	36
6	1470	116	0.46	0.028	28	52
7	2040	148	0.46	0.028	50	80
8	2090	148	0.46	0.022	50	130
9	2090	138	0.46	0.022	100	180
10	3040	150	0.38	0.02	30	280
11	3860	160	0.33	0.02	90	310
12	4150	160	0.33	0.02	Half-space	400

Site-specific ground response spectra appropriate at the free ground surface at Elevation 0 for each site profile, as shown in Figure 2-4, were used for this coherency study. Five percent damped site-specific response spectra are illustrated in Figures 2-5 and 2-6 for rock and soil sites, respectively. Also, plotted on the figures are the US NRC Regulatory Guide 1.60 design ground response spectra anchored to 0.3 g peak ground acceleration (PGA) for comparison purposes.

Deleted: SSI and Structure Response  
Deleted: SSI and Structure Response  
Deleted: SSI and Structure Response

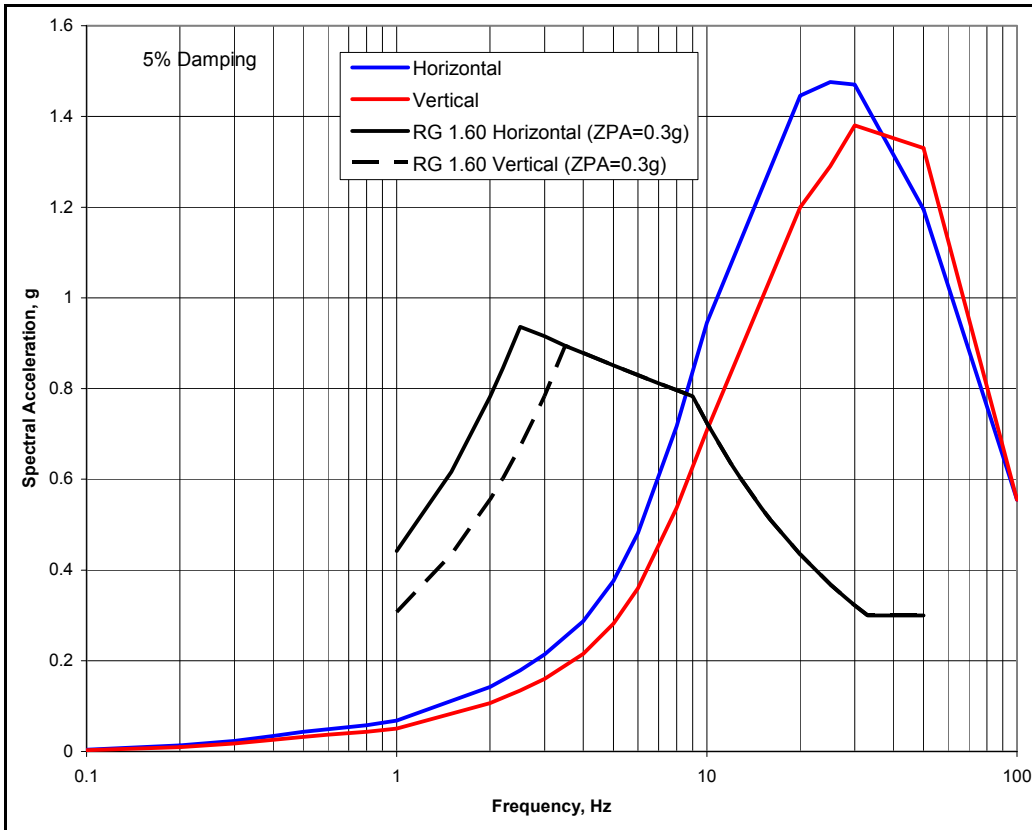
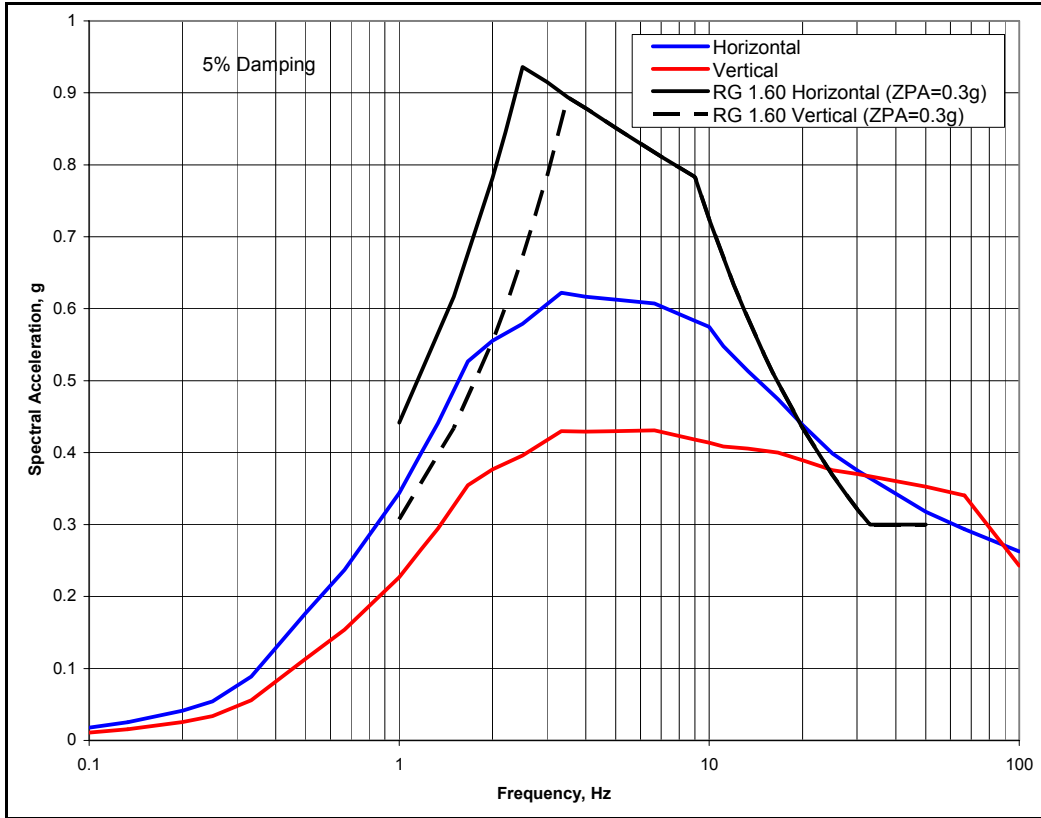


Figure 2-5 Site-Specific Response Spectra for Rock Site at Ground Surface (Depth 0-ft)

Deleted:  
SSI and Structure Response

Deleted:  
SSI and Structure Response

Deleted:  
SSI and Structure Response



**Figure 2-6**  
**Site-Specific Response Spectra for Soil Site at Ground Surface (Depth 0-ft)**

The rock site-specific ground response spectra have peak amplification in the 20 to 30 Hz range. The soil site-specific ground response spectra have peak amplification in the 3 to 8 Hz range.

For soil-structure interaction analyses and the evaluation of structure response including the effects of seismic wave incoherence, spectrum compatible time histories for the rock site were required. These were developed by Dr. Abrahamson. The computed spectra and the target spectra (Figure 2-5) are shown in Figure 2-7. Three uncorrelated components were generated for two horizontal directions and the vertical direction.

Deleted: SSI and Structure Response

Deleted: SSI and Structure Response

Deleted: SSI and Structure Response

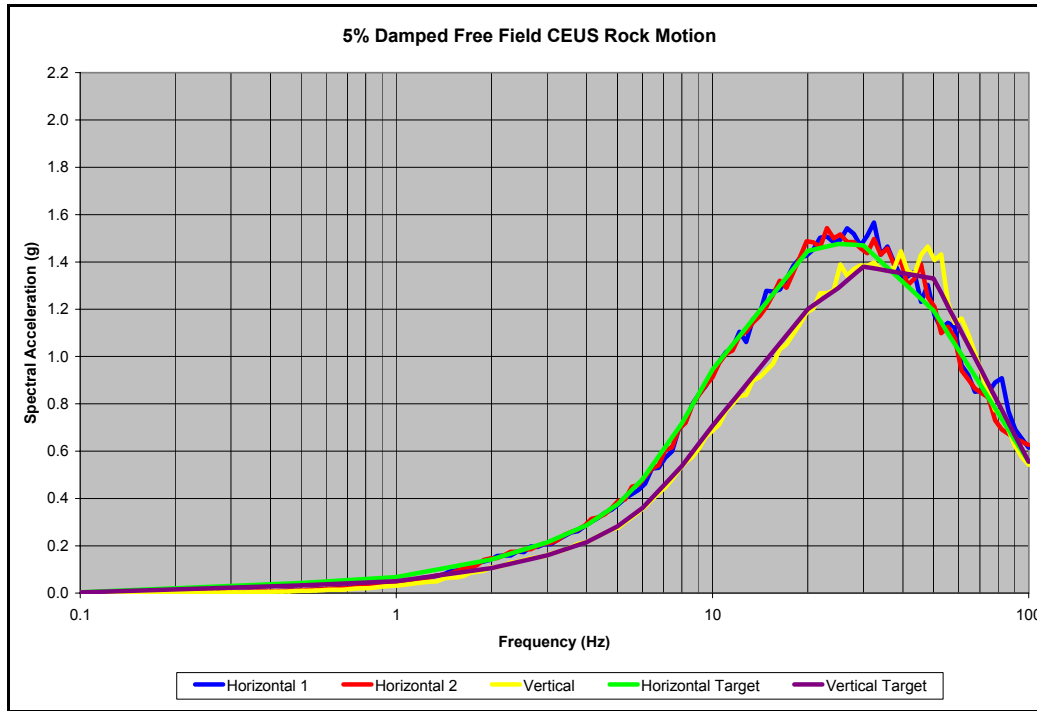


Figure 2-7  
Computed and Target Response Spectra for Rock Site

### Foundation Parameters

Descriptions of two advanced reactor designs (AP1000 and ESBWR) were reviewed in order to understand the foundation and building configurations. Based on the foundation configurations presented for these two new plant designs, a rectangular foundation that is 225 x 100-ft in plan, and a square foundation that is 150 x 150-ft in plan were selected for this study. These foundations have the same plan area such that analyses will be able to demonstrate the effect of foundation shape on seismic wave incoherence effects. In addition, a circular foundation footprint of the same area was also considered. The foundation circle had a radius of 84.63 feet. The benchmark comparison case between CLASSI and SASSI analyses utilized the 150-ft square foundation plan. To address the effect of foundation area, two additional square foundation footprints were considered, a 75-ft square foundation footprint, and a 300-ft square foundation footprint. The basic foundation area is 22,500-sq ft. The small foundation has one-fourth of this area and the large foundation has four times this area.

The SSI seismic analyses, by CLASSI and SASSI, were performed for the 150-ft square foundation footprint. For these analyses the foundation was assumed to be 15-ft thick. The resulting diagonal mass matrix terms are 1572 kip-sec<sup>2</sup>/ft in the horizontal and vertical

directions,  $2.98 \times 10^6$  kip-ft-sec<sup>2</sup> about the horizontal axes, and  $5.90 \times 10^6$  kip-ft-sec<sup>2</sup> about the vertical axes.

**Deleted:**  
*SSI and Structure Response*

**Deleted:**  
*SSI and Structure Response*

**Deleted:**  
*SSI and Structure Response*  
*SSI and Structure Response*

## Structure Properties

Soil-structure interaction seismic analyses for the purpose of evaluating structure and foundation response including the effects of seismic wave incoherence has been performed using a simple stick model of the main containment/auxiliary building based on the AP1000 advanced reactor design (Orr, 2003). This model is illustrated in Figure 2-8 with model properties presented in Tables 2-4 and 2-5. The model consists of three concentric sticks representing the Coupled Auxiliary and Shield Building (ASB), the Steel Containment Vessel (SCV), and the Containment Internal Structure (CIS). In order to incorporate the appropriate effects of incoherence induced rotations, modifications to this original stick model have been implemented as shown in Figure 2-9. At the top of the shield building, auxiliary building, steel containment vessel, and containment internal structure massless outrigger nodes have been added connected to the centerline by rigid links. The ASB and CIS outriggers extend 75 feet from the centerline in the X-direction. The SCV outrigger extends 65 feet from the centerline in the X-direction. These outriggers are intended to capture torsion at extreme locations of the structure. In order to make the model more realistic and to roughly correspond to AP1000 characteristics (Orr, 2006), the mass centers have been offset from the shear center at locations in the auxiliary building and the CIS as shown in Figure 2-9. The ASB and CIS structures were modeled including nominal torsion which was included by assuming approximate offsets between the centers of mass and the centers of rigidity. These offsets were intended to approximate the torsional behavior included in the more detailed stick models. Offsets were introduced at and below the roof level of the Auxiliary Building, and throughout the CIS structure model. These representations introduced natural torsion into the models. The shear centers of the three sticks are coincident along the Z-axis. The properties of the added outrigger and mass center nodes have been added to Tables 2-4 and 2-5. This model is utilized extensively in Chapter 5 for the evaluation of SSI and structure response. The model does not exactly match the AP1000 fundamental frequencies and mode shapes due to the simplifications and generalizations made in creating this example structure. However, the goal of this project was to utilize a representative nuclear structure and not to model any particular new plant design, thus, the model is considered to be adequate for the purposes of this study.

For CLASSI SSI seismic analyses, the structure properties input are described by the fixed-base dynamic modal properties including frequencies, mode shapes and participation factors. These dynamic properties were developed using the finite element program, SAP2000 (CSI, 2004). One hundred and sixty (160) modes were included with total mass participation in each direction of about 95 percent. The relative mass of the structures is approximately ASB – 86%, CIS – 11%, and SCV – less than 5%.

The fixed-base modes of the three structure sticks provide some insight into their dynamic behavior. Fundamental fixed-base frequencies for each of the Figure 2-8 three structure concentric sticks (similar frequencies resulted from the subsequent more detailed model shown in Figure 2-9) are:

- Coupled Auxiliary and Shield Building (ASB)
  - X-Horizontal – 3.2 Hz
  - Y-Horizontal – 3.0 Hz
  - Z-Vertical – 9.9 Hz
- Steel Containment Vessel (SCV)
  - X-Horizontal – 5.5 Hz, 9.5 Hz, 9.9 Hz
  - Y-Horizontal – 6.10 Hz
  - Z-Vertical – 16.0 Hz
- Containment Internal Structure (CIS)
  - X-Horizontal – 13.3 Hz, 20.1 Hz, 28.9 Hz
  - Y-Horizontal – 12.0 Hz, 14.9 Hz, 17.5 Hz
  - Z-Vertical – 41.4 Hz

The mode shapes for the fundamental modes of the Coupled Auxiliary and Shield Building (ASB), the Steel Containment Vessel (SCV), and the Containment Internal Structure (CIS) in the Y-horizontal direction are shown in Figures 2-9, 2-10, and 2-11, respectively.

**Deleted:**  
*SSI and Structure Response*

**Deleted:**  
*SSI and Structure Response*

**Deleted:**  
*SSI and Structure Response*  
*SSI and Structure Response*

**Deleted:**  
SSI and Structure Response

**Deleted:**  
SSI and Structure Response

**Deleted:**  
SSI and Structure Response

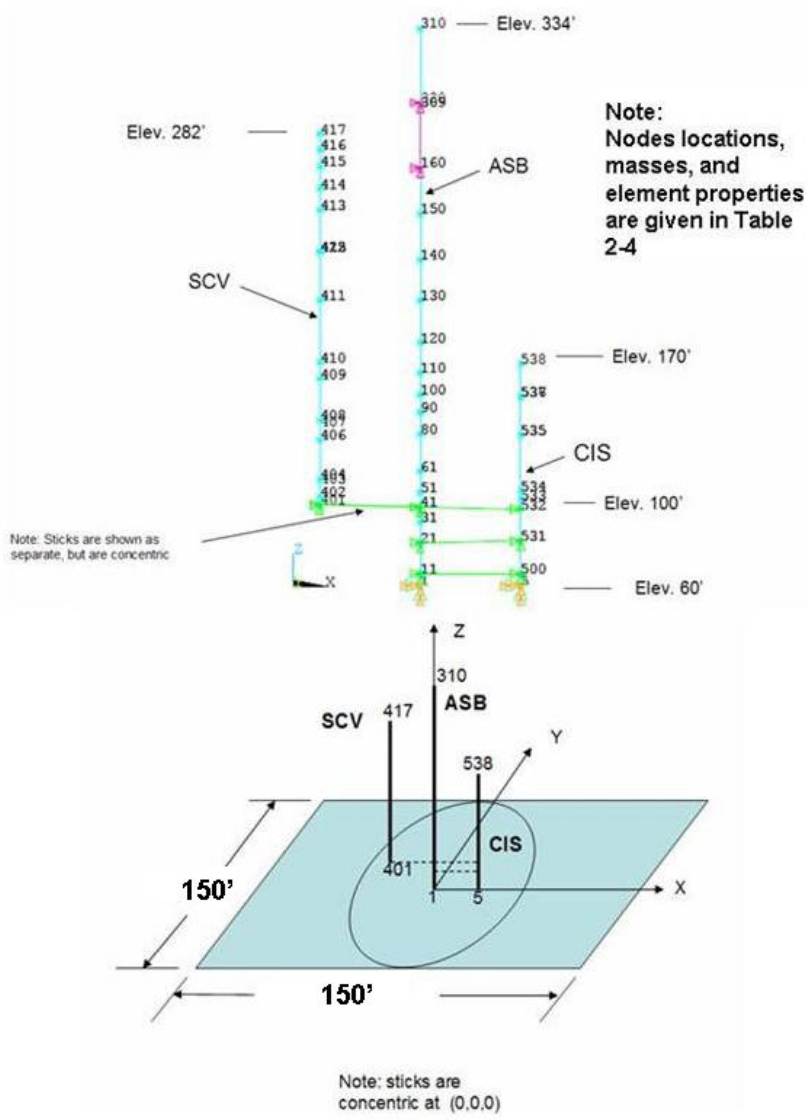


**Figure 2-8**  
**Advanced Reactor Structure Stick Model**

Deleted: .  
SSI and Structure Response

Deleted: .  
SSI and Structure Response

Deleted: .  
SSI and Structure Response .  
SSI and Structure Response

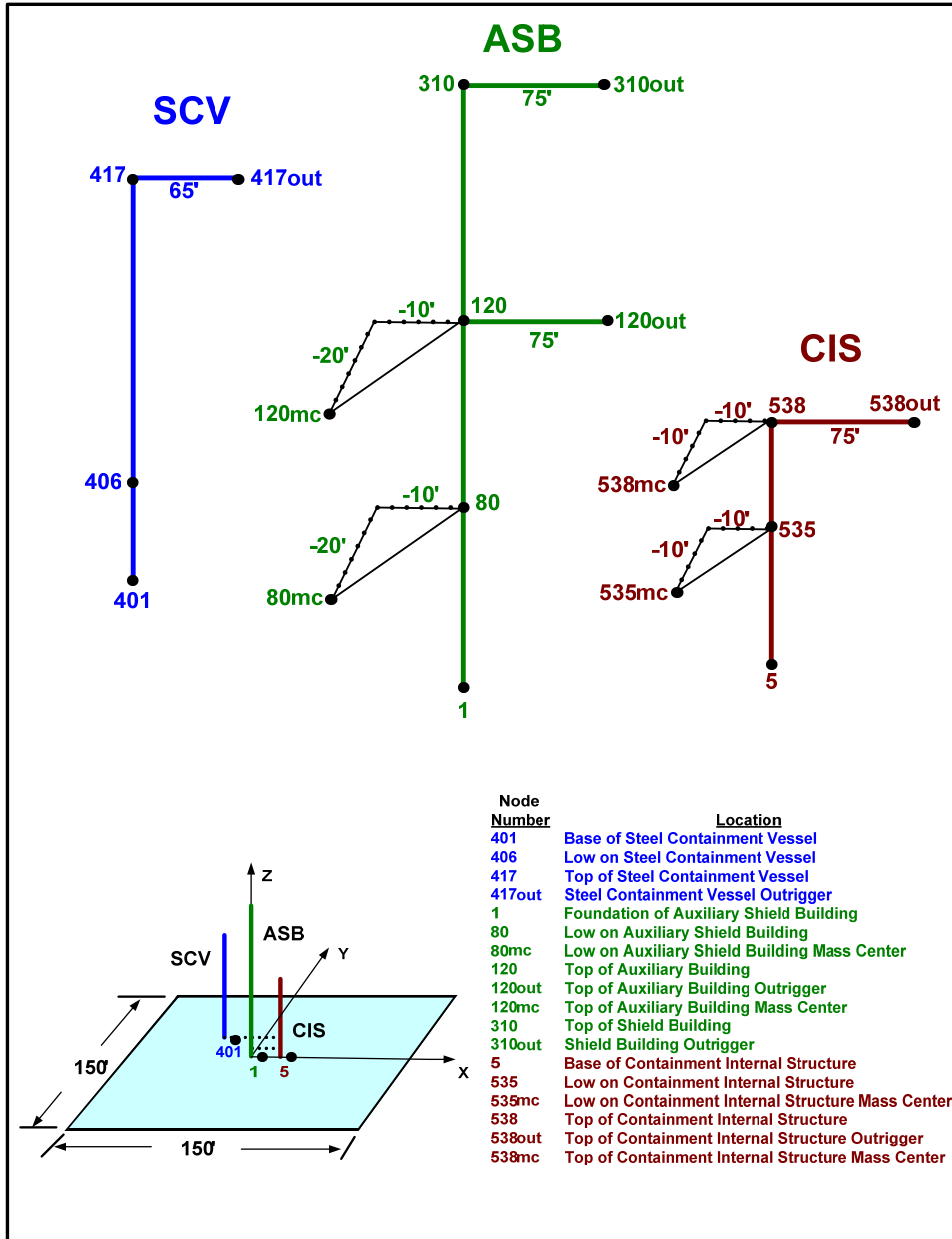


Figure 2-9  
Advanced Reactor Structure Stick Model with Outriggers and Offset Mass Centers

**Deleted:**  
SSI and Structure Response

**Deleted:**  
SSI and Structure Response

**Deleted:**  
SSI and Structure Response  
SSI and Structure Response

**Table 2-4  
Nodes and Mass Properties for Structural Model**

NODE	X	Y	Z	North-South Model			East-West Model		
				MX	MZ	Iy	MY	MZ	Ix
<b>ASB</b>									
1	0	0	60.50						
11	0	0	66.50	236.400	236.400	1641500	236.400	236.400	466740
21	0	0	81.50	494.260	494.260	3612000	494.260	494.260	847820
31	0	0	91.50	307.080	439.280	1938300	307.080	439.280	456250
41	0	0	99.00	330.460	330.460	2619900	330.460	330.460	484190
51	0	0	106.17	210.100	210.100	1287500	210.100	210.100	390700
61	0	0	116.50	597.740	465.540	2526200	597.740	465.540	764330
80	0	0	134.87	0	441.849	3448492	0	441.849	710952
80mc	-10	-20	134.87	441.849	0	0	441.849	0	0
90	0	0	145.37	165.406	165.406	933560	165.406	165.406	293100
100	0	0	153.98	190.099	190.099	1022510	190.099	190.099	316650
110	0	0	164.51	164.371	164.371	422680	164.371	164.371	271344
120	0	0	179.56	0	200.431	323582	0	200.431	349825
120out	75	0	179.56	0	0	0	0	0	0
120mc	-10	-20	179.56	200.431	0.00	0.00	200.431	0.00	0.00
130	0	0	200.00	126.050	126.050	317710	126.050	126.050	317710
140	0	0	220.00	132.470	132.470	333900	132.470	132.470	333900
150	0	0	242.50	140.260	140.260	353540	140.260	140.260	353540
160	0	0	265.00	231.223	231.223	529020	231.223	231.223	529020
309	0	0	295.23	263.980	433.530	276470	263.980	433.530	276470
310	0	0	333.13	135.590	91.320	63050	135.590	91.320	63050
310out	75	0	333.13	0	0	0	0	0	0
320	0	0	296.77	0.000	0.000	0	0.000	0.000	0

NODE	X	Y	Z	North-South Model			East-West Model		
				MX	MZ	Iy	MY	MZ	Ix
<b>CIS</b>									
5	0	0	60.5						
500	0	0	66.5	595.3	593.4	568000	595.3	595.3	568000
531	0	0	82.5	927.6	927.6	1422000	927.6	927.6	137100
532	0	0	98	468.7	468.7	70800	468.7	468.7	680000
533	0	0	103	146.3	286.2	185000	146.3	286.2	177000
534	0	0	107.17	319.1	238.7	358900	319.1	238.7	319130
535	0	0	134.25	0	238.6	282150	0	238.6	255550
535mc	-10	-10	134.25	298.2	0	0	298.2	0	0

**DRAFT**

*Study Input Parameters*

**Deleted:**  
SSI and Structure Response

**Deleted:**  
SSI and Structure Response

**Deleted:**  
SSI and Structure Response  
SSI and Structure Response

NODE	X	Y	Z	North-South Model			East-West Model		
				MX	MZ	Iy	MY	MZ	Ix
CIS									
536	0	0	153	14.6	14.6	2019	14.6	14.6	2504
537	0	0	153	30.8	30.8	6065	30.8	30.8	4321
538	0	0	169	0	9.4	748	0	9.4	696
538out	75	0	169	0	0	0	0	0	0
538mc	-10	-10	169	9.4	0	0	9.4	0	0

NODE	X	Y	Z	North-South Model			East-West Model		
				MX	MZ	Iy	MY	MZ	Ix
SCV									
401	0	0	100.000	1.739	1.739	3636	1.739	1.739	3636
402	0	0	104.125	5.541	5.541	11732	5.541	5.541	11732
403	0	0	110.500						
404	0	0	112.500	15.388	15.388	33362	15.388	15.388	33362
406	0	0	131.677	17.907	17.907	37914	17.907	17.907	37914
407	0	0	138.583						
408	0	0	141.500	17.904	17.904	38689	17.904	17.904	38689
409	0	0	162.000	18.349	18.349	38850	18.349	18.349	38850
410	0	0	169.927	28.994	28.994	61388	28.994	28.994	61388
411	0	0	200.000	28.340	28.340	60003	28.340	28.340	60003
412	0	0	224.000	40.251	51.739	81602	51.522	51.739	81602
413	0	0	224.208	15.746	15.746	33338	15.746	15.746	33338
414	0	0	255.021	11.271	11.271	21897	11.271	11.271	21897
415	0	0	265.833	10.288	10.288	14610	10.288	10.288	14610
416	0	0	273.833	10.070	10.070	8149	10.070	10.070	8149
417	0	0	281.901	5.618	5.618	0	5.618	5.618	0
417out	65	0	281.901	0	0	0	0	0	0
425	0	0	224.000	28.439	16.951		17.168	16.951	

Note: All values are in kip, seconds, feet units

Assume:  $I_z = I_x + I_y$

**Deleted:**  
SSI and Structure Response

**Deleted:**  
SSI and Structure Response

**Deleted:**  
SSI and Structure Response  
SSI and Structure Response

**Table 2-5  
Element Properties for Structural Model**

ELEM	North-South Model					East-West Model				Material	Modal damping
	NODES		A	IYY	AshearY	A	IZZ	AshearZ			
<b>ASB</b>											
1	1	11	15484.00	97176000	10322.67	15484.00	11236800	10322.67	Concrete	4 %	
2	11	21	3462.50	6266240	1366.35	3462.50	4061440	1011.30	Concrete	4 %	
3	21	31	3462.50	6266240	1366.35	3462.50	4061440	1011.30	Concrete	4 %	
4	31	41	3462.50	6266240	1366.35	3462.50	4061440	1011.30	Concrete	4 %	
5	41	51	3293.30	5744880	1214.35	3293.30	3562800	1008.14	Concrete	4 %	
6	51	61	3293.30	5744880	1214.35	3293.30	3562800	1008.14	Concrete	4 %	
7	61	80	3293.30	5744880	1214.35	3293.30	3562800	1008.14	Concrete	4 %	
	80	80mc	Rigid Link								
31	80	90	3197.52	4196560	1185.61	3197.52	4412370	1360.04	Concrete	4 %	
32	90	100	3197.52	4196560	1185.61	3197.52	4412370	1360.04	Concrete	4 %	
33	100	110	2501.52	3676560	874.54	2501.52	3311570	1121.07	Concrete	4 %	
34	110	120	1954.00	3083632	810.51	1954.00	3290960	746.70	Concrete	4 %	
	120	120out	Rigid Link								
	120	120mc	Rigid Link								
35	120	130	1338.00	2700000	535.20	1338.00	2700000	535.20	Concrete	4 %	
36	130	140	1338.00	2700000	535.20	1338.00	2700000	535.20	Concrete	4 %	
37	140	150	1338.00	2700000	535.20	1338.00	2700000	535.20	Concrete	4 %	
38	150	160	1338.00	2700000	535.20	1338.00	2700000	535.20	Concrete	4 %	
301	160	309	50.45	1	0.000	50.45	1	0.000	Concrete	4 %	
302	320	309	13.59	2680	10.872	13.59	2681.6	10.872	Concrete	4 %	
303	309	310	704.50	431720	281.800	704.50	431720	281.800	Concrete	4 %	
	310	310out	Rigid Link								
	160	320	Rigid	Rigid	Rigid	Rigid	Rigid	Rigid			

CIS										
500	5	500	15175	1.24E+07	9228.29	15175	1.11E+07	8311.88	Concrete	4 %
501	500	531	15175	1.24E+07	9228.29	15175	1.11E+07	8311.88	Concrete	4 %
502	531	532	6732	4.50E+06	2976.99	6732	3.33E+-6	2965.86	Concrete	4 %
503	532	533	7944	6.74E+06	4411.70	7944	5.95E+06	3948.04	Concrete	4 %
504	533	534	5160	4.60E+06	3026.91	5160	2.93E+06	2702.19	Concrete	4 %
505	534	535	1705	7.83E+05	613.65	1705	5.75E+05	405.33	Concrete	4 %
	535	535mc	Rigid Link							
506	535	536	326	3.15E+03	13.10	326	1.77E+04	67.36	Concrete	4 %
507	535	537	484	3.89E+04	93.98	484	1.58E+04	64.30	Concrete	4 %
508	537	538	164	2.11E+03	29.24	164	2.47E+03	17.16	Concrete	4 %
	538	538out	Rigid Link							

**DRAFT**

*Study Input Parameters*

**Deleted:**  
SSI and Structure Response

**Deleted:**  
SSI and Structure Response

**Deleted:**  
SSI and Structure Response  
SSI and Structure Response

<b>CIS</b>										
	538	538mc	Rigid Link							
506	535	536	326	3.15E+03	13.10	326	1.77E+04	67.36	Concrete	4 %
507	535	537	484	3.89E+04	93.98	484	1.58E+04	64.30	Concrete	4 %
508	537	538	164	2.11E+03	29.24	164	2.47E+03	17.16	Concrete	4 %

ELEM	NODES		North-South Model			East-West Model			Material	Modal damping
			A	IYY	AshearY	A	IZZ	AshearZ		
<b>SCV</b>										
401	401	402	14.49	29,107	27.6	14.49	29,107	27.6	Steel	4 %
402	402	403	59.63	126,243	29.81	59.63	126,243	29.81	Steel	4 %
403	403	404	59.63	126,243	29.81	59.63	126,243	29.81	Steel	4 %
405	404	406	59.63	126,243	29.81	59.63	126,243	29.81	Steel	4 %
406	406	407	59.63	126,243	29.81	59.63	126,243	29.81	Steel	4 %
407	407	408	59.63	126,243	29.81	59.63	126,243	29.81	Steel	4 %
408	408	409	59.63	126,243	29.81	59.63	126,243	29.81	Steel	4 %
409	409	410	59.63	126,243	29.81	59.63	126,243	29.81	Steel	4 %
410	410	411	59.63	126,243	29.81	59.63	126,243	29.81	Steel	4 %
411	411	412	59.63	126,243	29.81	59.63	126,243	29.81	Steel	4 %
412	412	413	59.63	126,243	29.81	59.63	126,243	29.81	Steel	4 %
413	413	414	13.15	110,115	27.1	13.15	110,115	27.1	Steel	4 %
414	414	415	4.58	83,714	24.6	4.58	83,714	24.6	Steel	4 %
415	415	416	1.74	46,047	19.89	1.74	46,047	19.89	Steel	4 %
416	416	417	0.55	13,850	8.56	0.55	13,850	8.56	Steel	4 %
	417	417out	Rigid Link							
	Spring		Kz	Kx		Kz	Ky			
	412	425	27630	80439		27630	9467			4 %

Notes:

All values are in kip, seconds, feet units

Material properties:

Concrete:

Elastic modulus = 519120 ksf

Poisson's ratio = 0.17

Steel:

Elastic modulus = 4248000 ksf

Poisson's ratio = 0.30

**DRAFT**  
*Study Input Parameters*

**Deleted:**  
SSI and Structure Response

**Deleted:**  
SSI and Structure Response

**Deleted:**  
SSI and Structure Response  
SSI and Structure Response

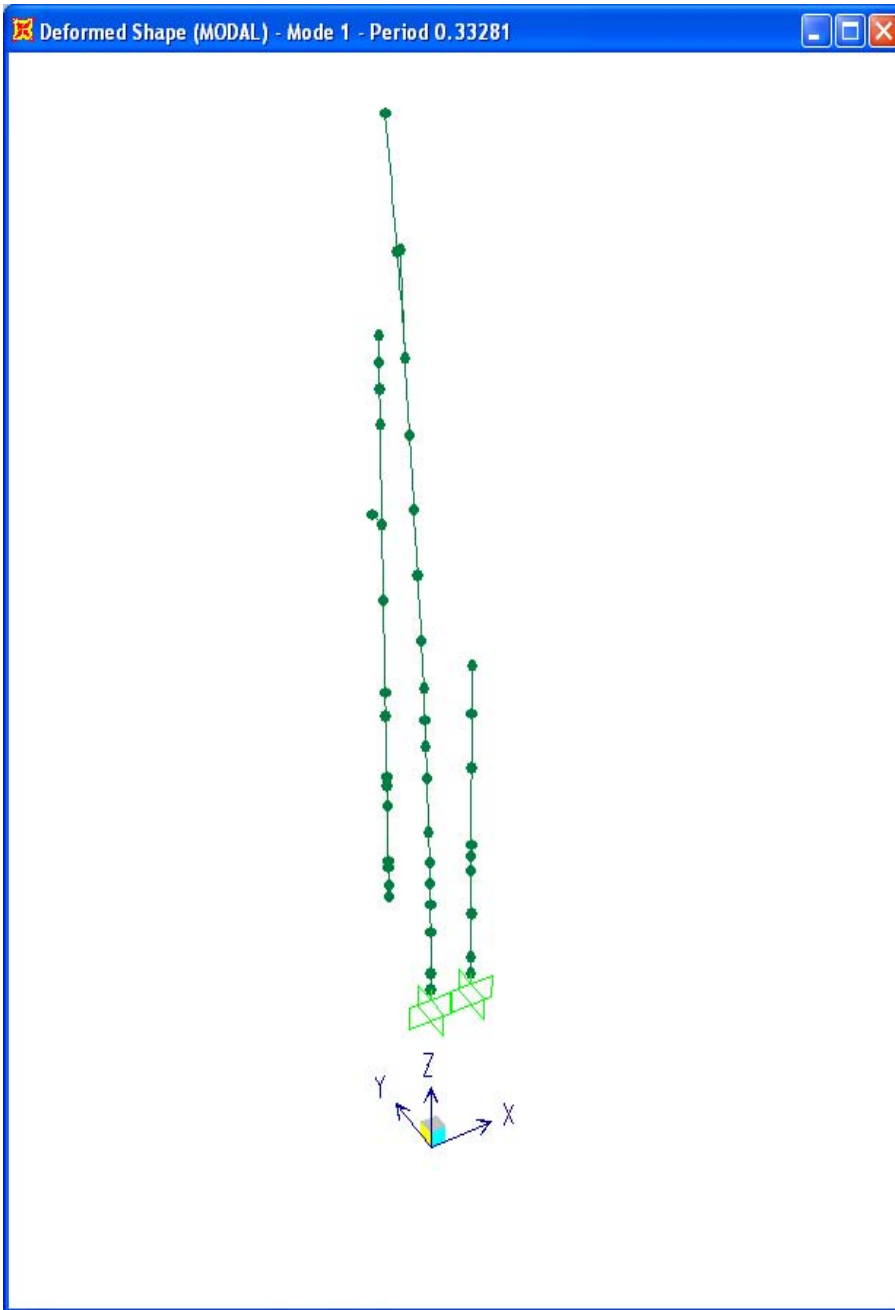
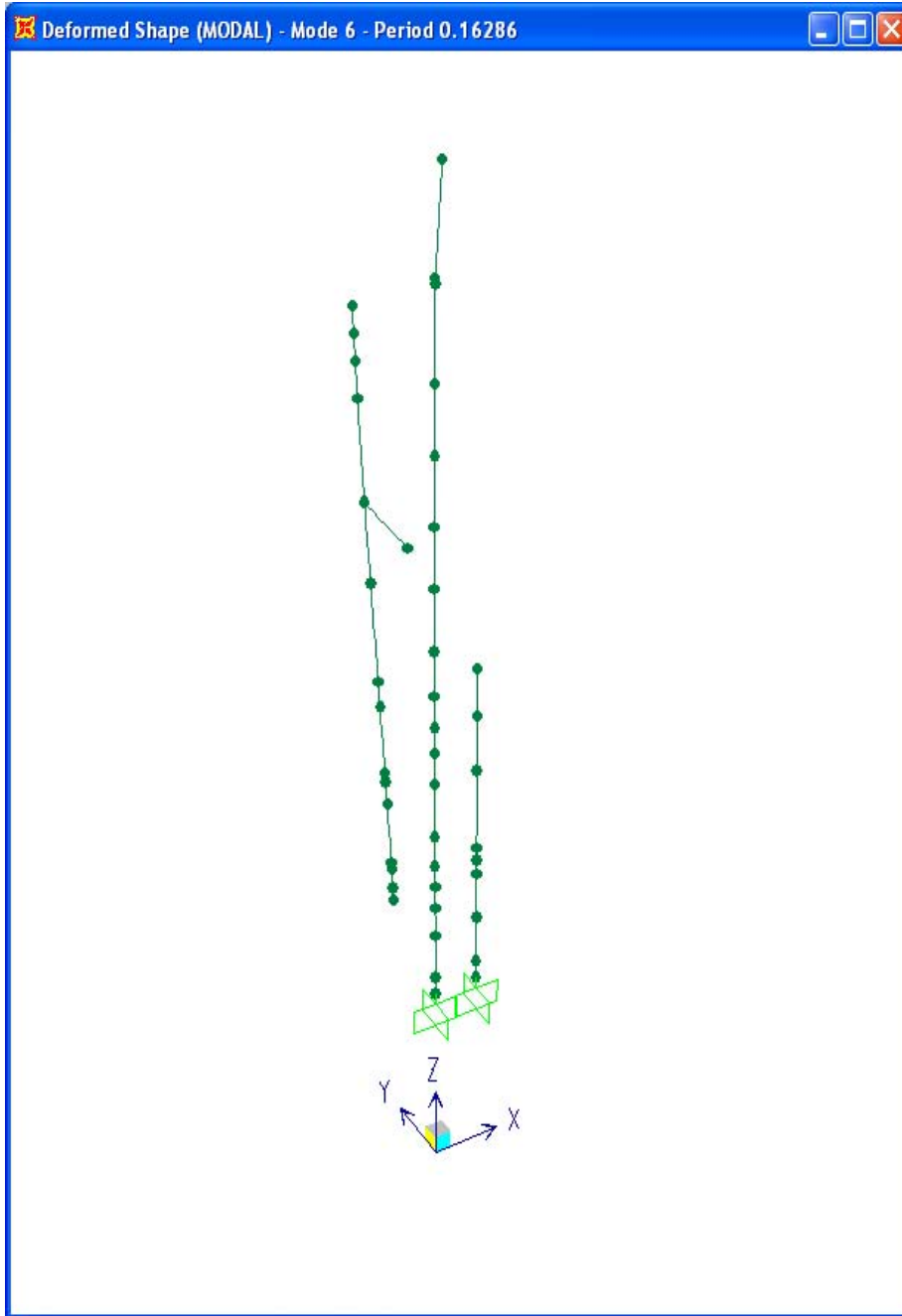


**Figure 2-10**  
Mode 1-ASB Fundamental Mode, Y-Direction,  $f = 3.0$  Hz



**Deleted:** .  
*SSI and Structure Response*

**Deleted:** .  
*SSI and Structure Response*

**Deleted:** .  
*SSI and Structure Response* .  
*SSI and Structure Response*

**Figure 2-11**  
**Mode 6–SCV Fundamental Mode, Y-Direction,  $f = 6.1$  Hz**

**DRAFT**  
*Study Input Parameters*

**Deleted:** .  
SSI and Structure Response

**Deleted:** .  
SSI and Structure Response

**Deleted:** .  
SSI and Structure Response .  
SSI and Structure Response

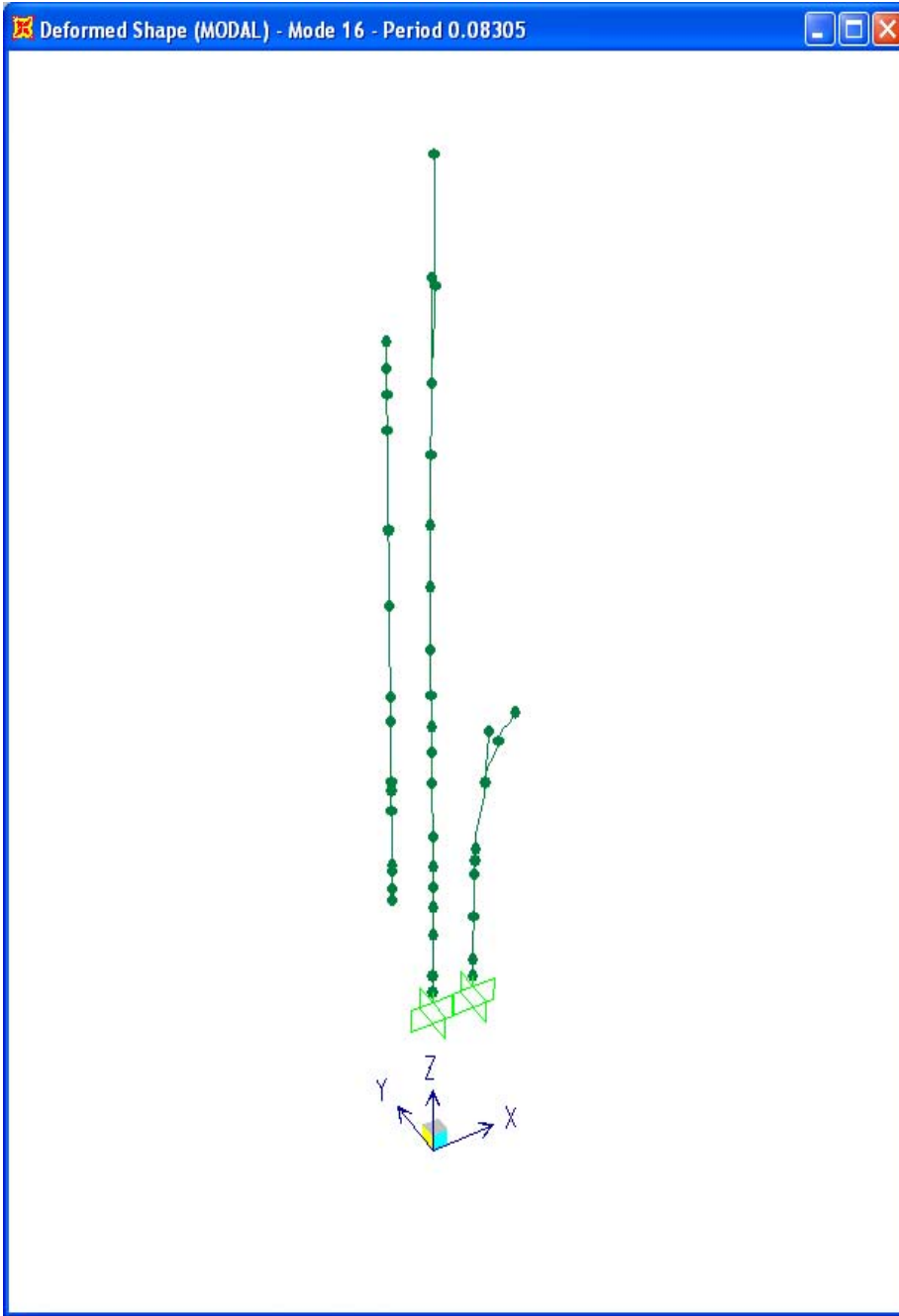


**Figure 2-12**  
**Mode 1–CIS Fundamental Mode, Y-Direction,  $f = 12.0$  Hz**



# 3

## TECHNICAL APPROACH

---

### General

In order to incorporate seismic wave incoherence into seismic analyses, a stochastic approach has been employed as described in this chapter. This approach is described in detail in EPRI Report TR-102631 2225 (EPRI, 1997) and briefly summarized in this chapter. By this approach, incoherency transfer functions have been developed for the rigid massless foundation and validated to be appropriate by evaluating structure response for a typical NPP structure. Random vibration theory (RVT) has been employed to convert response spectra to power spectral density (PSD) functions and PSD to response spectra in order to determine spectra incoherency corrections on the rigid, massless foundation. As described in Chapter 2, coherency functions as a function of separation distance, frequency, apparent wave velocity, and direction of motion from Abrahamson, 2005 are used as the basic input for all evaluations. The incoherency transfer functions and spectra corrections have been generated for the rigid, massless foundation using the computer program, CLASSI. In addition, CLASSI has been used to evaluate seismic structural response of example soil/structure systems. The procedures used to evaluate incoherency transfer functions, to evaluate foundation response of rigid, massless foundations, and to evaluate structure and foundation response of example structural models accounting for soil-structure interaction and seismic wave incoherence are described in this Chapter.

By these procedures, all elements of incoherence are appropriately treated. These elements include the reduction of the amplitude of translational motions and the effect of induced rotations. Chapters 4, 5, and 6 investigate the procedures. Chapter 4 deals with rigid, massless foundations of varying configurations, size, and site conditions. The rock site profile and the soil site profile of Chapter 2 and their companion free-field ground response spectra are considered in Chapter 4. Chapter 5 deals with a representative structure, i.e., a simplified model based on the AP1000, also described in Chapter 2. The rock site profile and associated ground response spectra of Chapter 2 are the examples considered. Chapter 6 summarizes the results and the conclusions.

### Procedure to Evaluate the Incoherency Transfer Function (ITF)

The incoherency transfer function is determined using the computer program, CLASSI following the procedure shown in Table 3-1. To run CLASSI (Wong and Luco, 1980), we must first define the foundation footprint plan dimensions, underlying soil layers with properties of density, shear wave velocity, Poisson's ratio, material damping, and layer thickness, and frequencies for analysis. The foundation footprint is divided into n sub-regions for input to CLASSI. The

**Deleted:**  
*SSI and Structure Response*

**Deleted:**  
*SSI and Structure Response*

**Deleted:**  
*SSI and Structure Response*  
*SSI and Structure Response*

coherency function is evaluated at the mid-point of each of these sub-regions with the separation distance being the distance between all of the combinations of sub-region mid-points.

Based on the assumption that ground motions can be represented by a stationary random process, the coherency function between ground motions  $x_i(t)$  and  $x_j(t)$ , denoted by  $\gamma(f)$ , is a complex function of frequency,  $f$ , defined by:

$$\gamma(f) = \frac{S_{ij}(f)}{\sqrt{S_{ii}(f)S_{jj}(f)}} \quad \text{(Equation 3-1)}$$

in which  $S_{ij}$  is the cross power spectral density function between motions  $x_i(t)$  and  $x_j(t)$  and  $S_{ii}$  and  $S_{jj}$  are the power spectral density functions for motions  $x_i(t)$  and  $x_j(t)$ , respectively.

$[\gamma]$  is evaluated as a  $3n$  by  $3n$  matrix of the Abrahamson coherency function based on the separation distances between sub-regions for each selected frequency and for input apparent wave velocity or slowness.

The incoherency transfer function, ITF( $f$ ) is equal to the amplitude of the square root of the diagonal terms of  $[S_{Uoi}]$  where  $[S_{Uoi}]$  is the 6 by 6 cross PSD matrix of rigid massless foundation motion subjected to unit PSD input.

$$[S_{Uoi}] = [F] [S_{UGi}] [FC]^T \quad \text{(Equation 3-2)}$$

where  $[F]$  is a 6 by  $3n$  scattering transfer function matrix relating sub-region displacements to rigid body displacements and  $[FC]$  is the complex conjugate of  $[F]$  and  $[S_{UGi}]$  is a  $3n$  by  $3n$  covariance matrix of incoherent ground motions for unit PSD input given by  $[I] [\gamma] [I]$  where  $[I]$  is an identity matrix.  $[F]$  is determined by:

$$[F] = [C] [T]^T \quad \text{(Equation 3-3)}$$

where  $[C]$  is the 6 by 6 compliance matrix (equal to the inverse of the impedance matrix  $[K]^{-1}$ ); and  $[T]$  is a  $3n$  by 6 traction matrix representing contact tractions on all  $n$  sub-regions subjected to unit rigid body motions.

$$[T] = [G]^{-1} [\alpha_b] \quad \text{(Equation 3-4)}$$

$[G]$  is the  $3n$  by  $3n$  Green's function matrix containing responses of the foundation to unit harmonic point loads and  $[\alpha_b]$  is a  $3n$  by 6 rigid foundation mode shape matrix. One of the program modules to CLASSI uses soil profile properties to determine the Green's function.

Even though the scattering transfer function matrix  $[F]$  is a function of the compliance matrix  $[C]$  and the traction matrix  $[T]$  (both of which are dependent on the soil properties) it is shown later in this section of the report that  $[F]$  is independent of the soil conditions. As a result, the incoherency transfer function (ITF) is independent of the soil conditions. The independence of the scattering transfer function  $[F]$  from soil properties is a direct result of the CLASSI

**Deleted:**  
SSI and Structure Response

**Deleted:**  
SSI and Structure Response

**Deleted:**  
SSI and Structure Response  
SSI and Structure Response

formulation which considers the SSI response of a rigid surface inclusion on a layered half-space (i.e., a rigid massless foundation).

Let the modification of the field-field surface motion due to the presence of the rigid surface inclusion be represented by six component vector  $\{U_0\}$ . The average free-field surface motion of each of  $n$  sub-regions that represents the interface of the rigid foundation area with the half-space surface is represented by the  $3n$  component vector  $\{U_n\}$ . The motion of a reference point of the rigid inclusion  $\{U_0\}$  in terms of the set of sub-region motions  $\{U_n\}$  is related by the  $6 \times 3n$  scattering transfer function  $[F]$ :

$$\{U_0\} = [F] \{U_n\} \quad \text{(Equation 3-5)}$$

It may be noted that the  $3n \times 6$  rigid body transformation array  $[\alpha_b]$  is defined by:

$$\{U_n\} = [\alpha_b] \{U_0\} \quad \text{(Equation 3-6)}$$

$[\alpha_b]$  is only a function of the foundation footprint geometry and the location of the  $n$  sub-regions and not of the properties of soil layers. As a result, comparison of Equations 3-5 and 3-6 shows that  $[F]$  must be independent of the soil conditions.

The  $6 \times 6$  impedance matrix  $[K]$  relates the driving forces applied to the rigid inclusion,  $\{P_0\}$  to the displacements of the rigid inclusion,  $\{U_0\}$  by:

$$\{P_0\} = [K] \{U_0\} \quad \text{(Equation 3-7)}$$

The impedance matrix may also be expressed in terms of the  $3n \times 3n$  array  $[G]$  of Green's functions integrated over each sub-region, and the  $3n \times 6$  rigid body transformation array  $[\alpha_b]$  by:

$$[K] = [\alpha_b]^T [G]^{-1} [\alpha_b] \quad \text{(Equation 3-8)}$$

Combining Equations 3-6, 3-7, and 3-8, it may be noted that  $\{P_0\} = [\alpha_b]^T [G]^{-1} [\alpha_b] \{U_0\} = [\alpha_b]^T [G]^{-1} \{U_n\}$ . The array  $[G]^{-1} [\alpha_b]$  may be identified as the  $3n \times 6$  traction array  $[T]$  from Equation 3-4. Transposing Equation 3-4 gives  $[T]^T = [\alpha_b]^T [G]^{-1}$ . As a result:

$$\{P_0\} = [T]^T \{U_n\} \quad \text{(Equation 3-9)}$$

Equating Equations 3-7 and 3-9 so that  $\{P_0\} = [K] \{U_0\} = [T]^T \{U_n\}$ , we may write express  $\{U_0\}$  in terms of  $\{U_n\}$  as:

$$\{U_0\} = [K]^{-1} [T]^T \{U_n\} = [C] [T]^T \{U_n\} = [F] \{U_n\} \quad \text{(Equation 3-10)}$$

where  $[C] = [K]^{-1}$  is the  $6 \times 6$  compliance array of the rigid inclusion reference point. The scattering transfer function,  $[F]$  is equal to  $[C][T]^T$  in accordance with Equation 3-3.

From Equation 3-6,  $\{U_n\} = [\alpha_b] \{U_0\}$ . Multiplying both sides to this equation gives  $[\alpha_b]^T \{U_n\} = [\alpha_b]^T [\alpha_b] \{U_0\}$ .  $\{U_0\}$  can then be related to  $\{U_n\}$  by  $\{U_0\} = ([\alpha_b]^T [\alpha_b])^{-1} [\alpha_b]^T \{U_n\}$  which may be

identified as the least squares solution for the average motion of the rigid surface inclusion given the over-determined free-field motion of the n sub-regions  $\{U_n\}$ . Hence, from Equation 3-5, it may be seen that the scattering transfer function  $\{F\}$  is given by:

$$[F] = ([\alpha_b]^T [\alpha_b])^{-1} [\alpha_b]^T \quad \text{(Equation 3-11)}$$

Equation 3-11 shows that the scattering transfer function is independent of any soil properties, being determined only by the rigid body kinematics of the rigid foundation motion. The use of the identity  $[F] = [C][T]^T$  is actually equivalent to the least squares solution, and is a convenient means of computation for the scattering transfer function given the CLASSI computation of  $[K]$  and  $[T]$  for solution of the SSI problem.

CLASSI is used to evaluate the impedance matrix  $[K]$  and the traction matrix  $[T]$  at each selected frequency. Normal outputs are impedance and scattering matrices. Also,  $[T]$ , a Green's function matrix  $[G]$ , and  $[\alpha_b]$  are generated internally by the program. Input is the foundation footprint and the definition of sub-regions along with soil properties. For this study, the foundation footprint was divided into 10-ft square sub-regions. Around the periphery of the foundation, the outside 10-ft was further divided into 5-ft square sub-regions.

Based on CLASSI determined  $[K]$ ,  $[T]$ ,  $[G]$ , and  $[\alpha_b]$  the 6 by 6 cross PSD,  $[S_{Uoi}]$  of the rigid massless foundation to unit PSD input due to incoherent input motion is generated. For this purpose, the coherency matrix,  $[\gamma]$ , the covariance matrix for unit PSD input,  $[S_{UGi}]$  and the scattering transfer function,  $[F]$  are evaluated. Also, incoherency transfer function, ITF, which is equal to the amplitude of the square root of the diagonal terms of  $[S_{Uoi}]$  is calculated.

**Table 3-1**  
**Procedure to Evaluate Incoherency Transfer Function**

<ul style="list-style-type: none"> <li>Define Soil Profile and Specify Properties by Soil Layers Define Foundation Footprint and Specify as n Sub-Regions</li> </ul>
<ul style="list-style-type: none"> <li>Input coherency function, <math>\gamma(f,s)</math> as a function of Frequency, f and Separation Distance, s</li> </ul>
<ul style="list-style-type: none"> <li>Run CLASSI modules to Evaluate the Impedance Matrix and Green's Function Matrix</li> </ul>
<ul style="list-style-type: none"> <li>From Green's Function Matrix and Rigid Foundation Assumption, Evaluate the Traction Matrix, <math>[T]</math>. Invert the Impedance Function to Evaluate the Compliance Function, <math>[C]</math></li> </ul>
<ul style="list-style-type: none"> <li>Evaluate <math>[S_{Uoi}]</math>, the Cross PSD matrix of Rigid Massless Foundation Motion Subjected to Unit PSD Input  <math>[S_{Uoi}] = [F] [S_{UGi}] [FC]^T</math>                      where <math>[F] = [C] [T]^T</math>                      and <math>[S_{UGi}] = [I] [\gamma] [I]</math></li> </ul>
<ul style="list-style-type: none"> <li>Evaluate the Incoherency Transfer Function, ITF(f) as the Amplitude of the Complex Square Root of the Diagonal Terms of <math>[S_{Uoi}]</math></li> </ul>

Deleted: SSI and Structure Response  
 Deleted: SSI and Structure Response  
 Deleted: SSI and Structure Response  
 Deleted: SSI and Structure Response

**Deleted:**  
SSI and Structure Response

**Deleted:**  
SSI and Structure Response

**Deleted:**  
SSI and Structure Response  
SSI and Structure Response

## Procedure to Evaluate the Rigid Massless Foundation Incoherent Response Spectra

In order to evaluate the foundation response spectra for the rigid massless foundation, it is necessary to input ground motion response spectra for CEUS rock sites,  $[RS_o]$  as described in Chapter 2. These response spectra are converted to power spectral density (PSD) functions, and procedures similar to that described in the previous sub-section are employed to evaluate the PSD of the foundation response. These output PSDs are then converted to response spectra. This process is shown in Table 3-2.

The PSD for a component of ground response spectrum,  $S_o(f)$ , is evaluated by random vibration theory as discussed below. Standard relationships of stationary random vibration theory are used to convert response spectra (RS) into power spectral density (PSD) functions, and vice versa. To calculate a PSD from a RS, an iterative process is used. A starting PSD uniform function (white noise) is used and iterations performed until the RS calculated from the new PSD matches the target RS. To calculate a RS from a PSD, a direct integral relationship exists. Numerical integration is performed to calculate the moments of the PSD and the peak factors relating the standard deviation of the maximum response to the mean of the maximum peak response (RS). Der Kiureghian, A., "Structural Response to Stationary Excitation," Journal of the Engineering Mechanics Division, American Society of Civil Engineers, December 1980 is the basic reference followed (Der Kiureghian, 1980).

The PSD of the rigid massless foundation to actual incoherent input motion is determined using  $[S_{UG}]$ , a  $3n$  by  $3n$  covariance matrix of actual incoherent ground motions as determined by Equation 3-12.

$$[S_{UG}] = [S_o^{1/2}] [Y] [S_o^{1/2}] \quad \text{(Equation 3-12)}$$

where  $[S_o^{1/2}]$  is a  $3n$  by  $3n$  on-diagonal PSD matrix on the input ground motion and  $S_o(f)$  is the power spectral density of the input ground motion. The difference between  $[S_{UG}]$  and  $[S_{UGI}]$  is that  $[S_o^{1/2}]$  is used instead of identity matrix,  $[I]$ .

$[S_{Uo}]$ , the 6 by 6 cross PSD of rigid massless foundation motion is determined from:

$$[S_{Uo}] = [F] [S_{UG}] [FC]^T \quad \text{(Equation 3-13)}$$

$[F]$  the 6 by  $3n$  scattering transfer function matrix relating sub-region displacements to rigid body displacements and its complex conjugate  $[FC]$  are determined in exactly the same manner as described in the previous sub-section.

The response spectrum for the foundation response,  $[RS_{Uo}]$  is then determined from the PSD defined by the diagonal terms of the  $[S_{Uo}]$  matrix using the random vibration approach.

**Deleted:**  
SSI and Structure Response

**Deleted:**  
SSI and Structure Response

**Deleted:**  
SSI and Structure Response  
SSI and Structure Response

**Table 3-2  
Procedure to Evaluate the Rigid Massless Foundation Incoherent Response Spectra**

<ul style="list-style-type: none"> <li>Define free-field ground response spectra, <math>[RS_o]</math></li> </ul>
<ul style="list-style-type: none"> <li>Evaluate the PSD for each component of ground response spectrum, <math>S_o(f)</math>, by random vibration theory. Evaluate <math>[S_o^{1/2}]</math>, a 3n by 3n on-diagonal PSD matrix of the input ground motion</li> </ul>
<ul style="list-style-type: none"> <li>Evaluate <math>[S_{Uo}]</math>, the cross PSD matrix of rigid, massless foundation motion <math>[S_{Uo}] = [F] [S_{UG}] [FC]^T</math> where <math>[S_{UG}] = [S_o^{1/2}] [\gamma] [S_o^{1/2}]</math></li> </ul>
<ul style="list-style-type: none"> <li>Response spectrum of foundation response, <math>[RS_{Uo}]</math> is determined from the PSD defined by the diagonal terms of the <math>[S_{Uo}]</math> matrix using random vibration theory.</li> </ul>

**Procedure to Evaluate the Foundation and Structure Incoherent Response Spectra by Random Vibration Theory**

The 6 by 6 cross PSD of foundation response motion,  $[S_{UF}]$  may be determined by pre-multiplying  $[S_{Uo}]$ , the 6 by 6 cross PSD of rigid massless foundation motion by  $[H_F]$  a 6 by 6 transfer function matrix between foundation response and the scattered foundation input motions and post-multiplying by  $[H_FC]$ , the complex conjugate of  $[H_F]$ :

$$[S_{UF}] = [H_F] [S_{Uo}] [H_FC]^T \tag{Equation 3-14}$$

The foundation transfer matrix is given by:

$$[H_F] = ([I] - \omega^2 [C] ([M_b] + [M_s(f)]))^{-1} \tag{Equation 3-15}$$

In the above equation,  $[I]$  is an identity matrix,  $\omega$  is the frequency of interest in radians per second,  $[C]$  is the compliance matrix previously defined,  $[M_b]$  is the 6 by 6 diagonal mass matrix containing the foundation mass and mass moment of inertia, and  $[M_s(f)]$  is the 6 by 6 equivalent mass matrix of the structure about its base computed by:

$$[M_s] = [\alpha_s]^T [M] [\alpha_s] + [\Gamma_s]^T [D(f)] [\Gamma_s] \tag{Equation 3-16}$$

where  $[D(f)]$  is the k by k diagonal modal amplification matrix (k is the number of fixed-base structure modes) given by:

$$[D] = \left[ \frac{(\omega/\omega_r)^2}{\left(1 - \frac{\omega^2}{\omega_r^2}\right) + 2i\beta_r(\omega/\omega_r)} \right] \text{ where } r \text{ goes from } 1 \text{ to } k \tag{Equation 3-17}$$

$[\alpha_s]$  is a q by 6 rigid body transformation matrix of the structure about its base where q is the number of structure dynamic degrees of freedom above its base.  $[\alpha_s]$  is given by:

**Deleted:**  
SSI and Structure Response

**Deleted:**  
SSI and Structure Response

**Deleted:**  
SSI and Structure Response  
SSI and Structure Response

$$[\alpha_s] = \begin{bmatrix} \dots\dots \\ \dots\dots \\ 1 & 0 & 0 & 0 & z^j & -y^j \\ 0 & 1 & 0 & -z^j & 0 & x^j \\ 0 & 0 & 1 & y^j & -x^j & 0 \\ 0 & 0 & 0 & 1 & 0 & 0 \\ 0 & 0 & 0 & 0 & 1 & 0 \\ 0 & 0 & 0 & 0 & 0 & 1 \end{bmatrix}$$

**(Equation 3-18)**

where j goes from 1 to q, the number of structure nodes with coordinates x, y, and z.  $[\Gamma_s]$  is a k by 6 matrix of modal participation factors given by:

$$[\Gamma_s] = [\phi_s]^T [M] [\alpha_s] \quad \text{(Equation 3-19)}$$

in which  $[\phi_s]$  is the q by k fixed-base mode shape matrix of the structure and  $[M]$  is the q by q structure mass matrix.

The response spectrum for the foundation response,  $[RS_{UF}]$  is then determined from the PSD defined by the diagonal terms of the  $[S_{UF}]$  matrix using the random vibration approach described above.

The q by q cross PSD of structural response motion,  $[S_{US}]$  is determined by pre-multiplying  $[S_{Uo}]$ , the 6 by 6 cross PSD of rigid massless foundation motion by  $[H_T]$  (a q by 6 transfer function matrix between structural response and the scattered foundation input motions) and post-multiplying by  $[H_T^C]$ , the complex conjugate of  $[H_T]$ :

$$[S_{US}] = [H_T] [S_{Uo}] [H_T^C]^T \quad \text{(Equation 3-20)}$$

The structure transfer function matrix is given by:

$$[H_T] = ([\alpha_s] + [\phi_s] [D] [\Gamma_s]) [H_F] \quad \text{(Equation 3-21)}$$

Where all matrices and terms have been previously defined.

The response spectrum for the foundation response,  $[RS_{US}]$  is then determined from the PSD defined by the diagonal terms of the  $[S_{US}]$  matrix using the random vibration approach described above.

## **Procedure to Evaluate the Foundation and Structure Incoherent Response Spectra by CLASSI**

The complete random vibration approach described above could have been employed herein. However, the formulation of CLASSI and its ease of use permitted implementation of a more direct approach to the SSI analysis of structure/foundation. The procedure used is shown in Table 3-3.

CLASSI program modules generate the complex impedance and scattering matrices at each frequency considered. The impedance matrix represents the stiffness and energy dissipation of the underlying soil medium. The foundation input motion is related to the free-field ground motion by means of a transformation defined by a scattering matrix. The term “foundation input motion” refers to the result of kinematic interaction of the foundation with the free-field ground motion. In general, the foundation input motion differs from the free-field ground motion in all cases, except for surface foundations subjected to vertically incident waves. The soil-foundation interface scatters waves because points on the foundation are constrained to move according to its geometry and stiffness. Modeling of incoherent ground motions is one aspect of this phenomena and the focus of this study.

In essence, the incoherency transfer function is the scattering matrix accounting for the effects of seismic wave incoherency over the dimensions of the foundation. For this application, a 6 by 6 complex incoherency transfer function matrix [ITF] is evaluated by taking the square root of the diagonal terms of  $[S_{Uoi}]$ , the 6 by 6 complex cross PSD matrix of rigid massless foundation motion to unit PSD input for each direction of translational input. Each column of the scattering matrix for vertically propagating waves is replaced by the diagonal terms from the incoherency transfer function matrix at each frequency of interest that correspond to each direction of input excitation. CLASSI SSI analyses are then performed in a conventional manner to evaluate the structure and foundation in-structure response spectra. CLASSI solves the SSI problem in the frequency domain. Ground motion time histories are transformed into the frequency domain, SSI parameters (impedances and scattering matrices) are complex-valued, frequency-dependent, and the structure is modeled using its fixed-base eigensystems.

In CLASSI, the dynamic characteristics of the structures to be analyzed are described by their fixed-based eigen-system and modal damping factors. Modal damping factors are the viscous damping factors for the fixed-base structure expressed as a fraction of critical damping. The structures’ dynamic characteristics are then projected to a point on the foundation at which the total motion of the foundation, including SSI effects, is determined.

The final step in the CLASSI substructure approach is the actual SSI analysis. The results of the previous steps – foundation input motion (scattering matrix defined by the incoherency transfer function), foundation impedances, and structure model – are combined to solve the equations of motion for the coupled soil-structure system. For a single rigid foundation, the SSI response computation requires solution of, at most, six simultaneous equations – the response of the foundation. The derivation of the solution is obtained by first representing the response in the structure in terms of the foundation motions and then applying that representation to the equation

**Deleted:**  
*SSI and Structure Response*

**Deleted:**  
*SSI and Structure Response*

**Deleted:**  
*SSI and Structure Response*  
*SSI and Structure Response*

defining the balance of forces at the soil/foundation interface. The formulation is in the frequency domain. Once the foundation motion is calculated (including all aspects of SSI), in-structure responses are determined for locations of interest in the structure, i.e., by solving the dynamic equations of motion in modal coordinates for the base excited system. The resulting in-structure response spectra at structure and foundation locations of interest include the effects of soil-structure interaction and seismic wave incoherence.

**Deleted:**  
*SSI and Structure Response*

**Deleted:**  
*SSI and Structure Response*

**Deleted:**  
*SSI and Structure Response*  
*SSI and Structure Response*

**Deleted:**  
*SSI and Structure Response*

**Deleted:**  
*SSI and Structure Response*

**Deleted:**  
*SSI and Structure Response*  
*SSI and Structure Response*

**Table 3-3**  
**Procedure to Evaluate the Foundation and Structure Incoherent Response Spectra by CLASSI**

<ul style="list-style-type: none"><li>• Define Free-Field Ground Motion Time Histories Compatible with Response Spectra, [RS<sub>o</sub>]</li></ul>
<ul style="list-style-type: none"><li>• Define Soil Profile and Specify Properties By Soil Layers Define Foundation Footprint and Specify As N Sub-Regions Define Foundation Thickness and Mass Properties Define a Fixed-Base Structural Model</li></ul>
<ul style="list-style-type: none"><li>• Input Coherency Function, <math>\gamma(F,S)</math> as a Function of Frequency, F and Separation Distance, S</li></ul>
<ul style="list-style-type: none"><li>• Run CLASSI Modules To Evaluate The Impedance Matrix</li></ul>
<ul style="list-style-type: none"><li>• Evaluate the Scattering Matrix as the Incoherency Transfer Function. Each Column of the Scattering Matrix Corresponds to a Direction of Input Excitation And is Given by the Diagonal Terms from the Incoherency Transfer Function at Each Frequency Of Interest.</li></ul>
<ul style="list-style-type: none"><li>• Evaluate Fixed-Base Modal Properties of the Structure</li></ul>
<ul style="list-style-type: none"><li>• Run CLASSI Modules That Combine the Structure Properties, Impedance Matrix, Scattering Matrix, And Input Time Histories, and Evaluates Output Time Histories</li></ul>
<ul style="list-style-type: none"><li>• Run Standard Response Spectrum Evaluation Program to Determine In-Structure Response Spectra for the Foundation and Structure Locations</li></ul>

# 4

## RIGID, MASSLESS FOUNDATION RESPONSE

---

### General

The effect of seismic wave incoherence is demonstrated in this chapter for the seismic response of a rigid massless foundation. Analyses reported in this chapter represent the essence of Task 2.1 developing the incoherency transfer functions that enable the effects of incoherence to be implemented into seismic analyses.

For most analyses the soil properties and foundation areas presented in Chapter 2 are used. These properties include the rock and soil profiles along with the corresponding high and low-frequency content site-specific ground response spectra.

A study of the effects of wave passage phenomena was performed to separate the effects of wave passage and local wave scattering. The wave passage study was performed for the 150-ft square foundation footprint and a rock half-space site condition of shear wave velocity of 6300 fps; the same site condition used in the benchmark comparison analyses documented in Appendix C.

### Wave Passage Effects

The Abrahamson coherency function accounts for horizontal spatial variation of ground motion from both wave passage effects and local wave scattering.

- Wave passage effects: Systematic spatial variation due to difference in arrival times of seismic waves across a foundation due to inclined waves.
- Local wave scattering: Spatial variation from scattering of waves due to the heterogeneous nature of the soil or rock along the propagation paths of the incident wave fields.

For the detailed efforts of this project, only local wave scattering of ground motion was considered. Local wave scattering results in large reductions in foundation motion and wave passage effects produce minimal further reductions. However, to take advantage of these further reductions in foundation motion due to wave passage, an apparent wave velocity must be assigned to the site. The apparent wave velocity is dependent on many parameters including earthquake source parameters, travel paths, and the earthquake source location relative to the site. Assigning an appropriate and defensible apparent wave velocity for free-field ground motion developed from probabilistic seismic hazard assessments is difficult and possibly controversial.

**Deleted:**  
SSI and Structure Response

**Deleted:**  
SSI and Structure Response

**Deleted:**  
SSI and Structure Response  
SSI and Structure Response

The effects of wave passage are demonstrated in terms of incoherency transfer functions and spectral corrections as shown in Figures 4-1, 4-2, 4-3, and 4-4. These results were generated for the 150-ft square foundation on a rock half-space of shear wave velocity of 6300 fps. The free-field ground motion was defined by site-specific ground response spectra, with high-frequency amplification, itemized in Appendix C. Earthquake ground motion recorded with adequate instruments to identify wave passage effects leads to the estimate of apparent wave velocities greater than 2 km/sec and more justifiably at 4 km/sec.

The wave passage analyses considered are:

- Apparent wave velocity of 2000 m/s (Slowness of 0.00050 s/m)
- Apparent wave velocity of 4000 m/s (Slowness of 0.00025 s/m)
- No wave passage effects (Apparent wave velocity = infinity - Slowness of 0 s/m)

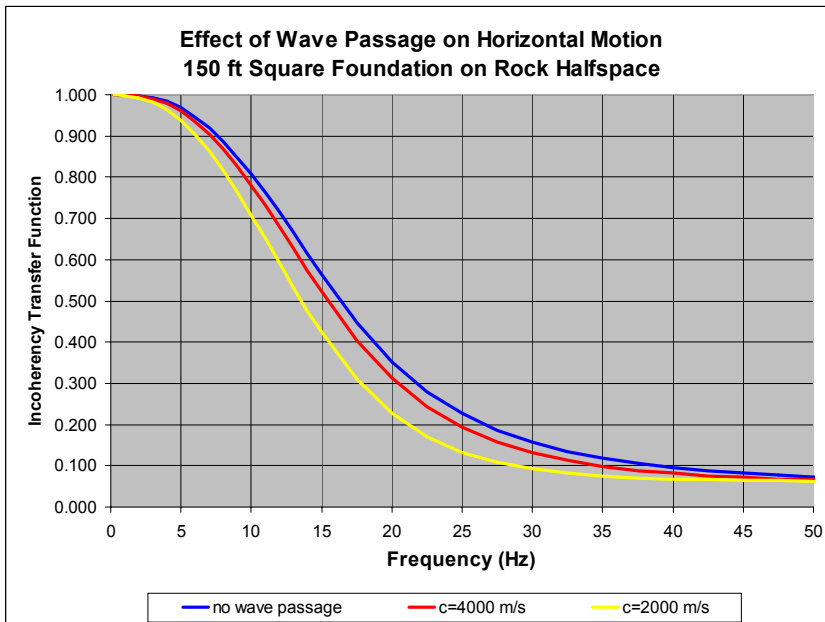


**Figure 4-1**  
**Effect of Wave Passage on Incoherency Transfer Function for Horizontal Motion**

**Deleted:** .  
SSI and Structure Response

**Deleted:** .  
SSI and Structure Response

**Deleted:** .  
SSI and Structure Response .  
SSI and Structure Response

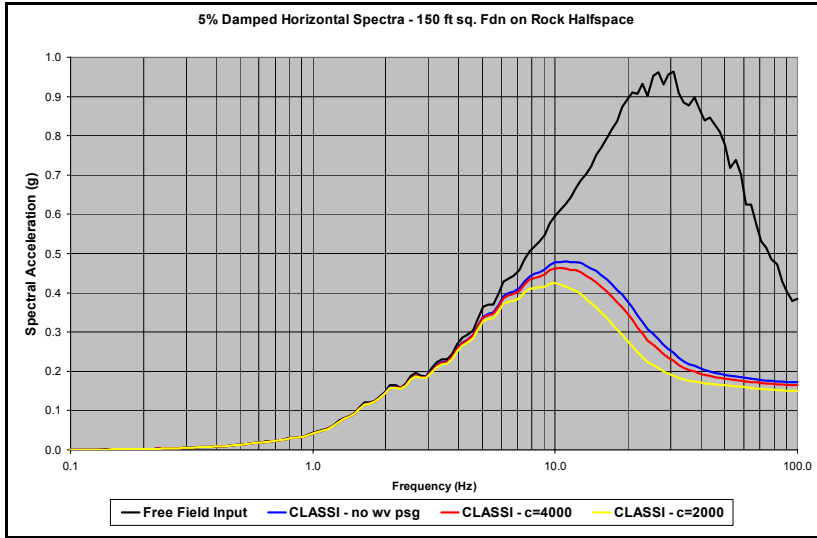


**Figure 4-2**  
Effect of Wave Passage on Foundation Horizontal Response Spectra

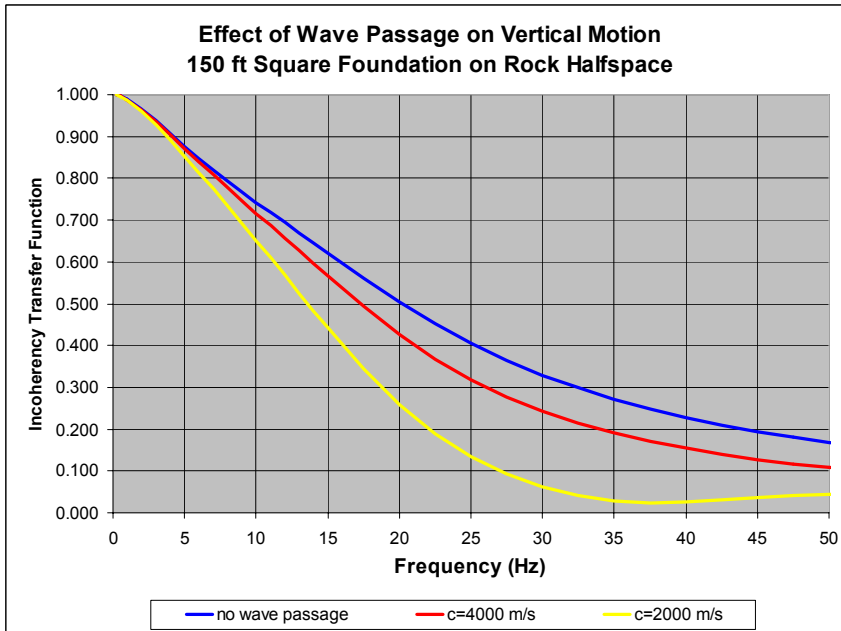
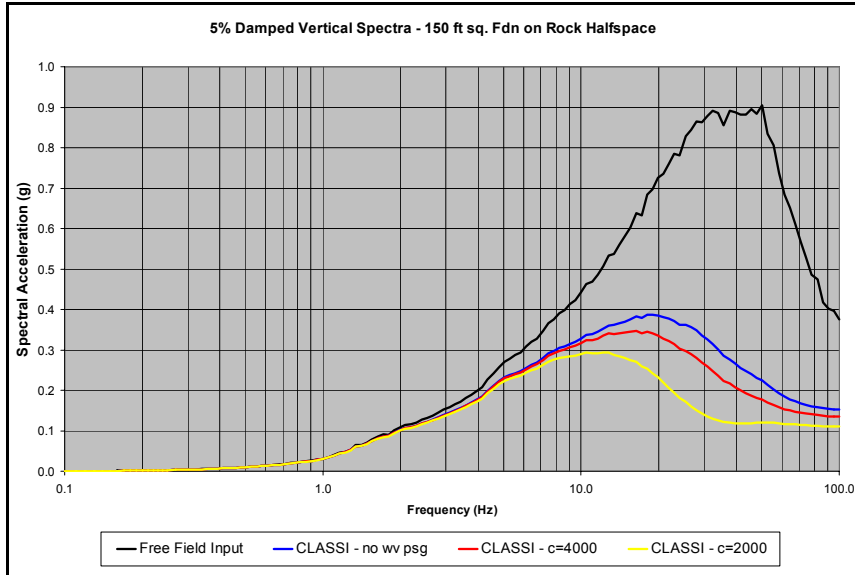


**Figure 4-3**  
Effect of Wave Passage on Incoherency Transfer Function for Vertical Motion



**Deleted:** .  
*SSI and Structure Response*

**Deleted:** .  
*SSI and Structure Response*

**Deleted:** .  
*SSI and Structure Response* .  
*SSI and Structure Response*

**Figure 4-4**  
**Effect of Wave Passage on Foundation Vertical Response Spectra**

### Incoherency Transfer Function

Incoherency transfer functions or wave scattering due to seismic wave incoherence have been computed in the manner described in Chapter 3. The incoherency transfer function demonstrates the effects of seismic wave incoherence as a function of frequency for the foundation footprint considered. Parametric studies have been performed for:

- Foundation Shape (Constant Area)
  - 150-ft square footprint
  - 100 by 225-ft rectangle footprint
  - 84.63-ft radius circle footprint
- Foundation Area (Constant Shape)
  - 75-ft square footprint
  - 150-ft square footprint
  - 300-ft square footprint

Calculations have been performed for local wave scattering effects only; wave passage effects have not been considered.

**Deleted:**  
SSI and Structure Response

**Deleted:**  
SSI and Structure Response

**Deleted:**  
SSI and Structure Response  
SSI and Structure Response

Soil profile. Chapter 3 demonstrated that the incoherency transfer functions are independent of site conditions. Hence, incoherency transfer functions as calculated for the rock site are presented. Foundation response is presented for the rock and soil site profiles since they are dependent on the site-specific ground motion, which differs for the two site conditions.

Foundation shape. The effects of foundation shape on the incoherency transfer functions for translational foundation motion are shown in Figures 4-5 and 4-6 for the horizontal and vertical directions, respectively. On these figures, the lines of different colors lie on top of each other so only one color is visible. The conclusion is that for these variations in foundation shape, i.e., square vs. rectangle (with reasonable aspect ratio of 2:1) vs. circle, the incoherency transfer function is independent of foundation shape. This conclusion applies only to the foundation shapes considered in this study and may change when foundations of different shapes (e.g., L shape) or larger aspect ratios are considered.

Foundation area. The effect of foundation area on the incoherency transfer function for translational foundation motion is presented in Figures 4-7 and 4-8. Square foundation footprints with area varying by a factor of 4 are considered. Although the variation on the plots appears small, the actual difference amounts to about 30 to 45 percent for an area difference of a factor of 4. Going from the 75-ft square foundation footprint to the 300-ft square foundation footprint results in an increased reduction from about 0.45 at 20 Hz and 0.23 at 30 Hz to about 0.27 at 20 Hz and 0.12 at 30 Hz.

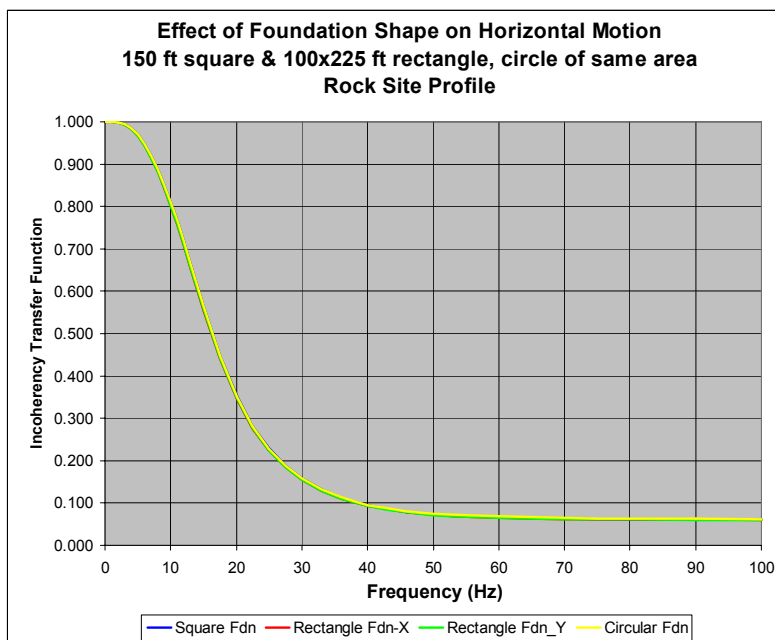


**Figure 4-5**  
**Horizontal Motion Incoherency Transfer Function – Effect of Foundation Shape**

Deleted: SSI and Structure Response

Deleted: SSI and Structure Response

Deleted: SSI and Structure Response

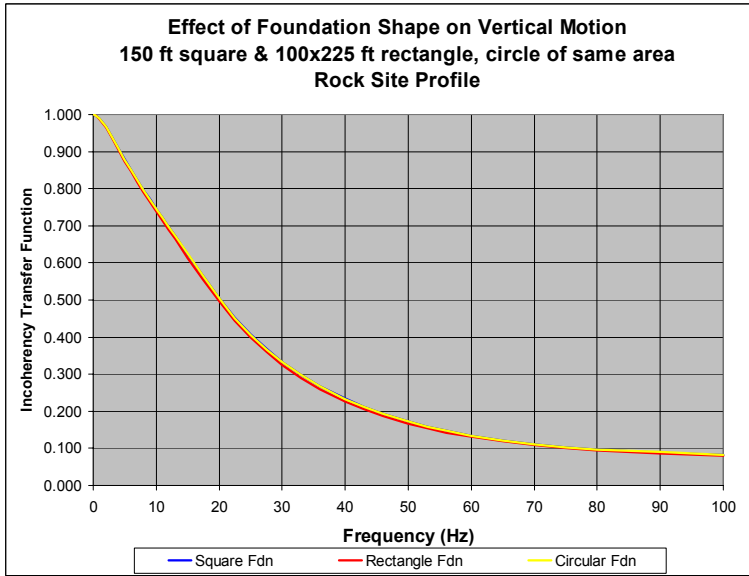


Figure 4-6 Vertical Motion Incoherency Transfer Function – Effect of Foundation Shape

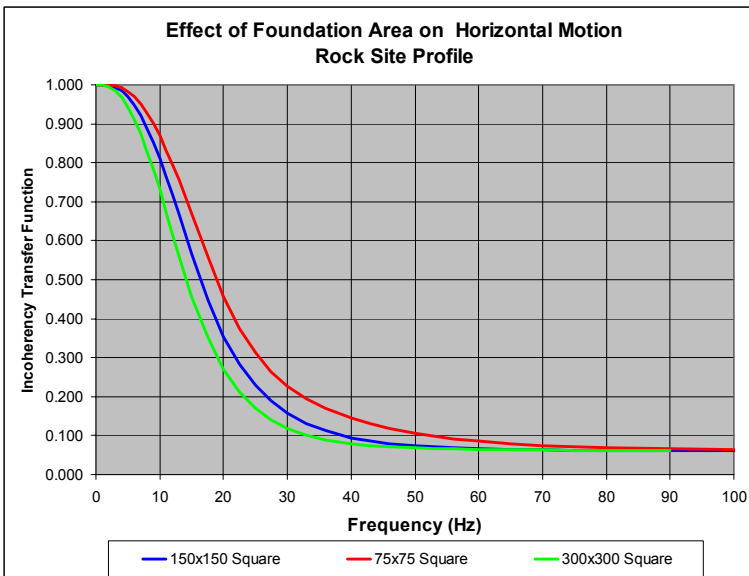
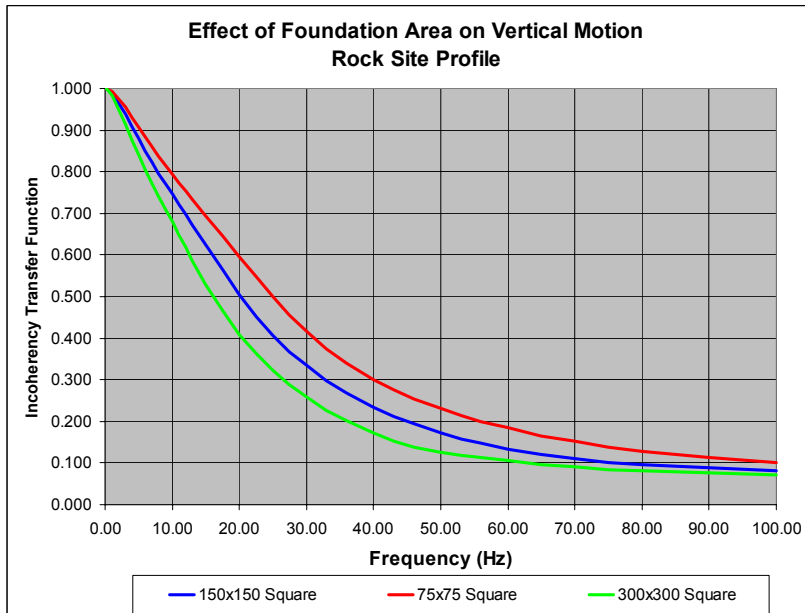


Figure 4-7 Horizontal Motion Incoherency Transfer Function – Effect of Foundation Area

**Deleted:**  
SSI and Structure Response

**Deleted:**  
SSI and Structure Response

**Deleted:**  
SSI and Structure Response  
SSI and Structure Response



**Figure 4-8**  
**Vertical Motion Incoherency Transfer Function – Effect of Foundation Area**

### Spectral Corrections

Foundation response spectra accounting for seismic wave incoherence have been computed in the manner described in Chapter 3. By this approach, the PSD is computed from the response spectra of the free-field input motion and input to CLASSI. The program then evaluates the PSD of the foundation motion including the effects of seismic wave incoherence. The resulting response PSD is then converted to foundation response spectra by random vibration theory. Foundation response spectra have been developed for both the rock and soil site profiles described in Chapter 2 using the compatible free-field high-frequency rock and lower frequency soil ground response spectra, respectively. Parametric studies have been performed for:

- Foundation Shape (Constant Area)
  - 150-ft square footprint
  - 100 by 225-ft rectangle footprint
  - 84.63-ft radius circle footprint (spectra are identical to the square and rectangle and are not presented herein)
- Foundation Area (Constant Shape)
  - 75-ft square footprint
  - 150-ft square footprint

- 300-ft square footprint

Results are shown in Figures 4-9 through 4-12.

Rock site. Figures 4-9 and 4-10 display response spectra for free-field ground motion and foundation response for the rock site. Figure 4-9 shows horizontal motion; Figure 4-10 shows vertical motion. Two free-field ground motion response spectra are plotted: the site-specific ground response spectra for the rock site and for reference, the US NRC Regulatory Guide 1.60 design response spectra (modified in the high-frequency region) anchored to a Peak Ground Acceleration of 0.3g (called the AP1000 SSE in the figures). Foundation response spectra for the four cases listed above are super-imposed on the free-field ground motion. It may be seen from these figures that the foundation spectra for the 150-ft square footprint, the 100 by 225-ft rectangle footprint, and the circle of the same area are the same. This is expected since the incoherency transfer functions are the same. These figures also show the effects of foundation area on response spectra for the 75-ft, 150-ft, and 300-ft square foundation footprint.

Soil site. Figures 4-11 and 4-12 display response spectra for the soil site in a similar manner to the data shown in Figures 4-9 and 4-10 for the rock site. Note however, that the site-specific free-field ground motion is significantly different than the site-specific rock motion. The same comparisons of foundation response spectra for the soil site are made. Note, there are reductions in response spectral values due to incoherence, but the most significant of those occurs in the frequency range above 10 Hz. The response spectra reductions as a function of foundation area are much more significant for the rock site than for the soil site. The effect of seismic wave incoherence is primarily a high-frequency phenomenon. Hence, the observed reductions in foundation response spectra are much less for the soil site since the soil site-specific ground motion is deficient in high-frequencies. For the rock site, the peak of the horizontal spectra is reduced from 0.85g for the 75-ft square foundation to 0.76g for the 150-ft square foundation to 0.67g for the 300-ft square foundation. All of these peak spectra values are much less than the 1.48g peak of the free-field input spectra in the horizontal direction. Similar behavior is observed for the vertical ground motion.

Approximate Treatment of Incoherency of Ground Motions. Spectral corrections taken from the figures are shown in Tables 4-1 and 4-2 for horizontal and vertical motion, respectively; along with the spectral corrections that are given in ASCE 4. Reductions are shown for the foundation dimensions of 75, 150, and 300 feet. It may be seen that spectral reductions are significantly greater than the ASCE 4 values for the rock site, but are actually somewhat similar for the soil site. This demonstrates that spectral reductions are not a proper way to account for seismic wave incoherence as they strongly depend on the frequency content of the free-field input ground response spectra. An approach based on the incoherency transfer function (ITF), modified to account for induced rotations, is more appropriate. The ITFs are independent of the input motion. However, the approximate rules to be applied differ depending on the predominant frequency content of the input motion.

**Deleted:**  
*SSI and Structure Response*

**Deleted:**  
*SSI and Structure Response*

**Deleted:**  
*SSI and Structure Response*  
*SSI and Structure Response*

**Deleted:**  
*SSI and Structure Response*

**Deleted:**  
*SSI and Structure Response*

**Deleted:**  
*SSI and Structure Response*  
*SSI and Structure Response*

**Table 4-1**  
**Spectral Corrections for Horizontal Motion**

Frequency	ASCE 4		Rock-H			Soil-H		
	150	300	75	150	300	75	150	300
5.00	1.00	1.00	0.95	0.93	0.89	0.98	0.97	0.95
10.00	0.90	0.80	0.84	0.78	0.71	0.90	0.85	0.79
15.00	0.86	0.71	0.68	0.59	0.49	0.78	0.71	0.63
20.00	0.82	0.65	0.50	0.41	0.33	0.68	0.62	0.56
25.00	0.80	0.60	0.38	0.30	0.24	0.64	0.60	0.55
30.00	0.80	0.60	0.32	0.25	0.20	0.64	0.60	0.56
40.00	0.80	0.60	0.27	0.22	0.19	0.65	0.62	0.59
50.00	0.80	0.60	0.26	0.22	0.19	0.68	0.66	0.63

**Table 4-2**  
**Spectral Corrections for Vertical Motion**

Frequency	ASCE 4		Rock-V			Soil-V		
	150	300	75	150	300	75	150	300
5.00	1.00	1.00	0.88	0.85	0.80	0.91	0.89	0.86
10.00	0.90	0.80	0.78	0.73	0.66	0.83	0.79	0.74
15.00	0.86	0.71	0.69	0.62	0.54	0.76	0.71	0.62
20.00	0.82	0.65	0.61	0.52	0.43	0.69	0.63	0.54
25.00	0.80	0.60	0.53	0.44	0.36	0.64	0.57	0.50
30.00	0.80	0.60	0.46	0.38	0.30	0.59	0.52	0.46
40.00	0.80	0.60	0.36	0.29	0.23	0.53	0.48	0.43
50.00	0.80	0.60	0.31	0.25	0.20	0.50	0.46	0.42

Deleted: SSI and Structure Response

Deleted: SSI and Structure Response

Deleted: SSI and Structure Response  
SSI and Structure Response

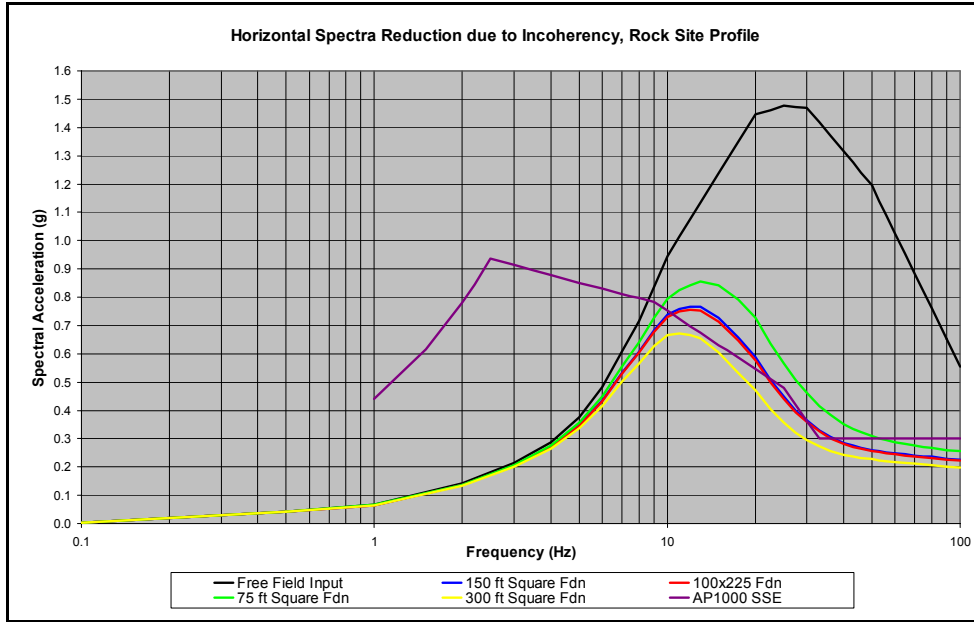


Figure 4-9  
Horizontal Motion Foundation Response Spectra, Rock Site

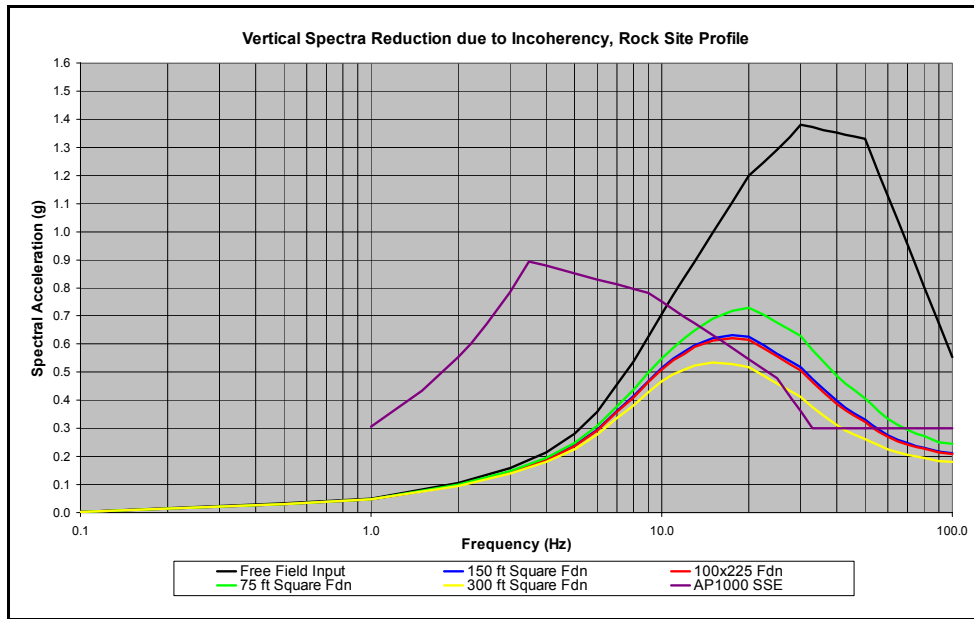


Figure 4-10  
Vertical Motion Foundation Response Spectra, Rock Site

Deleted: SSI and Structure Response

Deleted: SSI and Structure Response

Deleted: SSI and Structure Response

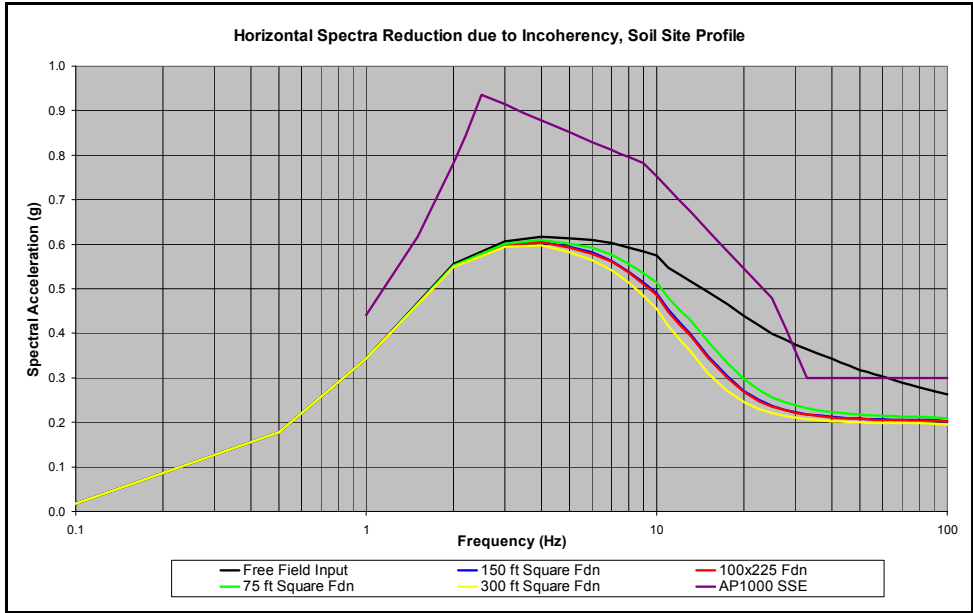


Figure 4-11  
Horizontal Motion Foundation Response Spectra, Soil Site

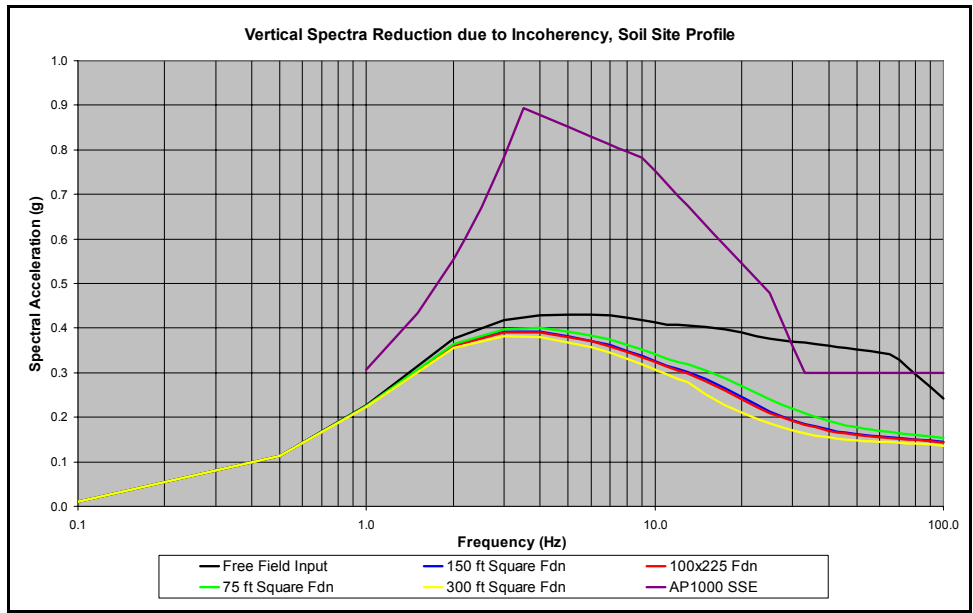


Figure 4-12  
Vertical Motion Foundation Response Spectra, Soil Site

**Deleted:**  
*SSI and Structure Response*

**Deleted:**  
*SSI and Structure Response*

**Deleted:**  
*SSI and Structure Response*  
*SSI and Structure Response*

## Rotations Induced by Incoherence

Thus far in this chapter it has been demonstrated that ground motion incoherence produces a reduction in the translational motion of the foundation relative to the free-field motion. It is known that incoherence can induce rotation due to the variability of the ground motion over the foundation footprint. For a rigid massless foundation, as is considered in this chapter, incoherent horizontal motion can induce torsional motion and incoherent vertical motion can induce rocking motion. To demonstrate the amplitude of induced rotations, the incoherency transfer function and the response spectrum for translational motion at the edge of the foundation caused by rotation are evaluated. These translational motions due to incoherence-induced rotations are compared to translational motions at the center of the foundation from the translational input to assess the effect of rotations.

As demonstrated in Chapter 3, the ITF is equal to the amplitude of the square root of the diagonal terms of the 6 by 6 cross PSD matrix of rigid massless foundation motion subjected to unit PSD input. The first three ITF terms are for translational motion and the last three ITF terms are for rotational motion. To quantify the maximum effect of the rotational terms on the response of the rigid massless foundation, the rotational ITF terms are converted to translational motions on the extreme edges of the foundation. To do so, they are scaled by the distance from the center of the foundation to the edge of the foundation of interest. Translations at these extreme points due to rotations induced by incoherence are evaluated for the 150-ft square foundation and the 100 by 225-ft rectangular foundation. The rock and soil site profiles described in Chapter 2 were considered for the evaluation of response spectra on the foundation.

For the 150-ft square foundation, the translation due to rotation is determined by multiplying the rotation by 75-ft, the distance from the foundation center to a wall at the edge of the foundation. Torsion due to horizontal motion and rocking due to vertical motion are illustrated in Figures 4-13 and 4-14.

For the 100 by 225-ft rectangular foundation, the 225-ft side is along the x or H1 axis and the 100-ft side is along the y or H2 axis. Vertical motion is in the z or V direction. For the rectangular foundation, H1 translation due to torsion is determined by multiplying the rotation by 50-ft, the distance from the foundation center to a wall at the edge of the foundation, and H2 translation due to torsion is determined by multiplying the rotation by 112.5-ft, the distance from the foundation center to a wall at the edge of the foundation. Vertical translation due to rocking is determined by multiplying the rotation by 112.5-ft, the largest distance from the foundation center to a wall at the edge of the foundation. Torsion due to horizontal motion and rocking due to vertical motion are illustrated in Figures 4-15, 4-16, and 4-17.

**Deleted:**  
*SSI and Structure Response*

**Deleted:**  
*SSI and Structure Response*

**Deleted:**  
*SSI and Structure Response*  
*SSI and Structure Response*

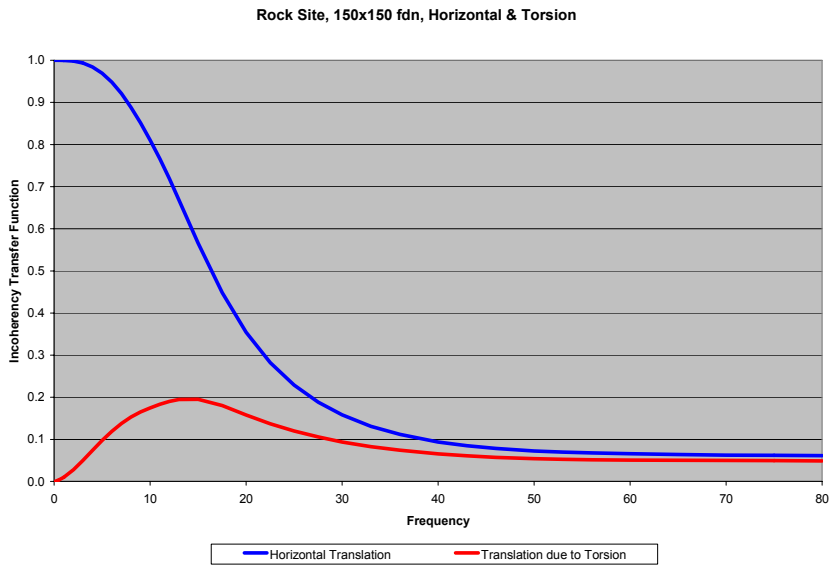


**Figure 4-13**  
**Torsion Induced by Incoherent Horizontal Input, Square Foundation**

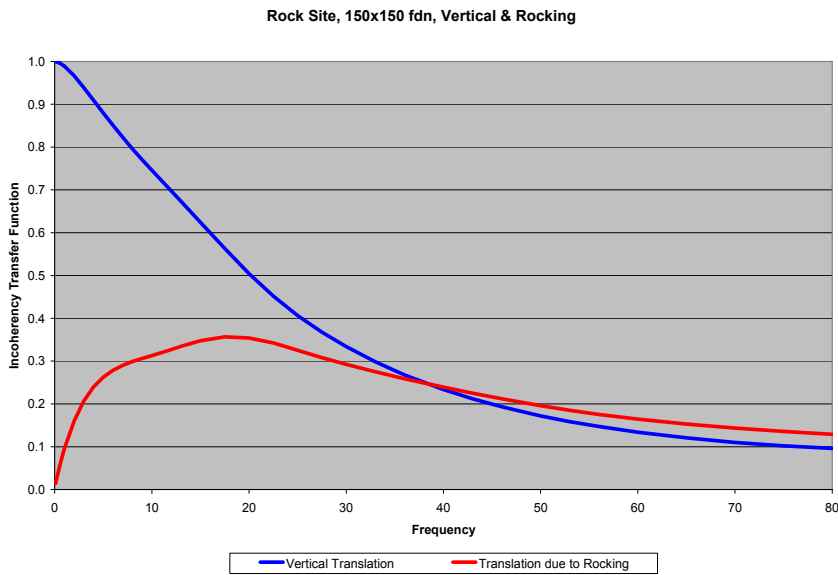


**Figure 4-14**  
**Rocking Induced by Incoherent Vertical Input, Square Foundation**

**Deleted:**  
*SSI and Structure Response*

**Deleted:**  
*SSI and Structure Response*

**Deleted:**  
*SSI and Structure Response*  
*SSI and Structure Response*

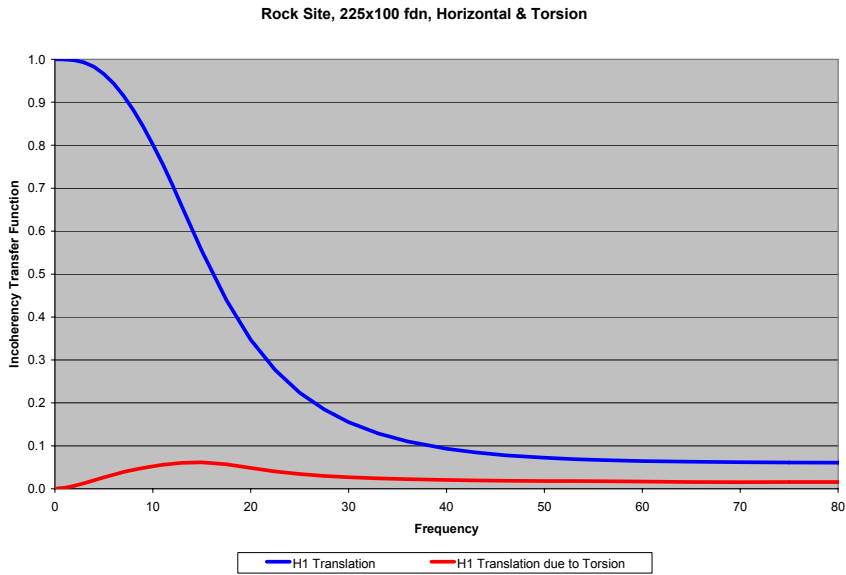


**Figure 4-15**  
**H1 Torsion Induced by Incoherent Horizontal Input, Rectangle Foundation**

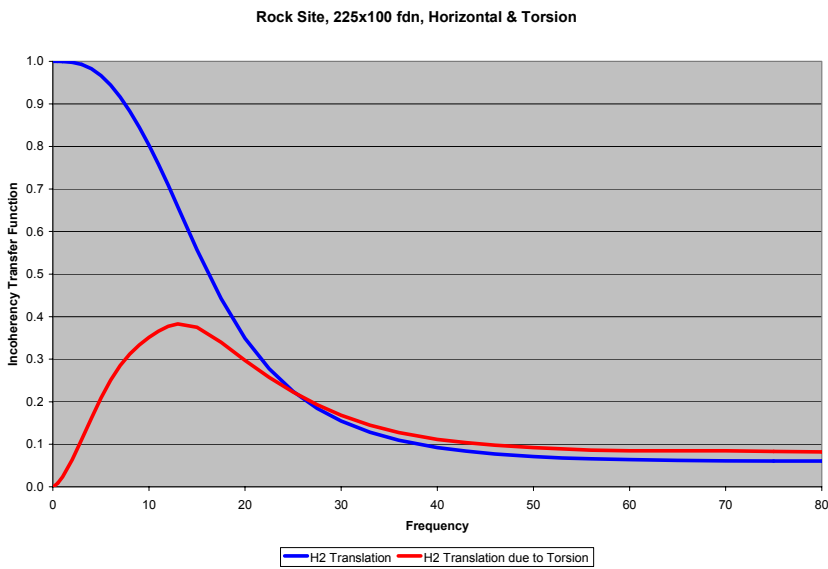


**Figure 4-16**  
**H2 Torsion Induced by Incoherent Horizontal Input, Rectangle Foundation**

**Deleted:**  
*SSI and Structure Response*

**Deleted:**  
*SSI and Structure Response*

**Deleted:**  
*SSI and Structure Response*  
*SSI and Structure Response*

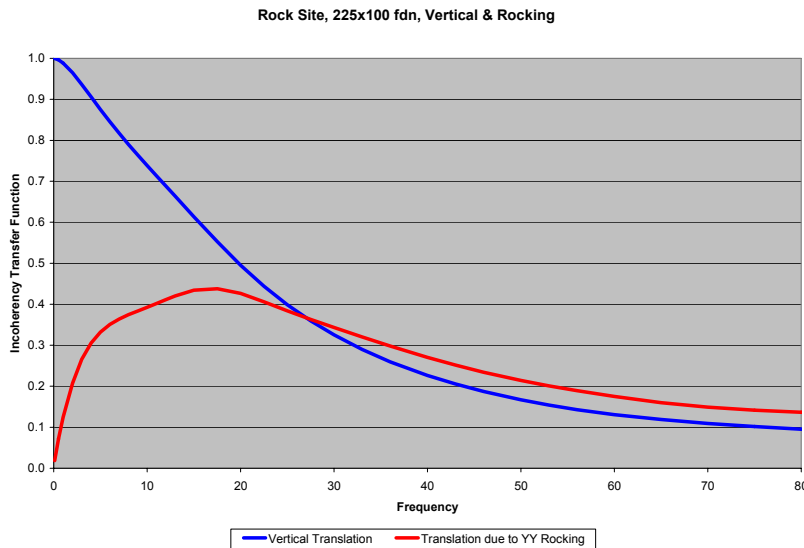


**Figure 4-17**  
**Rocking Induced by Incoherent Vertical Input, Rectangle Foundation**

Vertical motion due to rocking caused by incoherent vertical input appears to be more significant relative to vertical translation at the foundation center than the horizontal motion due to torsion caused by incoherent horizontal input relative to translational motion at the foundation center. The reason for this phenomenon is that the vertical coherency function is greater than the horizontal coherency function at the same frequencies and separation distances as demonstrated in Chapter 2.

The transfer functions shown above provide an indication of the effects of rotations and can be compared to results in the literature (Kim and Stewart, 2003). To gain a better understanding of the effect of rotation on structural response, foundation response spectra evaluated at the center and edge of the foundation were computed. In this manner, the effect of rotation on structural response can be better quantified.

Foundation response spectra accounting for seismic wave incoherence and including both translation and rocking effects have been computed in the manner described in Chapter 3. By this approach, the PSD is computed from the response spectra of the free-field input motion and input to CLASSI. The program then evaluates the PSD of the foundation motion including the effects of seismic wave incoherence. The resulting response PSD is then converted to foundation response spectra by random vibration theory. Foundation response spectra have been developed for both the rock and soil site profiles described in Chapter 2 using the compatible free-field high-frequency rock and lower frequency soil ground response spectra, respectively. Parametric studies have been performed for both the 150-ft square footprint and the 100 by 225-ft rectangular footprint. The resulting foundation response spectra for the square foundation are

**DRAFT**

*Rigid, Massless Foundation Response*

presented in Figures 4-18 through 4-21. Foundation spectra for the rectangular foundation are presented in Figures 4-22 through 4-25.

**Deleted:**  
*SSI and Structure Response*

**Deleted:**  
*SSI and Structure Response*

**Deleted:**  
*SSI and Structure Response*  
*SSI and Structure Response*

**Horizontal and Torsion, Response Spectra, 5% Damping  
Rock, 150 ft x 150 ft, H1 Input**

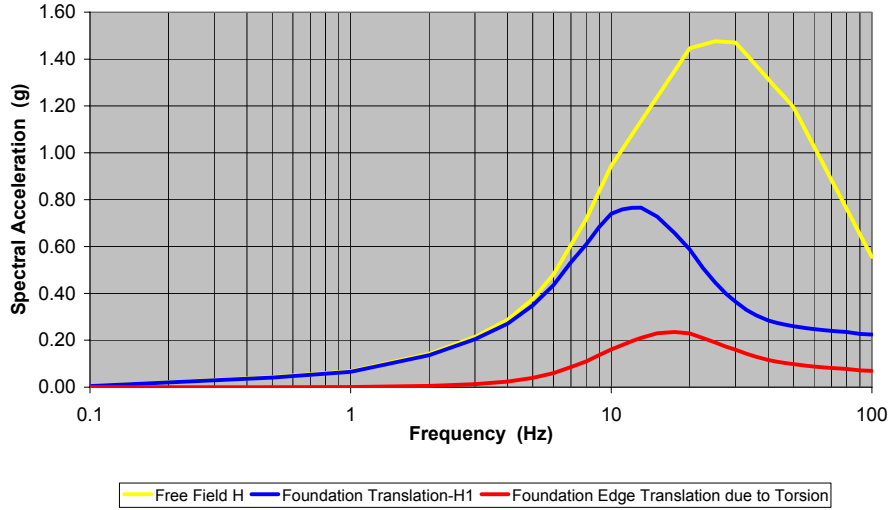


**Figure 4-18  
Response Spectra Including Torsion, Square Foundation, Rock Site**

**Deleted:**  
SSI and Structure Response

**Deleted:**  
SSI and Structure Response

**Deleted:**  
SSI and Structure Response

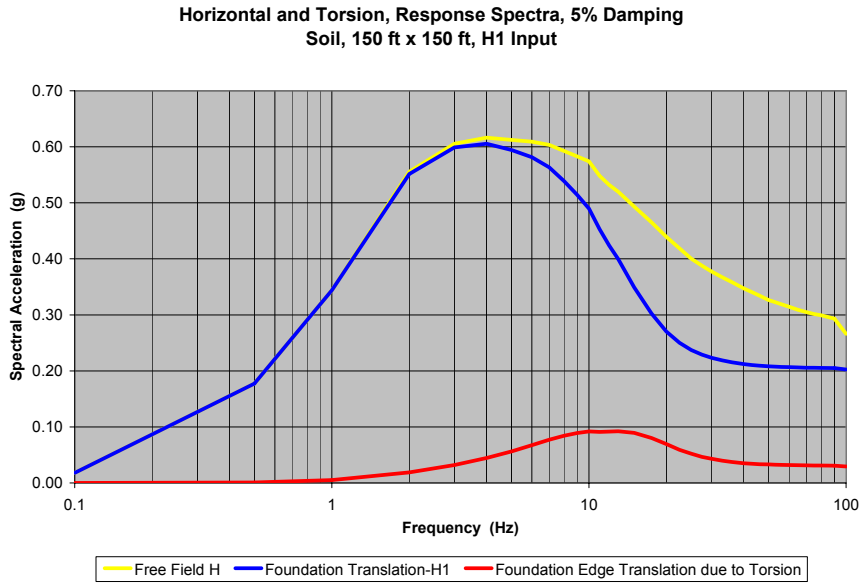


**Figure 4-19**  
Response Spectra Including Torsion, Square Foundation, Soil Site

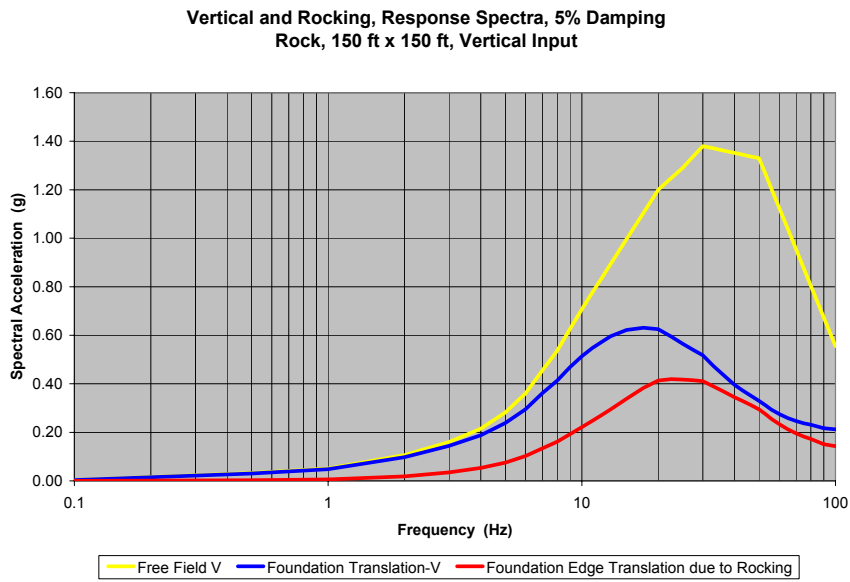


**Figure 4-20**  
Response Spectra Including Rocking, Square Foundation, Rock Site

Deleted: SSI and Structure Response

Deleted: SSI and Structure Response

Deleted: SSI and Structure Response

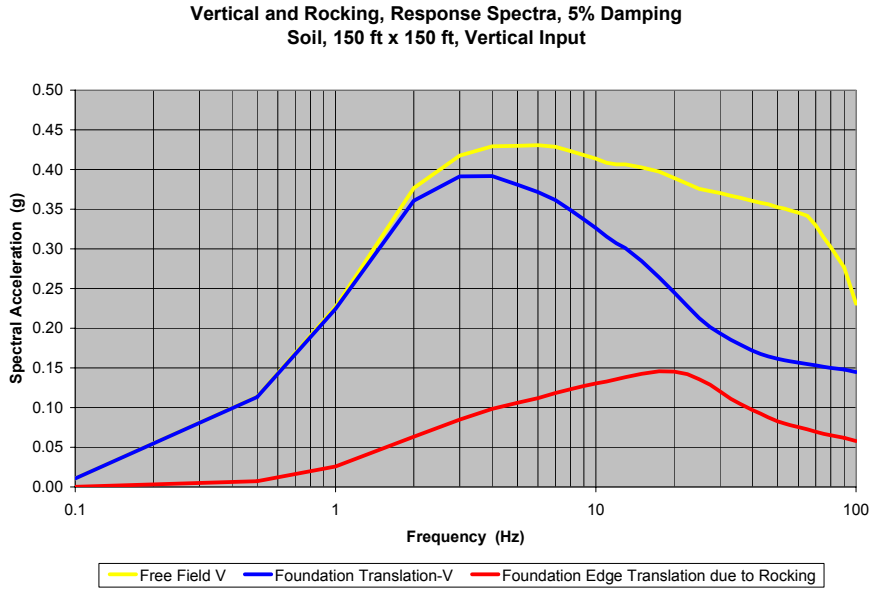


**Figure 4-21**  
Response Spectra Including Rocking, Square Foundation, Soil Site

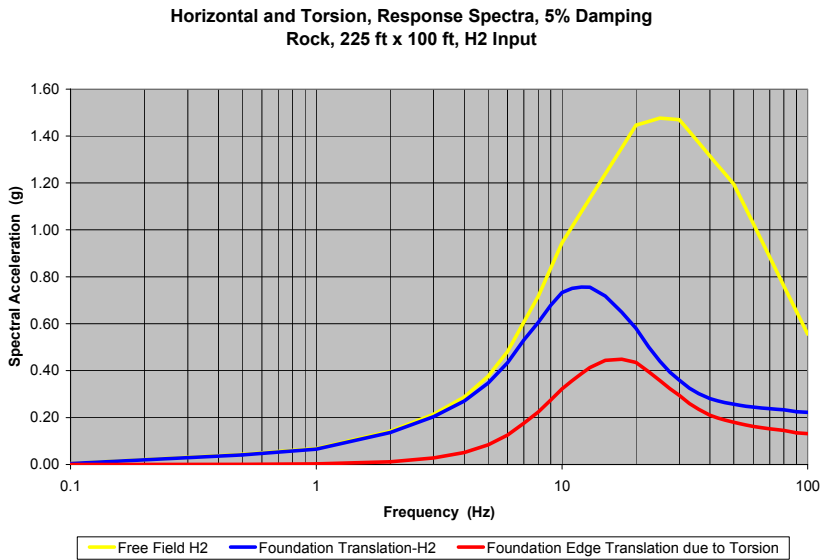


**Figure 4-22**  
Response Spectra Including Torsion, Rectangle Foundation, Rock Site

**Deleted:**  
*SSI and Structure Response*

**Deleted:**  
*SSI and Structure Response*

**Deleted:**  
*SSI and Structure Response*  
*SSI and Structure Response*

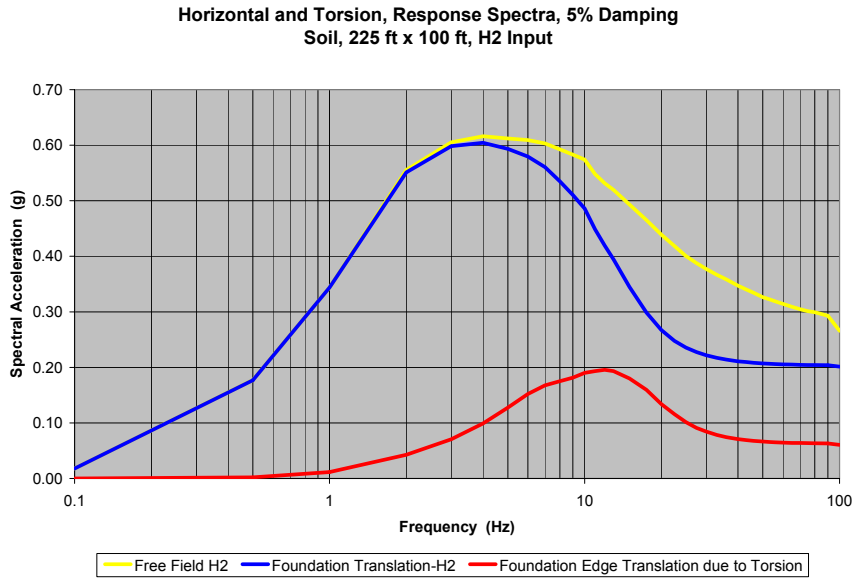


**Figure 4-23**  
**Response Spectra Including Torsion, Rectangle Foundation, Soil Site**

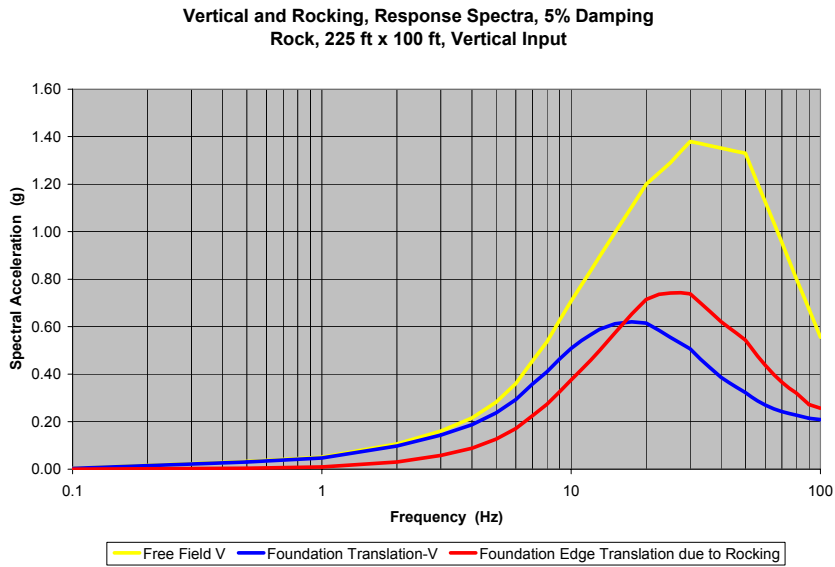


**Figure 4-24**  
**Response Spectra Including Rocking, Rectangle Foundation, Rock Site**

Deleted: SSI and Structure Response

Deleted: SSI and Structure Response

Deleted: SSI and Structure Response

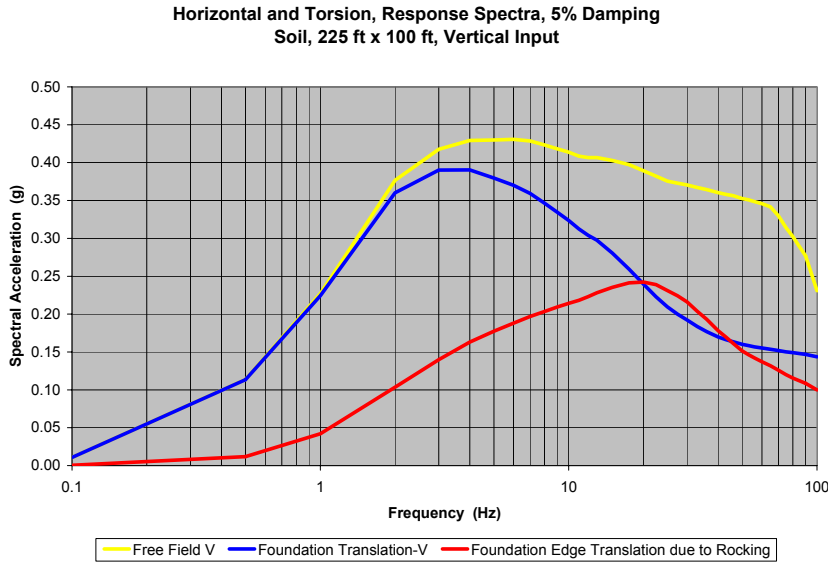


Figure 4-25  
Response Spectra Including Rocking, Rectangle Foundation, Soil Site

Effect of Torsion – The effect of incoherence-induced torsion on the foundation response is illustrated in Figures 4-18 and 4-19 for the square foundation, and Figures 4-22 and 4-23 for the rectangular foundation for rock and soil site conditions, respectively. For the rectangle foundation, torsion response was maximized by looking at the foundation edge that is 112.5-ft away from the foundation centerline. The effects of torsion are quantified by displaying the horizontal translation spectra at the foundation center and the response spectra of translational motion due to torsion at the foundation edge. The translation only and translation-torsion spectra must be combined in some manner such as SRSS or absolute sum depending on the phasing of incoherency-induced torsion relative to horizontal response due to horizontal ground motion. These spectra are not combined herein because the purpose of this section is only to understand the amplitude of incoherency induced rotations and not to compute total foundation response.

For the square foundation, Figures 4-18 and 4-19 indicate that translation induced by torsion is relatively small compared to the translation only spectra. For the square foundation on the rock site, the translation-torsion ZPA is about 30% of the ZPA for translational motion only. For this case, the translation only spectrum peaks at about 12 Hz and the translation-torsion spectrum peaks at about 18 Hz. At 12 Hz, the translation-torsion spectral acceleration is about 26% of the translation only spectral acceleration while at 18 Hz, the translation-torsion spectral acceleration is about 36% of the translation only spectral acceleration. For the square foundation on the soil site, the translation-torsion ZPA is about 14% of the ZPA for translational motion only. For this case, the translation only spectrum peaks at about 4 Hz and the translation-torsion spectrum peaks at about 13 Hz. At 4 Hz, the translation-torsion spectral acceleration is about 7% of the translation only spectral acceleration while at 13 Hz, the translation-torsion spectral acceleration

**Deleted:**  
*SSI and Structure Response*

**Deleted:**  
*SSI and Structure Response*

**Deleted:**  
*SSI and Structure Response*  
*SSI and Structure Response*

is about 23% of the translation only spectral acceleration. Incoherency-induced rotation is a high-frequency phenomenon and thus it is expected that it would have a smaller effect for lower frequency soil sites.

For the rectangular foundation, Figures 4-22 and 4-23 indicate that translation induced by torsion is a relatively large fraction of the translation only spectra. For this rectangle, torsion effects are amplified because the foundation edge at a large moment arm from the center is examined. For the rectangular foundation on the rock site, the translation-torsion ZPA is about 60% of the ZPA for translational motion only. For this case, the translation only spectrum peaks at about 12 Hz and the translation-torsion spectrum peaks at about 18 Hz. At 12 Hz, the translation-torsion spectral acceleration is about 50% of the translation only spectral acceleration while at 18 Hz, the translation-torsion spectral acceleration is about 70% of the translation only spectral acceleration. For the rectangular foundation on the soil site, the translation-torsion ZPA is about 30% of the ZPA for translational motion only. For this case, the translation only spectrum peaks at about 4 Hz and the translation-torsion spectrum peaks at about 12 Hz. At 4 Hz, the translation-torsion spectral acceleration is about 16% of the translation only spectral acceleration while at 12 Hz, the translation-torsion spectral acceleration is about 47% of the translation only spectral acceleration. Again, incoherency-induced rotation response is less significant for the lower frequency soil site.

Figures 4-18 and 4-22 for the high-frequency rock site, demonstrate that there are significant reductions due to incoherence even considering the added translational response at extreme locations due to torsion. This conclusion is apparent by comparison of the free-field spectra to the translation and torsion spectra no matter whether SRSS or absolute summation would be used. Even so, the contribution of additional torsion due to ground motion incoherence appears to be generally greater than what can be accommodated by considering 5% accidental eccentricity per ASCE 4.

Effect of Rocking - The effect of incoherence-induced rocking on the foundation vertical response is illustrated in Figures 4-20 and 4-21 for the square foundation, and Figures 4-24 and 4-25 for the rectangular foundation for rock and soil site conditions, respectively. For the rectangular foundation, rocking response was also maximized by looking at the foundation edge that is 112.5-ft away from the foundation centerline. The effects of rocking are quantified by displaying the vertical translation spectra at the foundation center and the response spectra of translational motion due to rocking at the foundation edge. The translation only and translation-rocking spectra must be combined in some manner such as SRSS or absolute sum depending on the phasing of incoherency-induced rocking relative to vertical response due to vertical ground motion. Again, these spectra are not combined herein because the purpose of this section is only to understand the amplitude of incoherency induced rotations and not to compute total foundation response.

For the square foundation, Figures 4-20 and 4-21 indicate that translation induced by rocking is significant compared to the translation only spectra. For the square foundation on the rock site, the translation-rocking ZPA is about 68% of the ZPA for translational motion only. For this case, the translation only spectrum peaks at about 18 Hz and the translation-rocking spectrum peaks at about 25 Hz. At 18 Hz, the translation-rocking spectral acceleration is about 61% of the translation only spectral acceleration while at 25 Hz, the translation-rocking spectral acceleration

is about 74% of the translation only spectral acceleration. For the square foundation on the soil site, the translation-rocking ZPA is about 40% of the ZPA for translational motion only. For this case, the translation only spectrum peaks at about 4 Hz and the translation-rocking spectrum peaks at about 20 Hz. At 4 Hz, the translation-rocking spectral acceleration is about 25% of the translation only spectral acceleration while at 20 Hz, the translation-rocking spectral acceleration is about 59% of the translation only spectral acceleration.

For the rectangular foundation, Figures 4-24 and 4-25 indicate that translation induced by rocking is even greater than the translation only spectra at some frequencies. For this rectangle, rocking effects are amplified because the foundation edge at a large moment arm from the center is examined. For the rectangular foundation on the rock site, the translation-rocking ZPA is about 23% greater than the ZPA for translational motion only. For this case, the translation only spectrum peaks at about 18 Hz and the translation-rocking spectrum peaks at about 28 Hz. At 18 Hz, the translation-rocking spectral acceleration is about equal to the translation only spectral acceleration while at 28 Hz, the translation-rocking spectral acceleration is about 40% greater than the translation only spectral acceleration. For the rectangular foundation on the soil site, the translation-rocking ZPA is about 70% of the ZPA for translational motion only. For this case, the translation only spectrum peaks at about 4 Hz and the translation-rocking spectrum peaks at about 20 Hz. At 4 Hz, the translation-rocking spectral acceleration is about 42% of the translation only spectral acceleration while at 20 Hz, the translation-rocking spectral acceleration is about equal to the translation only spectral acceleration. From 20 to 40 Hz, the translation-rocking spectrum is as much as 13% greater than the translation only spectrum.

Figures 4-20 and 4-24 demonstrate for the rock site that there are generally reductions due to incoherence even considering the added translational response at extreme locations due to rocking. This conclusion is apparent by comparison of the free-field spectra to the translation and torsion spectra no matter whether SRSS or absolute summation would be used. For the rectangular foundation, the translation plus rocking spectrum combined by absolute summation could exceed the spectrum for coherent motion at frequencies near 10 Hz. This behavior in which incoherent response from translation and incoherency-induced rotations exceeds the coherent response is observed at some locations in the SSI analysis results presented in Chapter 5.

The contribution of additional rocking due to ground motion incoherence produces a significantly higher foundation motion at the extremities of the foundation than the vertical motion of the foundation center. These results demonstrate that it is still worthwhile to pursue high-frequency reductions of ground motion due to incoherence but the effects of incoherence-induced rotations must be considered. Further evaluations of this point are presented in Chapter 5.

**Deleted:**  
*SSI and Structure Response*

**Deleted:**  
*SSI and Structure Response*

**Deleted:**  
*SSI and Structure Response*  
*SSI and Structure Response*

# 5

## SSI AND STRUCTURE RESPONSE

---

### General

The effect of ground motion incoherence on the response of rigid, massless foundations was treated in Chapter 4. These effects were presented as transfer functions between the free-field ground motion and the response of the rigid, massless foundations. In addition, the effect of incoherence was demonstrated by comparison of the response spectra on the foundation to the free-field ground response spectra. The transfer functions were denoted Incoherency Transfer Functions (ITFs).

Chapter 5 investigates the effects of incoherence of ground motion on the response of a nuclear power plant structure. The structure being analyzed is a simplified model based on some of the AP1000 properties (described in Chapter 2). Note the structure model is comprised of three sticks with limited inter-connectivity at upper elevations. The structure is anchored to a 15-ft thick, 150-ft square foundation. For the cases including soil-structure interaction (SSI), the rock site profile described in Chapter 2 was used. The free-field ground motion of interest is that motion compatible with the rock site profile, i.e., exhibiting significant high-frequency motion. For all analyses, the spectrum compatible time histories defined the free-field ground motion. All analyses considered 3 directions of simultaneous earthquake input motion.

In addition to evaluating the effects of incoherence on the response of the structure, a simplified method to incorporate seismic wave incoherence into seismic analysis of NPP structures, including SSI was investigated. Analyses described in this chapter are performed to demonstrate that the simplified approach of multiplying the Fourier amplitude of the input ground motion by a function derived from the ITF is a valid although conservative approach to accounting for incoherency of ground motion. This function takes into account translational and rotation effects of incoherency to form an engineering modified input motion.

Four sets of analyses have been performed for the example structural model:

1. SSI analysis with coherent input motion (dark blue curves in all Chapter 5 response spectra figures)
2. SSI analysis with incoherent input motion
  - a. Rigorous (direct) approach including all components of foundation input motion (three translations and three rotations) (green curves in all Chapter 5 response spectra curves)
  - b. Rigorous (direct) approach excluding rotational foundation input motion (red curves in all Chapter 5 response spectra figures)

3. SSI analysis with input motion modified by Incoherency Transfer Function (Simplified Approach) (light blue and yellow curves in all Chapter 5 response spectra curves)

It is recognized that rotations (torsion and rocking) are induced by incoherence as discussed in Chapter 4. To assess the impact of these rotations on structure response in a full SSI analysis as is conducted in this chapter, the rigorous SSI analysis with incoherent input motion is performed in two ways, Analyses 2a and 2b. In Analysis 2a, the effect of rotations will be realized in the SSI analysis. In Analysis 2b, the effect of rotations is deliberately eliminated for the purpose of assessing the rotation effects.

To evaluate the effects of incoherency on in-structure response, response spectra were calculated and compared for the various analyses at the tops of the structure sticks, at lower elevations on the structure sticks, and on outriggers extending 65 or 75-ft. from the top of each stick in the X direction (these dimensions were selected to approximately correspond to the AP1000 design dimensions). To evaluate the effects of induced rocking, the responses on the structure mass center and on the outrigger were used; to evaluate the effects of induced torsion, the responses on the outriggers were used.

Induced rocking due to vertical ground motion incoherence and induced torsion due to horizontal ground motion incoherence are considered. Their effect on vertical and horizontal response in the structure is presented.

### **SSI and Incoherence – Direct Method**

The results of Analyses 1 and 2 are presented here including SSI coherent and incoherent evaluations. The SSI incoherent analyses incorporate seismic wave incoherency through the scattering matrix populated by the incoherency transfer functions generated for the rock site and for the rigid massless foundation of 150-ft square. In this manner, incoherence is directly incorporated into the seismic analysis. In Analysis 2a, all terms of the scattering matrix are included, translations and rotations. In Analysis 2b, the rotational terms of the scattering matrix are set to zero.

As discussed more fully in Chapter 2, the fixed-base modes of the three structure sticks provide some insight into the dynamic behavior. The ASB has predominate modes with frequencies less than 10 Hz with fundamental modes in the horizontal directions of 3.2 Hz (X-direction) and 3.0 Hz (Y-direction); the fundamental mode in the vertical direction of frequency 9.9 Hz (Z-direction). Many modes participate in the response of the ASB. The predominate modes of the SCV in the horizontal directions also have frequencies less than 10 Hz – the lowest frequency of an important X-direction mode being 5.5 Hz; Y-direction mode being 6.14 Hz; the lowest frequency of an important vertical mode being 16 Hz. As with the ASB, many modes participate in the response of the SCV. The predominant modes of the CIS have frequencies greater than 10 Hz. Many modes participate in the response of the CIS.

The total mass of the structures is apportioned approximately ASB – 86%, CIS – 11%, and SCV – 3%, i.e., ignoring the mass of the foundation. The dynamic behavior of the three stick model is

**Deleted:**  
*SSI and Structure Response*

**Deleted:**  
*SSI and Structure Response*

**Deleted:**  
*SSI and Structure Response*  
*SSI and Structure Response*

**Deleted:**  
*SSI and Structure Response*

**Deleted:**  
*SSI and Structure Response*

**Deleted:**  
*SSI and Structure Response*

coupled through the inter-connectivity of the sticks and natural torsion is induced throughout the three structures due to the eccentricities assumed in the ASB and CIS structures.

Results presented are in-structure response spectra (5% damping) at the foundation and at points on each of the three models (ASB, SCV, CIS) as shown in Figure 5-1. Responses at the top of each model and at approximately mid-height (referred to as “low on” a particular structure within Figure 5-1), are calculated and compared. The near mid-height locations were selected to investigate the potential effect of incoherence on points where higher modes more fully participate in the response. Note that the ASB stick represents both the auxiliary building and the shield building. The combined auxiliary and shield building extends up to the top of the auxiliary building at Node 120. Above this node and elevation the ASB stick only represents the shield building. Hence, in addition to the top of the shield building and low in the combined ASB model, output was calculated and is presented at the top of the auxiliary building at the centerline (Z-direction), at the center of mass for the horizontal directions (X and Y), and at the outrigger (X, Y, Z).

In addition to foundation response, results are presented at Nodes 310, 310out, 120mc, 120out, and 80mc on the ASB, Nodes 417, 417out and 406 on the SCV, and Nodes 538mc, 538out, and 535mc on the CIS where node locations are illustrated in Figures 5-1 and 2-8. The “mc” designation added to the node number indicates that the mass and shear centers are not coincident and response is given at the mass center. The “out” designation added to the node number indicates an outrigger location used to display torsional response at the periphery of the structure. In-structure response spectra at these twelve locations for two horizontal, X and Y, and the vertical direction, Z, of ground motion are presented in Figures 5-2 through 5-37. Again, all analyses considered 3 directions of simultaneous earthquake input motion.

### **Foundation Response**

Foundation response is presented in Figures 5-2, 5-3, and 5-4. Comparing the foundation response spectra due to incoherency effects (Analysis 2a) with those of Analysis 1, generally shows significant reductions over those due to coherent SSI effects at frequencies greater than 10 Hz. Spectral accelerations are reduced by a factor of 1.5 to 3 over significant frequency ranges.

Comparison of the full incoherent results (Analysis 2a – green curve) with those excluding rotational effects (Analysis 2b – red curve) provides an indication of the effects of induced rotations on foundation response at its center. Any observed change in foundation response is due to the effects of the complete SSI phenomena (kinematic and inertial effects) of the rock structure system. For the foundation response, induced rotations have minimal effects on the horizontal response spectra. Relatively small perturbations about the full incoherent results are present for frequencies between 8 and 30 Hz where Analyses 2a and 2b ZPA values are coincident. In the vertical direction, there is no significant effect of rotations on the foundation response.

**Deleted:**  
*SSI and Structure Response*

**Deleted:**  
*SSI and Structure Response*

**Deleted:**  
*SSI and Structure Response*

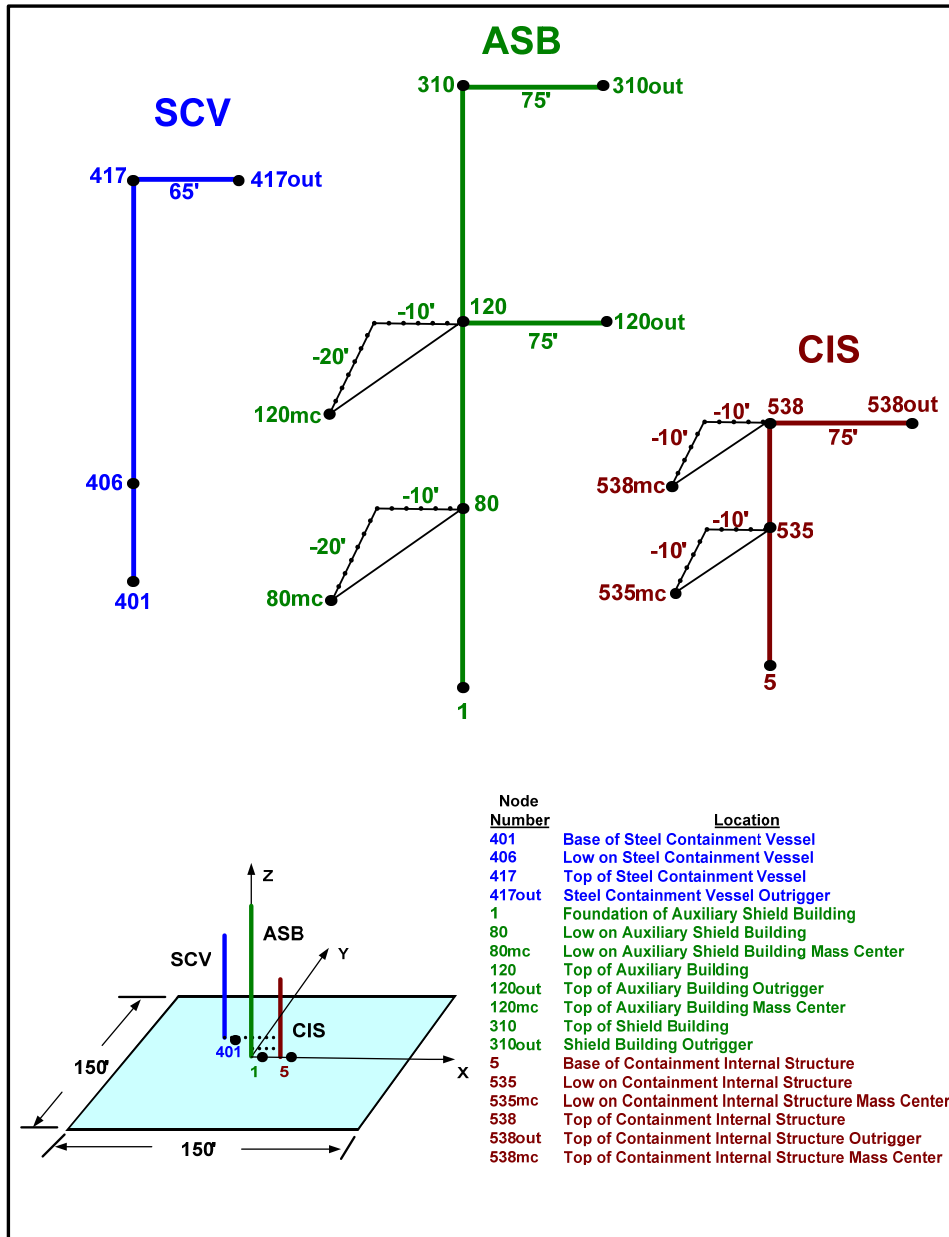


**Figure 5-1**  
**Locations on the AP1000-Based Stick Model Where In-Structure Response Spectra are Computed**

**Deleted:**  
*SSI and Structure Response*

**Deleted:**  
*SSI and Structure Response*

**Deleted:**  
*SSI and Structure Response*  
*SSI and Structure Response*

## **Auxiliary and Shield Building (ASB)**

- **Top of Shield Building.** Responses at the top of the coupled auxiliary and shield building (ASB) are presented in Figures 5-5, 5-6, and 5-7. Comparing the response spectra due to incoherency effects (Analysis 2a) with those of Analysis 1, generally, shows significant reductions due to incoherency for frequencies greater than 12 Hz. For horizontal directions, the reductions are, generally, greater than 30% up to 30 Hz and less as one approaches the ZPA frequency. For the vertical direction, substantial reductions are observed in the frequency range above 10 Hz, including at the ZPA frequency.

At frequencies of peak amplification less than 10 Hz (X-direction 3.2 and 6.5 Hz; Y-direction 3 Hz and 6 Hz), slight increases in spectral accelerations of the incoherent case above the coherent case are observed. Comparing Analyses 2a and 2b, one concludes this effect is due to induced rotations.

The responses of the outrigger, extending 75-ft. in the X-direction, are presented in Figures 5-14, 5-15, and 5-16. The reductions in response spectral accelerations generally follow the trend of the values on the centerline, but the reductions are observed to be less. The effects of incoherence induced torsion are shown in Figure 5-15 Y-direction response, where the responses calculated due to coherence and incoherence (blue and green curves) are relatively close for frequencies above 12 Hz. The specific effect of induced torsion can be observed by comparing the no rotation case (red curves) with the full incoherence case (green curves).

For this relatively low-frequency structure, additional horizontal response induced by rocking is observed only in the low-frequency range, i.e., at about 3 Hz. At frequencies of peak amplification less than 10 Hz (X-direction 3.2 and 6.5 Hz; Y-direction 3 Hz and 6 Hz), slight increases in spectral accelerations of the incoherent case above the coherent case are observed. The same phenomena observed above for frequencies less than 10 Hz is present on the outrigger, i.e., at frequencies of peak amplification, the incoherent response exceeds the coherent response. This is due to induced torsional response.

- **Top of Auxiliary Building.** Responses at the top of the auxiliary building are presented in Figures 5-8, 5-9, 5-10. In the X-direction, significant reductions due to incoherence are observed for frequencies greater than about 14 Hz to the ZPA frequency where the coherent and incoherent responses are the same. In the Y-direction, very significant reductions in the response are observed for frequencies greater than 10 Hz up to and including the ZPA. There are no observed low-frequency exceedances of the incoherent responses at this location.

The responses of the outrigger, extending 75-ft. in the X-direction, are presented in Figures 5-17, 5-18, and 5-19. The reductions in response spectral accelerations generally follow the trend of the values of the points at the mass centers, but the reductions are observed to be less. The effects of incoherence induced rocking and torsion is observed for the X-direction in Figure 5-15 and in Figure 5-16 for the Y-direction response.

**Deleted:**  
*SSI and Structure Response*

**Deleted:**  
*SSI and Structure Response*

**Deleted:**  
*SSI and Structure Response*  
*SSI and Structure Response*

- **Low in ASB.** Responses at a lower elevation of the coupled auxiliary and shield building (ASB) are presented in Figures 5-11, 5-12, and 5-13. These spectra demonstrate similar behavior to that seen at other locations in the ASB. Generally, the response reductions in the vertical direction are significant for frequencies greater than 10 Hz.

### **Steel Containment Vessel (SCV)**

- **Top of SCV.** Response at the top of the steel containment vessel (SCV) at the centerline is presented in Figures 5-20, 5-21, and 5-22. Comparing the response spectra due to incoherency effects (Analysis 2a) with those of Analysis 1, generally, show significant reductions in response for frequencies greater than about 12 Hz with less reductions at the ZPA. In the vertical direction, significant reductions are observed for all frequencies greater than 10 Hz. There are also no significant effects of induced rocking observed from these spectra.

The responses of the outrigger extending 75-ft in the X direction from the top of the steel containment vessel (SCV) are presented in Figures 5-26, 5-27, and 5-28. Significant reductions in response spectral accelerations are observed for frequencies greater than about 12 Hz in the X-direction and about 15 Hz in the Y-direction. Significant reductions in the vertical direction are observed for frequencies greater than about 12 Hz.

The effects of induced rotations are observed in the response spectra of Figure 5-27 when comparing the results due to Analyses 2a and 2b. Induced torsion is significant in the response for frequencies greater than 10 Hz. There are no rotational effects seen in the X-direction as the response spectra in Figures 5-20 and 5-26 are nearly identical. This is expected since the outrigger is placed on the X-axis and is considered to be representative of results away from the centers of mass of the structure. There are no effects of torsion seen in Z-direction response in Figure 5-28. Z direction outrigger response in Figure 5-28 is higher than center of mass response due to rocking. This rocking is structural seismic response and not due to incoherence.

- **Low in the SCV.** Responses at lower elevations of the steel containment vessel (SCV) are presented in Figures 5-23, 5-24, and 5-25. These spectra demonstrate similar behavior to that seen for the top of the SCV.

### **Containment Internal Structure (CIS)**

- **Top of CIS.** Responses at the top of the containment internal structure (CIS) at the center of mass are presented in Figures 5-29, 5-30, and 5-31. Comparing the response spectra due to incoherency effects (Analysis 2a) with those of Analysis 1, generally, shows significant reductions over those due to coherent SSI effects at frequencies greater than about 12 Hz. These reductions are 50% or greater. Compared to the SSI coherent ground motion case.

Responses of the outrigger extending 75-ft in the X direction from the top of the containment internal structure (CIS) are presented in Figures 5-35, 5-36, and 5-37. Significant reductions in response spectral accelerations are observed in all three directions at this location at frequencies greater than about 12 Hz. Reductions on the order of 40% and greater are observed.

Comparing the full incoherent results (Analysis 2a - green curve) with those excluding rotational effects (Analysis 2b – red curve) provides an indication of the effects of induced rotations on the CIS response. At the center of mass, the effect of induced rocking is observed to be significant in the frequency range of 12-25 Hz. These phenomena are due to induced rocking exciting horizontal modes. At the outrigger location, in the X- and Z- directions, the effects of induced rotations are observed in the frequency range above 10 Hz; in the Y-direction, the effect of induced rotations is due to the combination of torsion and rocking for frequencies greater than 10 Hz. Ignoring induced rotations under-estimates the response.

- **Low in the CIS.** Responses at lower elevations of the containment internal structure (CIS) are presented in Figures 5-32, 5-33, and 5-34. Generally, responses due to incoherence are significantly less than the case of coherent ground motions at frequencies greater than about 12 Hz. The importance of induced rotations is also evident from these plots.

### **Summary of Direct Method Results**

Figures 5-2 through 5-34 demonstrate significant reductions in high-frequency response as a result of seismic wave incoherence. In the horizontal response directions, these reductions in response spectra are tempered due to incoherency induced rocking and torsion. Even with this phenomena of incoherency induced rocking and torsion, the fundamental conclusion remains that there are significant reductions in high-frequency response due to seismic wave incoherence.

**Deleted:**  
*SSI and Structure Response*

**Deleted:**  
*SSI and Structure Response*

**Deleted:**  
*SSI and Structure Response*

Deleted: SSI and Structure Response

Deleted: SSI and Structure Response

Deleted: SSI and Structure Response

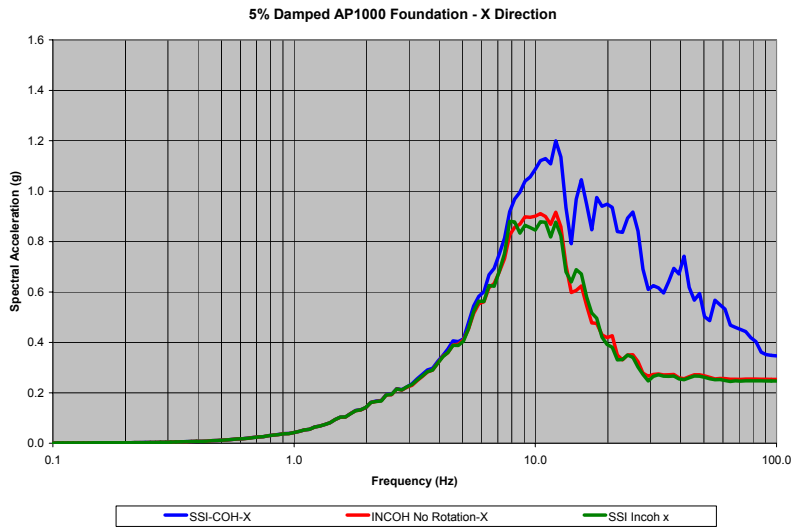


Figure 5-2 Foundation Response Spectra – X Direction –SSI Coherent, SSI Incoherent, SSI Incoherent with No Rotations (Node 1)

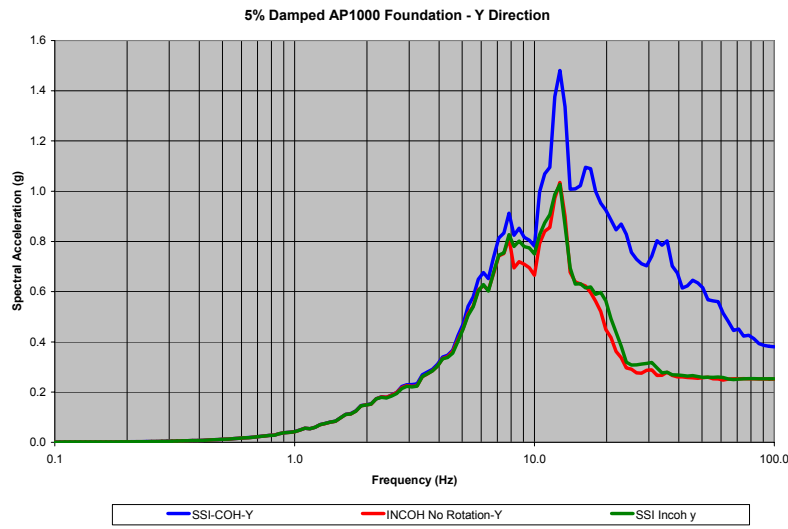
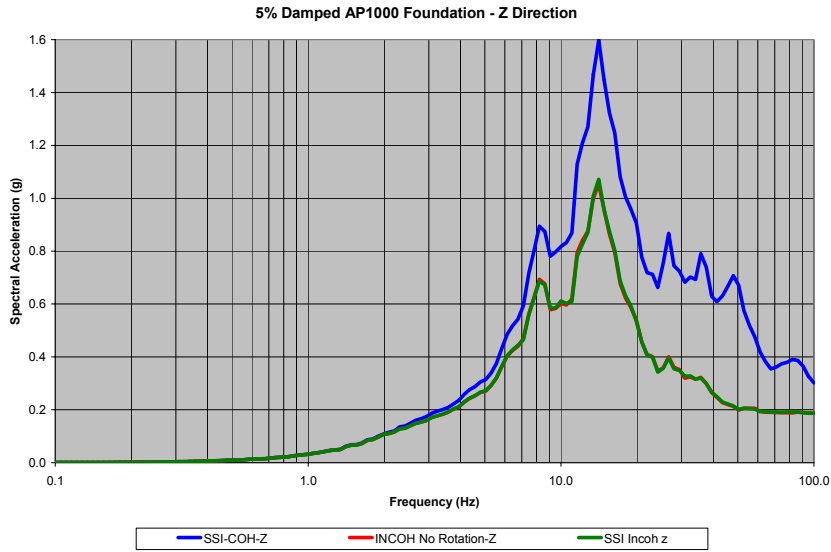


Figure 5-3 Foundation Response Spectra – Y Direction –SSI Coherent, SSI Incoherent, SSI Incoherent with No Rotations (Node 1)

**Deleted:**  
*SSI and Structure Response*

**Deleted:**  
*SSI and Structure Response*

**Deleted:**  
*SSI and Structure Response*  
*SSI and Structure Response*



**Figure 5-4**  
**Foundation Response Spectra – Z Direction –SSI Coherent, SSI Incoherent, SSI Incoherent with No Rotations (Node 1)**

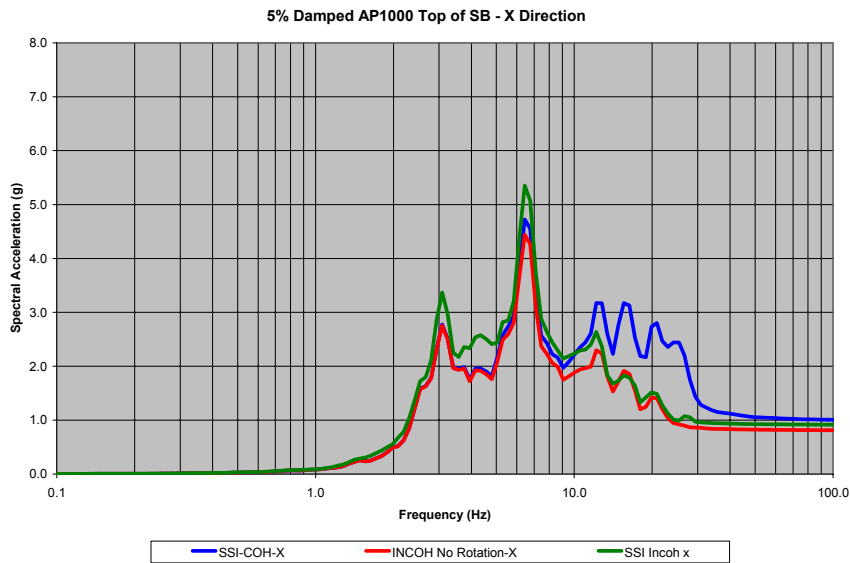


**Figure 5-5**  
**Top of Shield Building Response Spectra – X Direction –SSI Coherent, SSI Incoherent, SSI Incoherent with No Rotations (Node 310)**

Deleted: SSI and Structure Response

Deleted: SSI and Structure Response

Deleted: SSI and Structure Response

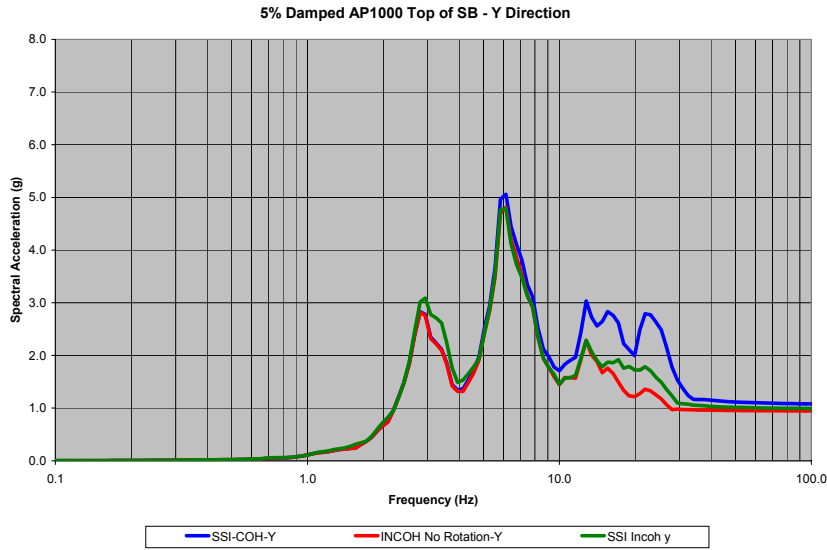


Figure 5-6  
Top of Shield Building Response Spectra – Y Direction –SSI Coherent, SSI Incoherent, SSI Incoherent with No Rotations (Node 310)

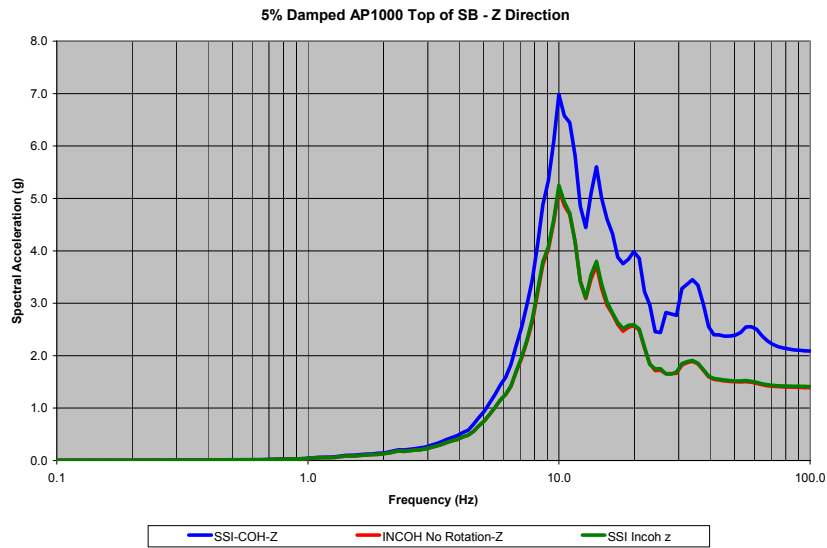
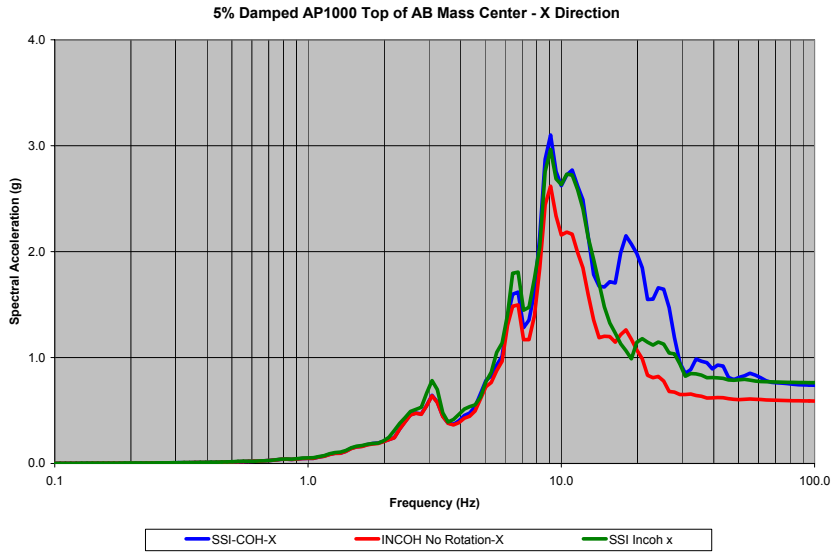


Figure 5-7  
Top of Shield Building Response Spectra – Z Direction –SSI Coherent, SSI Incoherent, SSI Incoherent with No Rotations (Node 310)

**Deleted:**  
*SSI and Structure Response*

**Deleted:**  
*SSI and Structure Response*

**Deleted:**  
*SSI and Structure Response*  
*SSI and Structure Response*



**Figure 5-8**  
Top of Auxiliary Building Response Spectra – X Direction –SSI Coherent, SSI Incoherent, SSI Incoherent with No Rotations (Node 120mc)

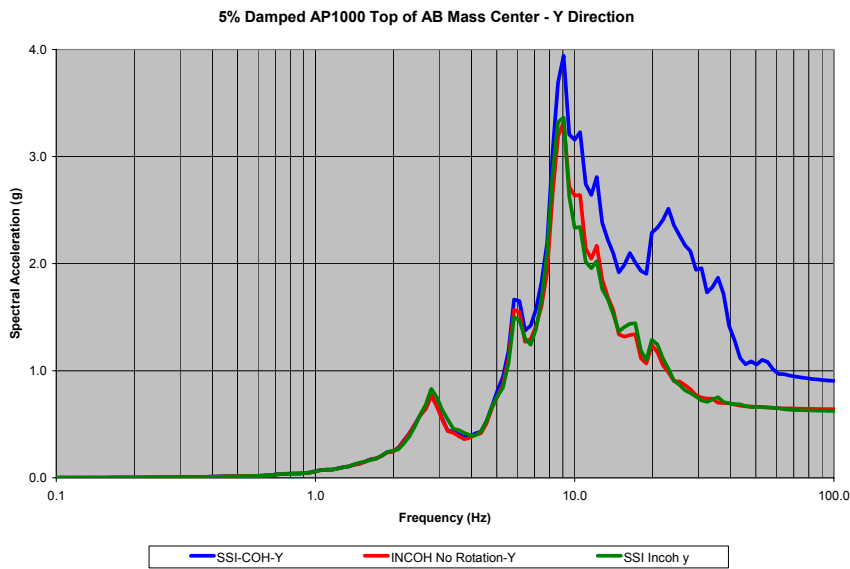


**Figure 5-9**  
Top of Auxiliary Building Response Spectra – Y Direction –SSI Coherent, SSI Incoherent, SSI Incoherent with No Rotations (Node 120mc)

Deleted: SSI and Structure Response

Deleted: SSI and Structure Response

Deleted: SSI and Structure Response

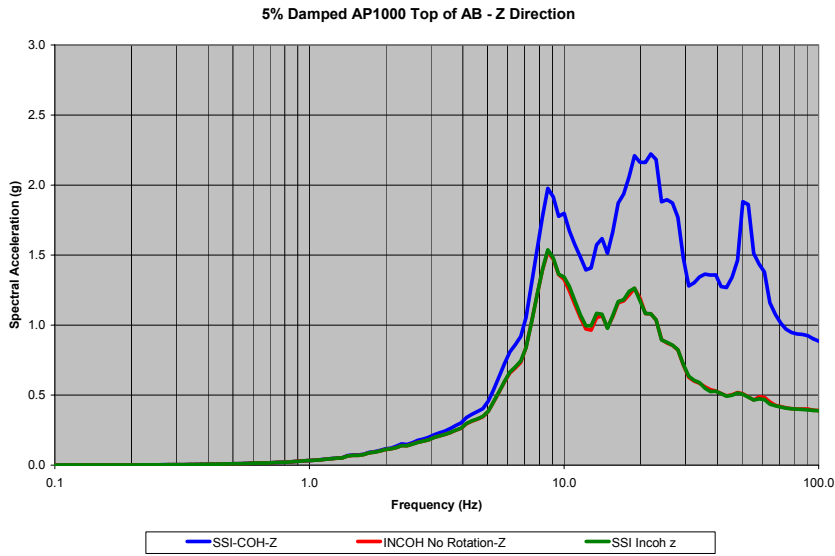


Figure 5-10  
Top of Auxiliary Building Response Spectra – Z Direction – SSI Coherent, SSI Incoherent, SSI Incoherent with No Rotations (Node 120)

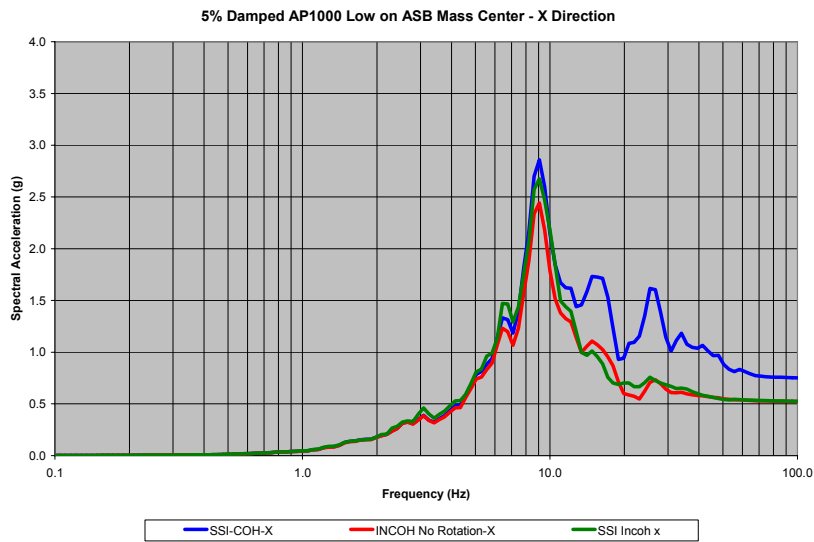
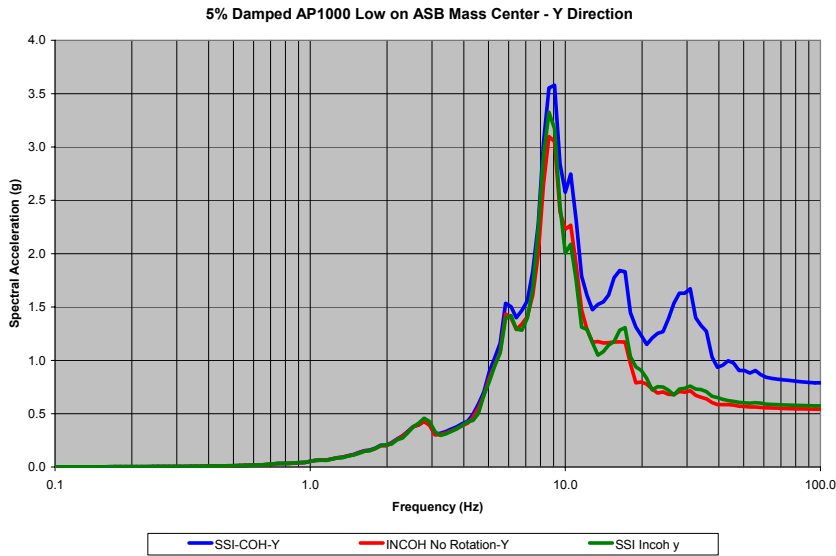


Figure 5-11  
Low on ASB Response Spectra – X Direction – SSI Coherent, SSI Incoherent, SSI Incoherent with No Rotations (Node 80mc)

**Deleted:**  
*SSI and Structure Response*

**Deleted:**  
*SSI and Structure Response*

**Deleted:**  
*SSI and Structure Response*  
*SSI and Structure Response*



**Figure 5-12**  
Low on ASB Response Spectra – Y Direction – SSI Coherent, SSI Incoherent, SSI Incoherent with No Rotations (Node 80mc)

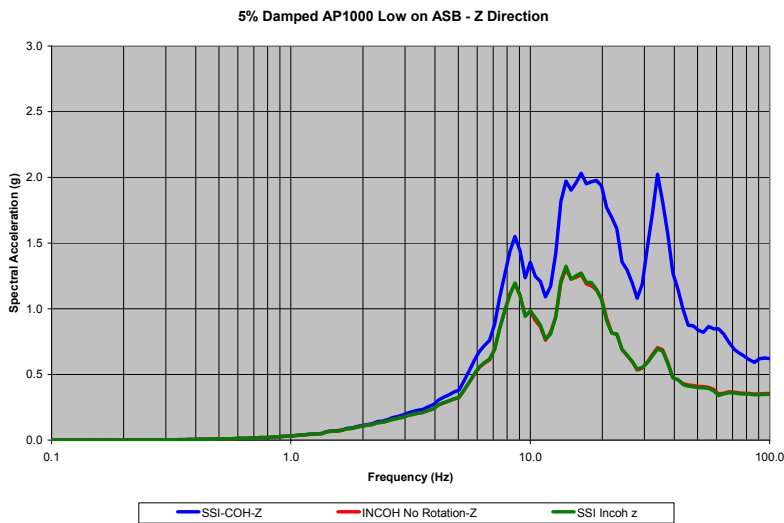


**Figure 5-13**  
Low on ASB Response Spectra – Z Direction – SSI Coherent, SSI Incoherent, SSI Incoherent with No Rotations (Node 80)

**Deleted:**  
*SSI and Structure Response*

**Deleted:**  
*SSI and Structure Response*

**Deleted:**  
*SSI and Structure Response*

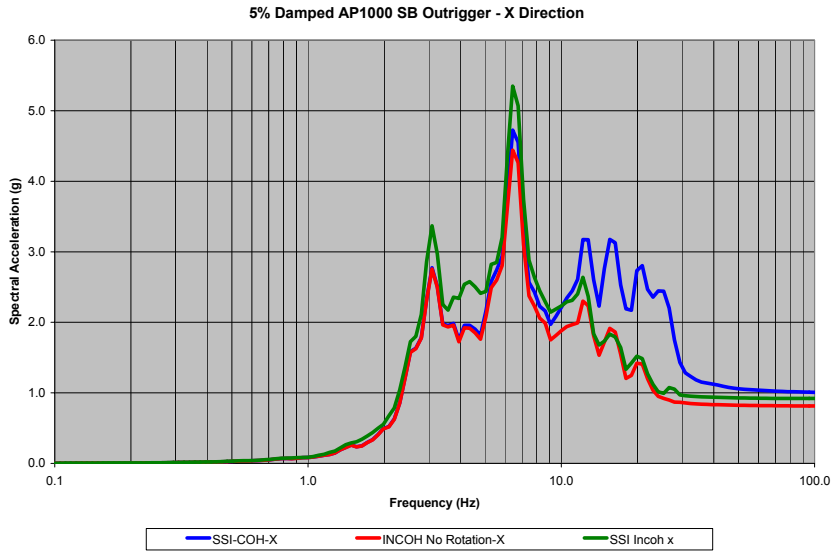


**Figure 5-14**  
**Shield Building Outrigger Response Spectra – X Direction – SSI Coherent, SSI Incoherent, SSI Incoherent with No Rotations (Node 310out)**

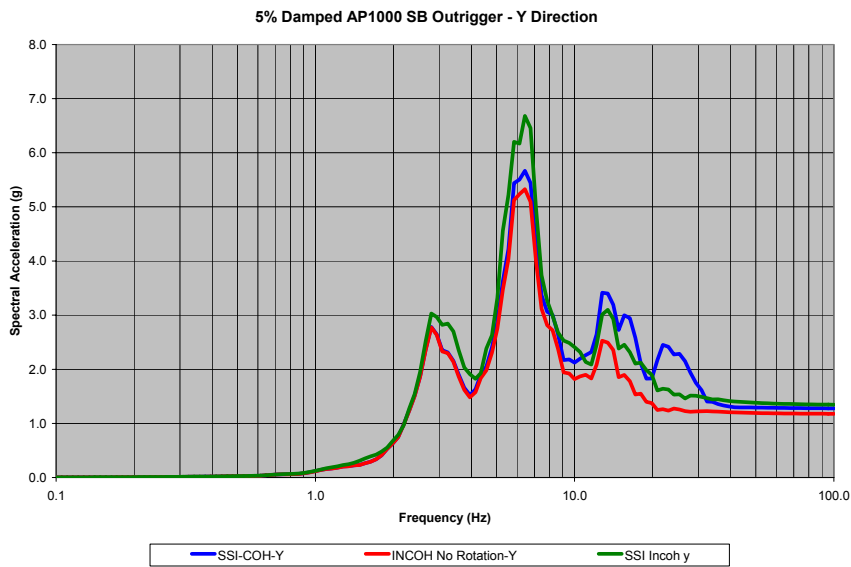


**Figure 5-15**  
**Shield Building Outrigger Response Spectra – Y Direction – SSI Coherent, SSI Incoherent, SSI Incoherent with No Rotations (Node 310out)**

Deleted: SSI and Structure Response

Deleted: SSI and Structure Response

Deleted: SSI and Structure Response  
SSI and Structure Response

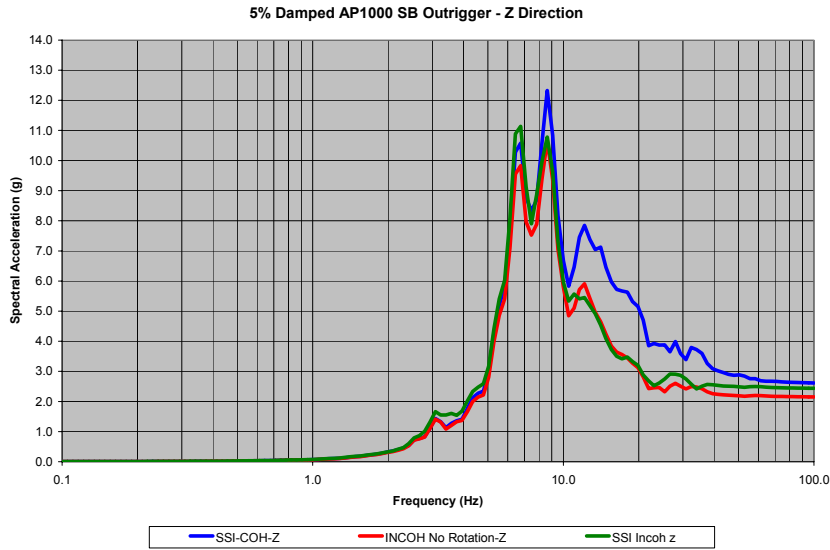


Figure 5-16  
Shield Building Outrigger Response Spectra – Z Direction – SSI Coherent, SSI Incoherent, SSI Incoherent with No Rotations (Node 310out)

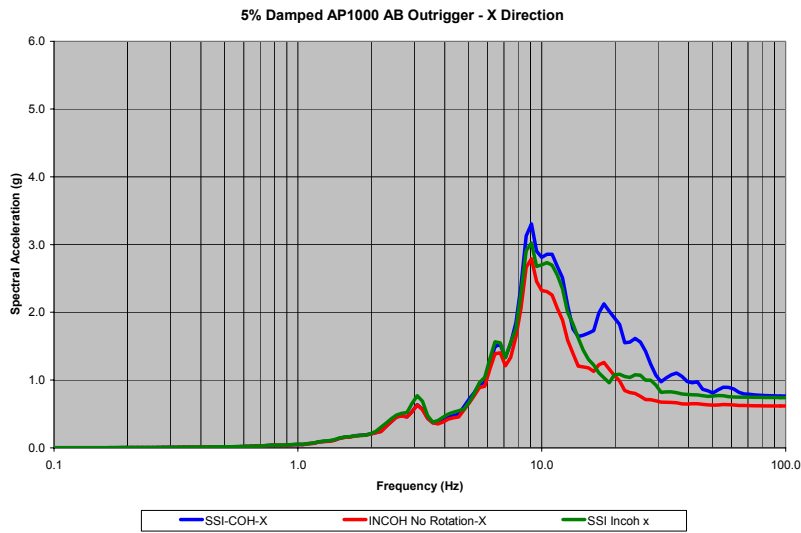


Figure 5-17  
Auxiliary Building Outrigger Response Spectra – X Direction – SSI Coherent, SSI Incoherent, SSI Incoherent with No Rotations (Node 120out)

Deleted: SSI and Structure Response

Deleted: SSI and Structure Response

Deleted: SSI and Structure Response

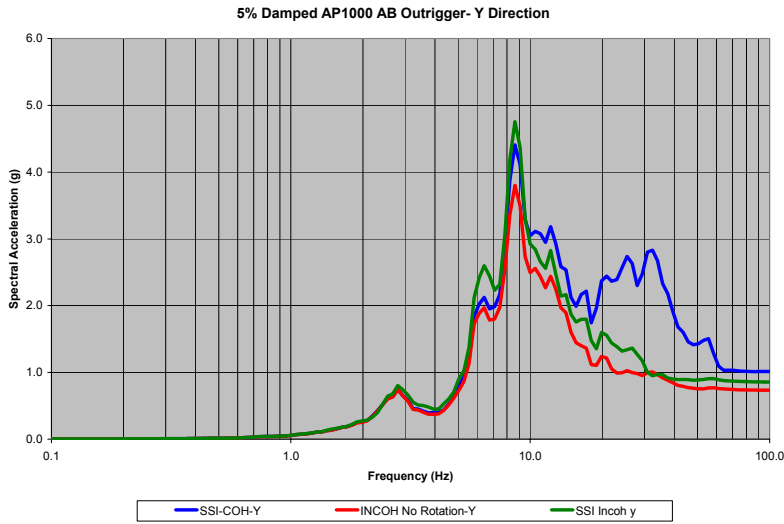


Figure 5-18  
Auxiliary Building Outrigger Response Spectra – Y Direction – SSI Coherent, SSI Incoherent, SSI Incoherent with No Rotations (Node 120out)

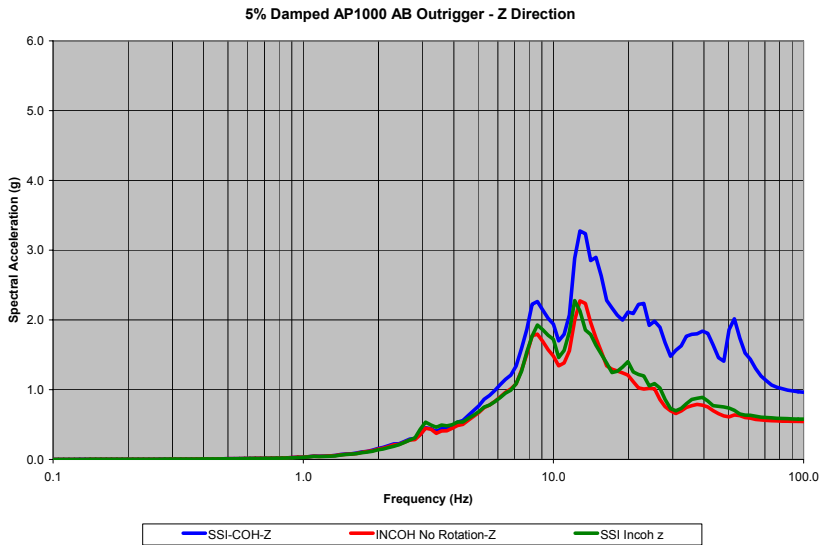
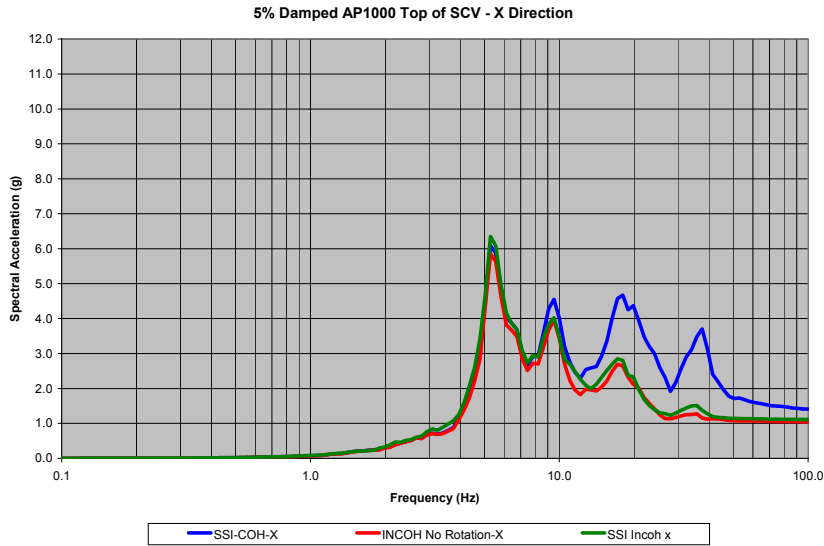


Figure 5-19  
Auxiliary Building Outrigger Response Spectra – Z Direction – SSI Coherent, SSI Incoherent, SSI Incoherent with No Rotations (Node 120out)

**Deleted:**  
*SSI and Structure Response*

**Deleted:**  
*SSI and Structure Response*

**Deleted:**  
*SSI and Structure Response*  
*SSI and Structure Response*



**Figure 5-20**  
**Top of SCV Response Spectra – X Direction –SSI Coherent, SSI Incoherent, SSI Incoherent with No Rotations (Node 417)**

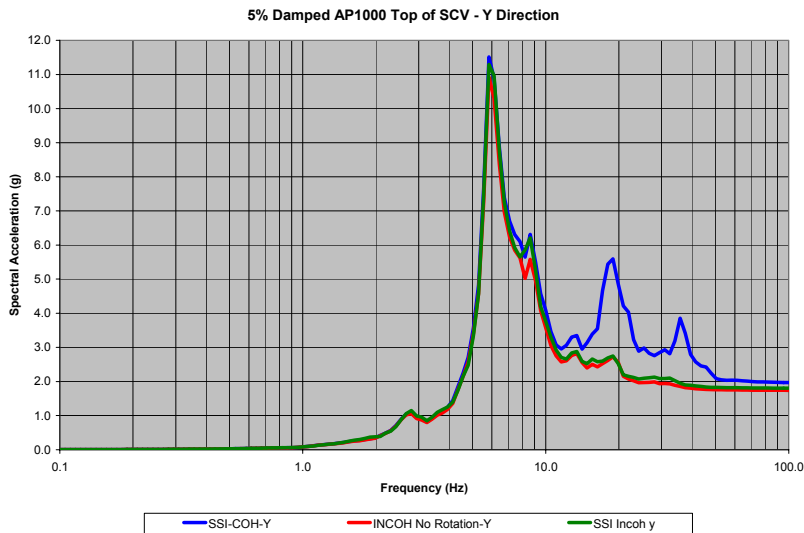


**Figure 5-21**  
**Top of SCV Response Spectra – Y Direction –SSI Coherent, SSI Incoherent, SSI Incoherent with No Rotations (Node 417)**

Deleted: SSI and Structure Response

Deleted: SSI and Structure Response

Deleted: SSI and Structure Response

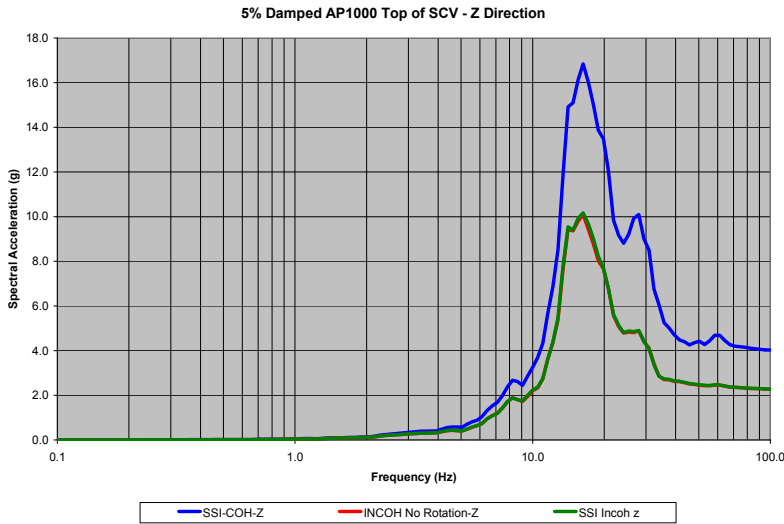


Figure 5-22  
Top of SCV Response Spectra – Z Direction – SSI Coherent, SSI Incoherent, SSI Incoherent with No Rotations (Node 417)

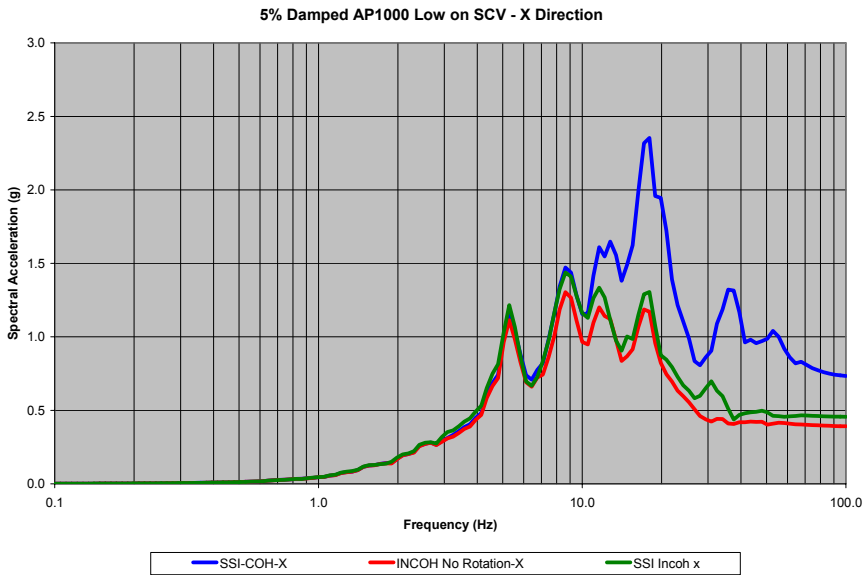


Figure 5-23  
Low on SCV Response Spectra – X Direction – SSI Coherent, SSI Incoherent, SSI Incoherent with No Rotations (Node 406)

Deleted:  
SSI and Structure Response

Deleted:  
SSI and Structure Response

Deleted:  
SSI and Structure Response  
SSI and Structure Response

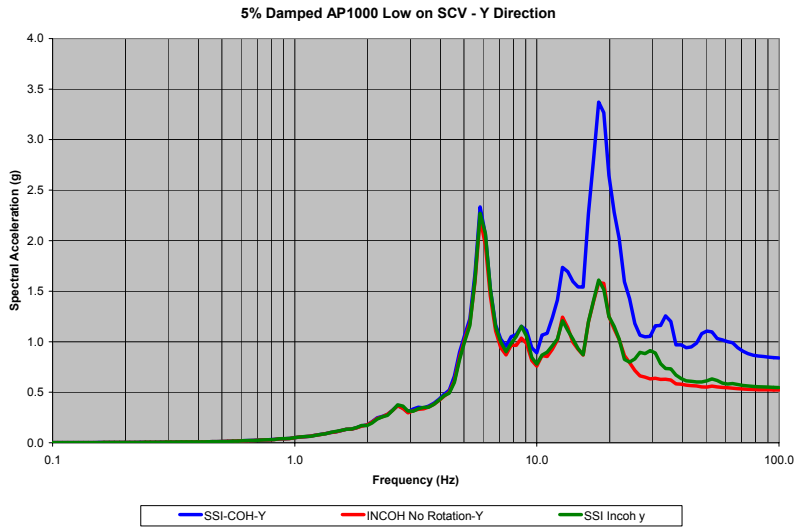


Figure 5-24  
Low on SCV Response Spectra – Y Direction – SSI Coherent, SSI Incoherent, SSI Incoherent with No Rotations (Node 406)

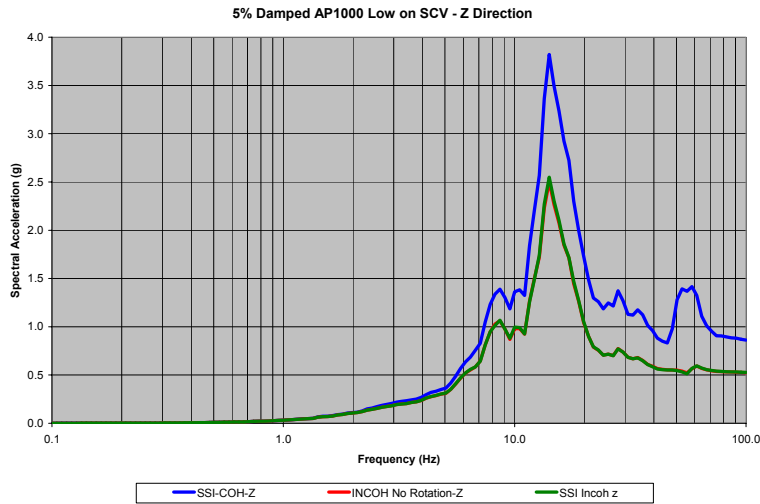


Figure 5-25  
Low on SCV Response Spectra – Z Direction – SSI Coherent, SSI Incoherent, SSI Incoherent with No Rotations (Node 406)

Note: The red SSI Incoh curve underlies the green INCOH No Rotation curve on this figure.

Deleted: SSI and Structure Response

Deleted: SSI and Structure Response

Deleted: SSI and Structure Response

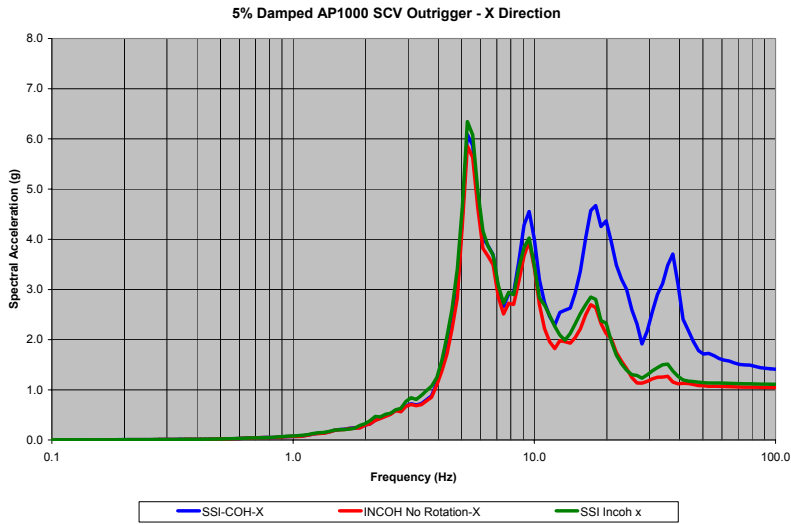


Figure 5-26  
SCV Outrigger Response Spectra – X Direction – SSI Coherent, SSI Incoherent, SSI Incoherent with No Rotations (Node 417out)

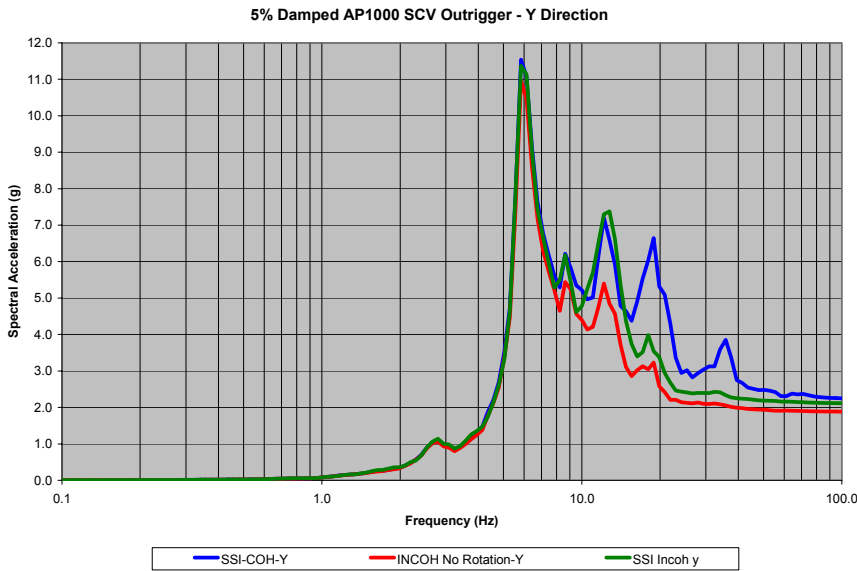
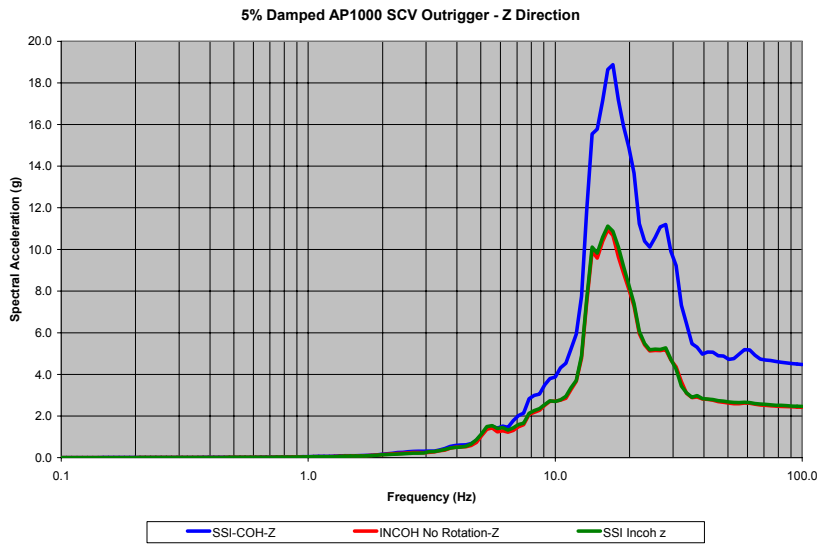


Figure 5-27  
SCV Outrigger Response Spectra – Y Direction – SSI Coherent, SSI Incoherent, SSI Incoherent with No Rotations (Node 417out)

**Deleted:**  
*SSI and Structure Response*

**Deleted:**  
*SSI and Structure Response*

**Deleted:**  
*SSI and Structure Response*  
*SSI and Structure Response*



**Figure 5-28**  
**SCV Outrigger Response Spectra – Z Direction – SSI Coherent, SSI Incoherent, SSI Incoherent with No Rotations (Node 417out)**

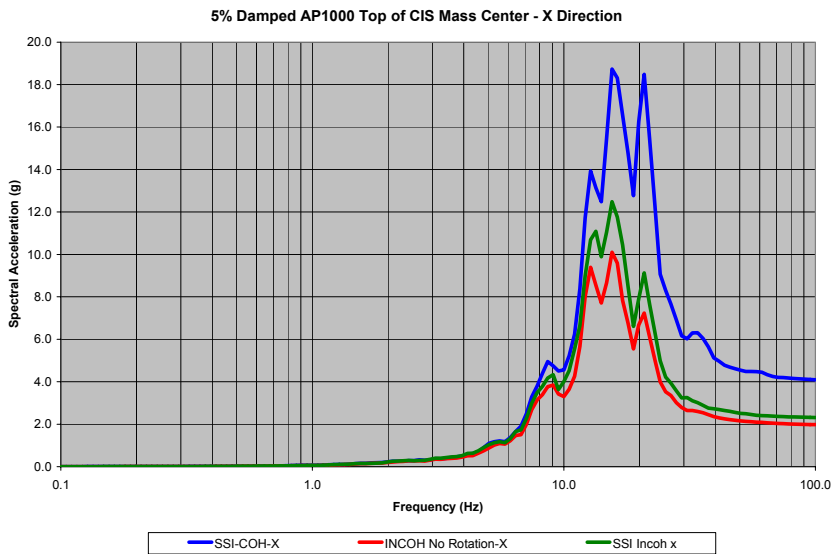


**Figure 5-29**  
**Top of CIS Response Spectra – X Direction – SSI Coherent, SSI Incoherent, SSI Incoherent with No Rotations (Node 538mc)**

Deleted: SSI and Structure Response

Deleted: SSI and Structure Response

Deleted: SSI and Structure Response

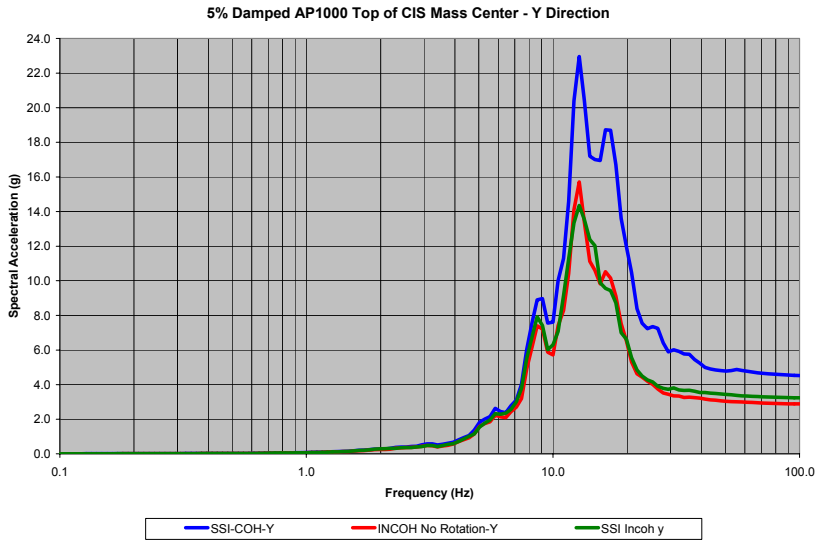


Figure 5-30  
Top of CIS Response Spectra – Y Direction –SSI Coherent, SSI Incoherent, SSI Incoherent with No Rotations (Node 538mc)

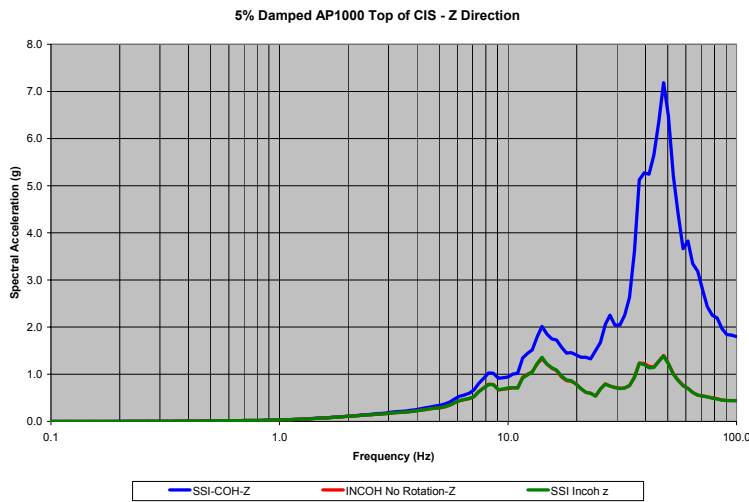


Figure 5-31  
Top of CIS Response Spectra – Z Direction –SSI Coherent, SSI Incoherent, SSI Incoherent with No Rotations (Node 538)

Note: The red SSI Incoh curve underlies the green INCOH No Rotation curve on this figure.

**Deleted:**  
*SSI and Structure Response*

**Deleted:**  
*SSI and Structure Response*

**Deleted:**  
*SSI and Structure Response*  
*SSI and Structure Response*

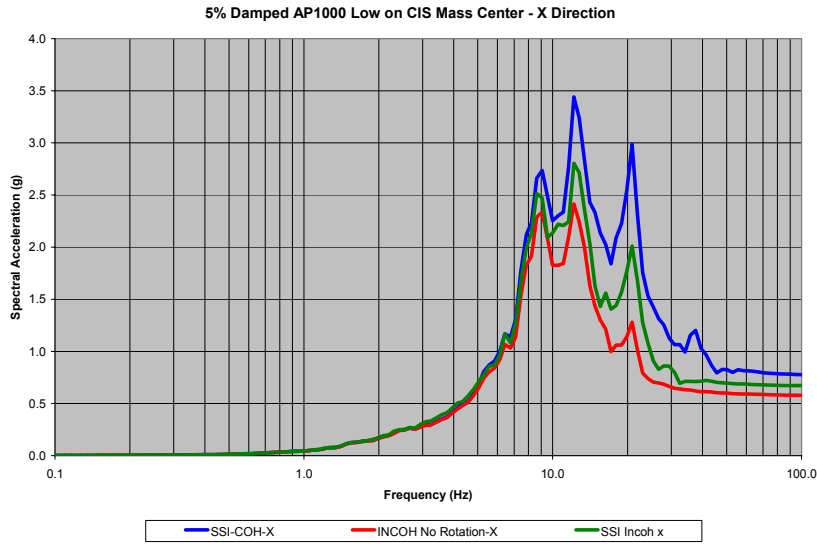


**Figure 5-32**  
**Low on CIS Response Spectra – X Direction –SSI Coherent, SSI Incoherent, SSI Incoherent with No Rotations (Node 535mc)**

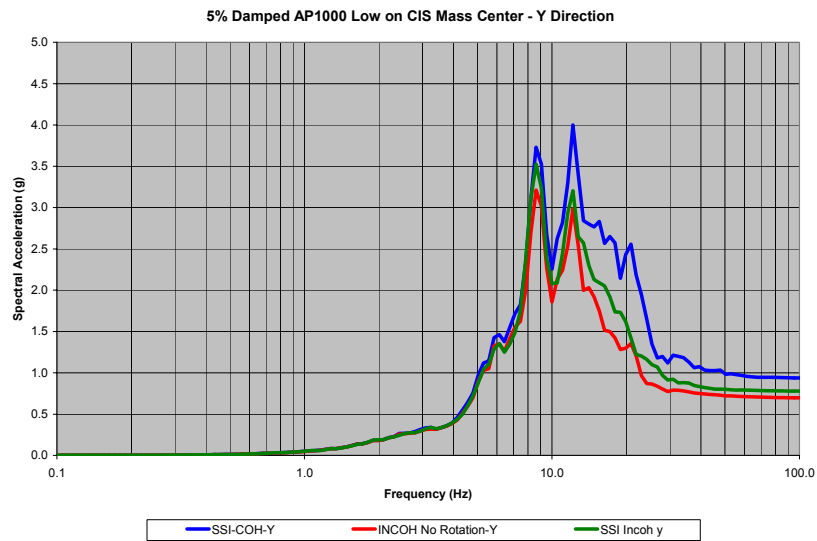


**Figure 5-33**  
**Low on CIS Response Spectra – Y Direction –SSI Coherent, SSI Incoherent, SSI Incoherent with No Rotations (Node 535mc)**

Deleted: SSI and Structure Response

Deleted: SSI and Structure Response

Deleted: SSI and Structure Response

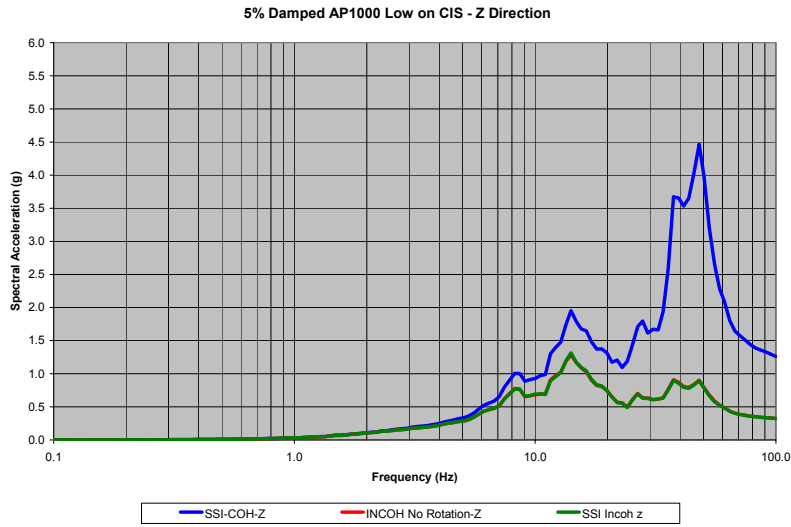


Figure 5-34  
Low on CIS Response Spectra – Z Direction – SSI Coherent, SSI Incoherent, SSI Incoherent with No Rotations (Node 535)

Note: The red SSI Incoh curve underlies the green INCOH No Rotation curve on this figure.

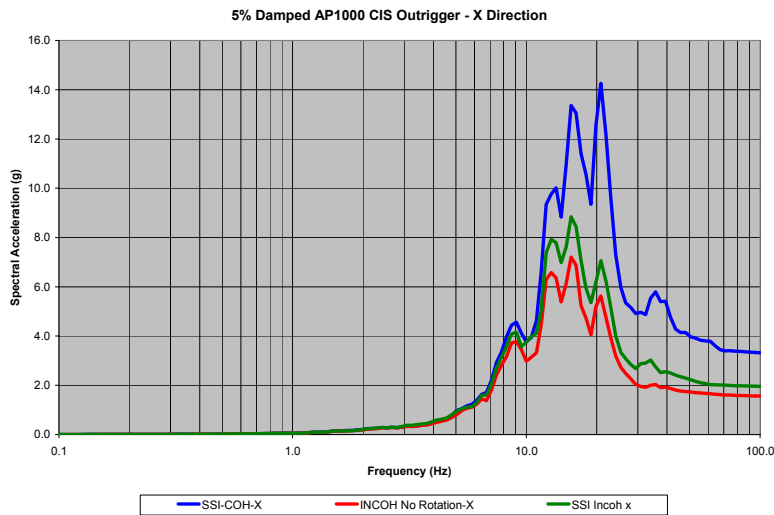
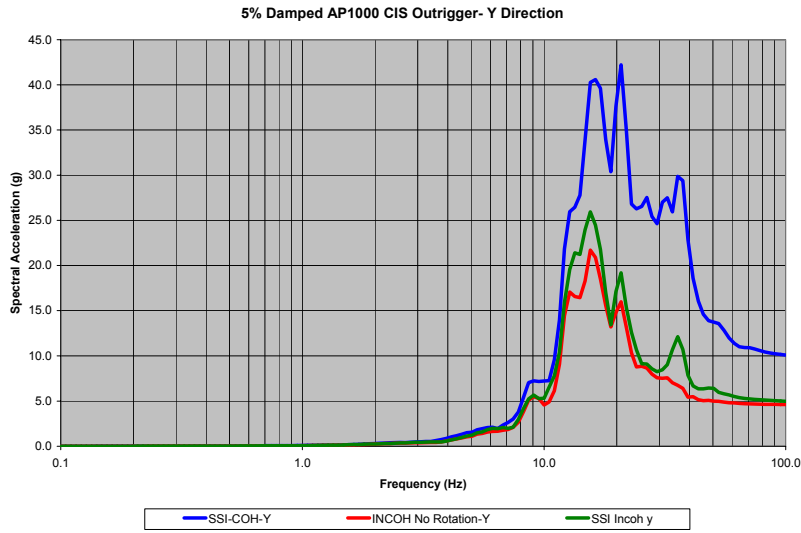


Figure 5-35  
CIS Outrigger Response Spectra – X Direction – SSI Coherent, SSI Incoherent, SSI Incoherent with No Rotations (Node 538out)

**Deleted:**  
*SSI and Structure Response*

**Deleted:**  
*SSI and Structure Response*

**Deleted:**  
*SSI and Structure Response*  
*SSI and Structure Response*



**Figure 5-36**  
**CIS Outrigger Response Spectra – Y Direction – SSI Coherent, SSI Incoherent, SSI Incoherent with No Rotations (Node 538out)**

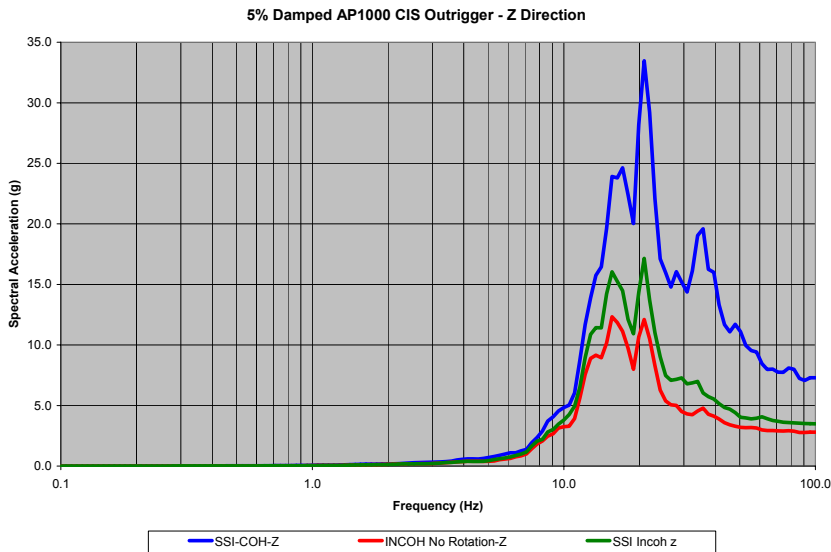


**Figure 5-37**  
**CIS Outrigger Response Spectra – Z Direction – SSI Coherent, SSI Incoherent, SSI Incoherent with No Rotations (Node 538out)**

Deleted: SSI and Structure Response

Deleted: SSI and Structure Response

Deleted: SSI and Structure Response

### SSI and Incoherence – Scaling Input Fourier Amplitude (Simplified Method)

An alternate and simplified means of incorporating seismic wave incoherence into seismic analyses is sought and discussed in this chapter. A simplified method for the representative structure/foundation model used within these incoherence studies is developed and implemented (Analysis 3 in the following section). Two candidate simplified methods were studied for this task and the results are depicted in the light blue and yellow curves on the response spectra that follow. The results of this simplified method are compared with the results generated by the direct or “exact” implementation (Analysis 2a, green curves). This alternative approach is to scale the Fourier amplitude spectrum of the free-field input motion by a function related to the Incoherency Transfer Function (ITF). The Fourier phase spectrum is unaffected. The result is a re-defined ground motion for SSI and dynamic structure analysis.

For illustration of the simplified method of analyses, the incoherency transfer function for the rock site profile and for the 150-ft square foundation footprint is used. This permits direct comparisons with the results presented earlier in this chapter. The incoherency transfer functions for horizontal and vertical motion as evaluated in Chapter 4 are shown as the dashed dark blue curves in Figures 5-38 and 5-39, respectively. Amplitudes of the Fourier transform of the free-field ground motion time histories were initially scaled by the ITF frequency-by-frequency.

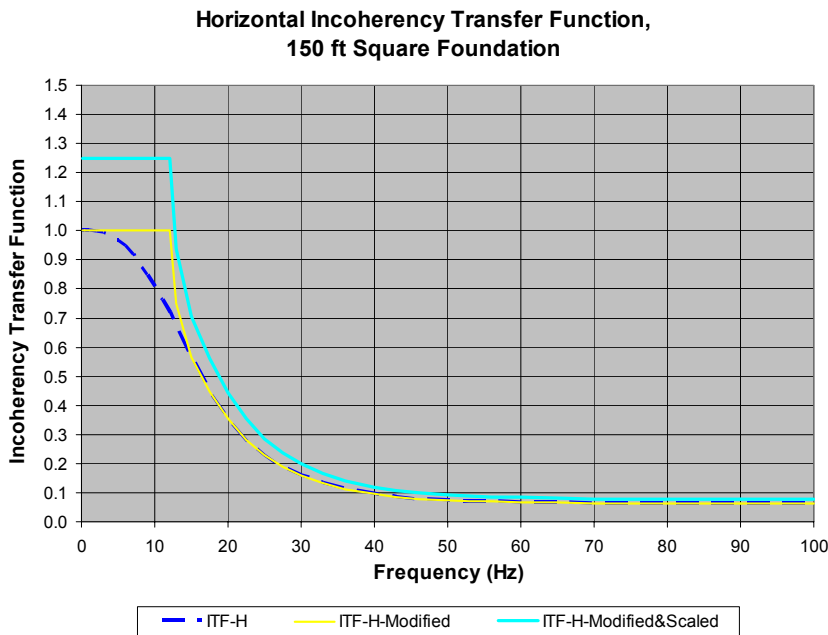
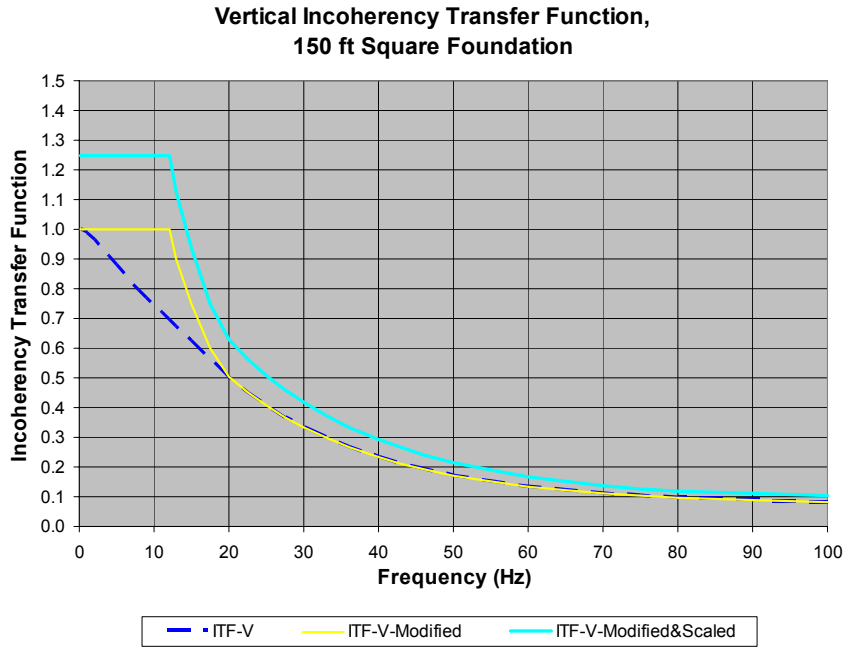


Figure 5-38  
Horizontal Incoherency Transfer Function Used for Simplified Approach

Deleted:  
SSI and Structure Response

Deleted:  
SSI and Structure Response

Deleted:  
SSI and Structure Response  
SSI and Structure Response



**Figure 5-39**  
**Vertical Incoherency Transfer Function Used for Simplified Approach**

Response from seismic analyses for incoherent ground motion by the initial simplified approach of scaling the free-field input motion Fourier amplitudes by the ITF were compared to seismic response from Analyses 2a and 2b. Example in-structure response spectra from these analyses are compared in Figures 5-40 through 5-43.

By using the ITF to scale the Fourier amplitude, the resulting response spectra exactly matched the Analysis 2b results in which incoherent motion was considered but induced rotations were not permitted. In Figures 5-40 through 5-43 as well as in spectra comparisons at all other locations considered, the ITF approach results (light blue curves) exactly matched the Analysis 2b results (red curves). However, the ITF approach did not adequately capture the effects of rotations induced by seismic wave incoherence. In general, there was not a good match between the ITF approach results (light blue curves) and the Analysis 2a results (green curves). As a result, it was decided that a function for scaling the Fourier amplitude would be developed and that function would be based on the ITF. Modifications to the ITF would be introduced in an effort to envelope the effects of rotations induced by seismic wave incoherence.

Deleted: SSI and Structure Response

Deleted: SSI and Structure Response

Deleted: SSI and Structure Response

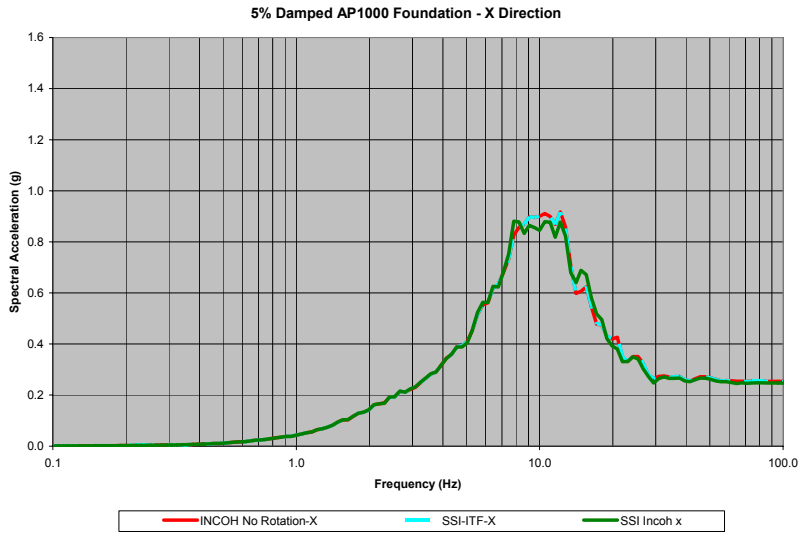


Figure 5-40 Foundation Response Spectra – X Direction – SSI Incoherent, SSI Incoherent with No Rotations, SSI Incoherent by ITF Scaling (Node 1)

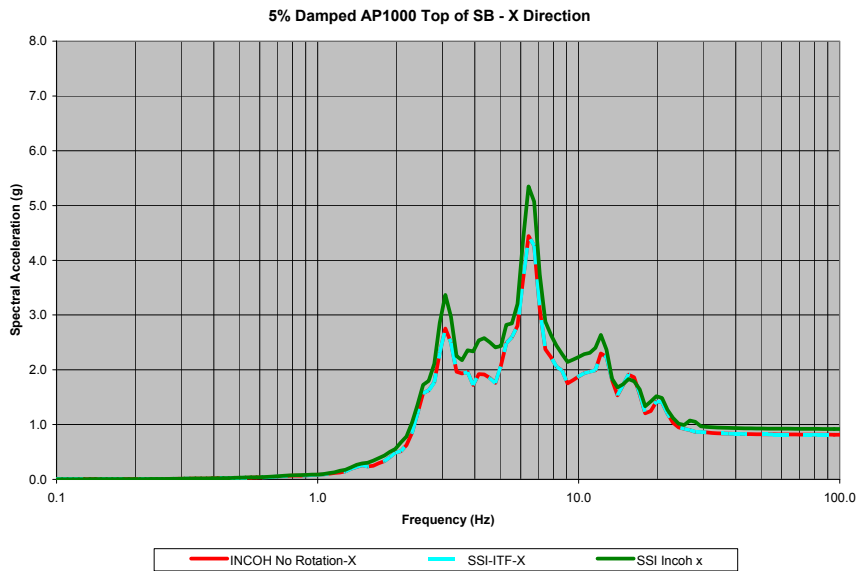
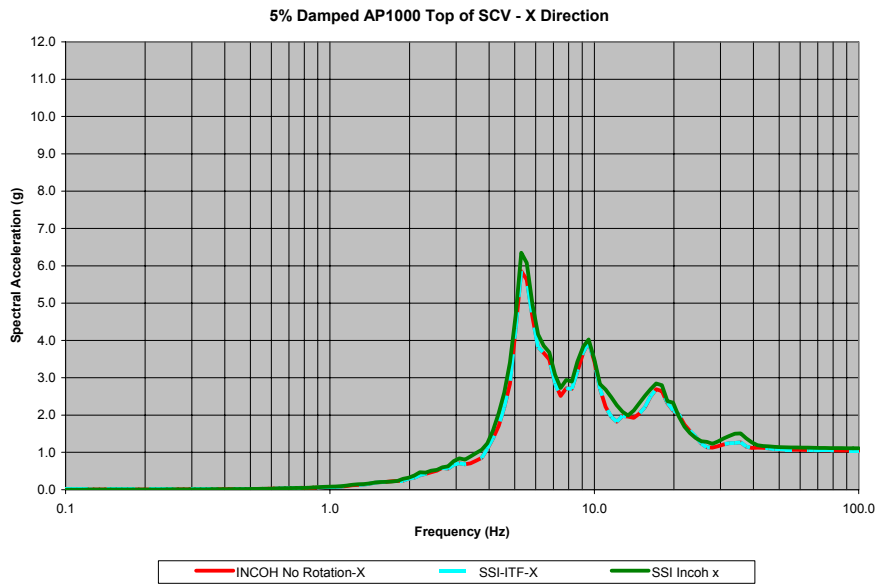


Figure 5-41 Top of Shield Building Response Spectra – X Direction – SSI Incoherent, SSI Incoherent with No Rotations, SSI Incoherent by ITF Scaling (Node 310)

**Deleted:**  
*SSI and Structure Response*

**Deleted:**  
*SSI and Structure Response*

**Deleted:**  
*SSI and Structure Response*



**Figure 5-42**  
**Top of SCV Response Spectra – X Direction – SSI Incoherent, SSI Incoherent with No Rotations, SSI Incoherent by ITF Scaling (Node 417)**

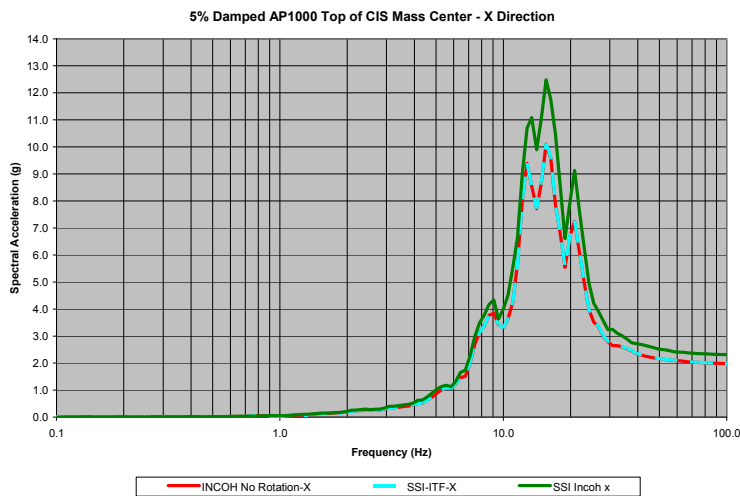


**Figure 5-43**  
**Top of CIS Response Spectra – X Direction – SSI Incoherent, SSI Incoherent with No Rotations, SSI Incoherent by ITF Scaling (Node 538mc)**

**Deleted:**  
*SSI and Structure Response*

**Deleted:**  
*SSI and Structure Response*

**Deleted:**  
*SSI and Structure Response*  
*SSI and Structure Response*

The analyses presented here are a pilot study to evaluate the feasibility of a simplified incoherency approach. An initial modified functional form was selected where the ITF amplitude is held to unity for frequencies less than 12 Hz and then reduced according to a functional relationship for higher frequencies. This modified ITF is shown as the yellow curves in Figures 5-38 and 5-39 for horizontal and vertical motion, respectively. Subsequent analyses as discussed below demonstrated that the modified ITF was not sufficient to adequately capture the incoherent response including induced rotations and the modified function was scaled by 1.25 as shown in the light blue curves in Figures 5-38 and 5-39 for horizontal and vertical motion, respectively.

The results of the analyses where the Fourier amplitude of the free-field input motion is scaled by the modified ITF (yellow curves) and the modified and scaled ITF (light blue curves) are shown in Figures 5-44 through 5-79. Results presented are in-structure response spectra (5% damping) at the foundation and at points on each of three structure models, ASB, SCV, and CIS as shown in Figure 5-1. In-structure response spectra are shown at the same locations for which response was computed by the direct approach as presented in Figures 5-2 through 5-37. Also shown on these figures are the SSI Coherent results (Analysis 1-dark blue curve) and the SSI Incoherent results by the direct or “exact” representation (Analysis 2a-green curve) as previously presented.

Figures 5-44 through 5-79 demonstrate that the modified ITF is not adequate to capture the effects of incoherency-induced rotations. The yellow modified ITF response spectra curves do not adequately envelope the green direct approach incoherent response spectra. As a result, the modified ITF was scaled by 1.25 at all frequencies as shown in Figures 5-38 and 5-39 and new response spectra were computed by scaling the Fourier amplitude of the free-field input motion by the modified and scaled ITF. The comparison of greatest interest is the comparison of the responses calculated by the modified and scaled ITF application to the Fourier amplitude of the free-field ground motion (Analysis 3 - light blue curve) with the “exact” incoherent SSI analysis (Analysis 2a - green curve).

Comparing these spectra in Figures 5-44 through 5-79 demonstrates that response spectra determined from the simplified approach (light blue curve, modified and scaled ITF) envelopes the computed in-structure response spectra by the direct approach (Analysis 2a, green curve) with a few exceptions. For each of the 48 locations at which spectra were computed, the simplified and direct approach are compared in Table 5-1. The results from the simplified approach envelopes the “exact” incoherent results at all frequencies at 38 of the 48 locations.

Exceptions to agreement between exact and simplified results are generally of low amplitude. In all cases, any exceedances by the direct approach over the simplified method occur in very narrow frequency bands. At 6 of the 10 locations where the exact response spectra exceed the spectra from the simplified method, the amount of exceedance is about 10% or less. The four locations where there are larger exceedances may be examined in the following figures:

- Figure 5-65 for a location low on the steel containment vessel (SCV) in the x direction

**Deleted:**  
*SSI and Structure Response*

**Deleted:**  
*SSI and Structure Response*

**Deleted:**  
*SSI and Structure Response*  
*SSI and Structure Response*

- Figure 5-74 for a location low on the containment internal structure (CIS) in the x direction
- Figures 5-78 and 5-79 for a location on the CIS outrigger (75-ft from the centerline) in the y and z directions, respectively.

At each of these locations, the exceedance of the “exact” incoherent response spectra appears to be very minor when compared to the large reduction due to incoherence (i.e., from the blue curve in these figures). As a result, it is judged that this simplified approach captures the effects of incoherence including reductions in translation response and increases response due to incoherency-induced rotations with sufficient accuracy.

### **Summary of Simplified Method Results**

The modified and scaled ITF-Fourier amplitude scaling method has been demonstrated to be appropriate for the conditions for which it was developed.

Observations and limitations of this approach are:

- An alternate means of incorporating seismic wave incoherence into seismic analyses has been developed and implemented. This alternative approach is to scale the Fourier amplitude spectrum of the free-field input motion by a function related to the Incoherency Transfer Function (ITF). The Fourier phase spectrum is unaffected. The result is a re-defined ground motion for SSI and dynamic structure analysis.
- For the recommended modified and scaled ITF, for frequencies less than 12 Hz, define the ITF scaling function to be 1.25, i.e., an increase in the amplitude of the Fourier transform of the free-field ground motion. Above 12 Hz, the modified and scaled ITF transitions smoothly to 1.25 times the ITF for the foundation footprint. This function is shown graphically in Figures 5-38 and 5-39 in the light blue curves.
- The results of this simplified method are compared with the results generated by the direct or “exact” implementation and are judged to adequately and conservatively represent those results.
- This simplified approach has been developed considering ground motion on a rock site in the central and eastern United States where the peak of the free-field ground motion is in the range of 20 to 30 Hz. It is judged that this simplified approach is applicable for other similar rock sites with high-frequency ground motion. It is further judged that this simplified approach would not necessarily (without additional studies) be applicable for soil sites with low-frequency ground motion. In fact, the low-frequency increase to 1.25 for frequencies less than 12 Hz would likely not be required.
- This simplified approach has been developed considering one representative structure model. The model considered has three major structure elements representing the Steel Containment Vessel, the Auxiliary Shield Building, and the Containment Internal Structure, and demonstrates the structural response behavior at a broad range of structural frequencies. The model is tall and has significant outriggers out to the periphery of the foundation in order to

understand the full effects of incoherence induced rotations (rocking and torsion). However, this simplified method would require validation with other structural models that differ significantly from the range of parameters (structural frequencies, foundation stiffness, site profile, etc.) utilized within this demonstration study.

- The simplified approach relies on conservative assumptions in order to envelope the exact responses at all the representative locations within the demonstration model. If new plants find this approach to be beneficial, i.e., this conservatism does not preclude its implementation, then further sensitivity studies could be warranted in the future. Examples are different foundation sizes and shapes, different structural models with frequency characteristics of interest, and different site conditions. The basic incoherency function used in this study is that for a 150-ft square foundation footprint. To augment this simplified approach, an algorithm could also be developed to estimate the ITF as a function of foundation area and, possibly shape.

**Deleted:**  
*SSI and Structure Response*

**Deleted:**  
*SSI and Structure Response*

**Deleted:**  
*SSI and Structure Response*

**Table 5-1**  
**Comparison of Incoherent Direct and Incoherent Simplified Spectra**

NODE	Location	Scaled (1.25) & Modified ITF Simplified vs. Incoherent
Fdn	Foundation - X Direction	Envelopes incoherent at all frequencies
Fdn	Foundation - Y Direction	Envelopes incoherent at all frequencies
Fdn	Foundation - Z Direction	Envelopes incoherent at all frequencies
45	Top of SCV - X Direction	Envelopes incoherent at all frequencies
45	Top of SCV - Y Direction	Envelopes incoherent at all frequencies
45	Top of SCV - Z Direction	Envelopes incoherent at all frequencies
18	Top of SB - X Direction	Incoherent exceeds from 4 to 5 Hz by 7%
18	Top of SB - Y Direction	Incoherent exceeds @ 20 Hz by 7%
18	Top of SB - Z Direction	Envelopes incoherent at all frequencies
12	Top of AB Shear Center - X Direction	Envelopes incoherent at all frequencies
12	Top of AB Shear Center - Y Direction	Envelopes incoherent at all frequencies
12	Top of AB Shear Center - Z Direction	Envelopes incoherent at all frequencies
112	Top of AB Mass Center - X Direction	Envelopes incoherent at all frequencies
112	Top of AB Mass Center - Y Direction	Envelopes incoherent at all frequencies
112	Top of AB Mass Center - Z Direction	Envelopes incoherent at all frequencies
29	Top of CIS Shear Center - X Direction	Incoherent exceeds from 32 to 34 Hz by 10%
29	Top of CIS Shear Center - Y Direction	Envelopes incoherent at all frequencies
29	Top of CIS Shear Center - Z Direction	Envelopes incoherent at all frequencies
129	Top of CIS Mass Center - X Direction	Envelopes incoherent at all frequencies
129	Top of CIS Mass Center - Y Direction	Envelopes incoherent at all frequencies
129	Top of CIS Mass Center - Z Direction	Envelopes incoherent at all frequencies
145	SCV Outrigger - X Direction	Envelopes incoherent at all frequencies
145	SCV Outrigger - Y Direction	Envelopes incoherent at all frequencies
145	SCV Outrigger - Z Direction	Envelopes incoherent at all frequencies

NODE	Location	Scaled (1.25) & Modified ITF Simplified vs. Incoherent
118	SB Outrigger - X Direction	Incoherent exceeds from 4 to 5 Hz by 7%
118	SB Outrigger - Y Direction	Envelopes incoherent at all frequencies
118	SB Outrigger - Z Direction	Envelopes incoherent at all frequencies
229	CIS Outrigger - X Direction	Incoherent exceeds @ 34 Hz by 11%
229	CIS Outrigger - Y Direction	Incoherent exceeds 32 to 40 Hz by as much as 34%
229	CIS Outrigger - Z Direction	Incoherent exceeds @ 21 Hz by 11% and from 27 to 33 Hz by as much as 26%
212	AB Outrigger - X Direction	Envelopes incoherent at all frequencies
212	AB Outrigger - Y Direction	Envelopes incoherent at all frequencies
212	AB Outrigger - Z Direction	Envelopes incoherent at all frequencies
34	Low on SCV - X Direction	Incoherent exceeds @ 31 Hz by 21%
34	Low on SCV - Y Direction	Incoherent exceeds @ 30 Hz by 7%
34	Low on SCV - Z Direction	Envelopes incoherent at all frequencies
8	Low on ASB Shear Center - X Direction	Envelopes incoherent at all frequencies
8	Low on ASB Shear Center - Y Direction	Envelopes incoherent at all frequencies
8	Low on ASB Shear Center - Z Direction	Envelopes incoherent at all frequencies
26	Low on CIS Shear Center - X Direction	Envelopes incoherent at all frequencies
26	Low on CIS Shear Center - Y Direction	Envelopes incoherent at all frequencies
26	Low on CIS Shear Center - Z Direction	Envelopes incoherent at all frequencies
108	Low on ASB Mass Center - X Direction	Envelopes incoherent at all frequencies
108	Low on ASB Mass Center - Y Direction	Envelopes incoherent at all frequencies
108	Low on ASB Mass Center - X Direction	Envelopes incoherent at all frequencies
126	Low on CIS Mass Center - X Direction	Incoherent exceeds from 19 to 24 Hz by 15%
126	Low on CIS Mass Center - Y Direction	Envelopes incoherent at all frequencies
126	Low on CIS Mass Center - Z Direction	Envelopes incoherent at all frequencies

**Deleted:**  
*SSI and Structure Response*

**Deleted:**  
*SSI and Structure Response*

**Deleted:**  
*SSI and Structure Response*  
*SSI and Structure Response*

Deleted: SSI and Structure Response

Deleted: SSI and Structure Response

Deleted: SSI and Structure Response

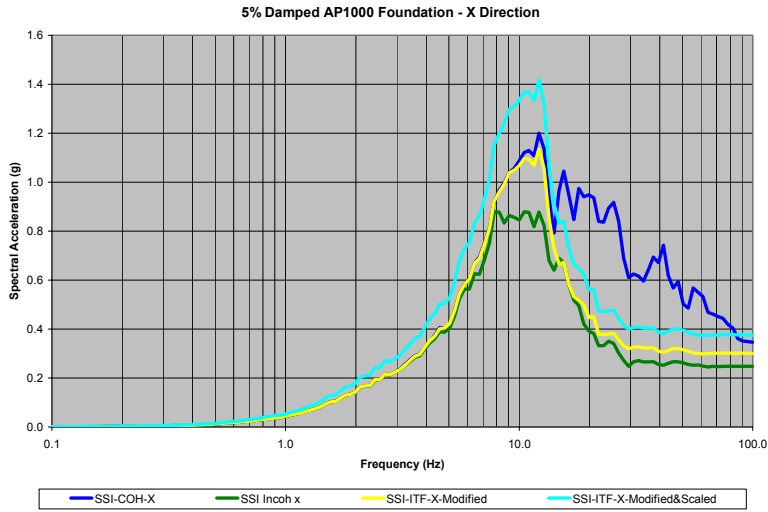


Figure 5-44 Foundation Response Spectra – X Direction – SSI Coherent, SSI Incoherent, SSI Incoherent by Modified ITF, SSI Incoherent by Modified and Scaled ITF (Node 1)

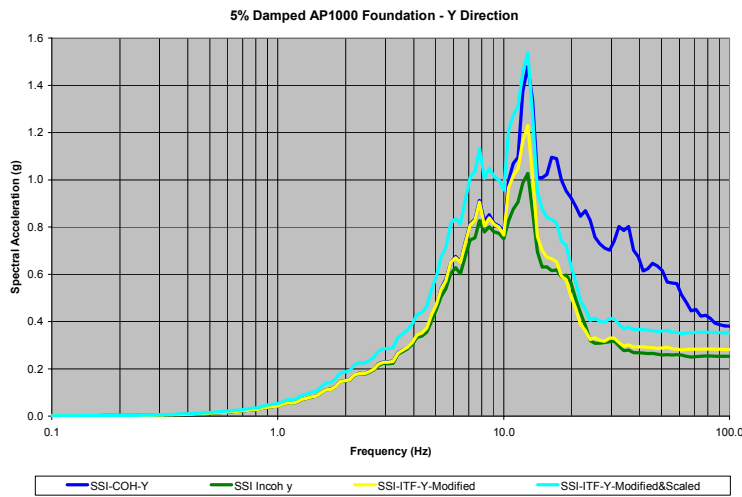
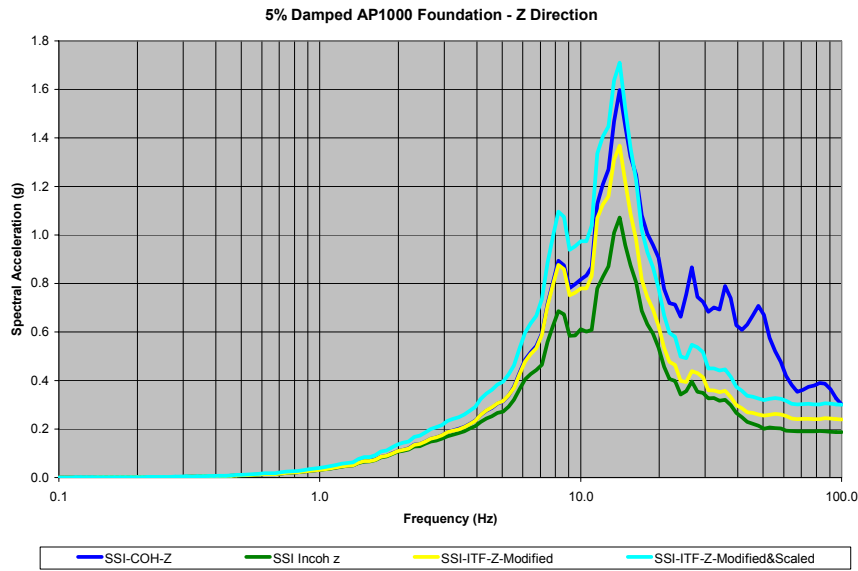
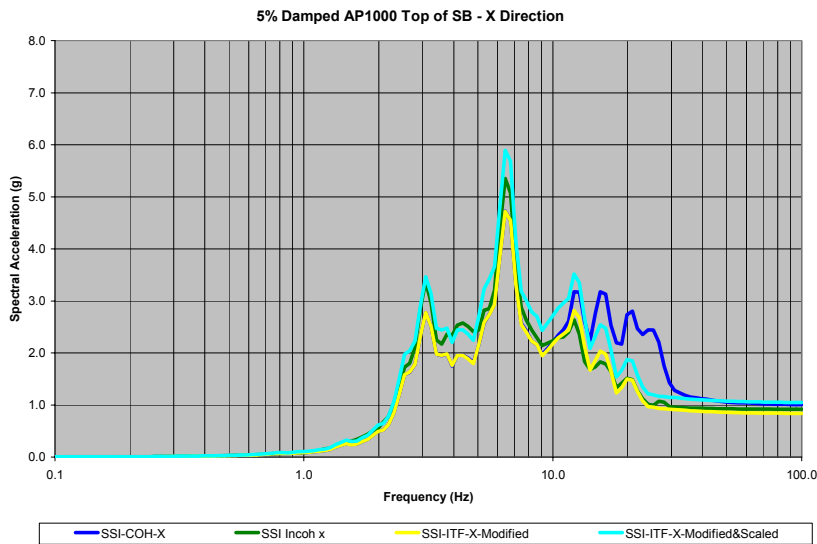


Figure 5-45 Foundation Response Spectra – Y Direction – SSI Coherent, SSI Incoherent, SSI Incoherent by Modified ITF, SSI Incoherent by Modified and Scaled ITF (Node 1)

**Deleted:** .  
*SSI and Structure Response*



**Figure 5-46**  
**Foundation Response Spectra – Z Direction – SSI Coherent, SSI Incoherent, SSI Incoherent by Modified ITF, SSI Incoherent by Modified and Scaled ITF (Node 1)**



**Figure 5-47**  
**Top of Shield Building Response Spectra – X Direction – SSI Coherent, SSI Incoherent, SSI Incoherent by Modified ITF, SSI Incoherent by Modified and Scaled ITF (Node 310)**

Deleted: SSI and Structure Response

Deleted: SSI and Structure Response

Deleted: SSI and Structure Response

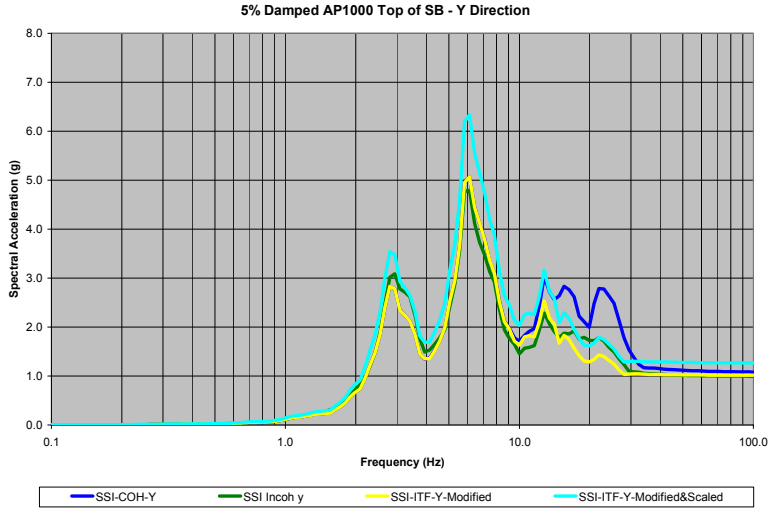


Figure 5-48  
Top of Shield Building Response Spectra – Y Direction – SSI Coherent, SSI Incoherent, SSI Incoherent by Modified ITF, SSI Incoherent by Modified and Scaled ITF (Node 310)

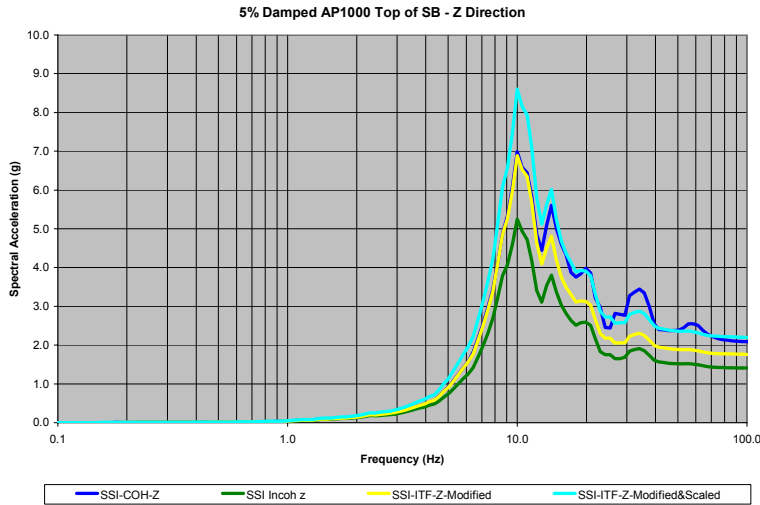
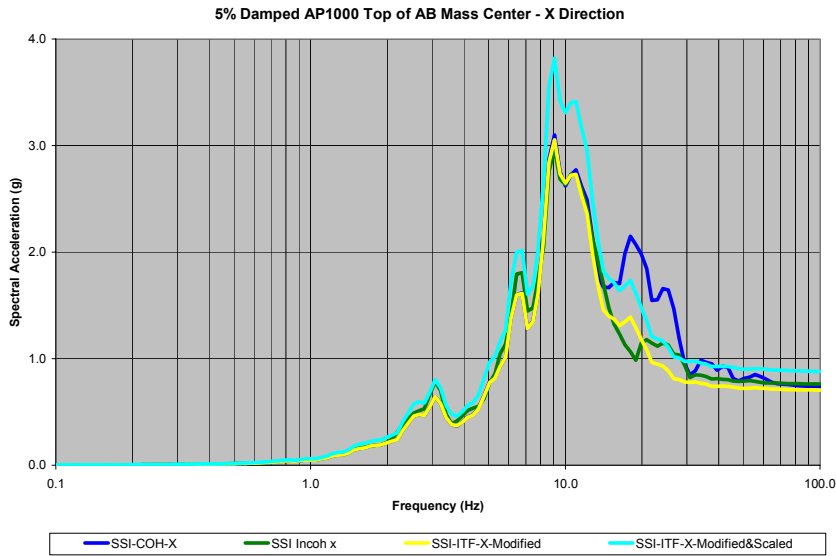


Figure 5-49  
Top of Shield Building Response Spectra – Z Direction – SSI Coherent, SSI Incoherent, SSI Incoherent by Modified ITF, SSI Incoherent by Modified and Scaled ITF (Node 310)

**Deleted:**  
*SSI and Structure Response*

**Deleted:**  
*SSI and Structure Response*

**Deleted:**  
*SSI and Structure Response*  
*SSI and Structure Response*



**Figure 5-50**  
Top of Auxiliary Building Response Spectra – X Direction – SSI Coherent, SSI Incoherent, SSI Incoherent by Modified ITF, SSI Incoherent by Modified and Scaled ITF (Node 120mc)

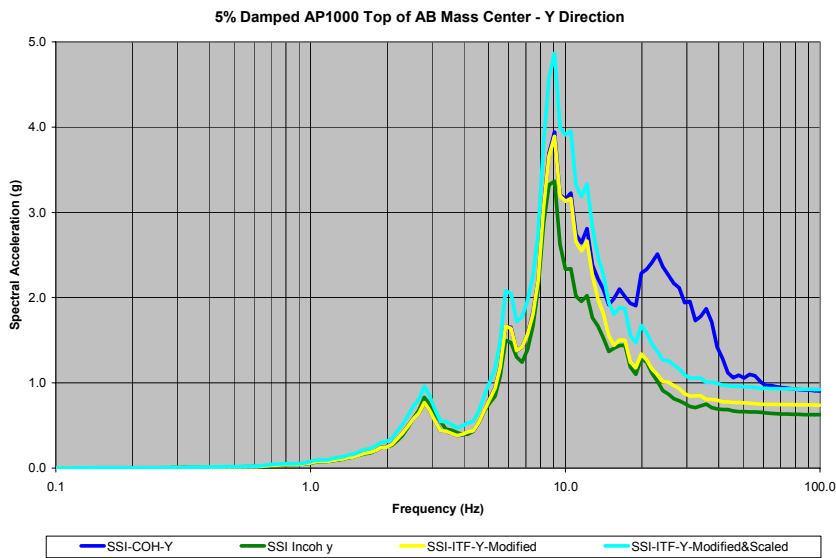


**Figure 5-51**  
Top of Auxiliary Building Response Spectra – Y Direction – SSI Coherent, SSI Incoherent, SSI Incoherent by Modified ITF, SSI Incoherent by Modified and Scaled ITF (Node 120mc)

Deleted: SSI and Structure Response

Deleted: SSI and Structure Response

Deleted: SSI and Structure Response

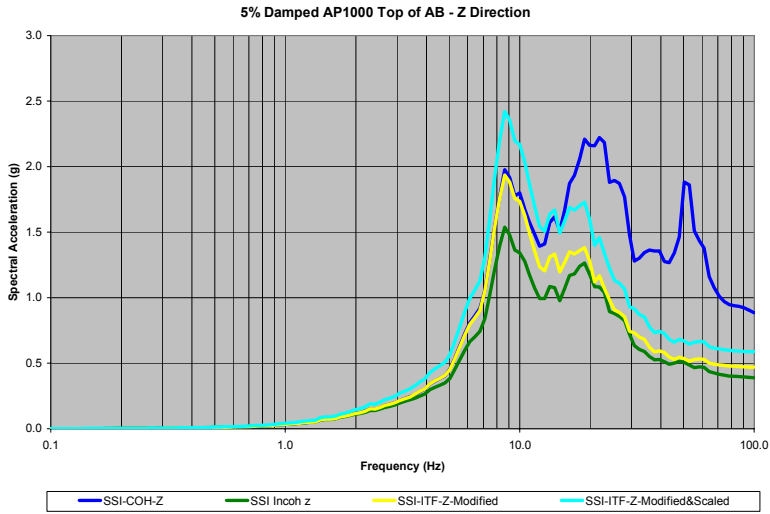


Figure 5-52  
Top of Auxiliary Building Response Spectra – Z Direction – SSI Coherent, SSI Incoherent, SSI Incoherent by Modified ITF, SSI Incoherent by Modified and Scaled ITF (Node 120)

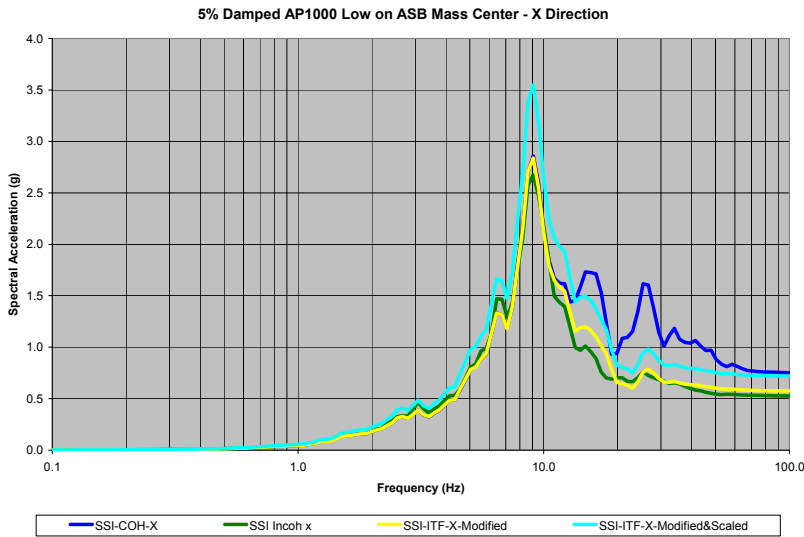
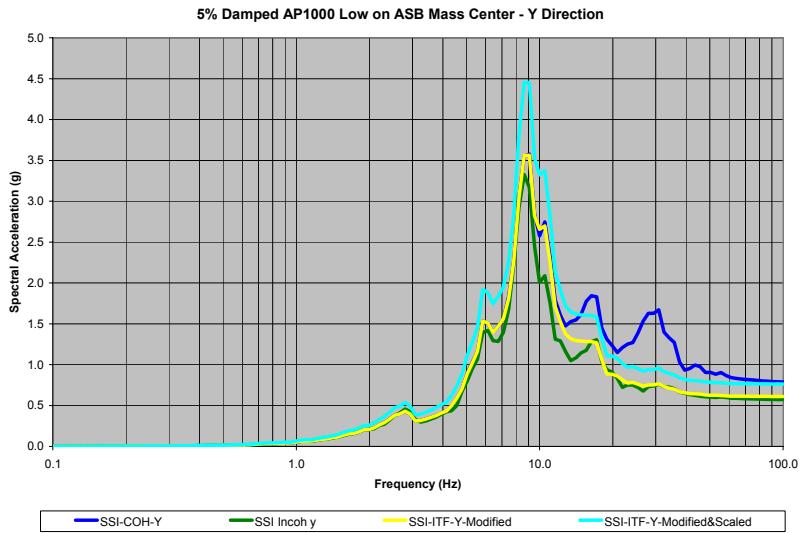


Figure 5-53  
Low on ASB Response Spectra – X Direction – SSI Coherent, SSI Incoherent, SSI Incoherent by Modified ITF, SSI Incoherent by Modified and Scaled ITF (Node 80mc)

**Deleted:**  
*SSI and Structure Response*

**Deleted:**  
*SSI and Structure Response*

**Deleted:**  
*SSI and Structure Response*  
*SSI and Structure Response*



**Figure 5-54**  
**Low on ASB Response Spectra – Y Direction – SSI Coherent, SSI Incoherent, SSI Incoherent by Modified ITF, SSI Incoherent by Modified and Scaled ITF (Node 80mc)**

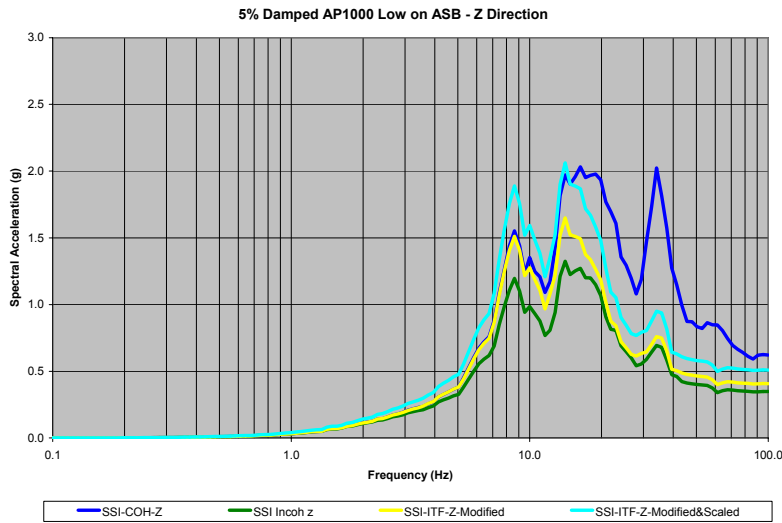


**Figure 5-55**  
**Low on ASB Response Spectra – Z Direction – SSI Coherent, SSI Incoherent, SSI Incoherent by Modified ITF, SSI Incoherent by Modified and Scaled ITF (Node 80)**

Deleted: SSI and Structure Response

Deleted: SSI and Structure Response

Deleted: SSI and Structure Response

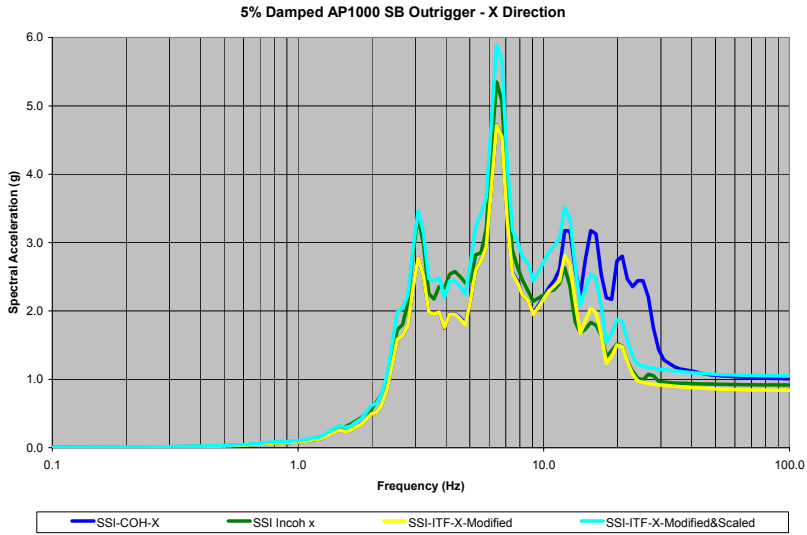


Figure 5-56  
Shield Building Outrigger Response Spectra – X Direction – SSI Coherent, SSI Incoherent, SSI Incoherent by Modified ITF, SSI Incoherent by Modified and Scaled ITF (Node 310out)

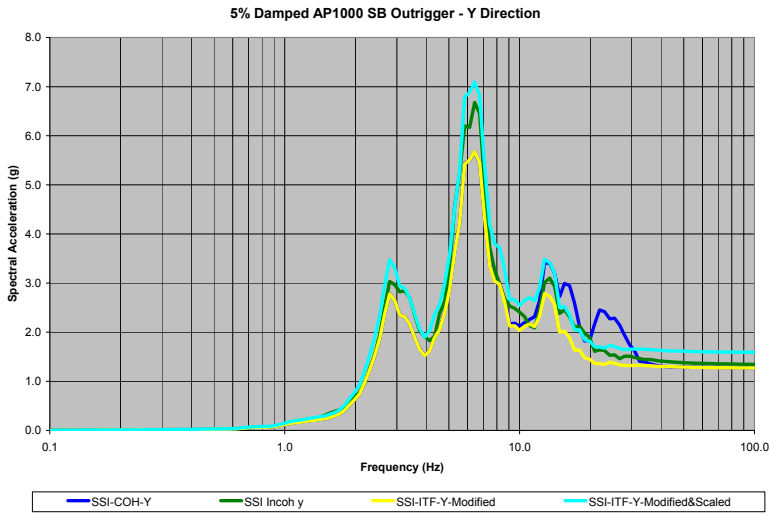


Figure 5-57  
Shield Building Outrigger Response Spectra – Y Direction – SSI Coherent, SSI Incoherent, SSI Incoherent by Modified ITF, SSI Incoherent by Modified and Scaled ITF (Node 310out)

Deleted: SSI and Structure Response  
Deleted: SSI and Structure Response  
Deleted: SSI and Structure Response

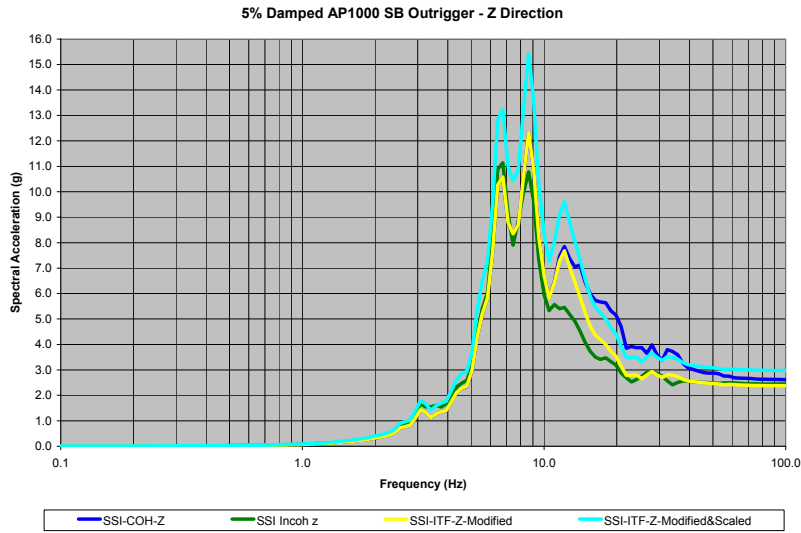


Figure 5-58  
Shield Building Outrigger Response Spectra – Z Direction – SSI Coherent, SSI Incoherent, SSI Incoherent by Modified ITF, SSI Incoherent by Modified and Scaled ITF (Node 310out)

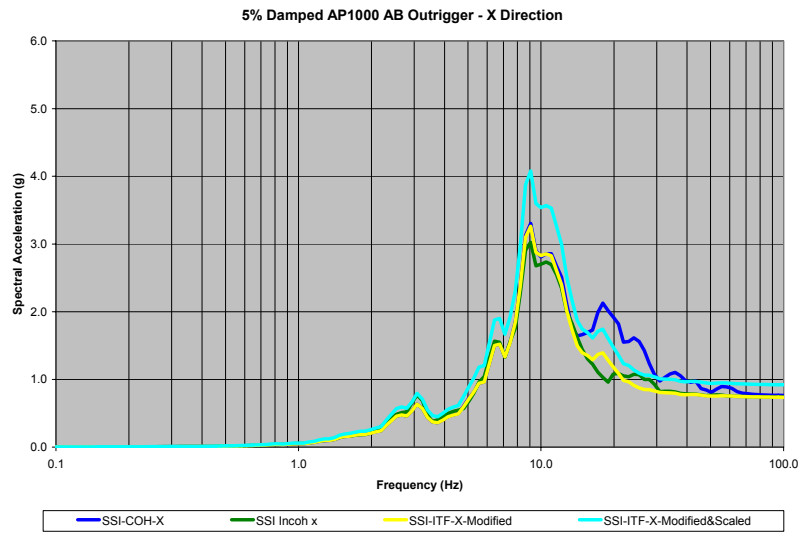


Figure 5-59  
Auxiliary Building Outrigger Response Spectra – X Direction – SSI Coherent, SSI Incoherent, SSI Incoherent by Modified ITF, SSI Incoherent by Modified and Scaled ITF (Node 120out)

Deleted: SSI and Structure Response

Deleted: SSI and Structure Response

Deleted: SSI and Structure Response

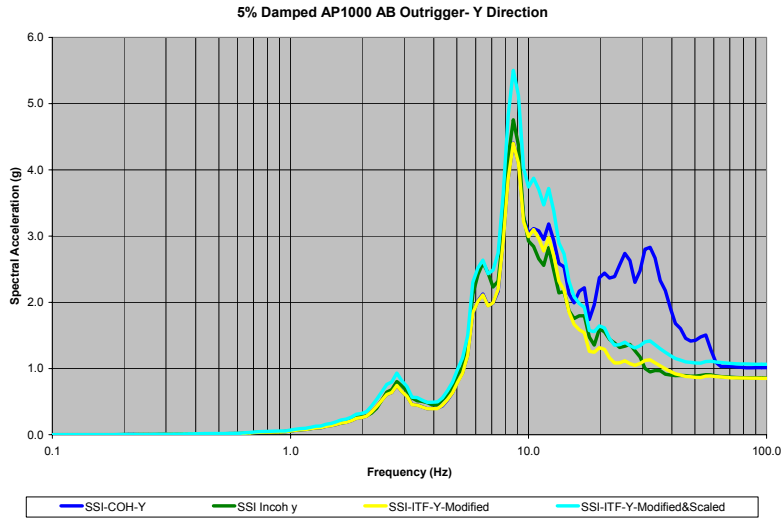


Figure 5-60  
Auxiliary Building Outrigger Response Spectra – Y Direction – SSI Coherent, SSI Incoherent, SSI Incoherent by Modified ITF, SSI Incoherent by Modified and Scaled ITF (Node 120out)

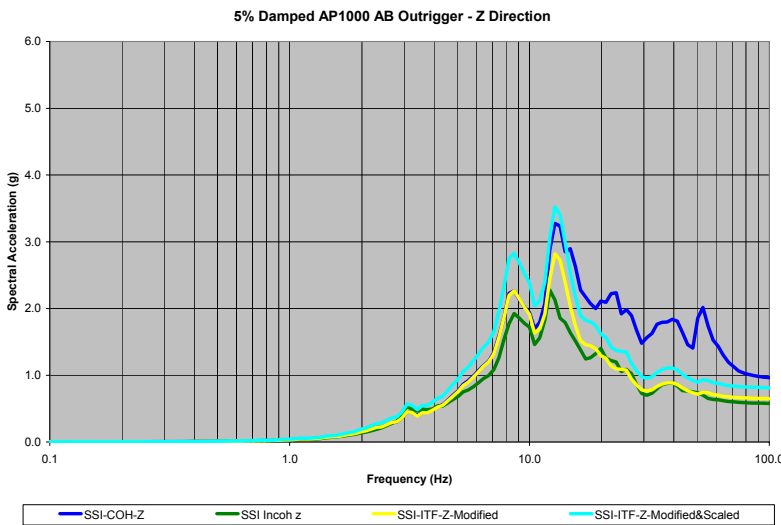
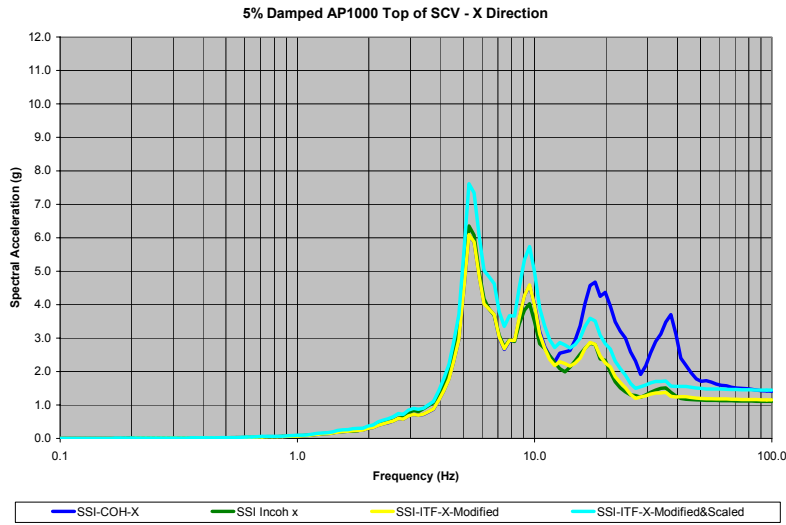


Figure 5-61  
Auxiliary Building Outrigger Response Spectra – Z Direction – SSI Coherent, SSI Incoherent, SSI Incoherent by Modified ITF, SSI Incoherent by Modified and Scaled ITF (Node 120out)

**Deleted:**  
*SSI and Structure Response*

**Deleted:**  
*SSI and Structure Response*

**Deleted:**  
*SSI and Structure Response*



**Figure 5-62**  
Top of SCV Response Spectra – X Direction – SSI Coherent, SSI Incoherent, SSI Incoherent by Modified ITF, SSI Incoherent by Modified and Scaled ITF (Node 417)

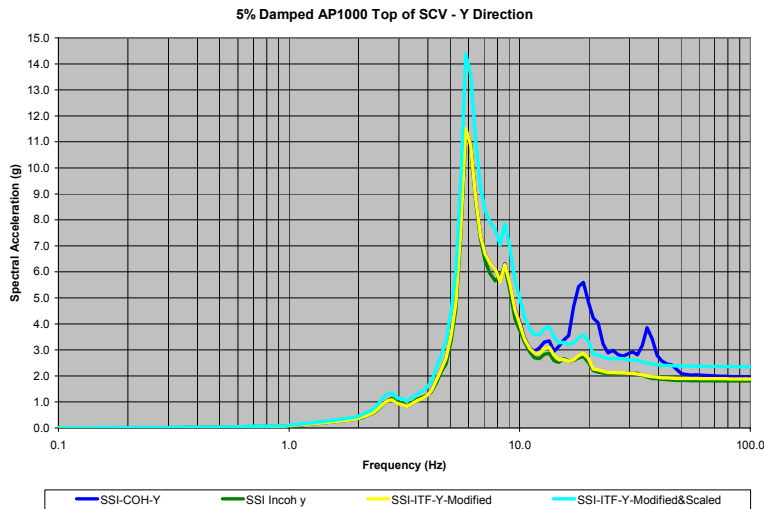


**Figure 5-63**  
Top of SCV Response Spectra – Y Direction – SSI Coherent, SSI Incoherent, SSI Incoherent by Modified ITF, SSI Incoherent by Modified and Scaled ITF (Node 417)

Deleted: SSI and Structure Response

Deleted: SSI and Structure Response

Deleted: SSI and Structure Response

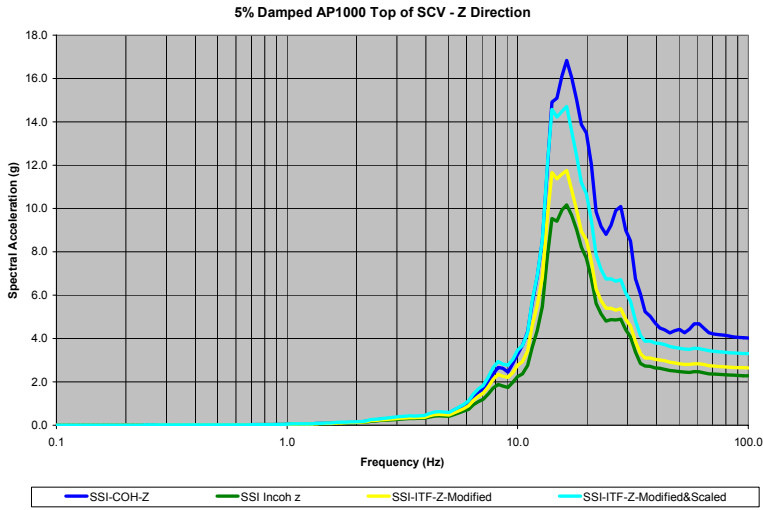


Figure 5-64  
Top of SCV Response Spectra – Z Direction – SSI Coherent, SSI Incoherent, SSI Incoherent by Modified ITF, SSI Incoherent by Modified and Scaled ITF (Node 417)

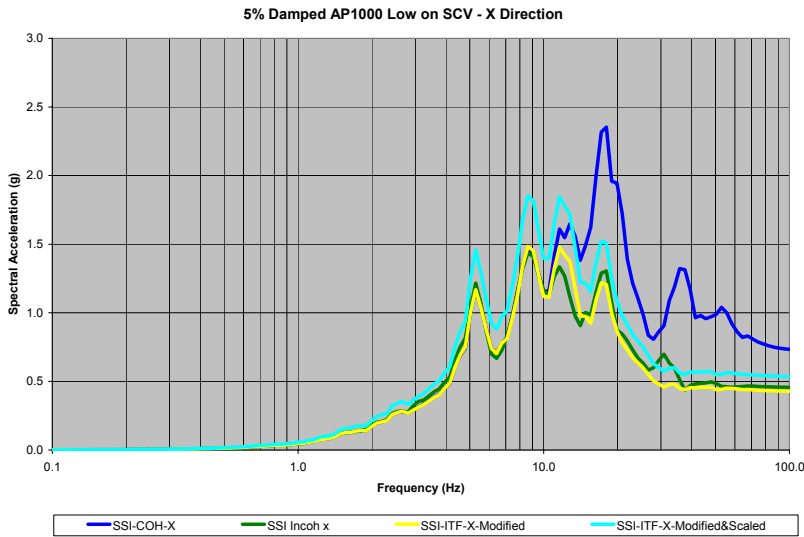


Figure 5-65  
Low on SCV Response Spectra – X Direction – SSI Coherent, SSI Incoherent, SSI Incoherent by Modified ITF, SSI Incoherent by Modified and Scaled ITF (Node 406)

Deleted:  
SSI and Structure Response

Deleted:  
SSI and Structure Response

Deleted:  
SSI and Structure Response  
SSI and Structure Response

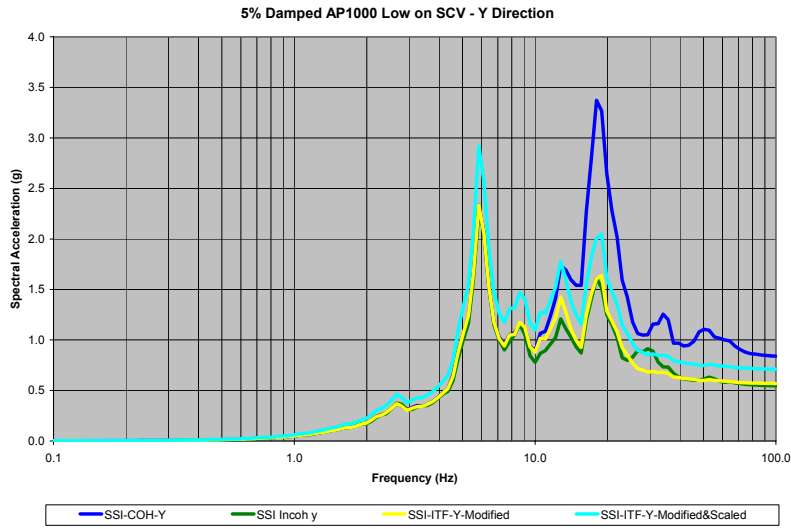


Figure 5-66  
Low on SCV Response Spectra – Y Direction – SSI Coherent, SSI Incoherent, SSI Incoherent by Modified ITF, SSI Incoherent by Modified and Scaled ITF (Node 406)

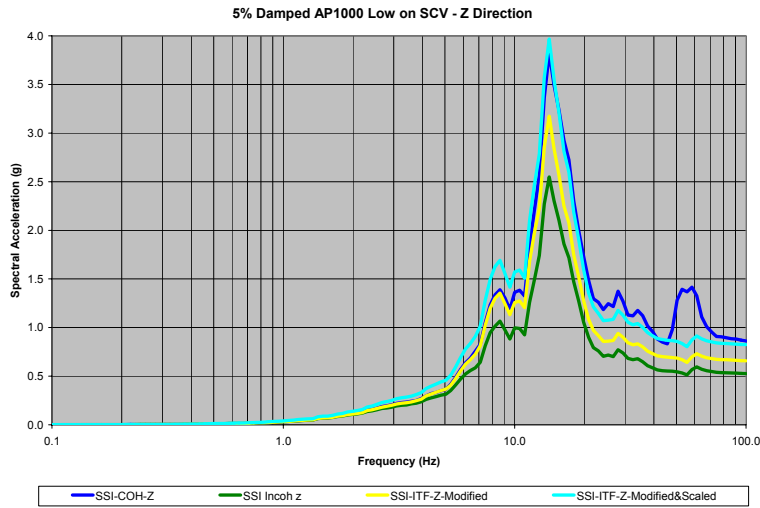


Figure 5-67  
Low on SCV Response Spectra – Z Direction – SSI Coherent, SSI Incoherent, SSI Incoherent by Modified ITF, SSI Incoherent by Modified and Scaled ITF (Node 406)

Deleted: SSI and Structure Response

Deleted: SSI and Structure Response

Deleted: SSI and Structure Response

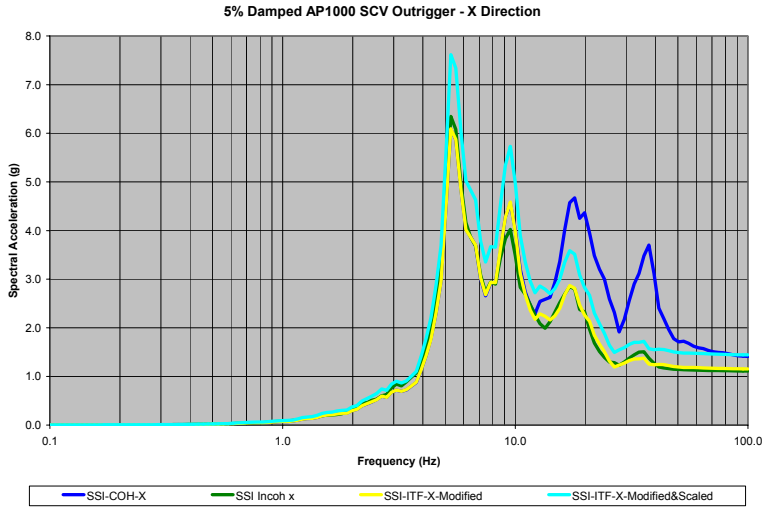


Figure 5-68  
SCV Outrigger Response Spectra – X Direction – SSI Coherent, SSI Incoherent, SSI Incoherent by Modified ITF, SSI Incoherent by Modified and Scaled ITF (Node 417out)

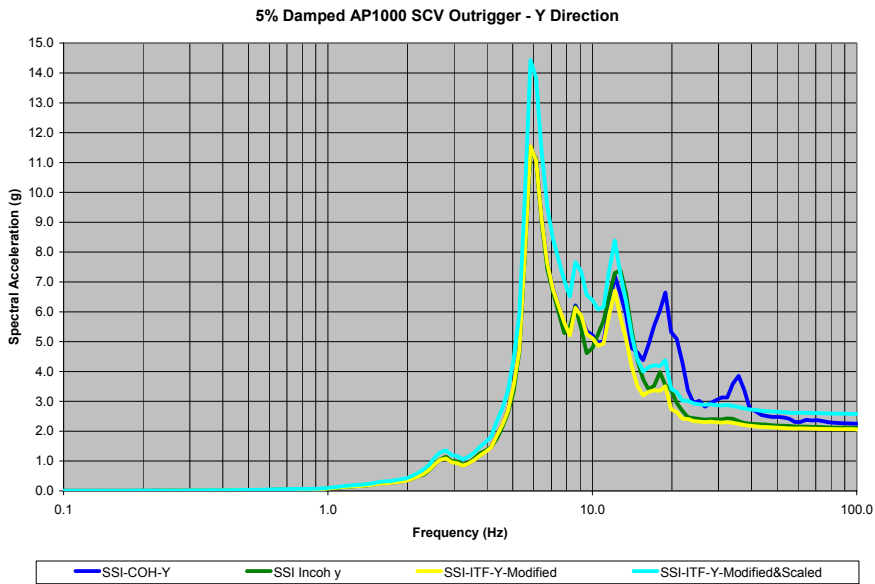
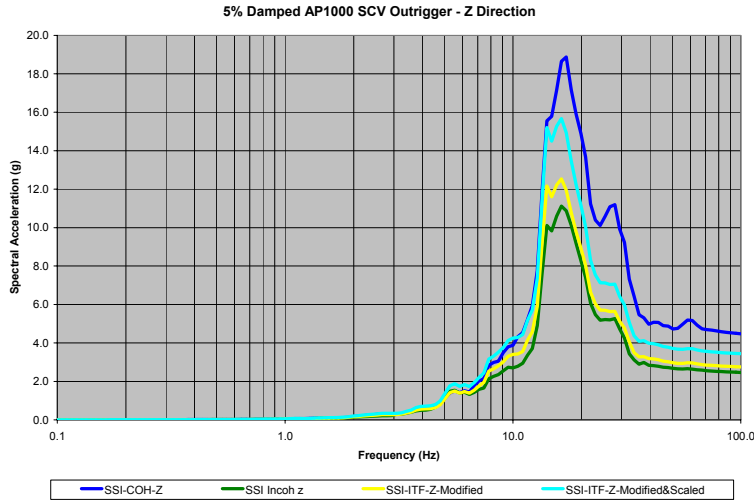


Figure 5-69  
SCV Outrigger Response Spectra – Y Direction – SSI Coherent, SSI Incoherent, SSI Incoherent by Modified ITF, SSI Incoherent by Modified and Scaled ITF (Node 417out)

**Deleted:** .  
*SSI and Structure Response*

**Deleted:** .  
*SSI and Structure Response*

**Deleted:** .  
*SSI and Structure Response*



**Figure 5-70**  
**SCV Outrigger Response Spectra – Z Direction – SSI Coherent, SSI Incoherent, SSI Incoherent by Modified ITF, SSI Incoherent by Modified and Scaled ITF (Node 417out)**

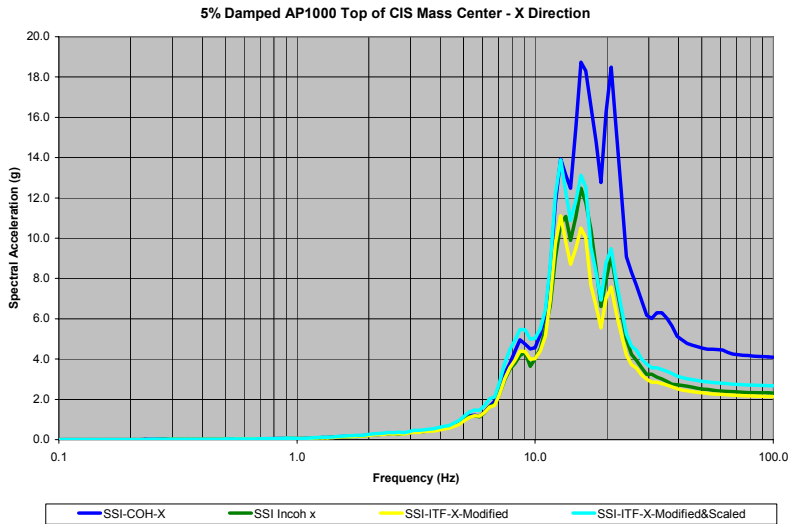


**Figure 5-71**  
**Top of CIS Response Spectra – X Direction – SSI Coherent, SSI Incoherent, SSI Incoherent by Modified ITF, SSI Incoherent by Modified and Scaled ITF (Node 538mc)**

Deleted: SSI and Structure Response

Deleted: SSI and Structure Response

Deleted: SSI and Structure Response

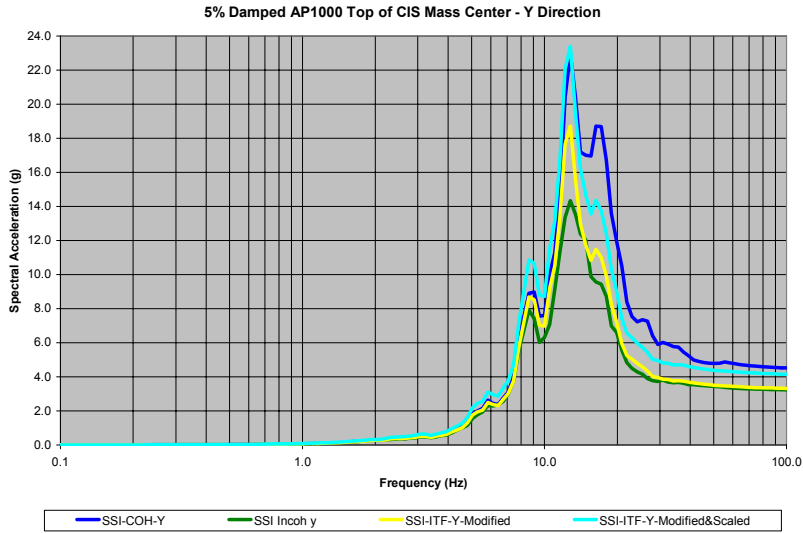


Figure 5-72  
Top of CIS Response Spectra – Y Direction – SSI Coherent, SSI Incoherent, SSI Incoherent by Modified ITF, SSI Incoherent by Modified and Scaled ITF (Node 538mc)

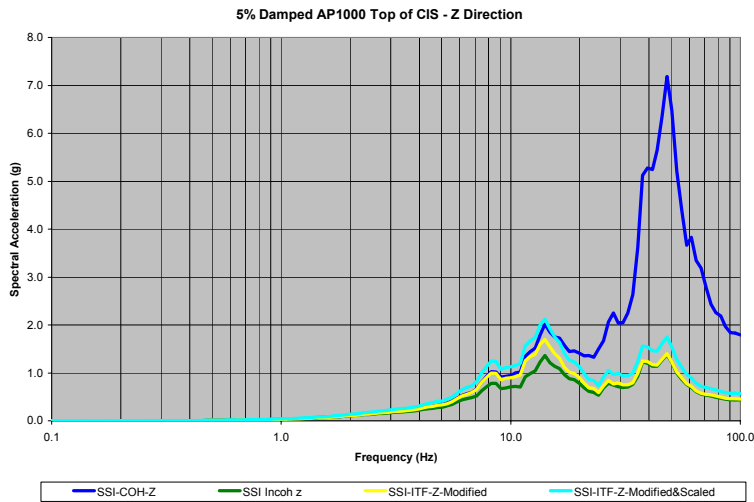
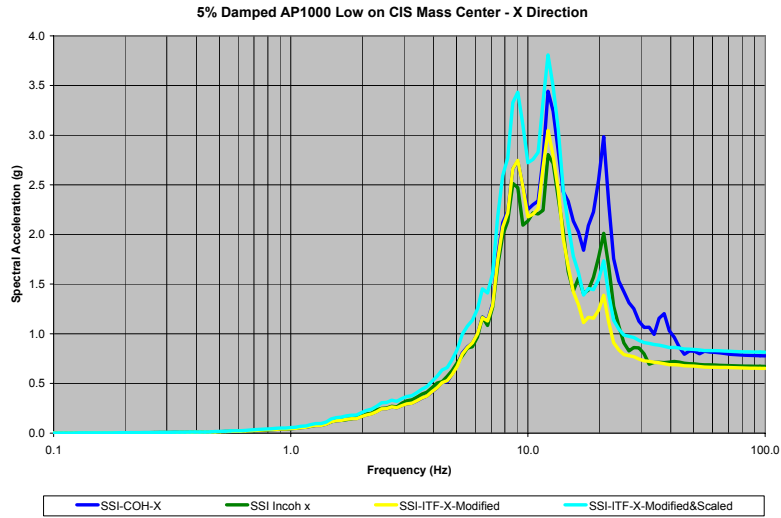


Figure 5-73  
Top of CIS Response Spectra – Z Direction – SSI Coherent, SSI Incoherent, SSI Incoherent by Modified ITF, SSI Incoherent by Modified and Scaled ITF (Node 538)

**Deleted:**  
*SSI and Structure Response*

**Deleted:**  
*SSI and Structure Response*

**Deleted:**  
*SSI and Structure Response*



**Figure 5-74**  
**Low on CIS Response Spectra – X Direction – SSI Coherent, SSI Incoherent, SSI Incoherent by Modified ITF, SSI Incoherent by Modified and Scaled ITF (Node 535mc)**

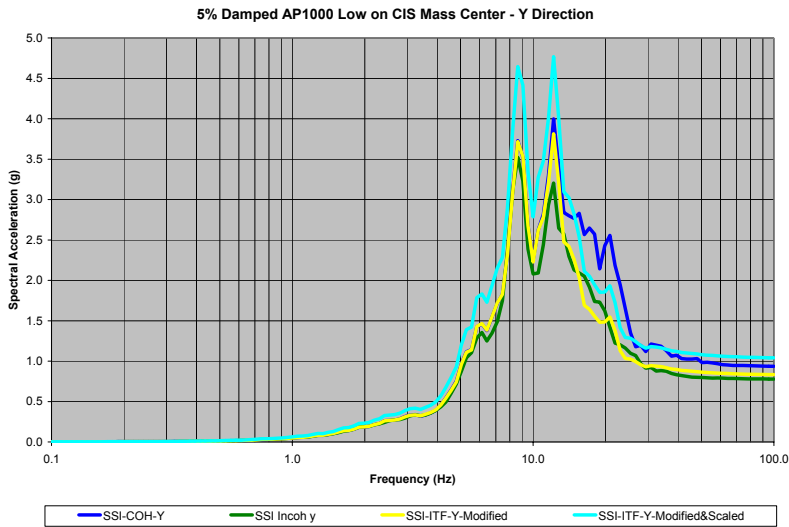


**Figure 5-75**  
**Low on CIS Response Spectra – Y Direction – SSI Coherent, SSI Incoherent, SSI Incoherent by Modified ITF, SSI Incoherent by Modified and Scaled ITF (Node 535mc)**

Deleted: SSI and Structure Response

Deleted: SSI and Structure Response

Deleted: SSI and Structure Response

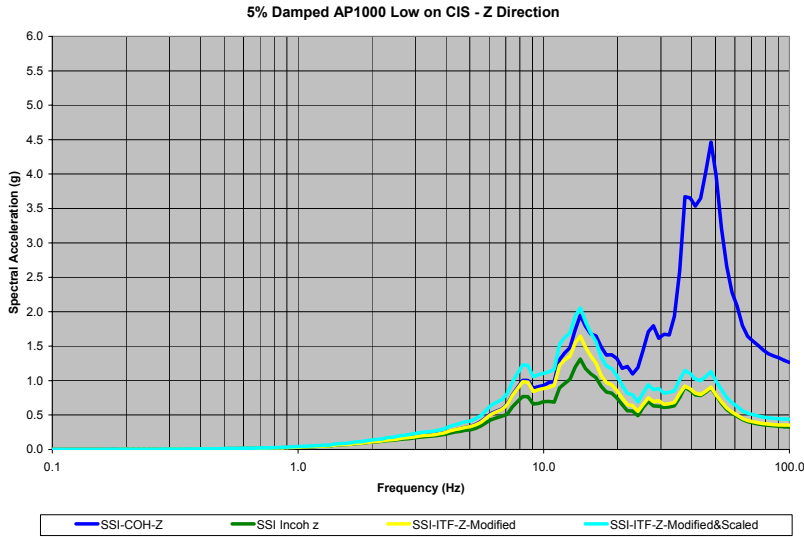


Figure 5-76 Low on CIS Response Spectra – Z Direction – SSI Coherent, SSI Incoherent, SSI Incoherent by Modified ITF, SSI Incoherent by Modified and Scaled ITF (Node 535)

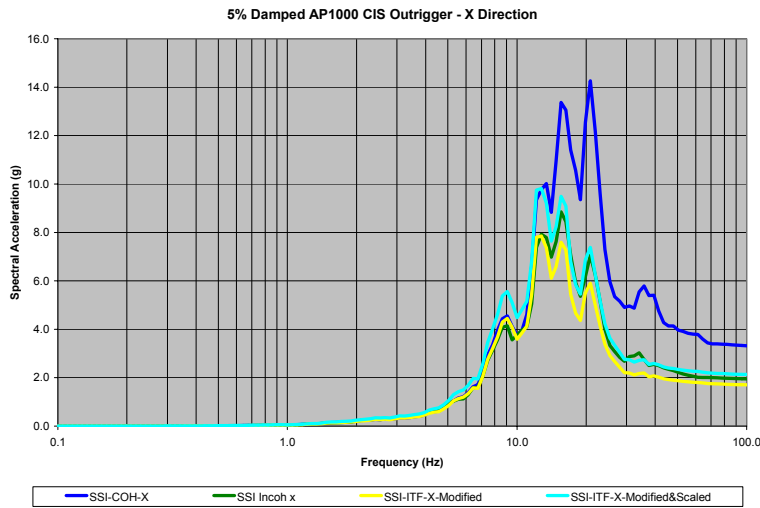


Figure 5-77 CIS Outrigger Response Spectra – X Direction – SSI Coherent, SSI Incoherent, SSI Incoherent by Modified ITF, SSI Incoherent by Modified and Scaled ITF (Node 538out)

Deleted:  
SSI and Structure Response

Deleted:  
SSI and Structure Response

Deleted:  
SSI and Structure Response  
SSI and Structure Response

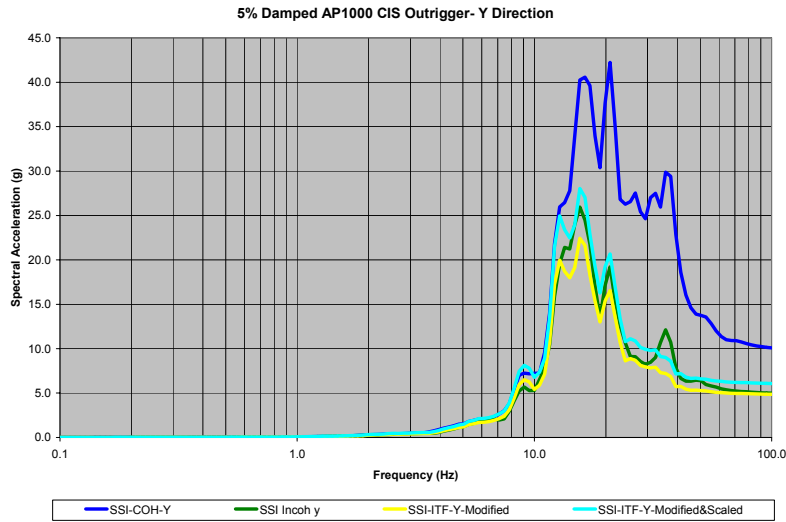


Figure 5-78  
CIS Outrigger Response Spectra – Y Direction – SSI Coherent, SSI Incoherent, SSI Incoherent by Modified ITF, SSI Incoherent by Modified and Scaled ITF (Node 538out)

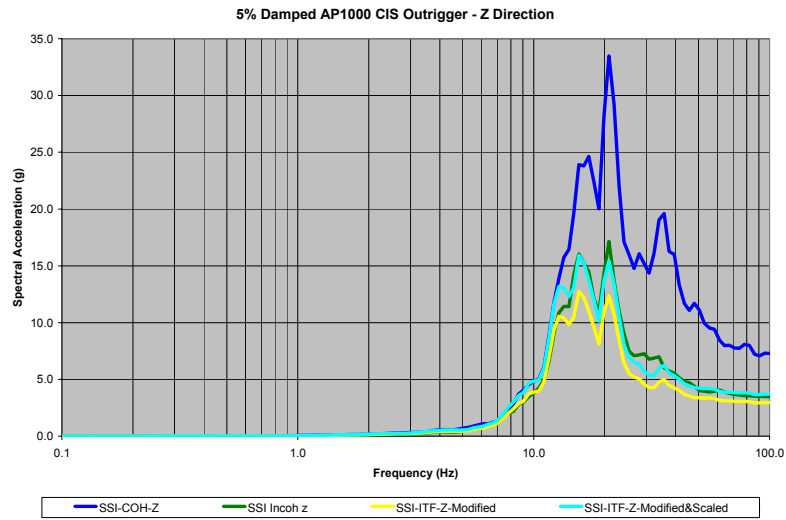


Figure 5-79  
CIS Outrigger Response Spectra – Z Direction – SSI Coherent, SSI Incoherent, SSI Incoherent by Modified ITF, SSI Incoherent by Modified and Scaled ITF (Node 538out)

**Deleted:**  
*SSI and Structure Response*

**Deleted:**  
*SSI and Structure Response*

**Deleted:**  
*SSI and Structure Response*  
*SSI and Structure Response*

## Effect of Embedment and Incoherence

The analyses reported to this point in Chapters 4 and 5 have considered surface foundations. However, many nuclear power plant structures have embedded foundations and partially embedded structures. The treatment of incoherence of ground motion for embedded foundation configurations is discussed next.

Embedment effects on SSI response of nuclear power plant structures are due to kinematic response and inertial response. Kinematic response effects are due to spatial variation of ground motion and the integrating effects of the embedded foundation and partially embedded walls. Two aspects of spatial variation of ground motion are to be considered: the variation of free-field ground motion with depth in the soil or rock over the embedded portions of the foundation/partially embedded structure; and the incoherency effects. The first has a significant effect on the foundation input motion generally reducing the translational motion of the foundation and increasing the rotational motion. This effect exists independent of incoherency. The second effect is that of incoherency, the subject of the current project.

A sensitivity study considering the effect of ground motion incoherence and embedded foundations has been performed and is presented in Appendix E. There were two objectives to the study:

1. Demonstrate the effects of combined incoherency and embedment on seismic response.
2. Assess whether it is possible to consider incoherency and embedment effects separately in which incoherency is treated by modified free-field motion per the simplified approach and embedment is treated by conventional SSI analysis.

The sensitivity study was conducted to investigate the combined effects of spatially varying ground motion with depth in the rock/soil due to foundation/structure embedment and incoherency of ground motion. The SSI analysis program ACS-SASSI was used. By comparing in-structure responses for the surface and embedded cases, the effect of embedment was observed. By comparing the incoherent transfer functions for the surface and embedded cases, the effect of incoherence of ground motion was assessed.

The functional form of the coherency functions at depth in the rock/soil is required for the sensitivity study. Dr. Abrahamson states that the coherency functions presented in Chapter 2 are equally applicable to surface motion and motion at depths typical of embedded foundations/partially embedded structures (Abrahamson, 2006). Therefore, they were used.

The sensitivity study utilizes a structure model representing a reactor building with an internal structure. Soil-structure interaction analyses are performed considering the reactor building to be surface founded and partially embedded. Incoherent-to-coherent spectral acceleration ratios are compared for the surface founded and embedded reactor building. In addition, incoherency transfer functions are computed by the approach described in Chapter 4, and for the surface founded and embedded reactor building.

**Deleted:**  
*SSI and Structure Response*

**Deleted:**  
*SSI and Structure Response*

**Deleted:**  
*SSI and Structure Response*

The effects of incoherency were demonstrated to be similar for the surface founded structure and the embedded structure. Incoherent to coherent spectral ratios were computed as a general indicator of the effect of incoherency and presented in Appendix E. The best indication of incoherency effects is the incoherency transfer function, which were also calculated and presented in Appendix E. In terms of ratios of in-structure response spectra (incoherent to coherent) and incoherency transfer functions, compared for surface founded and embedded cases, the results are very similar.

In conclusion, this sensitivity study demonstrates the significant reduction of high-frequency response for both surface founded and embedded structures. Generally, the results show the same behavior for the surface and embedded cases. All indications are that the effect of spatial variation of ground motion with depth can be treated independently from the effects of ground motion incoherency.

### **Effect of SSI on High-Frequency Seismic Response**

On rock sites such as that considered in this chapter, soil-structure interaction (SSI) is not generally considered. However, for the high-frequency content input motion considered herein, the effects of SSI are shown to be very significant. SSI generally consists of kinematic and inertial interaction. For the surface founded structure considered herein, the kinematic interaction effects are those associated with seismic wave incoherence. Inertial interaction includes the dynamic response of the soil-structure system and is characterized predominantly by shifting of structure frequencies to lower soil-structure frequencies and reduced response due to significant radiation damping. In the results presented in the chapter, those designated “SSI Coherent” include inertial interaction and those designated “SSI Incoherent” include both kinematic and inertial interaction. In this section, in-structure response spectra are presented without soil-structure interaction effects as a fixed-base structural model is used where the foundation motion is the same as the free-field input motion.

The effects of SSI are demonstrated in Figures 5-80 through 5-89 for X and Z direction response of the foundation and at the tops of the shield building, auxiliary building, steel containment vessel (SCV) and containment internal structure (CIS). The effects of inertial interaction may be seen by comparing the fixed-base ISRS (yellow curve) with the SSI Coherent ISRS (blue curve). The effects of incoherence may be seen by comparing the SSI Coherent ISRS (blue curve) with the SSI Incoherent ISRS (green curve). These figures demonstrate that significant reductions of the seismic response due to kinematic and inertial interaction exist at all frequencies greater than about 15 Hz for all of the locations considered. At lower frequencies, these figures also demonstrate where seismic response including SSI can exceed the fixed base results due to frequency shifts of the soil-structure system relative to structure fixed base frequencies.

Conclusions from this section are two-fold: (1) SSI effects can be very significant on a rock site where there is high-frequency input motion and (2) reductions due to inertial interaction of high-frequency seismic response are, in many cases, equal to or greater than the reductions due to seismic wave incoherence.

Deleted: SSI and Structure Response

Deleted: SSI and Structure Response

Deleted: SSI and Structure Response

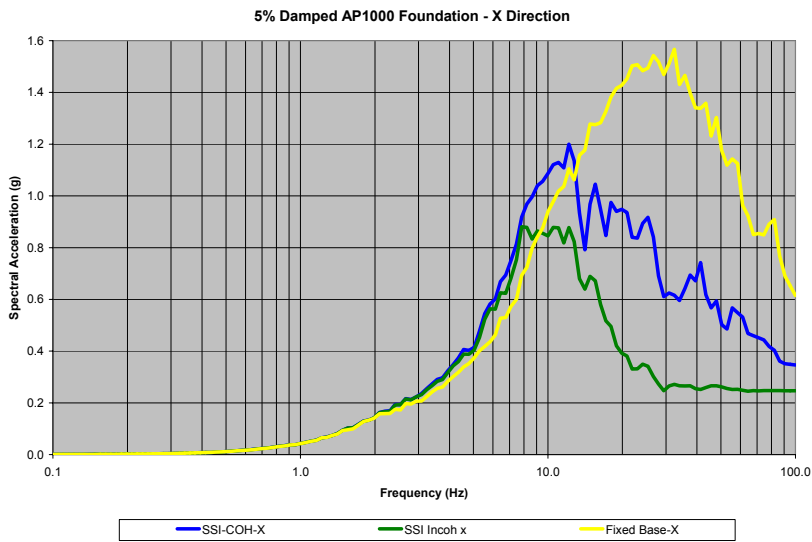


Figure 5-80  
Foundation Response Spectra – X Direction – SSI Coherent, SSI Incoherent, Fixed-Base (Node 1)

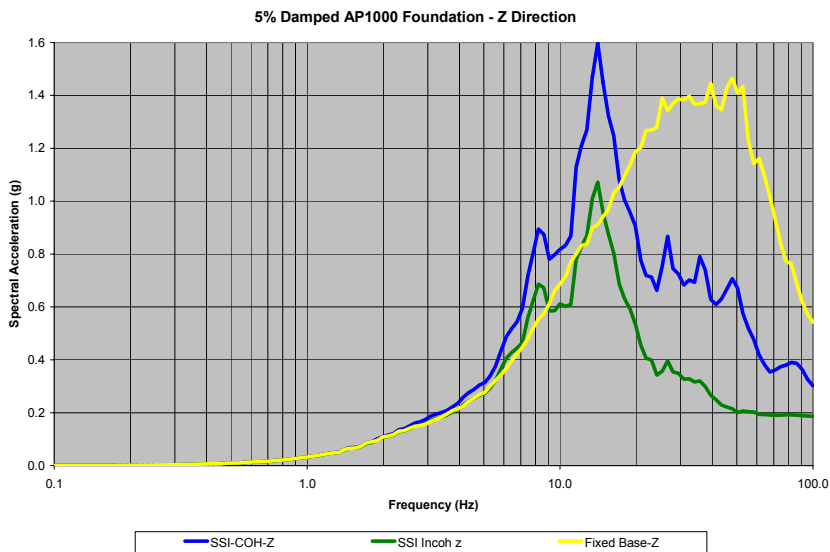
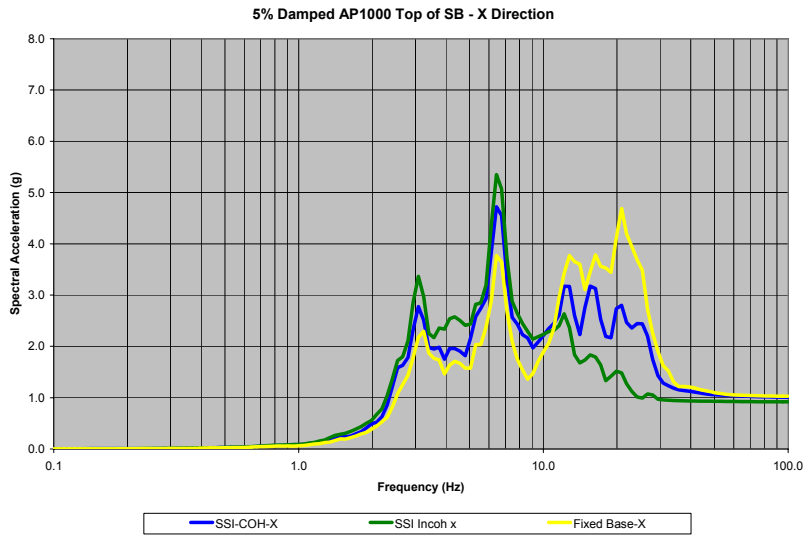


Figure 5-81  
Foundation Response Spectra – Z Direction – SSI Coherent, SSI Incoherent, Fixed-Base (Node 1)

**Deleted:**  
*SSI and Structure Response*

**Deleted:**  
*SSI and Structure Response*

**Deleted:**  
*SSI and Structure Response*



**Figure 5-82**  
**Top of Shield Building Response Spectra – X Direction – SSI Coherent, SSI Incoherent, Fixed-Base (Node 310)**

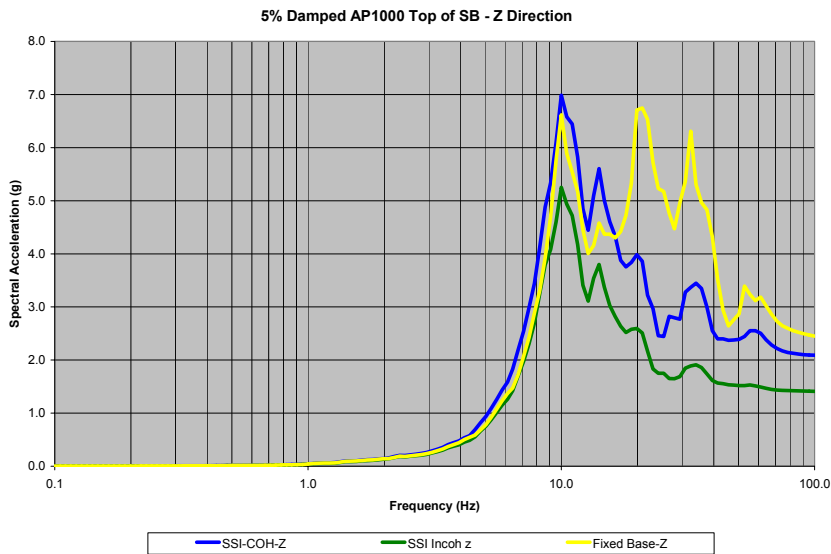


**Figure 5-83**  
**Top of Shield Building Response Spectra – Z Direction – SSI Coherent, SSI Incoherent, Fixed-Base (Node 310)**

Deleted: SSI and Structure Response

Deleted: SSI and Structure Response

Deleted: SSI and Structure Response

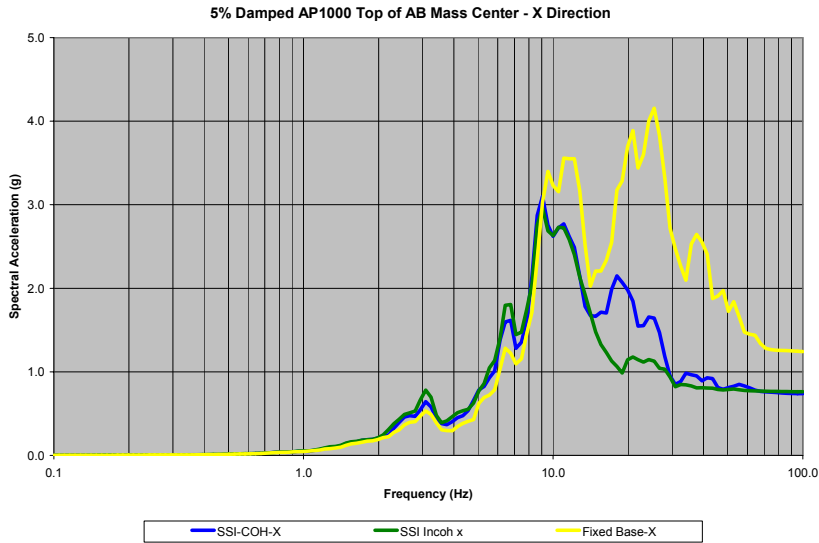


Figure 5-84  
Top of Auxiliary Building Response Spectra – X Direction – SSI Coherent, SSI Incoherent, Fixed-Base (Node 120mc)

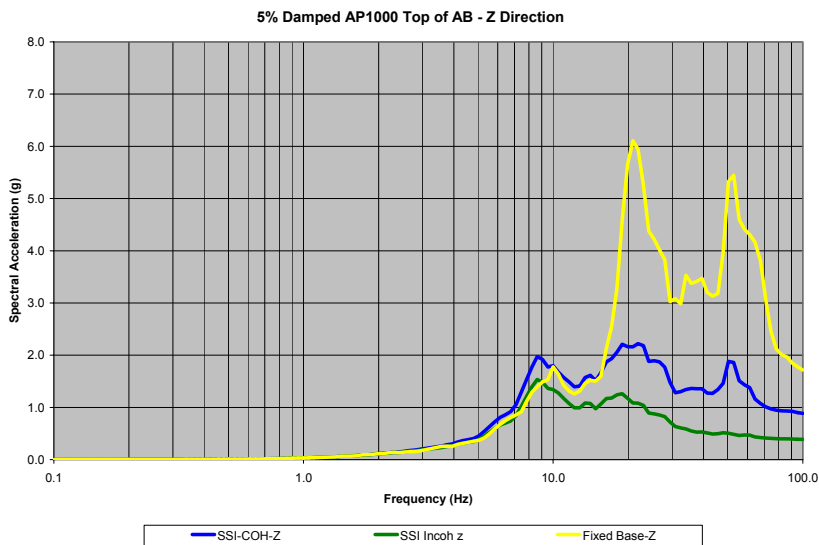
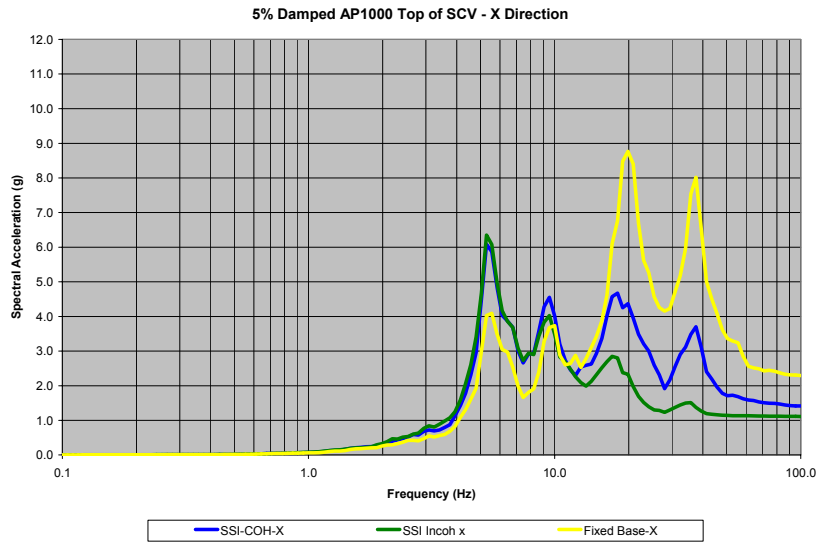


Figure 5-85  
Top of Auxiliary Building Response Spectra – Z Direction – SSI Coherent, SSI Incoherent, Fixed-Base (Node 120)

**Deleted:**  
*SSI and Structure Response*

**Deleted:**  
*SSI and Structure Response*

**Deleted:**  
*SSI and Structure Response*  
*SSI and Structure Response*



**Figure 5-86**  
**Top of SCV Response Spectra – X Direction – SSI Coherent, SSI Incoherent, Fixed-Base (Node 417)**

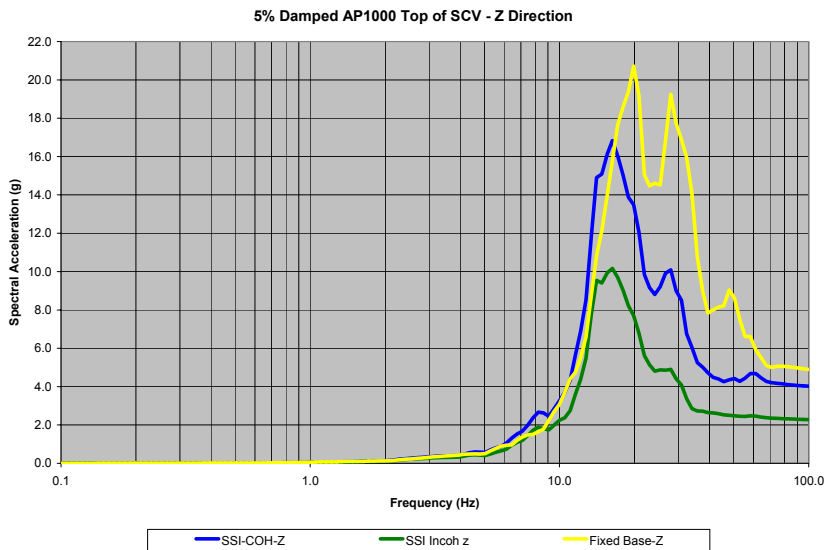


**Figure 5-87**  
**Top of SCV Response Spectra – Z Direction – SSI Coherent, SSI Incoherent, Fixed-Base (Node 417)**

Deleted: SSI and Structure Response

Deleted: SSI and Structure Response

Deleted: SSI and Structure Response

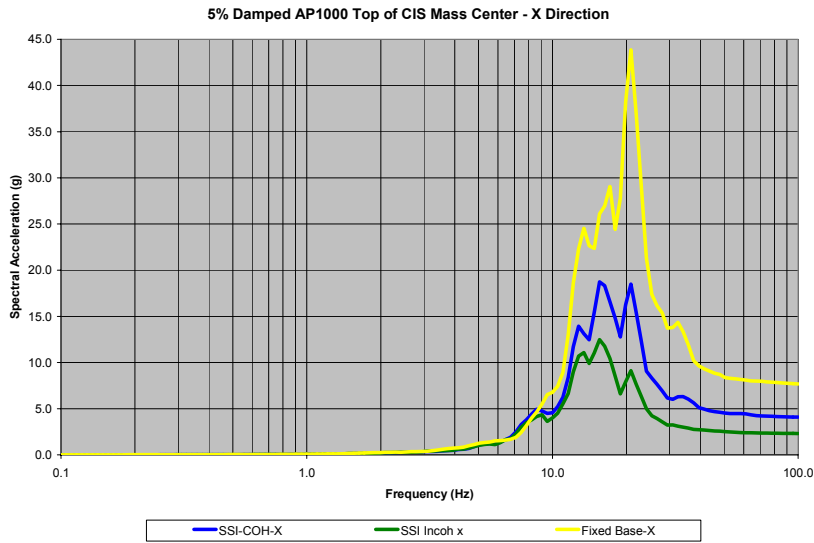


Figure 5-88  
Top of CIS Response Spectra – X Direction – SSI Coherent, SSI Incoherent, Fixed-Base (Node 538mc)

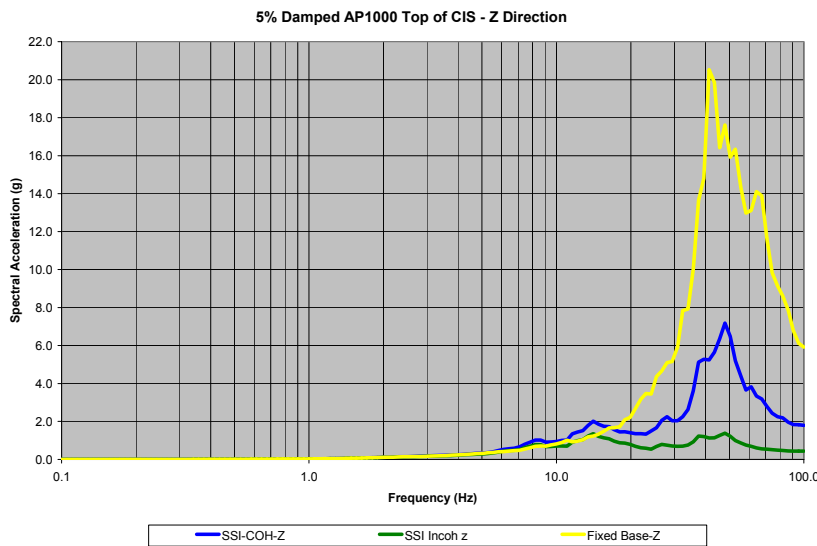


Figure 5-89  
Top of CIS Response Spectra – Z Direction – SSI Coherent, SSI Incoherent, Fixed-Base (Node 538)

# 6

## SUMMARY, CONCLUSIONS AND RECOMMENDATIONS

---

### SUMMARY

#### Tasks Performed and Approach

Task S2.1 of the EPRI/DOE New Plant Seismic Issues Resolution Program has been conducted with results presented herein. The objective of this task is to systematically study seismic wave incoherence effects on structures/foundations similar to those being considered for advanced reactor designs. Seismic wave incoherence arises from the horizontal spatial variation of earthquake ground motion. Spatial variation of horizontal and vertical ground motion can occur and are considered in this task. Two sources of incoherence or horizontal spatial variation of ground motion are:

1. Local wave scattering: Spatial variation from scattering of waves due to the heterogeneous nature of the soil or rock along the propagation paths of the incident wave fields.
2. Wave passage effects: Systematic spatial variation due to difference in arrival times of seismic waves across a foundation due to inclined waves.

This study considers both of these phenomena, but the final results are conservatively based only on local wave scattering.

Seismic response was evaluated for rigid, massless foundations and for example structural models on rigid foundation mats. The basic relationship between motion in the free-field and motion on the rigid massless foundation is developed based on random vibration theory. The starting points are the coherency functions developed by Dr. Abrahamson (Abrahamson, 2005, 2006). Coherency functions define the relationships between ground motion at separate locations as a function of the separation distance between the locations and the frequency of the ground motion. These coherency functions, combined with concepts of random vibration theory, were incorporated into the CLASSI system of SSI analysis programs. The next step is defining the relationship between free-field ground motion at discretized points on the foundation. The relationship is described by the cross power spectral density functions, normalized by the power spectral density (PSD) function of the free-field ground motion. The resulting PSDs of the motion of the rigid, massless foundation are used to define incoherency transfer functions (ITFs). The ITFs are equivalent to scattering functions in CLASSI nomenclature, i.e., frequency-dependent, complex-valued functions. The ITFs, when applied to the free-field ground motion, take into account the effects of incoherence on the foundation input motion. These scattering

**Deleted:** .  
References

**Deleted:** .  
*Summary, Conclusions and Recommendations*

**Deleted:** .  
References  
References

functions permit the evaluation of structure and foundation seismic response directly using the CLASSI family of SSI analysis programs. In general, each component of horizontal ground motion induces a horizontal translation and a companion torsional component. The vertical component of ground motion induces a vertical translation of the foundation and companion rocking components about the horizontal axes. The translational ITFs are principally a function of foundation area. The rotational ITFs are a function of foundation area and foundation shape.

### **Incoherency Transfer Function**

Incoherency transfer functions associated with local wave scattering due to seismic wave incoherence have been computed. The incoherency transfer function provides an indication of the reduction in translational foundation motion and induced rotations as a function of frequency due to seismic wave incoherence. Incoherency transfer functions have been developed for representative foundation shapes and areas. The free-field ground motion considered for the rock site profile is dominated by high-frequency motion, i.e., greater than 10 Hz. The free-field ground motion for the soil site profile is dominated by low-frequency motion, i.e., less than 10 Hz.

Parametric studies have been performed for:

- Foundation Shape, (Constant Area)
  - 150-ft square footprint
  - 100 by 225-ft rectangle footprint
  - 84.63-ft radius circle footprint
- Foundation Area, (Constant Shape)
  - 75-ft square footprint
  - 150-ft square footprint
  - 300-ft square footprint

Extensive calculations have been performed only for local wave scattering effects. The additional effect of wave passage was studied initially. It was found to provide additional reductions in foundation input motion. However, these additional reductions were small compared to those of local wave scattering and dependent on apparent wave velocity, which is a function of earthquake source and transmission path characteristics. These earthquake parameters are difficult to predict and are associated with individual events that are not the typical output of a probabilistic seismic hazard assessment. Therefore, it was judged to be slightly conservative to not include wave passage effects.

**Foundation shape.** Translational foundation response computed for a rectangle, a square of equal area, and a circle of equal area were determined to be essentially identical. This result indicates that for these shapes, the incoherency transfer function for translational response is independent of foundation shape considering a square, a circle, and a rectangle with about a 2 to 1 aspect ratio. This may not hold for more complicated or extended foundation shapes.

Deleted:  
Summary, Conclusions and  
Recommendations

Deleted:  
Summary, Conclusions and  
Recommendations

The measure of comparison for the effects of induced rotations vs. translations of the rigid, massless foundation are transfer functions of translations at the center of the foundation vs. the translations at the periphery of the foundation induced by the rotations of the center. This measure is the maximum effect of the induced rotations. The incoherency transfer functions for induced rotations are similar for the square and circle of equal areas. The relative amplitude of their effect increases with increasing frequency as expected; the largest effect being above 20 or 30 Hz. Comparing vertical response at the center and at the periphery, induced rocking of the foundation is greater than induced torsion due to the difference in the horizontal and vertical coherency functions.

For the rectangular foundation, the torsional and rocking behavior differ significantly from the square foundation of equal area. Significantly greater torsion is induced due to ground motion perpendicular to the long side of the rectangle than for the short side. Similarly, significantly greater rocking is induced about the short axis compared to the long axis.

**Foundation area.** To investigate the effect of foundation area on the translational incoherency transfer function, square foundation footprints with varying area were considered. Larger foundation footprints correspond to much larger reductions in foundation response at high-frequencies. Increasing foundation area from a 75-ft square foundation to a 300-ft square foundation, a factor of 16 on area, results in an increased reduction at 20 Hz from about 0.45 to 0.27 and at 30 Hz from 0.23 to 0.12. Foundation area is demonstrated within this study to be a key parameter.

**Site conditions.** The effect of soil profile on the incoherency transfer function was also investigated. As shown in Chapter 3, even though the scattering transfer function matrix is a function of the compliance matrix and the traction matrix (both of which are dependent on the soil properties), the scattering transfer function itself is independent of soil conditions. As a result, the incoherency transfer function is independent of site conditions and are identical at all frequencies for soil and rock.

## Impact on Response Spectra Due to Incoherence Effects

### Foundation response

For a rigid, massless foundation, foundation response spectra accounting for seismic wave incoherence were computed. By this approach, the PSD is computed from the response spectra of the free-field input motion and input to CLASSI. The program then evaluates the PSD of the foundation motion including the effects of seismic wave incoherence. The resulting response PSD is then converted to foundation response spectra by random vibration theory. Foundation response spectra were developed for the rock and soil site profiles using the compatible free-field high-frequency rock and lower frequency soil ground response spectra, respectively. Parametric studies were performed for:

- Foundation Shape, (Constant Area)
  - 150-ft square footprint

Deleted: .  
References

Deleted: .  
Summary, Conclusions and Recommendations

Deleted: .  
References  
References

- 100 by 225-ft rectangle footprint
- 84.63-ft. radius circle footprint
- Foundation Area (Constant Shape)
  - 75-ft square footprint
  - 150-ft square footprint
  - 300-ft square footprint

**Center of foundation.** Comparison of translational foundation response spectra for the 150-ft square footprint, the circle of equal area, and the 100 by 225-ft rectangle footprint are the same, as would be expected because the incoherency transfer functions are essentially the same and induced rotations do not play a role. The effects of foundation area on translational foundation response spectra were evaluated for the 75-ft, 150-ft, and 300-ft square foundation footprints. These modified spectra or spectra corrections as a function of foundation area are much more significant for the rock site than for the soil site. Again, this is expected because the site-specific free-field ground motion for the soil site is significantly different than the site-specific rock motion. The effect of seismic wave incoherence is primarily a high-frequency phenomenon. Hence, the observed reductions in foundation response spectra are much less for the soil site since the soil site-specific ground motion is deficient in high-frequencies. For the rock site, the peak of the horizontal spectra is reduced from 0.85g for the 75-ft square foundation to 0.76g for the 150-ft square foundation to 0.67g for the 300-ft square foundation. All of these peak spectra values are much less than the 1.48g peak of the horizontal free-field ground motion spectra. Similar behavior is observed for the vertical ground motion.

Spectral corrections from these analyses were also compared to the spectral corrections that are recommended to account for incoherence of ground motion in ASCE 4 (ASCE, 2000). Comparing the recommendations of ASCE 4 with the results generated within this study, the following points are apparent. The methodology of treating the phenomena should be as described herein, i.e., either treat the phenomena in a direct manner or modify the free-field ground motion according to a modified form of the ITF, which accounts for the effects of induced rotations on response, rather than applying a scale factor to the end result in-structure response spectra. This is clearly demonstrated by comparing the correction factors of ASCE 4 with the calculated reductions from the current study. For the rock site, for translations, the reductions calculated here are significantly greater than those recommended in ASCE 4. For the soil site, the calculated reductions are comparable to those of ASCE 4. This demonstrates the need to perform SSI analyses accounting properly for the effects of incoherence or to apply modified incoherency transfer functions to the free-field ground motion, if appropriate. The simplified approach based on the incoherency transfer function as proposed in this study is appropriate because the functions are independent of the input motion.

**Periphery of foundation.** The effect of induced rotations (torsion due to horizontal ground motion and rocking due to vertical ground motion) can be significant at points away from the center of the foundation. In the extreme, these phenomena are observed on the periphery of the foundation. The impact on foundation response will decrease as one moves to the center. In direct treatments, the effect of induced rotations is directly taken into account. For simplified or

approximate methods, the effects of these rotations is incorporated into function generated to increase the Incoherency Transfer Function (ITF) in the lower frequency part of the function (as described in Chapter 5).

The effect of incoherence of ground motion on foundation response in the frequency range above 10 Hz is substantial even considering these induced rotations.

### **Structure response**

The effects on in-structure response spectra due to seismic wave incoherence were calculated for a simplified structural model accounting for soil-structure interaction effects. The structure utilized for these studies is represented by a simplified structural model of three sticks supported by a 15-ft thick foundation mat with 150-ft square plan dimensions. The three simplified structural models represented an Auxiliary Shield Building (ASB), Steel Containment Vessel (SCV), and a Containment Internal Structure (CIS). The ASB and CIS structures were modeled including nominal torsion which was included by assuming approximate offsets between the centers of mass and the centers of rigidity. These offsets were intended to approximate the torsional behavior included in the more detailed stick models. Offsets were introduced at and below the roof level of the Auxiliary Building, and throughout the CIS structure model. These representations introduced natural torsion into the models. The shear centers of the three sticks are coincident along the Z-axis.

The fixed-base modes of the three structure sticks provide some insight into their dynamic behavior. The ASB has predominate modes with frequencies less than 10 Hz with fundamental modes in the horizontal directions of 3.2 Hz (X-direction) and 3.0 Hz (Y-direction); the fundamental mode in the vertical direction of frequency 9.9 Hz (Z-direction). Many modes participate in the response of the ASB. The predominate modes of the SCV in the horizontal directions also have frequencies less than 10 Hz – the lowest frequency of an important X-direction mode being 5.5 Hz; Y-direction mode being 6.1 Hz; the lowest frequency of an important vertical mode being 16 Hz. As with the ASB, many modes participate in the response of the SCV. The predominant modes of the CIS have frequencies greater than 10 Hz. Many modes participate in the response of the CIS.

Four sets of analyses were performed:

1. SSI analysis with coherent input motion
2. SSI analysis with incoherent input motion
  - a. Rigorous approach including all components of foundation input motion (three translations and three rotations)
  - b. Rigorous approach excluding rotational foundation input motion
3. SSI analysis with input motion modified by a function based on the Incoherency Transfer Function to reflect incoherence-induced rotation effects

Results presented are in-structure response spectra at the foundation and at representative points in the structure models for two horizontal, X and Y, and the vertical direction, Z of ground

**Deleted:** .  
References

**Deleted:** .  
*Summary, Conclusions and Recommendations*

**Deleted:** .  
References .  
References

motion. In addition, rigid “outrigger” elements were added to the selected node points to assess the effect of induced rotations on the response of extreme locations. For each of the structures, the responses at the following locations were calculated and evaluated:

- Auxiliary Shield Building (ASB)
  - Top of the Shield Building
    - Approximately 265-ft above the foundation
    - Centerline (Node 310) and outrigger at 75-ft from the centerline (Node 310out)
  - Top of the Auxiliary Building
    - Approximately 113-ft above the foundation
    - Centerline (Node 120), center of mass (Node 120mc), and outrigger at 75-ft from the centerline (Node 120out)
  - Low on the Auxiliary Shield Building
    - Approximately 68-ft above the foundation
    - Centerline (Node 80) and center of mass (Node 80mc)
- Containment Internal Structure (CIS)
  - Top of CIS
    - Approximately 102-ft above the foundation
    - Centerline (Node 538), center of mass (Node 538mc), and outrigger at 75-ft from the centerline (Node 538out)
  - Mid-Height of CIS
    - Approximately 67-ft above the foundation
    - Centerline (Node 535) and center of mass (Node 535mc)
- Steel Containment Vessel (SCV)
  - Top of SCV
    - Approximately 215-ft above the foundation
    - Centerline (Node 417) and outrigger at 65-ft from the centerline (Node 417out)
  - Mid-Height of SCV
    - Approximately 65-ft above the foundation
    - Centerline (Node 406)

All analyses were performed using the computer program CLASSI. The rock site profile and the spectrum compatible time histories for the high-frequency rock site response spectra were used for Analyses 1, 2 and 3.

**Deleted:**  
*Summary, Conclusions and Recommendations*

**Deleted:**  
*Summary, Conclusions and Recommendations*

Analysis 1 was performed with CLASSI assuming the free-field ground motion was comprised of vertically propagating waves and with no incoherence effects. In CLASSI nomenclature, the scattering functions were frequency-independent and equal to 1.0, i.e., there is no kinematic interaction such that the foundation input motion was identical to the free-field ground motion.

Analysis 2a was performed with CLASSI accounting for the incoherency of the ground motion through the ITFs. The ITFs were defined from the PSDs of the motion of the rigid, massless foundation described above. The ITFs are equivalent to scattering functions in CLASSI nomenclature, i.e., frequency-dependent, complex-valued functions. ITFs, when applied to the free-field ground motion, take into account the effects of incoherence on the foundation input motion. These scattering functions permit the evaluation of structure and foundation seismic response directly using the CLASSI family of SSI analysis programs. This approach is direct and “exact”.

Comparison of the results of Analyses 1 and 2a show:

- **Centerline of the structure.** The response spectra at the tops of the Shield Building and Steel Containment Vessel, both at high elevations in the structural complex, demonstrate significant reductions in spectral accelerations due to incoherence of ground motions. The reductions at frequencies greater than approximately 12 Hz range from minimal to above 50 percent. In the case of the Shield Building, at frequencies less than 10 Hz, the incoherent response slightly exceeds the coherent response at frequencies of peak amplification. The response spectra at the top of the Auxiliary Building demonstrate similar reductions due to incoherence, but smaller in amplitude. The response spectra at the top of the CIS demonstrate significant reductions due to incoherence. The mid-height reductions for the ASB, SCV, and CIS follow similar trends.

For the Containment Internal Structure (CIS), a structure with predominant fixed-base frequencies greater than 10 Hz, induced rocking is extremely important to calculating total horizontal response. It is surmised that the high-frequency characteristics of this structure play a role in the importance of induced rocking for the high-frequency ground motion.

- **Periphery of structures (outriggers).** Generally, the trends noted above concerning the coherent vs. incoherent response hold at the periphery of the structures. However, the amounts of the reductions are less in some cases. The effect of torsional response is clearly observed in the response comparisons of Analyses 2a and 2b. Thus, induced torsion needs to be taken into account in calculating the structure response to incoherent motion.

Analysis 2b was performed with CLASSI only accounting for the incoherency of the ground motion on the translational components of foundation input motion. The translational ITFs (or scattering functions) were those of Analysis 2a; the rotational ITFs (or scattering functions) were set to zero. Analysis 2b permits an evaluation of the importance of induced rotations on structure response. The results of Analysis 2b highlighted the importance of induced rocking on in-structure horizontal response and the importance of induced torsion on horizontal response at peripheries of the structure.

Simplified methods to incorporate the effects of ground motion incoherence have also been a goal of this project. The generic approach for the simplified method is to generate a modification

**Deleted:** .  
References .

**Deleted:** .  
*Summary, Conclusions and Recommendations*

**Deleted:** .  
References .  
References

of the free-field ground motion as a function of foundation size and frequency of the ground motion to incorporate the effects of incoherence. Simplified approaches have numerous benefits if validated. In particular, if the approach focuses on modifying the free-field ground motion accounting for incoherence, standard seismic analysis programs and methods could then be employed directly without special routines or programs written. The simplified approach is to scale the Fourier amplitude spectra of the free-field ground motion by a function derived from the ITFs and modified as necessary to incorporate the effects of induced rotations. This function is then applied to the Fourier amplitude function of the free-field ground motion. The Fourier phase spectrum is unaffected. Trial applications of this approach are described below.

## **Benchmark Comparison**

The development of incoherency transfer functions, their impact on response spectra for an example rigid, massless foundation and the in-structure response of a typical nuclear power plant structure have been validated by independent benchmark comparisons of results (Appendix C). For this purpose, the effect of incoherent ground motion has been evaluated by:

- Two different SSI computer programs; CLASSI and SASSI.
- Two different algorithms; CLASSI-stochastic method and SASSI-eigen decomposition method.
- Two different analytical approaches; random vibration theory (RVT) by CLASSI, and time history dynamic analyses by SASSI.
- Two different organizations conducting the analyses; CLASSI by the ARES team, and SASSI by the ARES team and the Bechtel Corp.

Excellent agreement is obtained for both incoherency transfer functions and in-structure response spectra on the foundation and locations on the structures. Although the benchmark studies focused on translational responses rather than the combination of translations and rotations, the team is confident that when considering all effects, the benchmark comparison will meet engineering acceptability. The benchmark comparison is validation of the technical approach being employed in Task S2.1.

## **APPLICATIONS**

Two approaches have been evaluated in the present study: direct incorporation of the Abrahamson coherency functions into soil-structure interaction computer programs CLASSI and SASSI; and the simplified approach of modifying the free-field ground motion and performing SSI analysis for the resulting modified ground motion assuming coherent input motions.

- **Direct incorporation into SSI analysis computer programs.**
  - Incorporation of the Abrahamson coherency functions into CLASSI follows a random vibration approach and is considered “exact” for the assumptions of the CLASSI methodology. These assumptions are the effective foundation stiffness is rigid and the foundations are surface-founded. The effective foundation stiffness is the result of the

**Deleted:**  
Summary, Conclusions and Recommendations

**Deleted:**  
Summary, Conclusions and Recommendations

foundation itself and the stiffening effects of the inter-connecting structure with the foundation. The mat foundations of heavy shear wall structures and containment/internal structures behave rigidly when taking into account the inter-connecting structural elements. Other configurations, such as structures with spread footings or strip foundations will not meet this assumption. Structures with embedded foundations and partially embedded walls can be treated with SSI analysis programs such as CLASSI, but require input in the form of scattering and impedance matrices from finite element representations.

- The Abrahamson coherency functions have been successfully implemented in versions of SASSI. The approach taken in SASSI is a deterministic approach. It requires the eigen-decomposition of the coherency function matrix which defines the coherency relationship between interaction node points. By the ARES version of SASSI implementing incoherency all modes are used and combined by absolute summation. This approach is shown to match the CLASSI results very closely in Appendix C. SASSI is not limited to foundations behaving rigidly or to surface-founded configurations.

Hence, the direct implementation approach has been validated and is available to treat the SSI response of nuclear power plant structures.

- **Simplified approach of modifying the free-field ground motion.**

- An alternate means of incorporating seismic wave incoherence into seismic analyses has been developed and implemented. This alternative approach is to scale the Fourier amplitude spectrum of the free-field input motion by a function related to the Incoherency Transfer Function (ITF). The Fourier phase spectrum is unaffected. The result is a re-defined ground motion for SSI and dynamic structure analysis.
- For the recommended modified and scaled ITF, for frequencies less than 12 Hz, define the ITF scaling function to be 1.25, i.e., an increase in the amplitude of the Fourier transform of the free-field ground motion. Above 12 Hz, the modified and scaled ITF transitions smoothly to 1.25 times the ITF for the foundation footprint. This function is shown graphically in Figures 5-38 and 5-39 in the light blue curves.
- The results of this simplified method are compared with the results generated by the direct or “exact” implementation and are judged to adequately and conservatively represent those results.
- This simplified approach has been developed considering ground motion on a rock site in the central and eastern United States where the peak of the free-field ground motion is in the range of 20 to 30 Hz. It is judged that this simplified approach is applicable for other similar rock sites with high-frequency ground motion. It is further judged that this simplified approach would not necessarily (without additional studies) be applicable for soil sites with low-frequency ground motion. In fact, the low-frequency increase to 1.25 for frequencies less than 12 Hz would likely not be required.
- The simplified approach has been developed to empirically match direct incoherent analysis results for a single representative NPP nuclear island. The model used included three structures of various dynamic characteristics ranging from a flexible shield building to a stiff containment internal structure.

**Deleted:** .  
References

**Deleted:** .  
*Summary, Conclusions and Recommendations*

**Deleted:** .  
References  
References

- The simplified approach relies on conservative assumptions in order to envelope the exact responses at all the representative locations within the demonstration model. If new plants find this approach to be beneficial, i.e., this conservatism does not preclude its implementation, then further sensitivity studies could be warranted in the future.

## CONCLUSIONS

The conclusions of this study are:

- The phenomena of incoherence are important for high-frequency ground motions (primarily greater than 10 Hz) and high-frequency response of structures. Realistically accounting for ground motion incoherence on the seismic response of nuclear power plant structures is significant and should be properly incorporated into seismic design analyses.
- Consideration of coherent earthquake ground motion that results from the assumption of vertically propagating plane waves, generally, produces conservative (and in some cases overly conservative) foundation motion at frequencies greater than 10 Hz. Seismic wave incoherence or spatial variation from scattering of waves due to the heterogeneous nature of the soil or rock along the propagation paths of the incident wave fields results in averaging or integrating effects of high-frequency ground motions by stiff nuclear power plant structures' foundations.
- Generally, for the rock site and corresponding high-frequency free-field ground motion considered in this study, incoherent earthquake ground motion results in calculated in-structure response spectra at the tops of the structures and at mid-heights showed minimal effects below 10 Hz. For the case of the top of the Shield Building, the incoherent responses showed amplification in spectral accelerations above those for the coherent case at frequencies of peak amplification less than 10 Hz. In frequency ranges above 10 Hz, the ratio of coherent response spectra to incoherent response spectra varied from about 1 to greater than 2. Generally, above 10 Hz, there is significant conservatism in the coherent spectra. This includes the principal effect of induced rocking, i.e., excitation of horizontal modes and the resulting amplification of horizontal response in the structure.
- Induced rotations may be important to in-structure response depending on the structure and its dynamic characteristics.
  - The effect of induced torsional response was quantified for the three structure models of interest by evaluating response at outriggers placed at structure peripheries. Induced torsion is important, but does not invalidate the significant reductions observed in in-structure response spectra for frequencies greater than approximately 12 Hz.
  - The effect of induced rocking on horizontal structure response was evaluated. For those portions of the structure model with frequencies of important fixed-base horizontal modes below 10 Hz, i.e., the ASB and SCV, induced rotations had minimal impact on in-structure response. For the CIS with frequencies of important fixed-base horizontal modes greater than 10 Hz, the impact of induced rocking on in-structure response was significant. This is expected from two regards: the rocking ITFs gain importance as frequency increases above 10 Hz; and the free-field ground motion has significant frequency content above 10 Hz.

**Deleted:**  
Summary, Conclusions and Recommendations

**Deleted:**  
Summary, Conclusions and Recommendations

- The phenomena of incoherence are three-dimensional. Induced torsion couples horizontal response in the two horizontal directions. Induced rocking couples horizontal and vertical response, i.e., incoherent vertical ground motion induces horizontal response in the structure.
- Two valid direct approaches for accurately addressing incoherency effects have been studied and recommendations for their implementation have been provided within this report:
  - The primary direct approach utilized within these studies incorporates the Abrahamson coherency functions directly into the CLASSI soil-structure interaction program
  - As a result of the effort to benchmark the CLASSI direct incoherency approach, the SASSI method by Bechtel and the ACS SASSI method by ARES are also available to treat the effects of incoherence on structures. A benefit of this study is that there are multiple direct methods that may be used to account for incoherency effects on nuclear power plant structures.
- Another valid, but conservative approach for addressing incoherency effects has been studied, and recommendations for its implementation have been provided within this report. The simplified approach applies a modified form of the Incoherency Transfer Function (ITFs) to the free-field ground motion and allows for the performance of the SSI analysis for the resulting modified ground motion assuming coherent input motions.
- Regarding the simplified approach, a recommendation has been provided for a simplified approach which will provide insight into the effects of incoherence on foundation and structure response. The simplified approach is applicable to rock sites and the corresponding free-field ground motion with significant high-frequency content. The concept of the simplified approach has been validated herein. However, its generalization to foundation/structure systems of all types will require additional sensitivity studies to be performed. These sensitivity studies would include variations in structure and foundation conditions and ground motion characteristics. This simplified approach is necessarily conservative due to its goal of being generically applicable to as broad a range of structures and foundations as possible and due to the incoherency-induced rotations that exist for some structure/foundation configurations.
- For realistic, but simplified, foundation shapes studied herein, the most important parameter was found to be foundation area. Foundation shape (square vs. rectangle vs. circle) and site soil conditions were found to have minimal effect on the translational component ITFs. Foundation shape does have an effect on induced rotational ITFs.
- The CLASSI analyses performed in this study rely on the assumption that the foundation of the structure behaves rigidly when subjected to earthquake ground motion. The behavior of a foundation is dependent on the effective stiffness, which is a function of the foundation itself and the stiffening due to the interconnecting structural elements anchored to the foundation. The results of this study are applicable to typical nuclear power plant structures whose foundations are significantly stiffened by inter-connecting structural systems. Examples of such structures are reactor containments with internal structures and heavy shear wall structures. It is important to note that SSI analysis programs utilizing finite element modeling of the foundation, such as SASSI, are not restricted to the assumption of foundations behaving rigidly. An additional observation is that any effective flexibility of the foundation will likely reduce the effect of induced rocking on structure response.

<b>Deleted:</b> References
<b>Deleted:</b> <i>Summary, Conclusions and Recommendations</i>
<b>Deleted:</b> References References

- The combined effects of spatial variation of ground motion with depth in the rock/soil and the effect of incoherence of ground motion for structures with embedded foundations and partially embedded walls is judged to be analyzable by considering the effects simultaneously or by separation of the two effects and superimposing the results. Appendix E documents a sensitivity study performed to evaluate the effects of incoherence on surface/embedded foundation/structure systems. A representative reactor containment/internal structure, supported on the rock site profile and subjected to the companion high-frequency ground motion was analyzed. Surface founded coherent and incoherent responses were calculated and the effects of incoherence quantified. The same structure was analyzed for an embedment ratio of 0.5. Coherent and incoherent responses were calculated. Isolating the effects of incoherence from the other aspects of SSI was done. In general terms, the results demonstrate that the effects of incoherence and embedment are separable. In addition, the effects of embedment on response for coherent and incoherent ground motions were demonstrated to significantly reduce response. The ACS-SASSI program was used.
- Computer programs that model flexible foundations and embedment, such as SASSI (when modified to treat the phenomena of incoherency), can effectively analyze soil-structure systems including those effects.
- Appendix B highlights the difficulties of validating the effects of incoherence of ground motion on nuclear power plant structures with currently existing data. The approach taken in the present study to account for incoherence of ground motion is compatible with that taken by Stewart and colleagues to evaluate recorded data and to implement the results into the seismic design process. Recorded data at Diablo Canyon and Perry nuclear power plants, as well as the data used in the Stewart and Kim studies, highlight the difficulties in using recorded data to validate specific elements of SSI. Carefully designed instrumentation schemes will be required in the future to validate these individual elements.

In summary, seismic analyses incorporating ground motion incoherence demonstrate a significant reduction in high-frequency seismic response as measured by in-structure response spectra. The computed incoherency transfer functions depend on the foundation area and are independent of site soil conditions. However, the resulting spectral reductions strongly depend on the site soil conditions. The effect of seismic wave incoherence is primarily a high-frequency phenomenon. Hence, the observed reductions in foundation response spectra are much less for soil sites since the soil site-specific ground motion is generally deficient in the high-frequency portion of the spectra. The project effectively demonstrated the validity of using SSI codes modified to incorporate incoherency effects as a method for deriving structural responses for nuclear structures. The CLASSI program approach was validated using a series of benchmark problems with the SASSI code. A variety of sensitivity studies were completed which resulted in key insights as to the effects that foundation size, shape and soil properties have on the results. The project studied the options available to generate a simplified approach toward incorporation of incoherence effects that eliminates the need to perform a specific SSI analysis which incorporates the incoherence effect. A recommendation for this simplified approach has been provided based on the studies performed on the three example structures. The benefits of utilizing this simplified approach are that it is easier to implement and does not require the use of a modified version of a SSI computer program. The trade-off for that simplification is that the

method is more conservative than the direct approach and may not provide the degree of realistic response desired by a specific new plant application.

**Deleted:**  
*Summary, Conclusions and Recommendations*

**Deleted:**  
*Summary, Conclusions and Recommendations*



# 7

## REFERENCES

---

- Abrahamson, N. (2006). *Spatial Coherency for Soil-Structure Interaction*, Electric Power Research Institute, Final Report 1014101, Palo Alto, CA. August (Draft).
- Abrahamson, N. (2005). *Spatial Coherency for Soil-Structure Interaction*, Electric Power Research Institute, Technical Update Report 1012968, Palo Alto, CA. December.
- ASCE (2000). *Seismic Analysis of Safety-Related Nuclear Structures and Commentary*, American Society Civil Engineers, Report. ASCE 4-98.
- Chang, C.-Y., M.S. Power, I.M. Idriss, P. Sommerville, W. Silva, and P.C. Chen. (1986). *Engineering Characterization of Ground Motion, Task II: Observational Data on Spatial Variations of Earthquake Ground Motion*, NUREG/CR-3805, Vol. 3.
- CSI (2004). Computers and Structures Incorporated, SAP2000, Integrated Software for Structural Analysis and Design, Version 9.
- Der Kiureghian, A. (1980). *Structural Response to Stationary Excitation*, Journal of the Engineering Mechanics Division, American Society Civil Engineers, December.
- EPRI (1997). *Soil-Structure Interaction Analysis Incorporating Spatial Incoherence of Ground Motions*, Electric Power Research Institute, Report TR-102631 2225, Palo Alto, CA. November.
- EPRI (1993) *Guidelines for Determining Design Basis Ground Motions, Volume 1: Method and Guidelines for Estimating Earthquake Ground Motion in Eastern North America*, Electric Power Research Institute, Report TR-102293, Palo Alto, CA. November.
- EPRI (1991). *A Methodology for Assessment of Nuclear Power Plant Seismic Margin (Rev 1)*, Electric Power Research Institute, Report NP-6041-SL, Palo Alto, CA. August.
- Ghiocel Predictive Technologies, Inc. (2006). ACS-SASSI, An Advanced Computational Software for 3D Dynamic Analysis Including Soil-Structure Interaction, Version 2.1, Pittsford, New York.
- Johnson, J.J. (2003). *Soil-Structure Interaction*, Earthquake Engineering Handbook, Chapter 10, W-F Chen, C. Scawthorn, eds., CRC Press, New York, NY.
- Kim, S. and J.P. Stewart (2003). *Kinematic Soil-Structure Interaction from Strong Motion Recordings*, Journal of Geotechnical and Geoenvironmental Engineering, ASCE, April.

McCann, M., J. Marrone, and R. Youngs (2004). *CEUS Ground Motion Project Final Report*, TR-1009684, Electric Power Research Institute, Palo Alto, CA, December.

Orr, R. (2003). *AP1000 Inputs for 2D SASSI Analyses*, Calculation No. APP-1000-S2C-052, Rev. 0, Westinghouse.

Orr, R., Westinghouse Corporation (2006). Personal email communication on AP1000 Model Properties to Greg Hardy, ARES Corporation, August.

Ostadan, F., Bechtel Corporation (2006). Personal email communication on SASSI SSI Analysis Results to Steve Short, ARES Corporation, August.

Rood, H., et al (1991). *Safety Evaluation Report Related to the Operation of Diablo Canyon Nuclear Power Plant 2*, NUREG-0675, Supplement No. 34, USNRC, June.

U.S. Department of Energy (2002). *Natural Phenomena Hazards Design and Evaluation Criteria for Department of Energy Facilities*, DOE-STD-1020-2002, January.

Wong, H.L. and J.E. Luco (1980). *Soil-Structure Interaction: A Linear Continuum Mechanics Approach (CLASSI)*, Report CE, Department of Civil Engineering, University of Southern California, Los Angeles, California.

**Deleted:** .  
References

**Deleted:** .  
Summary, Conclusions and Recommendations

**Deleted:** .  
References  
References

# A

## COMMENTS AND RESPONSES TO NRC REQUESTS FOR ADDITIONAL INFORMATION (RAIs)

---

The NRC submitted 53 RAIs related to the S2.1 Task on June 1, 2006. These RAIs were titled “Section 4.0 –Comments on EPRI Report 1012966 *Effect of Seismic Wave Incoherence on Foundation and Building Response (S2.1)*”. The industry responses and resolutions for these 53 RAIs are documented below.

**NRC Comment/Question:**

4.1 The report seems to be written well and different topics of discussion are well laid out.

**Industry Response/Resolution:**

4.1 Thank you.

---

**NRC Comment/Question:**

4.2 An important gap in this study is the lack of any treatment of kinematic interaction of embedded foundations or any questioning of the validity of the use of the proposed Abrahamson coherency function for those foundations.

**Industry Response/Resolution:**

4.2 Embedment – the question of validity of Abrahamson coherency function at depth is addressed in EPRI Report 1014101 (Spatial Coherency Models for Soil-Structure Interaction). Dr. Abrahamson has included additional material within this report relative to the data available to support the validity of using the coherency function with depth.

Embedment effects on SSI response of NPP structures are due to kinematic response and inertial response. Kinematic response effects are due to spatial variation of ground motion and the integrating effects of the embedded foundation and partially embedded walls. Two aspects of spatial variation of ground motion are to be considered: the variation of free-field ground motion with depth in the soil or rock from the surface to foundation for a partially embedded structure; and the incoherency effects. The first has a significant effect on the foundation input motion generally reducing the translational motion of the foundation and increasing the rotational motion. This effect exists independent of incoherency. The assumption and judgment is that the effects of incoherency are separable from this aspect of spatial variation of ground motion with depth. Appendix E on effects of embedment and incoherence will address this assumption and judgments in this area. A further assumption is that the coherency

**Deleted:**  
*Effect of Embedment and Incoherence*

**Deleted:**  
*Effect of Embedment and Incoherence*

**Deleted:**  
*Effect of Embedment and Incoherence*

functions are applicable at depth as well as on the surface of the soil or rock. Given these assumptions, kinematic interaction effects can be treated separately and combined at the later stage or treated simultaneously in a methodology, such as SASSI. If treated separately, one needs to be careful not to double count the effect of incoherence and vertical spatial variation of motion. It should be noted that Abrahamson coherency function is developed for horizontal separation distance only. Any ground motion incoherency effects due to elevation (or depth) differences of ground nodal points is ignored. In SASSI, the Abrahamson coherency model is applied at all horizontal planes within the embedded part of the foundation based on the horizontal distance of the nodal points. Appendix E addresses the subject of embedment in more detail.

---

**NRC Comment/Question:**

4.3 The standard practice of performing SSI analysis using coherent ground motion was based on observation and interpretation of data from down hole arrays that show a large percentage of the power of ground motion comes from vertically propagating waves. It appears that the recommended method of SSI analysis in this report is simply to reduce the amplitudes of ground motion at frequencies generally above 10 Hz, and then apply the reduced motion uniformly (coherently) across the entire foundation.

**Industry Response/Resolution:**

4.3 Chapter 6 itemizes the two methods of treating incoherency of ground motion:

- 1) Take the coherency function directly and input to the SSI analysis using a program that incorporates both the SSI and incoherence effects (what we have labeled as the direct approach).
- 2) Modify the input motion and evaluate the new input as coherent motion (what we have labeled as the simplified approach).

Both of these methods are considered to be acceptable approaches for the treatment of incoherency effects and further elaboration will also be provided within the EPRI I1.1 integration report.

---

**NRC Comment/Question:**

4.4 This report needs to clearly layout the approach and implementation scheme for using the SSE (design ground motion) derived from a performance-based approach in conducting engineering analyses. Detailed steps of the implementation in carrying out the SSI analysis using the incoherent motion approach, including guidance on soil parameter modeling are needed.

**Industry Response/Resolution:**

4.4 This requested overall approach and implementation scheme will be defined in the EPRI Integration task I1.1 and documented within that report. The overall implementation approach is a broader scope than that of this incoherence task and will include the risk

calculations and SSE determination in tasks G1.1, G1.2 and G1.3, as well as the implementation of the results from S2.1. Chapter 6 describes two alternatives to incorporating the effects of incoherency of ground motion and its association with the SSI analysis.

**Deleted:**  
*Effect of Embedment and Incoherence*

**Deleted:**  
*Effect of Embedment and Incoherence*

**Deleted:**  
*Effect of Embedment and Incoherence*

---

**NRC Comment/Question:**

4.5 Complicated equations are described that use rectangular and square matrices, which are appropriately multiplied by column matrices to obtain resulting equations. These are described in text, however a step-by-step process of converting the matrices using conceptual layout in matrix form will enhance the reader's understanding.

**Industry Response/Resolution:**

4.5 We reviewed the text in Chapter 3 and introduced some further clarifications to assist with the enhancement of the reader's understanding.

---

**NRC Comment/Question:**

4.6 The ASCE Journal of Geotechnical and GeoEnvironmental Engineering issue of April 2003, Volume 129, Number 4 published an article, "Kinematic Soil-Structure Interaction from Strong Motion Recordings" by Seunghyun Kim and Jonathan Stewart. This article points out that the incoherence parameter is dependent on the site shear wave velocity. This paper also points out that the use of incoherent motion introduces torsional motion.

**Industry Response/Resolution:**

4.6 Appendix B of this report discusses the Kim and Stewart paper and its applicability to the present study. The Kim and Stewart paper and its ramifications were also discussed at the May 11-12 meetings at the NRC.  
Incoherency does introduce both torsion and rocking. Chapters 4, 5, and 6 have been expanded in this area and discuss the impact of induced rotations on foundation and structure response.  
In Chapter 3, it is demonstrated that the incoherency transfer function for random spatial variations is independent of any soil properties. Of course, incoherence effects on response spectra are dependent on soil properties.

---

**NRC Comment/Question:**

4.7 Page iv: As discussed here, seismic wave incoherence occurs because of the horizontal spatial variation of both horizontal and vertical ground motions. The variation in the horizontal input motions will result in torsional input at the foundation while the variation in the vertical motions will cause rocking of the base mat. Please discuss in detail the basis for not considering the torsion and rocking effects and state whether these effects will be considered in the individual plant ESP and/or COL applications.

**Deleted:**  
*Effect of Embedment and Incoherence*

**Deleted:**  
*Effect of Embedment and Incoherence*

**Deleted:**  
*Effect of Embedment and Incoherence*

**Industry Response/Resolution:**

4.7 Torsion and rocking have been considered in this study. See the response to question 4.6 and the new material within Chapters 4, 5 and 6 of this report.

---

**NRC Comment/Question:**

4.8 Page iv: This section states that the seismic response is evaluated for rigid, massless foundations and for example structural models on foundation mats that behave rigidly. Please discuss how the results would be impacted by taking into account the flexibility and mass of the foundation and state whether these effects will be considered in the individual plant ESP and/or COL application. (See also page 1-2 for the same subject).

**Industry Response/Resolution:**

4.8 a. Flexibility - the industry teams' recommendation that the S2.1 methodology is applicable to NPP structures (containments, internal structure/NSSS, and heavy shear wall structures) is based on published data, including ASCE (2000), *Seismic Analysis of Safety-Related Nuclear Structures and Commentary*, American Society Civil Engineers, Report ASCE 4-98, and engineering judgment. The SSI analysis procedures implemented in CLASSI and SASSI validated the approach to treating the phenomena. CLASSI is limited to foundations effectively behaving "rigidly", i.e., the combined effective stiffness of the inter-connecting structure and the foundation behaves rigidly for overall soil-structure response analysis. This assumption is applicable to NPP structures mentioned above. The SASSI implementation of the incoherence effects is not limited to foundations behaving "rigidly" and foundation flexibility can be considered in the SASSI solution.

b. Mass – the substructure approach to SSI as implemented in CLASSI was discussed at the May 12 meeting. The foundation input motion is derived by multiplying the free-field ground motion times the scattering matrices and accounts for kinematic interaction – the next step is solving the SSI problem including mass of foundation and dynamic characteristics of the structure.

---

**NRC Comment/Question:**

4.9 Page iv: This section states that the incoherency transfer functions depend on the foundation area and are independent of site soil conditions but that the resulting spectral reductions strongly depend on site soil conditions. This seems to be inconsistent. Please explain. (This statement also appears on page ix.)

**Industry Response/Resolution:**

4.9 The transfer functions are not dependent on the site conditions (See response to RAI 4.47). The effects on free-field response spectra are highly dependent on these free-field ground response spectra: those with significant high-frequency content (rock site profile) will experience significant reductions in frequency content above 10 Hz; those with minimal amplified frequency content above 10 Hz (soil site profile) will experience

minimal impact on the free-field response spectra. The report text (Chapters 4 and 5) has been modified to make the description of this more complete in order to alleviate any misconception of an inconsistency.

**Deleted:**  
*Effect of Embedment and Incoherence*

**Deleted:**  
*Effect of Embedment and Incoherence*

**Deleted:**  
*Effect of Embedment and Incoherence*

---

**NRC Comment/Question:**

4.10 Page v: This section describes some of the research activities and uncertainties that have been identified. These include: additional analyses for different and more complex foundation shapes; verification based on foundation responses in real earthquakes; sensitivity study; and validation through peer review. Please discuss the status of these tasks and provide assurance that these tasks will not impact the incoherency functions presented in this report.

**Industry Response/Resolution:**

- 4.10 In response to the 4 different areas from the RAI above:
- a. Additional studies.
    - (i) Different and more complex foundation shapes
      - a circular foundation was analyzed and the results reported in Chapter 4.
    - (ii) Verification based on foundation responses in real earthquakes. Appendix B discusses the validation of the SSI incoherence phenomena with recorded data.
    - (iii) Sensitivity study – sensitivity studies on foundation shapes and coherency uncertainty are being conducted. Foundation shape was addressed in (i). Sensitivity study concerning the effect of uncertainty in the coherence function is discussed in Appendix D. Neither of these sensitivity studies produced results that impacted the methods/results in this study.
  - b. Peer Review for the coherency function has been completed (see Abrahamson 2006 report), with no effect or changes to the coherency function results.

---

**NRC Comment/Question:**

4.11 Page viii: This page states that in this study, the assumption was made that mat foundations of typical nuclear power plant (NPP) structures behave rigidly. This assumption may not be valid in all cases. Please discuss the effect of mat flexibility on the results reported in this study and whether the mat flexibility will be considered in the individual plant ESP and/or COL application.

**Industry Response/Resolution:**

4.11 The issue of flexibility of foundations is discussed in section 4.8a above.

---

**NRC Comment/Question:**

4.12 Page 1-1: This page states that this study considers both the “local wave scattering” and “wave passage effects” but that the final results are based on “local wave scattering”

**Deleted:** .  
*Effect of Embedment and Incoherence*

**Deleted:** .  
*Effect of Embedment and Incoherence*

**Deleted:** .  
*Effect of Embedment and Incoherence*

only. Please provide the basis of excluding “wave passage effects” and state whether the “wave passage effects” will be considered in the individual plant ESP and/or COL applications. See also Page 5-1.

**Industry Response/Resolution:**

4.12 Wave passage vs. local wave scattering (randomness) is discussed and results presented in Chapter 4. Excluding wave passage effects is conservative and, thus, individual plants would not be required to address either within ESP or COL applications.

---

**NRC Comment/Question:**

4.13 Page 2-2: It is not clear which equation is plotted in Figures 2-1 and 2-2, and which equation is to be used for “no wave passage effect”. Please explain.

**Industry Response/Resolution:**

4.13 The curves plotted in Figures 2-1 and 2-2 are derived from Equation 2-1 for local wave scattering only. No wave passage effects are included. The report (Chapter 2) was updated to ensure this is clear.

---

**NRC Comment/Question:**

4.14 Page 2-3: This section states that the ground motion data analyzed to develop the coherency functions have frequency content of 20 Hz and less, but that the trends can be extrapolated to higher frequencies. It is not obvious why and how these trends can be extrapolated. Please explain.

**Industry Response/Resolution:**

4.14 These bullets are merely a summarization of the conclusions from EPRI report 1012968 “Spatial Coherency Models for Soil-Structure Interaction”. The bases for this extrapolation are described within that report (Abrahamson, 2005a). Extrapolation of coherency function values for frequencies greater than 20 Hz as constant and equal to the 20 Hz value or extrapolated to smaller values has no material effect on the results. That is, the coherency values at 20 Hz are already so small that the incoherency transfer functions would be minimally affected by reducing them further. Similarly for foundation and structure response.

---

**NRC Comment/Question:**

4.15 Page 2-3: This section rightfully states that the mean input ground motion is the goal for the design of NPP structures, and as a result, the goal is to use mean coherency. However, this section further states that the coherency functions stated in the report are median coherency functions. Please provide justification for using the median instead of the mean coherency functions.

**Deleted:**  
Effect of Embedment and Incoherence

**Deleted:**  
Effect of Embedment and Incoherence

**Deleted:**  
Effect of Embedment and Incoherence

**Industry Response/Resolution:**

4.15 The mean and median are approximately the same with a difference of only a few percent. The median is slightly higher than the mean, as has been documented in the report by Dr. Norm Abrahamson in *Spatial Coherency Models for Soil-Structure Interaction*, EPRI 1012968. Thus, the justification for using the median is that it is slightly conservative to do so.

---

**NRC Comment/Question:**

4.16 Page 2-3: Tables 2-2 and 2-3 do not seem to be consistent with Figure 2-4. Please explain.

**Industry Response/Resolution:**

4.16 The soil curve in Figure 2.4 is the low strain shear wave velocity. Table 2-3 lists the properties associated with the assumed  $10^{-2}$  % strain level. The text has been changed to reflect this and to clarify any inconsistency.

---

**NRC Comment/Question:**

4.17 Page 2-5: This section states that the shear wave velocity of the bedrock is 4300 fps but Table 2-3 indicates a value of 4150 fps. Please explain the discrepancy and its potential impact.

**Industry Response/Resolution:**

4.17 The 4150 fps value is consistent with the assumed  $10^{-2}$  % earthquake strain level and this section has been modified to clarify any inconsistency.

---

**NRC Comment/Question:**

4.18 Page 2-5 and 2-6: This section quotes the EPRI 1993 Guidelines for Determining Design Basis Ground Motion. Please provide the full reference.

**Industry Response/Resolution:**

4.18 Agree. The full reference has been provided within the reference list.

---

**NRC Comment/Question:**

4.19 Page 2-6: This section states that the soil damping and shear modulus were determined based on an earthquake strain level of  $10^{-2}$ %. This is the same strain value as was stated for rock. Please explain why the strain value for the soil is not higher than that of the rock.

**Deleted:**

*Effect of Embedment and Incoherence*

**Deleted:**

*Effect of Embedment and Incoherence*

**Deleted:**

*Effect of Embedment and Incoherence*

**Industry Response/Resolution:**

4.19 The 10<sup>-2</sup> % strain level was assumed for the entire profile (including bedrock) for the purpose of developing an example soil case. CLASSI and SASSI are based on equivalent linear response, thus, the soil properties of each layer are associated with a strain level. These values were assumed for illustrative purposes only to develop an example to show the effect of incoherence on a soil site. The text has been clarified that this is not a recommended design practice which, in general, would need to demonstrate that the properties are consistent with strain levels obtained from a SHAKE analysis or other analytical technique.

**NRC Comment/Question:**

4.20 The structural model to evaluate kinematic interaction is presented in Figure 2-8. The stick model has mass, stiffness and damping representing a fixed-base condition. The use of this model for studying the kinematic interaction should be further explained. Presumably the inertial interaction part is to be evaluated in a separate step. In this context, the use of superstructure with masses hinders the demonstration of kinematic effects. Please explain.

**Industry Response/Resolution:**

4.20 See response 4.8b above. Figure 2-8 is a schematic of the structure/foundation used as an example. The solution to the problem is performed in steps; the first step is to solve the kinematic interaction problem, the final step is to solve the inertial interaction problem including the impedances, the foundation mass and structure dynamic properties subjected to the foundation input motion derived as the scattering functions times the ground motion. The scattering functions times the ground motion are the kinematic interaction effects.

**NRC Comment/Question:**

4.21 It is stated in the general section that the goal is to obtain an engineering-modified input ground motion accounting for incoherency effects. Presumably, the modified ground motion will be applied as a completely coherent time function in the SSI analysis. It appears that the effect of the proposed incoherency is only to reduce time histories along three orthogonal directions without any rotational input. This seems to render the very idea of incoherency incongruent. Please explain the value of this approach.

**Industry Response/Resolution:**

4.21 The effect of incoherence of ground motion on foundation/structure response is detailed in Chapters 4, 5, and 6. These effects include alterations in translational input motions and induced rotations. At the rigid, massless foundation level, the results are presented in Chapter 4. The effect on structure response is presented in Chapter 5. A simplified, but

conservative approach for considering incoherence in which free-field ground motion is modified is presented in Chapter 5. This approach includes both the effects of translation and rotation.

**Deleted:**  
*Effect of Embedment and Incoherence*

**Deleted:**  
*Effect of Embedment and Incoherence*

**Deleted:**  
*Effect of Embedment and Incoherence*

---

**NRC Comment/Question:**

4.22 Based on Figure 4-1, the effect of incoherency transfer functions for the vertical and horizontal directions are about a factor of 2 apart. Can this be validated from actual recordings, or is this to be expected in the CEUS region? This effect also shows up later in the report.

**Industry Response/Resolution:**

4.22 Generally, the coherency functions (Figures. 2-1 and 2-2) are less for horizontal motions than vertical. Hence, the ITFs for horizontal should be less than for the vertical. The basis for these vertical and horizontal coherency functions were developed from all applicable ground motion recordings available from dense instrument arrays as described in Abrahamson (2005). As a result, this behavior is expected in the CEUS region.

---

**NRC Comment/Question:**

4.23 Page 5-4: This section states that to study the effect of foundation shape, square vs. rectangular foundations were considered, while different foundation sizes of square foundations were investigated to study the effect of foundation area. Please explain whether you have studied circular foundations, especially in light of the fact that a significant number of NPP foundations are circular. Please explain whether this effect will be considered in the individual plant ESP and/or COL application.

**Industry Response/Resolution:**

4.23 A circular foundation shape was considered and the results are presented in Chapter 4.

---

**NRC Comment/Question:**

4.24 At the end of this chapter it is concluded that the incoherency transfer function (ITF) is independent of the input motion. This would be one of the most important points that would allow the use of the ITF without any dependence on the seismologically (performance-based) obtained ground motion spectrum. The validation of this point needs to be demonstrated by observed behavior.

**Industry Response/Resolution:**

4.24 EPRI 1012968 concludes that the coherency functions are independent of many ground motion attributes. The development of the ITF as described in Chapter 3 demonstrates the independence from the input motion.

---

**Deleted:**  
*Effect of Embedment and Incoherence*

**Deleted:**  
*Effect of Embedment and Incoherence*

**Deleted:**  
*Effect of Embedment and Incoherence*

**NRC Comment/Question:**

4.25 Figures 5-17 and 5-18 show the reduction effect at PGA, but the reduced vertical PGA (0.15g) is less than the horizontal (0.2g). Can this be validated by observed data?

**Industry Response/Resolution:**

4.25 Looking at the response, the free-field motion has amplified spectral accelerations of over 0.6g for the horizontal direction and over 0.4g for the vertical. This portion of the spectra likely drives the response of the structure/foundation – hence, the lower PGA is not surprising.

---

**NRC Comment/Question:**

4.26 Page 6-10: This section discusses whether correction factors need to be applied to take into account rotational effects of torsion and rocking. Please elaborate on the statement “*The exact solution includes rocking induced by consideration of incoherence but the incoherence transfer function (ITF) scaled solution only includes translational input motion.*”

**Industry Response/Resolution:**

4.26 The descriptions of the effects of induced rotations have been significantly expanded to address multiple similar RAI questions on rotations. Chapters 4, 5, and 6 contain expanded descriptions that should address the treatment of both rocking and torsion.

---

**NRC Comment/Question:**

4.27 This section also states that translational foundation response after SSI when subjected to rotations only were less than 0.01g, and the in-structure response was similarly low. Were these results for a soil or rock site? A soil site may be subject to more rocking. The staff would like to see the details of these results.

**Industry Response/Resolution:**

4.27 The expanded descriptions of the effects of induced rotations are discussed in Chapters 4, 5, and 6. Note the effect of incoherency on in-structure response is dependent on the free-field ground motion. Incoherence has the greatest effect on free-field ground motion with high-frequencies, i.e., frequency content greater than 10 Hz, representative of rock sites. The effect on in-structure response is less mainly due to the differences in the free-field ground motion characteristics.

---

**NRC Comment/Question:**

4.28 Furthermore, this section states that for the rock condition, no additional consideration of rotations due to ground motion incoherence appears to be warranted. Please explain if

additional consideration of rotations due to ground motion incoherence would be warranted for a soil site.

**Deleted:**  
*Effect of Embedment and Incoherence*

**Deleted:**  
*Effect of Embedment and Incoherence*

**Deleted:**  
*Effect of Embedment and Incoherence*

**Industry Response/Resolution:**

4.28 See above discussions on the treatment of rotations. The revised Chapters 4, 5, and 6 contain additional details on this subject.

---

**NRC Comment/Question:**

4.29 Page 6-17: This section states that all the analyses in this report are conducted for surface foundations even though many NPP structures have embedded foundations. This section further states that it is anticipated that the effects of embedment and the effects of incoherence are independent of each other but that analyses to demonstrate this relationship have not been performed. Please provide the basis of this assumption and state whether embedment effects will be considered in the individual plant ESP and/or COL application.

**Industry Response/Resolution:**

4.29 Embedment effects. See response to 4.2.  
A sensitivity study demonstrating the effects of incoherency on surface founded and embedded structures has been added as Appendix E of this report. This work demonstrates the relation between incoherence and embedment. Considerations for individual plant ESP and/or COL application content are not part of this project. These considerations will be addressed within the EPRI Integration report (Task I1.1) as appropriate.

---

**NRC Comment/Question:**

4.30 Page 6-17: This section states that in-structure spectra for one horizontal direction and for a surface founded and embedded model are shown in Figures 6-26 and 6-27, respectively. It is not clear what these Figures illustrate. Please elaborate.

**Industry Response/Resolution:**

4.30 These results were removed because the case analyzed did not have significant embedment effects, i.e., the embedment depth compared to the plan dimensions was small.

---

**NRC Comment/Question:**

4.31 PGAs for horizontal and vertical direction are almost a factor of 2 apart, see series of figures marked 6 -1 through 6-6.

**Deleted:**  
Effect of Embedment and Incoherence

**Deleted:**  
Effect of Embedment and Incoherence

**Deleted:**  
Effect of Embedment and Incoherence

**Industry Response/Resolution:**

4.31 Agree. See response to 4.22. Not sure what the question is here, but we assume it is similar or the same as RAI 4.22.

---

**NRC Comment/Question:**

4.32 Figures 6-14 through 6-25 use the label SSI-CTF, but CTF does not seem to have a definition.

**Industry Response/Resolution:**

4.32 Agree – Figures 6-14 through 6-25 in the original report use “CTF”. This should be “ITF”. This typo was corrected in this revised report.

---

**NRC Comment/Question:**

4.33 Page 7-2: This section states that it was judged to be slightly conservative to not include wave passage effects. Please explain if the wave passage effect might have a bigger impact on rocking and torsion.

**Industry Response/Resolution:**

4.33 Wave passage might have larger effect on torsion and rocking, but only accompanied with a corresponding reduction in effective translational input. It is judged to be slightly conservative to ignore wave passage because, at the well-recognized apparent wave velocities (values approximating 4 km/sec or greater), the effect of wave passage on SSI response of these types of foundations/structures is calculated to be minimal. Results have been added to the report for the cases of apparent wave velocities of 2 km/sec and 4 km/sec in Chapter 4. The results show that it is conservative to ignore the effects of wave passage.

---

**NRC Comment/Question:**

4.34 The conclusions are well laid out; however the issue of embedded foundations is not discussed and majority of reactor designs use structures that are embedded to depths between 20 to 60 ft.

**Industry Response/Resolution:**

4.34 Thank you. Please see response to 4.2 above for embedment.

---

**NRC Comment/Question:**

4.35 p. ix first bullet and p. 8-6 second bullet: It is stated that: *“The basic effect of incoherence on seismic response of structures has been demonstrated and validated through recorded ground motions and analyses of their effects with alternative methods and programs.”*

**Deleted:**  
*Effect of Embedment and Incoherence*

**Deleted:**  
*Effect of Embedment and Incoherence*

**Deleted:**  
*Effect of Embedment and Incoherence*

The report presents analyses utilizing a simulated time history based on the response spectra of Fig. 2-5 or using random vibration theory with power spectra derived from the response spectra of Figs. 2-5 and 2-6. Was there a separate analysis performed with recorded ground motions?

**Industry Response/Resolution:**

4.35 This conclusion bullet has been modified in response to this RAI in order to alleviate any confusion on the review performed relative to recorded ground motions. Appendix B addresses the review of recorded ground motions to assess the potential to validate the methods recommended within this study on seismic wave incoherence.

---

**NRC Comment/Question:**

4.36 There are two typos in Table 2-1, p. 2-1: for the horizontal ground motion  $f_c$  the first term in the expression should be  $-1.886+...$  instead of  $1.886+...$ , and for the vertical ground motion  $f_c$  the last term of the expression should be  $...(1))^2$  instead of  $...(1))2$ .

**Industry Response/Resolution:**

4.36 Agree, these two typos were corrected. Thank you.

---

**NRC Comment/Question:**

4.37 The variation of the soil shear wave velocity with depth in Fig. 2-4 (p. 2-5) does not fully correspond to the values provided in Table 2-3 (p. 2-6). Additionally, it is stated on bottom of p. 2-5 that "...and then a half-space of bedrock at a shear wave velocity of 4300 fps". The entry for the half-space shear wave velocity in Table 2-3 is 4150 fps. Which is the soil profile used in the analysis?

**Industry Response/Resolution:**

4.37 See answers to previous RAIs 4.16 and 4.17. Appropriate clarifications have been made in the report.

---

**NRC Comment/Question:**

4.38 It is stated on p. 2-8 last paragraph that: "For soil-structure interaction analyses and the evaluation of structure response including the effects of seismic wave incoherence, spectrum compatible time histories for the rock site were required. Three uncorrelated components were generated for two horizontal directions and the vertical direction." What was the time step for the generation of the time histories? What was the duration? What amplitude modulating function was utilized to transform the generated stationary time histories to non-stationary? It would be helpful if the time histories were presented.

**Deleted:**

*Effect of Embedment and Incoherence*

**Deleted:**

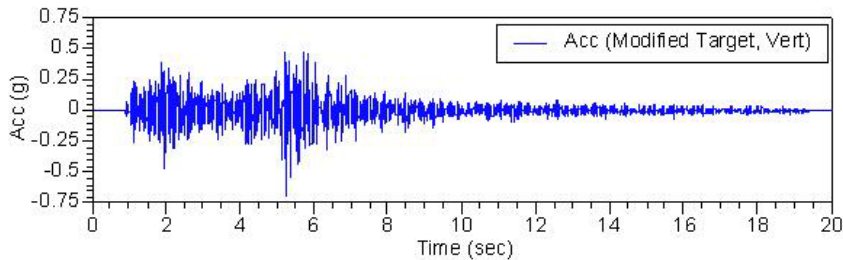
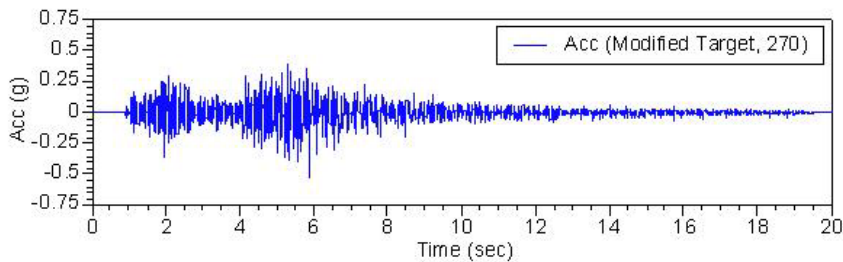
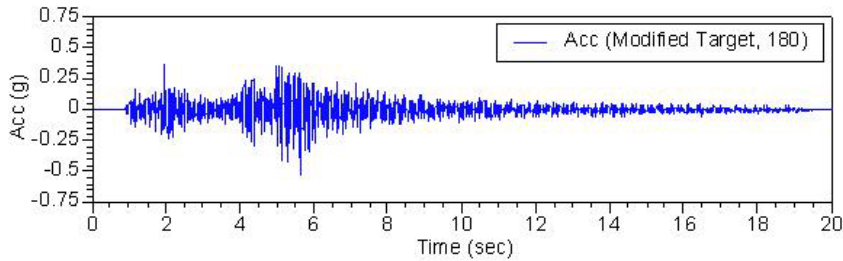
*Effect of Embedment and Incoherence*

**Deleted:**

*Effect of Embedment and Incoherence*

**Industry Response/Resolution:**

4.38 These were generated by Dr. Abrahamson as being appropriate to the site conditions and the likely earthquake parameters. The reference time history that was selected for the development of the spectrum compatible time histories was recorded at the USGS station at the Keenwild Fire Station in Southern California (June 12, 2005 Anza Earthquake). The time duration was approximately 15 seconds. The time step was 0.005 seconds. The acceleration time histories are depicted below.



**NRC Comment/Question:**

4.39 It is stated on p. 2-9 that: “The SSI seismic analyses, by CLASSI and SASSI, were performed for the 150-ft square foundation footprint. For these analyses the foundation was assumed to be 15-ft thick. ...” Wasn’t the foundation massless in the CLASSI and SASSI benchmark problem comparisons (Section 4)? Were there additional comparisons made? Why was a 15-ft foundation thickness selected?

**Deleted:**  
*Effect of Embedment and Incoherence*

**Deleted:**  
*Effect of Embedment and Incoherence*

**Deleted:**  
*Effect of Embedment and Incoherence*

**Industry Response/Resolution:**

4.39 Original benchmark problems were for rigid massless foundation response. Recently, benchmark problems have been added comparing CLASSI, Bechtel SASSI, and ACS SASSI by ARES. These new benchmark problems included the 3 stick structural model and the 15-ft thick foundation. In addition, all analyses described in Chapter 5 of the current report utilized the 3 stick structure model with the 15-ft thick foundation. All of the benchmark comparison problems are documented in Appendix C. We examined the basemats of several new plant designs and the foundation thicknesses vary between designs and over the plan dimensions. A 15-ft uniform thickness was assumed for the benchmark models for comparison purposes only, and is not meant to represent an AP1000 specific model.

---

**NRC Comment/Question:**

4.40 Figure 2-8: Shouldn't the foundation footprint dimensions be < 150' or 225' > instead of < 100' or 225' > in the X-direction and < 150' or 100' > instead of < 100' > in the Y-direction?

**Industry Response/Resolution:**

4.40 Dimensions on Figure 2-8 have been revised.

---

**NRC Comment/Question:**

4.41 There are some typos in Eq. 3-14 (p. 3-5): It should read  $[HT] = ([\alpha s] + [\phi s] [D] [\Gamma s]) [HF]$  instead of  $[HT] = ([\alpha s] / [\phi s] T [D] [\Gamma s]) [HF]$ .

**Industry Response/Resolution:**

4.41 Agree. Equation 3-14 has been changed to reflect the removal of the transpose. The Wen Tseng 1997 EPRI report contained a typo and the divide symbol was included in the equation. This also has been changed.

---

**NRC Comment/Question:**

4.42 It is stated in subsection "Procedure to Evaluate the Foundation and Structure Incoherent Response Spectra by CLASSI" that "The complete random vibration approach described above could have been employed herein" (p. 3-5), but that "Ground motion time histories are transformed into the frequency domain, SSI parameters (impedances and scattering matrices) are complex-valued, frequency-dependent, and the structure is modeled using fixed-base eigen systems. SSI analyses are performed—output are time histories of interest from which in-structure response spectra are computed. The resulting in-structure response spectra at structure and foundation locations of interest include the effects of

**Deleted:**

*Effect of Embedment and Incoherence*

**Deleted:**

*Effect of Embedment and Incoherence*

**Deleted:**

*Effect of Embedment and Incoherence*

soil-structure interaction and seismic wave incoherence” (p. 3-6). This process is not random vibration analysis – this is a deterministic time history analysis utilizing the frequency domain.

**Industry Response/Resolution:**

4.42 The actual text follows for p. 3-5:

“The complete random vibration approach described above could have been employed herein. However, the formulation of CLASSI and its ease of use permitted implementation of a more direct approach to the SSI analysis of structure/foundation.”

The random vibration approach was used to generate the incoherency transfer functions (ITFs), which in CLASSI nomenclature are the scattering functions. These scattering functions are the key element to account for the effects of incoherence on the foundation input motion. This approach is described in detail in Chapter 3.

Once having determined the scattering functions, their application to the SSI analysis of a foundation/structure system could have been performed assuming random vibration theory only. This approach would have consisted of converting the free-field ground response spectra into PSDs, analyze the soil-structure system using the frequency-dependent impedance matrix and scattering functions, incorporating the dynamic characteristics of the foundation and structure system, and solving for the PSDs of in-structure response. Then, converting those in-structure response PSDs to in-structure response spectra as appropriate.

The alternative was to use CLASSI in a conventional manner, i.e., perform all of the above solution steps, again with scattering functions developed from RVT approaches as described in detail in Chapter 3, perform SSI analyses in the frequency domain, which entails converting the free-field ground motion time histories (derived to be compatible with the free-field ground response spectra) into its FFT, performing SSI analysis in the frequency domain, i.e., using the same steps as described above, calculating the Fourier Transform of in-structure response and Inverse Fourier transform those into the time domain. These in-structure time histories are processed to calculate in-structure response spectra for response comparisons.

In conclusion, the RVT approach is used to develop the ITFs, or scattering functions, which are used in the standard CLASSI SSI analysis procedure.

**NRC Comment/Question:**

4.43 It is stated on p. 3-6 that “For this application, a 6 by 6 complex incoherency transfer function matrix [ITF] is evaluated by taking the square root of  $[S_{UoI}]$ , the 6 by 6 complex cross PSD matrix of rigid massless foundation motion to unit PSD input. The scattering matrix for vertically propagating waves is replaced by the columns of the incoherency transfer function matrix at each frequency of interest that correspond to the directions of input excitation”. Was the square root of the entire  $[S_{UoI}]$  matrix considered in the

**Deleted:**  
*Effect of Embedment and Incoherence*

**Deleted:**  
*Effect of Embedment and Incoherence*

**Deleted:**  
*Effect of Embedment and Incoherence*

approach by replacing all columns of the scattering matrix by the columns of the ITF matrix, as indicated on p. 3-6, or were only the diagonal elements of the ITF matrix considered as indicated throughout the rest of the report?

**Industry Response/Resolution:**

- 4.43 The diagonal elements of the CPSD matrix were used to define the scattering functions. For developing these scattering functions, each of the three directions was analyzed separately and the scattering functions extracted for the each of the three directions of free-field ground motion.

---

**NRC Comment/Question:**

- 4.44 In Section 4 it is stated that the benchmark problem comparison utilized:

Two different algorithms; CLASSI–stochastic method and SASSI-eigen decomposition method

Two different analytical approaches; random vibration theory (RVT) by CLASSI and time history dynamic analyses by SASSI

Regarding the second bullet: Both CLASSI and SASSI utilize a time history analysis, with the only difference being that the CLASSI approach described in the report transforms the time history in the frequency domain, conducts the evaluation in the frequency domain and transforms the results back into the time domain as noted in I-8. Hence, the results regarding this aspect should be expected to be identical, assuming that CLASSI and SASSI have been validated before regarding fully coherent incident motions.

Regarding the first bullet: The approach used in CLASSI is described in the report, whereas that of SASSI is not. However, Report TR-102631 (1997) describes an eigen decomposition approach for the incorporation of the spatial incoherence of seismic ground motions in SASSI through the module “INCOH”, which also utilizes eigen decomposition. If the evaluations by SASSI are based on the approach described in Report TR-102631 (1997), the following is observed regarding the benchmark comparison: The CLASSI – stochastic method described in this report in Section 3 is identical to the stochastic approach described in the TR-102631 report (1997), also in their Section 3.

The only difference is that this report incorporates the coherency matrix  $[\gamma]$  fully in the analysis by using matrix analysis and taking the square root of the cross spectral density matrix of the rigid massless foundation motion  $[S_{u_o}]$  (Eq. 3-2 on p. 3-2), whereas the “INCOH” module of the TR-102631 report performs an eigenvalue decomposition of  $[\gamma]$  and retains its dominant modes. The module “INCOH” was validated in Section 5 of Report TR-102631 (1997) utilizing SASSI with previous studies conducted by Luco and Mita (1987) for a circular, rigid, massless foundation and Mita and Luco (1986) for the response of a flexible, cylindrical structure.

If the evaluations by SASSI are based on the “INCOH” module described in Report TR-102631 (1997), the benchmark comparison in this report simply suggests that the eigen

**Deleted:** .  
*Effect of Embedment and Incoherence*

**Deleted:** .  
*Effect of Embedment and Incoherence*

**Deleted:** .  
*Effect of Embedment and Incoherence*

decomposition of the coherency matrix  $[\gamma]$  by SASSI contained sufficient number of modes to capture the full effect of  $[\gamma]$  considered by CLASSI. Additionally, if this is the case, retaining higher modes in the decomposition would render the SASSI results in Figs. 4-1, 4-2 and 4-3 smoother, as are those evaluated by CLASSI.

**Industry Response/Resolution:**

4.44 The approach to modeling incoherence of ground motion in CLASSI is derived in detail in Chapter 3 of the report. The approach follows EPRI (1997). Changes to the methodology are in the form of the coherency of ground motion and its application to the particular problems investigated. The approach of SASSI is similar to that described in EPRI (1997). Two versions of SASSI were used in the comparison studies. The two versions have been generated from the same basic approach, but have evolved separately over time. The approaches, including key differences, are summarized in Chapter 6.

The comparisons of the foundation and in-structure responses as reported in Appendix C are remarkably close. The differences in methodologies, computer programs (CLASSI, and two versions of SASSI), and analysts performing the analyses would be expected to lead to some greater differences than observed. The one similarity in methodology for the CLASSI and SASSI is the fact that they both solve the SSI problem in the frequency domain. These very good comparisons adequately validate the two approaches.

**NRC Comment/Question:**

4.45 What input motion was used in the benchmark comparison? It is stated on p. 4-1 that “Input earthquake excitation was the rock input motion for which the response spectra are shown in Figure 2-5”. However, the maximum horizontal acceleration in Fig. 2-5 is ~ 1.48g whereas the maximum horizontal acceleration in Fig. 4-2 is ~ 1.0g, and the maximum vertical acceleration in Fig. 2-5 is ~ 1.38g whereas the maximum vertical acceleration in Fig. 4-3 is ~ 0.9g.

**Industry Response/Resolution:**

4.45 The rock input motion used for studies reported in the body of the report are those of Figure 2-7. Some of the Benchmark Comparisons documented in Appendix C were based on ground motions with the same basic characteristics, but with different amplitudes.

**NRC Comment/Question:**

4.46 It is stated on p. 2-3 that a damping ratio of 0.02 is assumed, whereas on p. 4-1 for the benchmark problem the damping is considered as 1 percent. Also, the bedrock shear wave velocity for the bedrock is considered as 4300 fps on p. 2-5, 4150 fps in Table 2-3 and 6300 fps for the benchmark comparison. Which damping values and shear wave velocities were used? Or were there different response spectra and corresponding time histories developed for the benchmark problem? This may also be associated with I-11.

Deleted:  
Effect of Embedment and Incoherence

Deleted:  
Effect of Embedment and Incoherence

Deleted:  
Effect of Embedment and Incoherence

**Industry Response/Resolution:**

4.46 Tables 2-2 and 2-3 itemize the rock and soil properties used in the studies presented in the body of the report. Appendix C itemizes rock material properties used in the Benchmark Analyses.

**NRC Comment/Question:**

4.47 It is stated on p. 5-4 that the soil profile does not affect the ITFs, which are basically identical at all frequencies for soil and rock (Figs. 5-13 and 5-14). This should be expected if the matrix  $[S_{U_{ol}}]$  in Eq. 3-2 were controlled by  $[\gamma]$  only, which is considered identical for rock and soil sites according to the coherency model. However,  $[S_{U_{ol}}] = [F][S_{UGI}] [FC]^T$  (Eq. 3-2) also contains the scattering transfer function  $[F]$ , and the ITFs are the square root of the diagonal terms of  $[S_{U_{ol}}]$ . How dependent is  $[F]$  (Eq. 3-3) on the site properties or is it only function of location and frequency? If  $[F]$  depends on the site properties, this should be reflected in the ITFs, which, consequently, should differ for soil and rock sites.

**Industry Response/Resolution:**

4.47 The independence of the scattering transfer function  $[F]$  from soil properties is a direct result of the CLASSI formulation which considers the response of a rigid surface inclusion on a layered half-space (i.e., a rigid massless foundation) as the driving input motion for the SSI solution. Let the modification of the field-field surface motion due to the presence of the rigid surface inclusion be represented by six component vector  $\{U_0^*\}$ . The average free-field surface motion of each of  $n$  sub-regions that represents the interface of the rigid foundation area with the half-space surface is represented by the  $3n$  component vector  $\{U_n\}$ . We seek the motion of a reference point of the rigid inclusion  $\{U_0^*\}$  in terms of the set of sub region motions  $\{U_n\}$  and define the  $6 \times 3n$  scattering transfer function  $[F]$  as  $\{U_0^*\} = [F] \{U_n\}$ . Given the  $3n \times 3n$  array  $[G]$  of Green's functions integrated over each sub-region, and the  $3n \times 6$  rigid body transformation array  $[\alpha_b]$ , defined by  $\{U_n\} = [\alpha_b] \{U_0^*\}$ , we may compute the impedance of the driving forces  $\{P_0\}$  applied to the rigid inclusion as the  $6 \times 6$  array,  $[K] = [\alpha_b]^T [G]^{-1} [\alpha_b]$ , where  $\{P_0\} = [K] \{U_0^*\}$ . We note that  $\{P_0\} = [\alpha_b]^T [G]^{-1} [\alpha_b] \{U_0^*\} = [\alpha_b]^T [G]^{-1} \{U_n\}$ . The array  $[G]^{-1} [\alpha_b]$  may be identified as the  $3n \times 6$  traction array  $[T]$  for which  $[T]^T = [\alpha_b]^T [G]^{-1}$  and thus  $\{P_0\} = [T]^T \{U_n\}$ . Since,  $\{P_0\} = [K] \{U_0^*\} = [T]^T \{U_n\}$ , we may write  $\{U_0^*\} = [K]^{-1} [T]^T \{U_n\} = [C] [T]^T \{U_n\}$  where  $[C] = [K]^{-1}$  is the  $6 \times 6$  compliance array of the rigid inclusion reference point. Referring to the definition of the scattering transfer function we may identify  $[F] = [C] [T]^T$ .

Since  $\{U_n\} = [\alpha_b] \{U_0^*\}$ , we may also form,  $[\alpha_b]^T \{U_n\} = [\alpha_b]^T [\alpha_b] \{U_0^*\}$ . Now,  $\{U_0^*\} = ([\alpha_b]^T [\alpha_b])^{-1} [\alpha_b]^T \{U_n\}$  which may be identified as the least squares solution for the average motion of the rigid surface inclusion given the over-determined free-field motion of the  $n$  sub-regions  $\{U_n\}$ . Again, referring to the definition of the scattering transfer function, we may identify  $[F] = ([\alpha_b]^T [\alpha_b])^{-1} [\alpha_b]^T$  from which it may be verified that the scattering transfer function is independent of any soil properties, being

**Deleted:**

*Effect of Embedment and Incoherence*

**Deleted:**

*Effect of Embedment and Incoherence*

**Deleted:**

*Effect of Embedment and Incoherence*

determined only by the rigid body kinematics of the rigid foundation motion. The use of the identity  $[F] = [C][T]^T$  is actually equivalent to the least squares solution and is a convenient means of computation for the scattering transfer function given the CLASSI computation of  $[K]$  and  $[T]$  for solution of the SSI problem.

Now, given the  $3n \times 3n$  cross spectral density response matrix of the rigid massless foundation accounting for incoherence as  $[SUG] = [S01/2][\gamma][S01/2]$ , then the  $6 \times 6$  cross PSD of the rigid massless foundation is found from  $[SU0^*] = [F] [SUG][FC]T$ , where  $[FC]$  is the complex conjugate of  $[F]$ . Thus, the response of the rigid massless foundation is controlled by  $[\gamma]$  only.

---

**NRC Comment/Question:**

4.48 In the subsection “Spectral Corrections” on p. 5-10, where random vibration analysis is utilized, what was the equivalent duration of the seismic motions used in the conversion between power spectra and response spectra?

**Industry Response/Resolution:**

4.48 Six seconds was used for the seismic motions, which was judged to be typical/representative of EUS rock motions.

---

**NRC Comment/Question:**

4.49 It is stated in the subsection “Spectral Corrections” on p. 5-10, as well as earlier on p. 5-4, that the response spectra for the square 150 ft x 150 ft and the rectangular 100 ft x 225 ft are identical. Is there an explanation for this? It is also mentioned that the ITFs are identical for the two foundation shapes. Are all terms of the  $[S_{UoI}]$  matrix in Eq. 3-2 identical (or close) for both foundation shapes?

**Industry Response/Resolution:**

4.49 The studies performed in this scope of work have demonstrated that the most important parameter affecting translational responses is the area of the foundation. Induced rotations are dependent on the foundation shape. These observations are discussed in detail in Chapter 4.

---

**NRC Comment/Question:**

4.50 On p. 5-11 it is stated that “It may be seen that spectral reductions are significantly greater than the ASCE 4 values for the rock site but are actually somewhat similar for the soil site.” There seem, however, to be very significant differences between the ASCE 4 and the soil spectral corrections especially for the 150-ft square foundation in both horizontal and vertical directions, and the 300-ft square foundation in the vertical direction. Also, is there a reason behind the increase in the values of the horizontal spectral corrections at the 50.0 Hz frequency for all foundations supported on soil?

**Deleted:**  
 Effect of Embedment and Incoherence

**Deleted:**  
 Effect of Embedment and Incoherence

**Deleted:**  
 Effect of Embedment and Incoherence

**Industry Response/Resolution:**

4.50 Chapter 4 revises these observations.

**NRC Comment/Question:**

4.51 A previous analysis by Luco and Wong (1986) evaluated the response of a rectangular, rigid, massless foundation subjected to spatially random ground motions. Because their analysis and results are closely related to those presented in this report, their work is briefly described herein for clarity in this question.

**Industry Response/Resolution:**

4.51 Thank you for the effort undertaken to summarize that work here. This NRC comment labeled 4.51 is not a question and thus, doesn't require a response. The question is within RAI 4.52.

**NRC Comment/Question:**

4.52 Figure I-1 presents the layout and coordinate system of the Luco and Wong analyses. It is considered that the rectangular ( ) massless, rigid foundation is bonded to a visco-elastic half-space with Poisson's ratio of 1/3 and material damping ratio of 0.01.

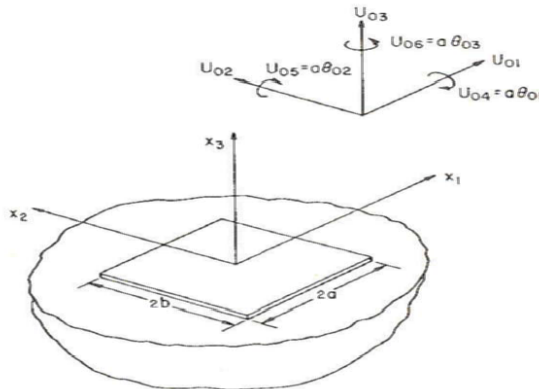


Figure I-1. Layout of foundation and coordinate system (from Luco and Wong, 1986).

The coherency expression of Luco and Wong (1986) is of the form:

$$\gamma_{LW}(f, \xi) = \exp[-(v2\pi f \xi / \beta)^2] \quad (I-1)$$

where  $v$  is a coherency drop parameter associated with random inhomogeneities and variations in elastic properties along the path of body waves,  $\beta$  is an estimate of the elastic wave velocity,  $f$  is frequency in Hz and  $\xi$  is separation distance in m. Figure I-2 presents a comparison of the Abrahamson coherency model used in this report for horizontal and vertical motions (Eqs.

Deleted: Effect of Embedment and Incoherence  
Deleted: Effect of Embedment and Incoherence  
Deleted: Effect of Embedment and Incoherence

2-1 and 2-2 in the report) with the Luco and Wong coherency (Eq. I-1 herein) for  $\beta = 1921.5$  m/sec (=6300 fps), i.e., the one used in the benchmark problem,  $\nu = 0, 0.1, 0.2, 0.3, 0.4,$  and  $0.5$  as used by Luco and Wong, and at separation distances of 10 m and 45.75 m (= 150 ft), the latter being the length of each side of the foundation in the benchmark problem. The approach described in Luco and Wong assumes that the coherency decay is the same in the two horizontal and the vertical directions. The value  $\nu = 0$  represents fully coherent motions. The model of Luco and Wong decays more slowly with frequency at the shorter separation distances than the Abrahamson coherency model. At the longer separation distance, the value of  $\nu = 0.5$  falls in-between the horizontal and vertical Abrahamson models. At longer separation distances, the Luco and Wong model falls off more sharply with frequency than the Abrahamson models.

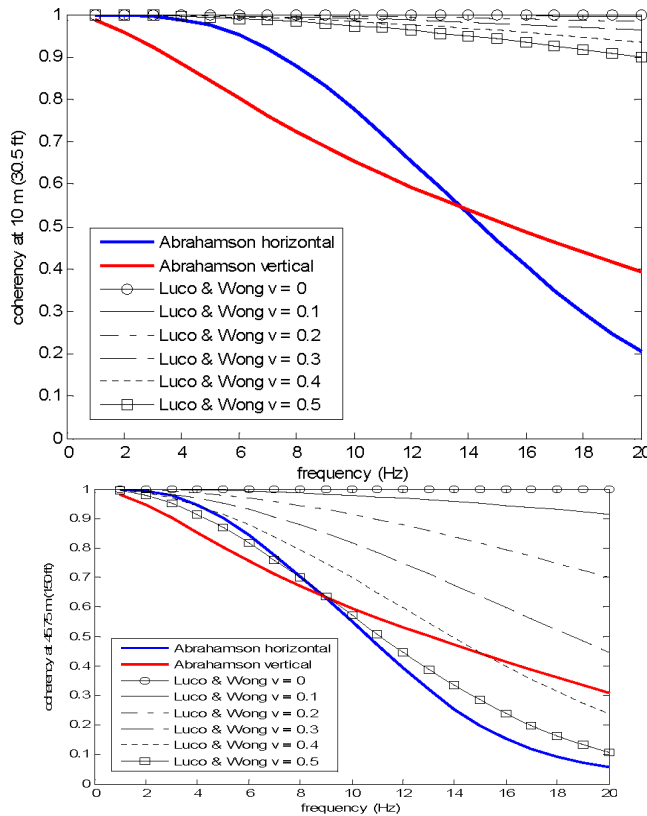


Figure I-2. Comparison of the Abrahamson and the Luco and Wong coherency models at separation distances of 10 m and 45.75 m (= 150 ft).

Luco and Wong's (1986) results for a square ( $2a \times 2a$ , Fig. I-1) foundation subjected to motions experiencing loss of coherency are presented in Fig. I-3a for the translational response components, and Fig. I-3b for the rotational response components. The results are presented as functions of the dimensional parameter  $\sigma$  and for variable values of  $\nu$ . An increase of " $\sigma$ " in the dimensional parameter in the figures, considering that  $a = 150$  ft, is equivalent to 13.37 Hz for  $\beta =$

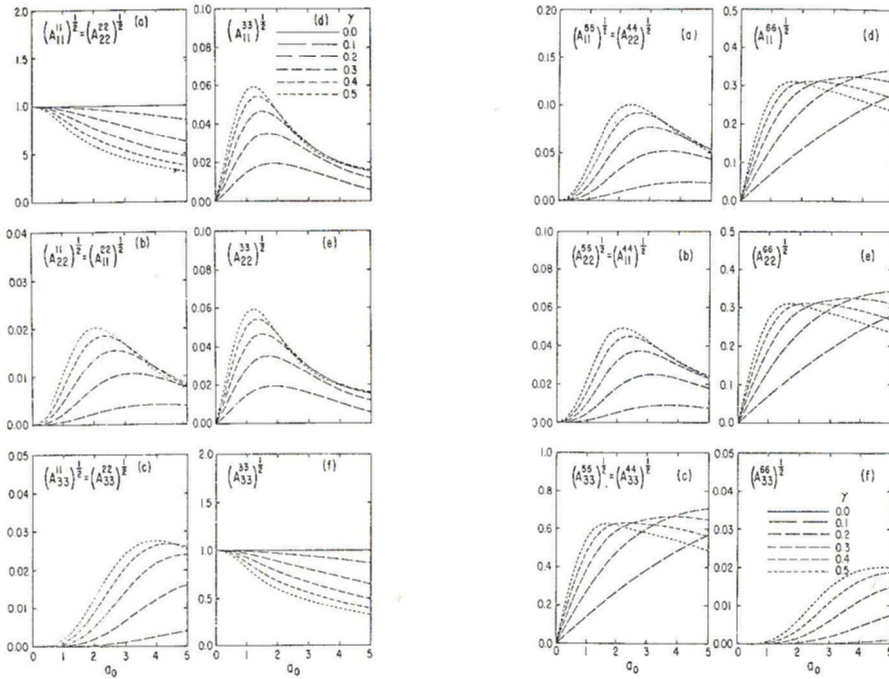
Deleted: Effect of Embedment and Incoherence

Deleted: Effect of Embedment and Incoherence

Deleted: Effect of Embedment and Incoherence

6300 fps used in the benchmark comparison, and 9.125 Hz for  $\beta = 4300$  fps suggested on p. 2-5, yielding maximum values for the frequency at = 5 of 66.85 Hz and 45.62 Hz, respectively.

According to Luco and Wong (1986),  $a_e \sqrt{A_{ij}^{ij}}$ ,  $i=1, 2, 3$  and  $j = 1, 2, \dots, 6$ , can be interpreted as the amplitude of a transfer function between the  $i$ -th component of the excitation and the  $j$ -th component of the response (Fig. I-1). In this sense,  $\sqrt{A_{11}^{11}} = \sqrt{A_{22}^{22}}$  in Fig. I-3a, subplot (a), corresponds to the ITFs provided in the report in any of the two horizontal directions, and in Fig. I-3a, subplot (f), to the ITF in the vertical direction. As can be seen from Fig. I-3a, loss of coherency in a specific direction results in significant reduction of translation in the corresponding direction ( $\sqrt{A_{11}^{11}}$ ,  $\sqrt{A_{22}^{22}}$ ,  $\sqrt{A_{33}^{33}}$ ), but affects only minimally the translational response in the other directions.



(a) translational response

(b) rotational response

The decay of the transfer functions  $\sqrt{A_{11}^{11}} A_{11}^{11}$ ,  $\sqrt{A_{22}^{22}}$ ,  $\sqrt{A_{33}^{33}}$  in Fig. I-3a is much slower than the ITFs presented in the EPRI report, possibly because the Luco and Wong model produces significantly higher coherency values than the EPRI model (Fig. I-2). Figure I-3b presents the results for the rotational components of the foundation. According to Luco and Wong (1986), can be interpreted as the amplitude of the transfer function between the  $i$ -th component of the excitation and the foundation response  $\tilde{U}_{05} = a\tilde{\theta}_{05}$  (Fig. I-1), i.e., rocking about the  $x_2$  axis.

**Deleted:**

*Effect of Embedment and Incoherence*

**Deleted:**

*Effect of Embedment and Incoherence*

**Deleted:**

*Effect of Embedment and Incoherence*

Hence, and represent the rocking transfer functions due to the vertical excitation, and  $\sqrt{A_{11}^{66}}$  and  $\sqrt{A_{22}^{66}}$  the torsional response caused by the horizontal motions. Figure I-3b then suggests that the rocking response about the  $x_1$  and  $x_2$  axis are mostly associated with the vertical component of the free-field ground motion, and the torsional response about the  $x_3$  axis is associated with the  $x_1$  and  $x_2$  components of the Figure I-3. Foundation response to seismic ground motions exhibiting loss of coherence (from Luco and Wong, 1986). The coherency drop parameter “ $\gamma$ ” in the figure is referred to in the text as “ $\nu$ ” because “ $\gamma$ ” in the EPRI reports refers to the coherency function.

Figure I-3b indicates that rocking caused by the vertical motions (subfigure (c)), and torsion caused by the horizontal motions (subfigures (d) and (e)) can be significant, and increase as  $\nu$  increases (and coherency decreases, Fig. I-2). It is also noted from Fig. I-3b, subfigures (c), (d) and (e), that as  $\nu$  increases, the peaks of  $\sqrt{A_{33}^{44}}$ ,  $\sqrt{A_{33}^{55}}$ ,  $\sqrt{A_{11}^{66}}$  and  $\sqrt{A_{22}^{66}}$  shift towards the lower frequencies. On the other hand, the negligible effect of rocking discussed on p. 6-10 of the EPRI report appears to be counter-intuitive, in that the large reductions in the translational response due to incoherency presented in the report do not result in any rotational effects. Since the Abrahamson coherency model drops more rapidly with frequency and separation distance than the Luco and Wong model (Fig. I-2), this should lead to even higher values for the rotational transfer functions, but it is stated in the report that their effect is negligible. Does the rotational effect become negligible in the report’s study, because, due to the sharp decay of the Abrahamson coherency model, the peak of the rotational transfer functions shifts to such low-frequencies where the ground motions do not contain much energy? How do all elements of the  $[S_{Uol}]$  matrix of Eq. 3-2 (not only the translational ITFs) behave at different frequencies?

**Industry Response/Resolution:**

4.52 The ITFs calculated in the present study are presented in Figures 4-13, 4-14, 4-15 and 4-16. These ITFs demonstrate the same shape and trends as Figure 2 of the study by Kim and Stewart (*Kinematic Soil-Structure Interaction from Strong Motion Recordings* by Seunghyun Kim and Jonathan Stewart, Journal of Geotechnical and Geoenvironmental Engineering, April 2003). This Figure 2 depicts the amplitude of the transfer function between free-field motion and the foundation input motion for different foundation shapes based on analytical formulations from Veletsos, Prasad, Luco, Wong, etc. as described in the above reference.

In addition, as discussed within the responses to several previous RAIs, there has been an expanded treatment of both rocking and torsion within Chapters 4, 5 and 6 to reflect additional models/studies in this area.

**NRC Comment/Question:**

4.53 There is insufficient information provided in the report to evaluate the effect of embedment and incoherence on p. 6-17. It is stated that “It is anticipated that the effects of embedment and the effects of seismic wave incoherence are independent of each other”. This depends on whether coherency is a function of depth or not. It is also stated on p. 6-17 that Figures 6-26 and 6-27 suggest “independency of embedment and

incoherency". If the same coherency model was used for the surface and the embedded structure, then the comparison between Figs. 6-26 and 6-27 indicates only the effect of embedment, not coherency. Also, in Fig. 6-26, what is the meaning of the response at an El. -21' for a surface structure?

**Deleted:**  
*Effect of Embedment and Incoherence*

**Deleted:**  
*Effect of Embedment and Incoherence*

**Deleted:**  
*Effect of Embedment and Incoherence*

**Industry Response/Resolution:**

4.53 The issue of embedment has been addressed in more detail in several places within the report (Chapters 5 and 6 and Appendix E) and in the response to RAI 4.2.

---



# B

## VALIDATION OF INCOHERENCY EFFECTS THROUGH RECORDED EVENTS

---

Over the course of this incoherence structural response task, the project team has utilized the talents of the Technical Review and Advisory Group (TRAG) and individual NRC staff members to provide comments and insights on the use of incoherency relative to the new plant seismic response. One goal within this task has been to research whether actual recorded data could be utilized to provide specific validation of incoherent ground motion effects on foundations and structures reflected within the studies documented in this report. During a meeting at the NRC in late 2005 discussions centered around the review of past studies by researchers in this field such as Dr. Stewart and Dr. Kim, and on the earthquake recordings that have occurred at the Diablo Canyon and the Perry nuclear power plants. To address the potential of using recorded data for validation purposes, the project team researched the technical literature for studies that reflected such validation efforts and also collected available recording data for the Deer Canyon earthquake that affected the Diablo Canyon NPP and the Leroy earthquake that affected the Perry NPP. The results of these efforts are documented in the following sections of Appendix B. The overall conclusions from these studies are contained in section B.4.

### B.1 Technical Literature on Validation of Incoherency Effects

Significant effort has been expended over the last three decades to validate the effects of soil-structure interaction (SSI) on structure response with one emphasis being on recorded earthquake motions. The majority of these efforts have focused on total SSI effects, i.e., the combined effects of kinematic and inertial interaction. It is well recognized that it is very difficult to separate the effects of kinematic and inertial interaction in recorded responses. The most successful attempts to separate the effects are for structures where one of the phenomena is not deemed to be important. For example, a structure such as a stiff tank embedded in soil with relatively small mass may serve to demonstrate the effects of kinematic interaction with minimal inertial interaction effects (Ishii et al., 1984).

Kinematic interaction is due to the variation in ground motion over the contact surface of the soil/rock and structure/foundation. For surface-founded structures, this variation is that at the interface of the foundation and the surface of soil or rock, and due to horizontal spatial variation of motion. Generally, this horizontal variation is due to wave passage effects and incoherence of ground motion. The effects of wave passage on nuclear power plant structures, for reasonable wave propagation parameters, have been shown to be of minimal consequence. However, the effects of incoherence of ground motion are significant for nuclear power plant structures founded on rock sites. For embedded foundations, kinematic interaction is due to the above

**Deleted:**  
*Effect of Embedment and Incoherence*

**Deleted:**  
*Effect of Embedment and Incoherence*

**Deleted:**  
*Effect of Embedment and Incoherence*

phenomena and due to the spatial variation of the ground motion with depth in the soil or rock. Until recently, studies where kinematic interaction has been the primary focus were performed to investigate the spatial variation of ground motion with depth in the soil or rock and its effects on the response of structures with embedded foundations and partially embedded walls. These field observations of embedment verified the physics of the problem, i.e., generally, there is a reduction in motion with depth in the soil or rock and a corresponding reduction in foundation motion of structures. Chang et al. (1985) and Johnson (2003) summarize many of the efforts to document these phenomena.

Seismic wave incoherence has been recognized as a phenomenon of particular interest to structures of large plan dimensions and for structures with multiple supports and large distances between supports, e.g., bridges. As reported by Chang et al. (1985), the horizontal variation of ground motion was observed many years ago, but only verified through very limited recorded data.

In more recent times, significant free-field data has been recorded, which illuminates the phenomena of incoherence of ground motion particularly the horizontal variation of ground motion due to incoherence (Abrahamson 2005a, 2006a). It is this significant body of data, which has permitted the development and benchmarking of the techniques in the present report.

Taking into account the effect of seismic wave incoherence on seismic response of nuclear power plant structures is particularly important given the seismic hazards calculated for rock sites in the Central and Eastern United States (CEUS). Current probabilistic seismic hazard assessments (PSHAs) for rock sites in the CEUS result in site-specific Uniform Hazard Spectra (UHS) that contain significant amplified response in the frequency range above 10 Hz. As demonstrated earlier in this report, the effects of incoherence of ground motion increase with increasing frequency and distance between observation points. The most significant effects are for frequencies greater than 10 Hz. These effects of incoherence are to reduce the effective translational motion of the foundation and induce additional rotational excitations of the foundation for frequencies greater than 10 Hz. The effect on in-structure response is to reduce the high-frequency content response for high-frequency input ground motion. For these current CEUS ground motions, it is important to account for all aspects of SSI in calculating structure response of these structures.

Over the last decade, Stewart and colleagues have devoted significant effort to evaluating the effects of kinematic interaction on structures through observations. This body of work includes Stewart and Stewart (1997), Stewart et al. (1999a), Stewart et al. (1999b), and Kim (2001). Kim and Stewart (2003) summarize these efforts including results and recommendations for incorporation of incoherency effects into the design of conventional structures. Key points from the Kim and Stewart (2004) study are presented below:

- The approach taken to calculate transfer functions between recorded free-field ground motion and recorded foundation motion parallels that of Chapter 3 here, i.e., at a given frequency, the transfer function is the square root of the ratio of the diagonal terms of the cross power spectral density function (CPSD) matrix divided by the PSD of the input motion.

**Deleted:**  
Effect of Embedment and Incoherence

**Deleted:**  
Effect of Embedment and Incoherence

**Deleted:**  
Effect of Embedment and Incoherence

- The complete data set included twenty-nine instrumented sites: fourteen with near surface foundations and fifteen with piles. Multiple earthquakes were recorded at some of the fourteen sites. The fourteen near surface cases were evaluated, incoherency parameters estimated, and the results compared to the transfer functions of Veletsos et al. (1997). The structure-foundations systems were conventional structures.
- The focus of the studies was on foundation response. However, an important aspect of the evaluation was to approximately account for inertial interaction effects in the data. This was achieved for cases where in-structure response was recorded. In-structure response provided information as to the soil-structure frequencies at which corrections to the data or elimination of the data could be done. As mentioned above, it is very difficult to separate the phenomena of kinematic and inertial interaction. However, attempts were made to do so in the studies cited. Other considerations in the selection of data sites to be included were foundation conditions (near surface foundations, mat foundations, etc.), relatively close proximity of free-field instruments to the structures of interest, free-field instruments not so close that their recordings were significantly affected by structure response.
- Translational response of the foundations were taken from one of three sources: foundation response recorded at or near the foundation centroid, averaged response from multiple recordings on the foundation to estimate the centroid values, or the translational response recorded at the recording station uncorrected to the centroid, if that was the only data available. Rotational motion (torsion and rocking) was calculated from differences in recorded translational motions at points on the foundation divided by the distance between the points.
- An assessment was made of the suitability of the data based on signal processing concepts and only those ordinates found to meet the criteria were included. Generally, this led to the focus being on frequencies less than 10 Hz. Further, the highest confidence in the data was for translations. Rotations being calculated as differences in translations divided by a distance measure were much less reliable. In all cases, there is a great deal of scatter in the data.

Figure B.1-1 is reproduced from Kim (2001) to demonstrate a number of points.

- The quantity plotted is transmissibility, which is consistent with the ITF calculated in the body of this report. The transmissibility is a function of the ratio of the foundation response to the free-field motion. The three plots are for two components of horizontal ground motion and torsion.
- Kim and Stewart (2003) exercised several criteria to determine the data to be included in the regression analysis as discussed in the text herein. The conclusion was to perform the regression analysis to fit the parameters of the Veletsos model for frequencies less than 10 Hz. The frequency range of main interest to this study is greater than 10 Hz.
- Inertial interaction effects were isolated to the extent possible and the data points near the soil-structure fundamental frequency were adjusted.

In conclusion, the transmissibility functions oscillate significantly over the entire plotted frequency range (0 to 25 Hz). It is clear that matching the trend of the results is achievable,

**Deleted:** .  
*Effect of Embedment and Incoherence*

**Deleted:** .  
*Effect of Embedment and Incoherence*

**Deleted:** .  
*Effect of Embedment and Incoherence*

but matching the ITF or transmissibility of an individual earthquake will be extremely difficult.

- For correlation with theoretical representations, in addition to the factors discussed above, a number of other factors complicated the comparisons: foundation conditions (rigidity, embedment, etc.), assumption of purely vertically incident incoherent waves is likely not strictly correct (dispersion of motion due to reflections within the site), differences in the effects as measured for the two horizontal directions, the models assumed half-space or very simplified site profiles where certainly non-homogeneity of the site is the actual situation, etc.
- The conclusions of the evaluations are that the phenomena of incoherence of ground motion exists and should be taken into account when specifying the design ground motion for structures. The approach to account for incoherence is to apply a transfer function to the free-field ground motion to develop a design ground motion for the design seismic analysis – the same concept as proposed herein but without added provisions to account for induced rotations. The recommended transfer functions to be applied are the theoretical functions of Veletsos et al. (1997) with the assumption of ground motion incoherence given by an exponential decay. Limitations or caveats of this approach are principally on the foundation, i.e., foundations that are continuous or behave in a continuous manner (mat foundations or inter-connected spread footings), foundation dimensions less than 60 m. (presumably to more closely approximate rigid foundation behavior for conventional structures), and embedment ratios less than 0.5.

The approach recommended by Kim and Stewart (2003) is identical to the simplified method proposed within the body of this report with the following exceptions:

- The assumed ground motion coherency function is distinctly different from the Abrahamson functions (Abrahamson, 2005, 2006), which are based on the extensive body of recorded data – recorded over the last decade or so.
- No additional consideration for induced rotations is included in the recommended approach. The simplified method of Chapter 5 includes an added provision to account for induced rotations.

The majority of incoherency response validation studies to date have focused on conventional structures for many reasons. At the present time, due to the number of instrumented structures and the frequency of earthquakes (particularly in California), the only extensive data base of recordings exists for conventional structures. Studies such as the body of work by Stewart and colleagues are extremely valuable in validating the effects of incoherence on structure response. However, further validation of the phenomena for nuclear power plant structures is sought. The following two sections discuss the observed behavior of the Diablo Canyon Nuclear Power Plant and the Perry Nuclear Power Plant subjected to earthquake ground motions.

Deleted: Effect of Embedment and Incoherence

Deleted: Effect of Embedment and Incoherence

Deleted: Effect of Embedment and Incoherence

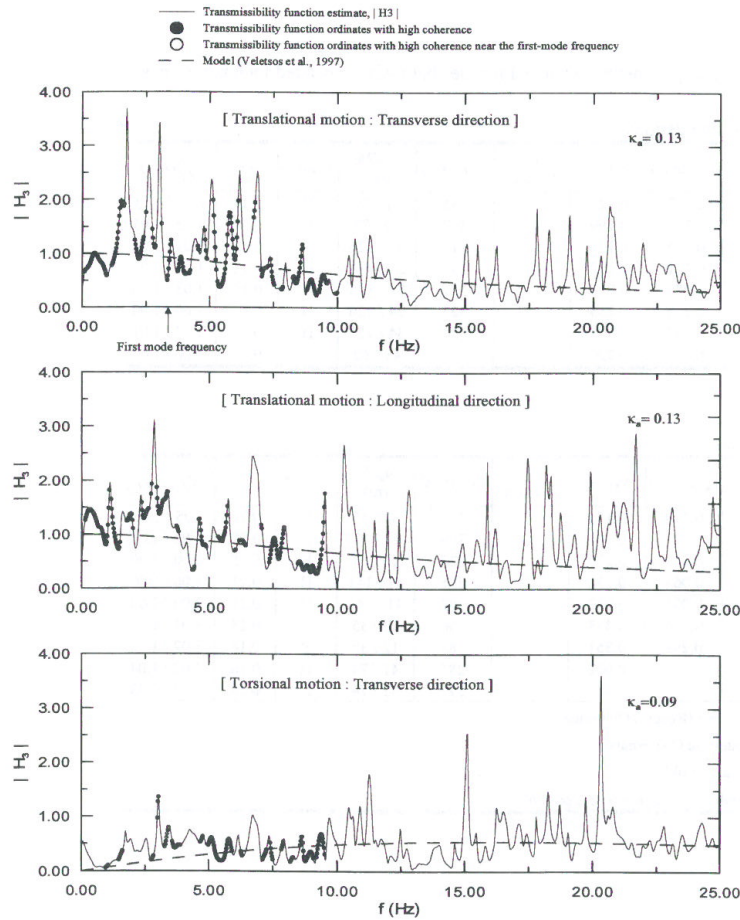


Figure B.1-1  
Example of Transmissibility Functions for a Single Earthquake, Data Processed, and  
Estimation of Incoherence Parameter of the Free-Field Motion (Kim, 2001)

**Deleted:** .

*Effect of Embedment and Incoherence*

**Deleted:** .

*Effect of Embedment and Incoherence*

**Deleted:** .

*Effect of Embedment and Incoherence*

## **B.2 Diablo Canyon Earthquakes**

The Diablo Canyon nuclear power plant in California has experienced recent earthquakes in which ground motion was recorded on the containment foundation and in the free-field. A magnitude 6.5 San Simeon earthquake was studied but found to have only low-frequency motion (due to the high magnitude and being relatively far from the Diablo Canyon site). The Magnitude 3.4 Deer Canyon Earthquake that occurred October 18, 2003, however, provides an opportunity to compare calculated and measured incoherency effects. This relatively low magnitude earthquake ground motion is narrow banded with high-frequencies in the 10 to 20 Hz range making this motion a good candidate for the study of ground motion incoherence effects. The peak ground acceleration is in the range of 0.01 and 0.02g depending on the component. Measured free-field and containment foundation motion are shown in Figure B.2-1. The containment motion is significantly reduced from the free-field motion at frequencies greater than 10 to 12 Hz.

Calculations simulating incoherent Deer Canyon foundation motion for the Diablo Canyon foundation footprint and soil conditions are compared to measured foundation and free-field Deer Canyon earthquake motion in this appendix. However, this approach does not account for SSI effects that may be a significant reason for high-frequency reductions of foundation motion relative to the free-field motion. To account for SSI effects, a transfer function relating horizontal foundation motion to horizontal free-field ground motion determined from soil-structure analyses of the Diablo Canyon plant many years ago is available in the literature (PG&E, 1988). The total transfer function between foundation and free-field motion is the product of an SSI transfer function and an incoherency transfer function. For purposes of discussion, the SSI transfer function, as used here, is comprised of two parts: the effects of vertical spatial variation of the ground motion, i.e., the combination of spatial variation with depth in the rock/soil at the site and the effects of the excavation and embedment of the foundation; and the inertial interaction effects. To compute an SSI transfer function for comparison to the transfer function from the SSI analyses, the transfer function of the total motion was estimated from the measured foundation and containment foundation motions and divided by the computed incoherency transfer function (ITF) determined by the CLASSI random vibration approach.

It should be recognized that the free-field seismic instrument at the time of the Deer Canyon earthquake was not located on the same rock type/formation as the Diablo Canyon containment foundation. A new free-field seismic instrument will be or has been installed to the north of the containment structure on the same rock type/foundation. Hence, difference in rock conditions is another difference between the free-field and containment foundation during the Deer Canyon earthquake.

Deleted:  
Effect of Embedment and Incoherence

Deleted:  
Effect of Embedment and Incoherence

Deleted:  
Effect of Embedment and Incoherence

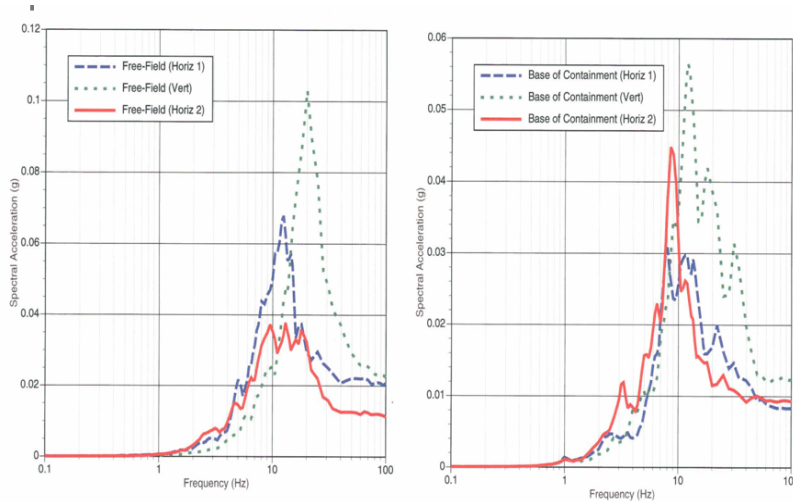
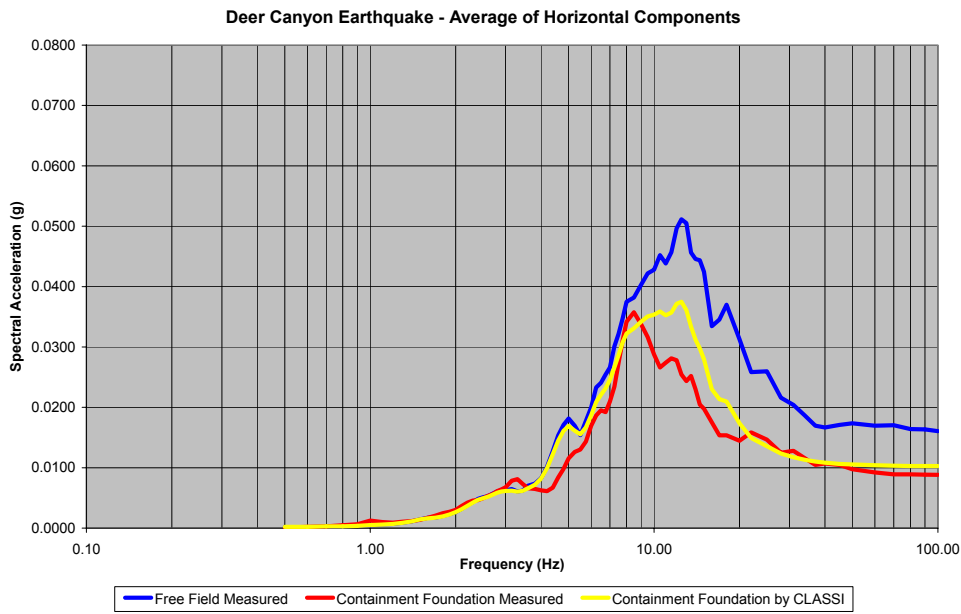


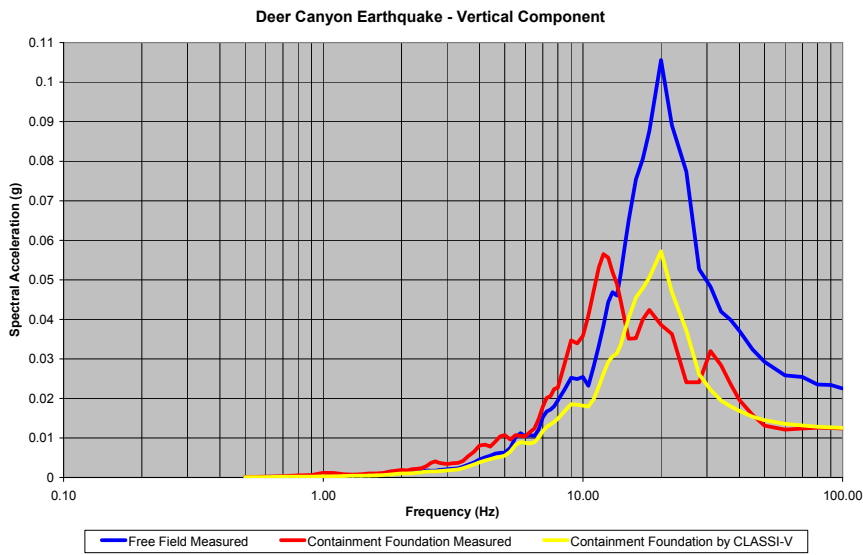
**Figure B.2-1**  
**Measured Earthquake Motion at Diablo Canyon from the 2003 Deer Canyon Earthquake**

The foundation of the Diablo Canyon containment structure has a 153 foot diameter circular footprint. Soil properties consist of a 3 layers over a half space. The layers are 10, 20, and 125 feet with shear wave velocities of 2600, 3300, and 4000 fps. The half space has a shear wave velocity of 4800 fps. Soil damping and densities used in the 1988 SSI analyses were also used. The free-field ground response spectra was input as a PSD using the CLASSI RVT approach in order to evaluate the containment motion PSD due to ground motion incoherence only considering the Diablo Canyon foundation as rigid and massless. The resulting PSD was then converted to a response spectra by random vibration theory for comparison to the measured foundation response spectra. The results of this calculation are shown in Figure B.2-2. The computed foundation motion is of the same amplitude as the measured motion but with slightly different frequency content. The measured motion has lower frequency content than the computed foundation motion indicating the effects of soil-structure interaction. As stated above, any difference in foundation and free-field motion is due to the combination of ground motion incoherence and soil-structure interaction. Hence, Figure B.2-2 is interesting but does not isolate the effects of ground motion incoherence and soil-structure interaction.

Deleted: Effect of Embedment and Incoherence  
Deleted: Effect of Embedment and Incoherence  
Deleted: Effect of Embedment and Incoherence



a. Horizontal Motion



b. Vertical Motion

Figure B.2-2  
Comparison of Measured and Computed Foundation Motion at Diablo Canyon

**Deleted:**  
*Effect of Embedment and Incoherence*

**Deleted:**  
*Effect of Embedment and Incoherence*

**Deleted:**  
*Effect of Embedment and Incoherence*

In order to isolate the effects of incoherency from other SSI effects (i.e., inertial interaction, embedment), the Diablo Canyon existing SSI transfer functions were compared to transfer functions computed from the total motion transfer function and the incoherency transfer function. The total motion transfer function is estimated as the square root of the ratio of the foundation motion power spectral density to the free-field motion power spectral density. Each of these power spectral density functions are determined by random vibration theory using the foundation and free-field response spectra respectively. The incoherency transfer function is determined for the Diablo Canyon foundation footprint and soil properties in the same manner described in Chapter 4. The measured transfer function for the ratio of the square root of PSDs and the incoherency transfer function (ITF) are shown in Figure B.2-3. The estimated SSI transfer function is then equal to the measured transfer function divided by the incoherency transfer function and this result is also shown in Figure B.2-3.

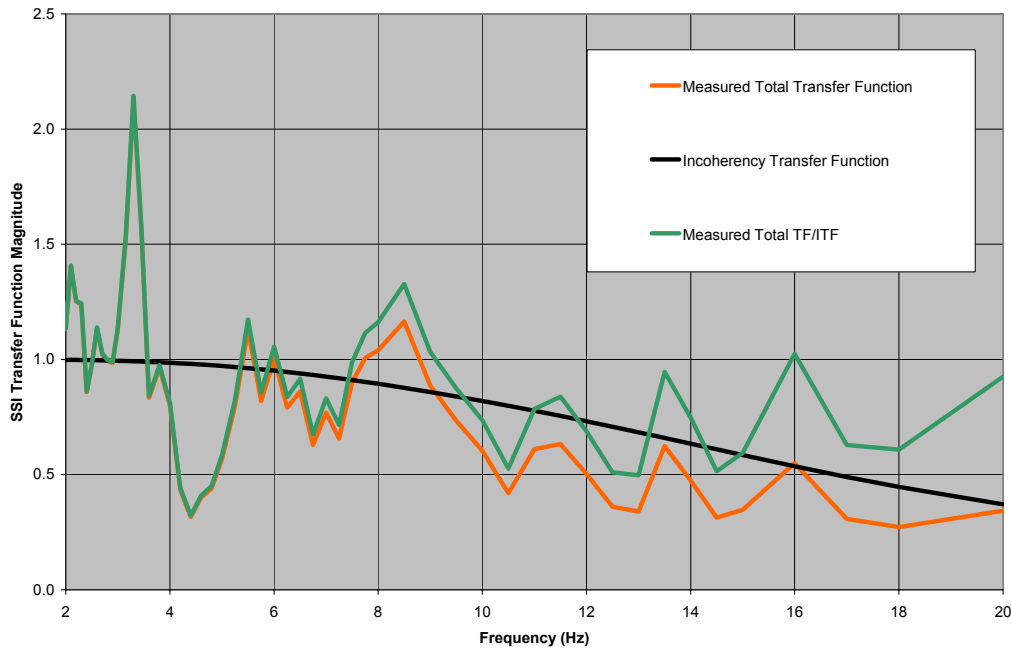


**Figure B.2-3**  
**Total Motion, Incoherency, and Estimated SSI Transfer Functions**

SSI transfer functions determined from the 1988 soil-structure interaction analyses are available for horizontal motion and for mean, upper bound and lower bound soil profiles. These SSI transfer functions are compared to the estimated SSI transfer function determined as the ratio of total to incoherency transfer functions in Figure B.2-4. It may be seen that the SSI transfer functions from SSI analyses are highly variable but the estimated SSI transfer function from measured ground motion and incoherence calculations lies in the same range as the SSI analyses results over a wide frequency range. The results presented in Figures B.2-2 and B.2-4 support that the differences in foundation and free-field motion at Diablo Canyon from the 2003 Deer

Deleted: Effect of Embedment and Incoherence  
Deleted: Effect of Embedment and Incoherence  
Deleted: Effect of Embedment and Incoherence

Canyon earthquake could be due to ground motion incoherence combined with SSI effects. In the frequency range from 11 to 20 Hz the estimated SSI transfer function is reasonably close to the mean soil SSI transfer function from SSI analyses.

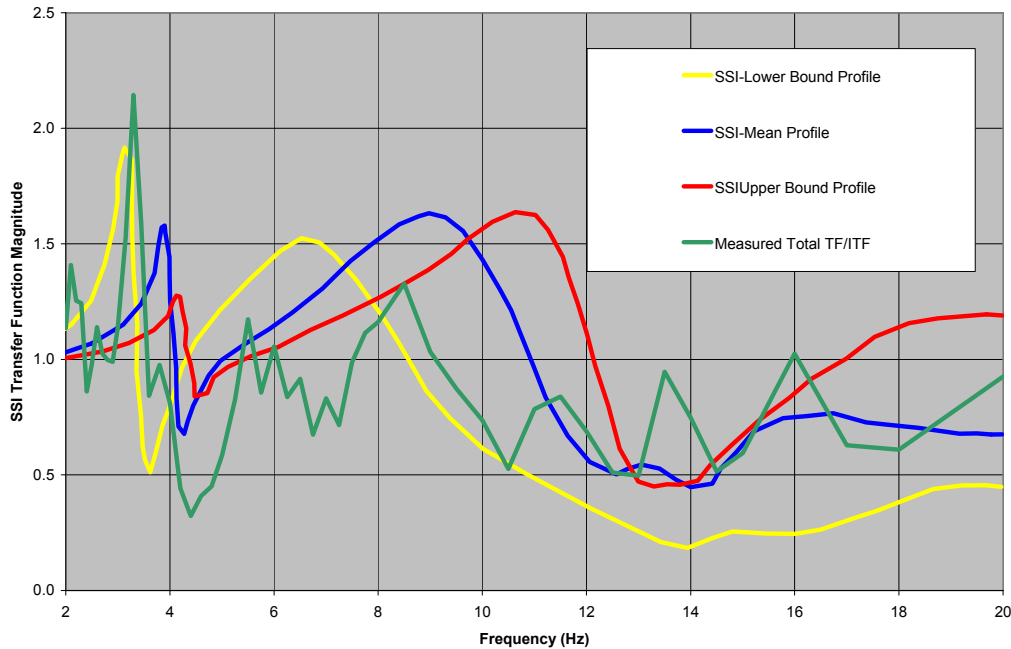


Figure B.2-4 Comparison of Estimated and Calculated SSI Transfer Functions

### B.3 Measured Response of the Perry Nuclear Power Plant during the Northeastern Ohio Earthquake of January 31, 1986

On January 31, 1986, an earthquake with an estimated moment magnitude of 4.6 occurred in the vicinity of Leroy, Ohio. The Perry Nuclear Power Plant, which was undergoing pre-operational testing (prior to fuel load), is located approximately 17 km to the north of the epicentral area. The plant is a Mark III BWR with a free-standing steel containment shell surrounded by a concrete shield building. The estimated epicentral intensity of the earthquake was VI (MMI scale) and the Perry site intensity was estimated to be V (MMI scale). The Perry Plant has a Kinometrics SMA-3 strong recording system with two tri-axial transducer units (force balance accelerometers) mounted on cantilever steel brackets attached to the shield wall near the base mat and the steel containment shell at the approximate elevation of the operating floor. Figure 1 shows the general plan and section of the Perry Plant with the instrument locations identified. As can be noted, there are no free-field instruments.

**Deleted:**  
Effect of Embedment and Incoherence

**Deleted:**  
Effect of Embedment and Incoherence

**Deleted:**  
Effect of Embedment and Incoherence

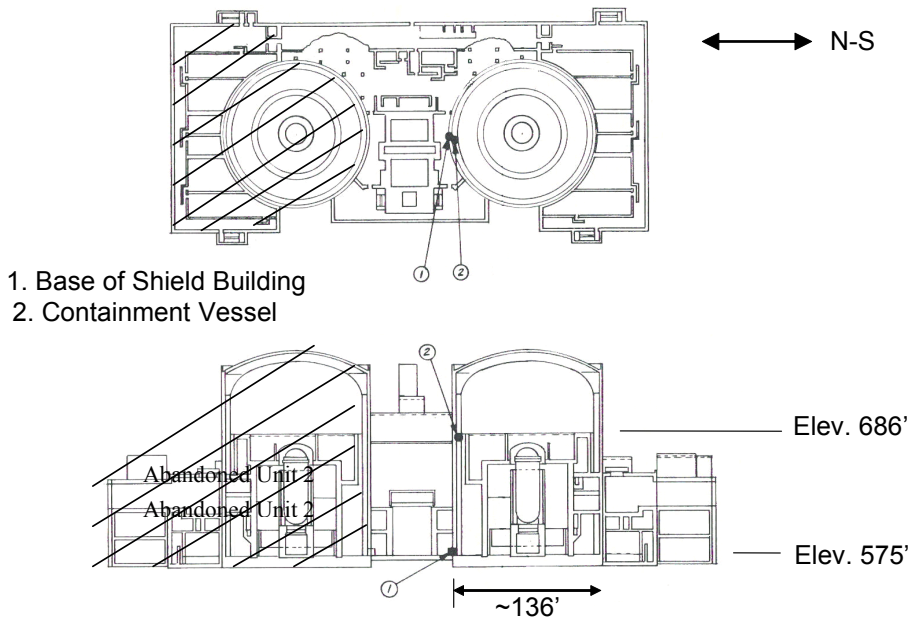


**Figure B.3-1**  
**Perry Plant Configuration Showing Strong Motion Instrument Locations**

The common base mat of the containment and shield buildings is directly founded on rock with a surface shear wave velocity of 4900 fps. The containment and shield buildings are physically separated from the other plant structures. In the north-south direction, the base mat is not embedded while in the east-west direction a portion of the shield building is embedded.

Figure B.3-2 shows the recorded accelerations (processed and corrected) at the base of the shield building.

Deleted: Effect of Embedment and Incoherence  
Deleted: Effect of Embedment and Incoherence  
Deleted: Effect of Embedment and Incoherence

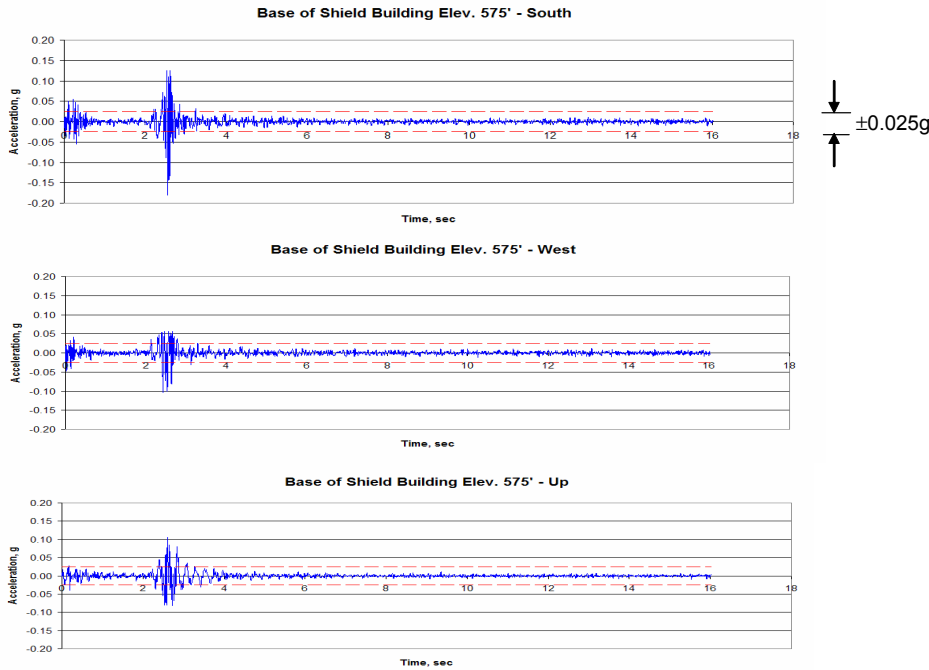


**Figure B.3-2**  
**Processed and Corrected Acceleration Records Obtained from the Base of Shield Building Instruments**

As can be noted, the duration of the strong motion response is less than one second. Since the base mat was founded on sound rock, the base record was inferred to be equivalent to a free-field record. The maximum response (peak acceleration) of the base motion is 0.18 g and occurs in the north-south direction. Walkdown inspections of the plant revealed that no damage had occurred nor were any spurious activation of the plant controls noted. However, the response spectra of the recorded base motion indicated that the OBE of the plant had been exceeded in the 20 Hz region. This evidence of a non-damaging event, which would have led to plant shutdown under the then current rules, prompted both the NRC and EPRI to initiate studies that ultimately led to the establishment of Regulatory Guides 1.166 and 1.167. One of the criteria of RG 1.166 is the CAV threshold of 0.16 g-sec, where the CAV is the integral of the absolute acceleration of the free-field motion greater than 0.025 g. Figure B.3-3 shows the calculation of the CAV for the Perry Plant records which is approximately one-fourth of the limiting value, indicating that the recorded motion (inferred to be a free-field motion) has very low damage potential.

**Deleted:**  
Effect of Embedment and Incoherence

**Deleted:**  
Effect of Embedment and Incoherence

**Deleted:**  
Effect of Embedment and Incoherence

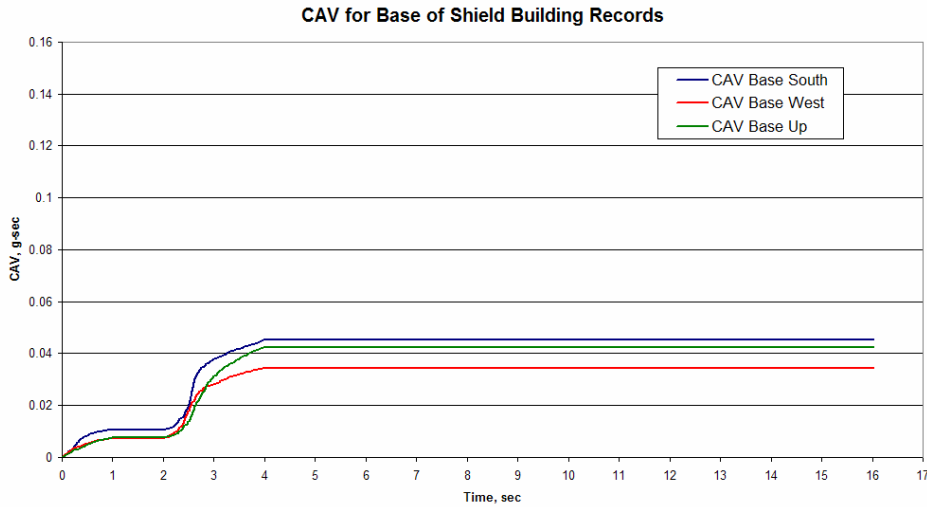


**Figure B.3-3**  
**CAV Computation from Recorded Base of Shield Building Acceleration Records**

Figures B.3-4 through B.3-6 compare the response spectra of the recorded motions, both at the base of the Shield Building and the Containment Vessel at the operating floor elevation.

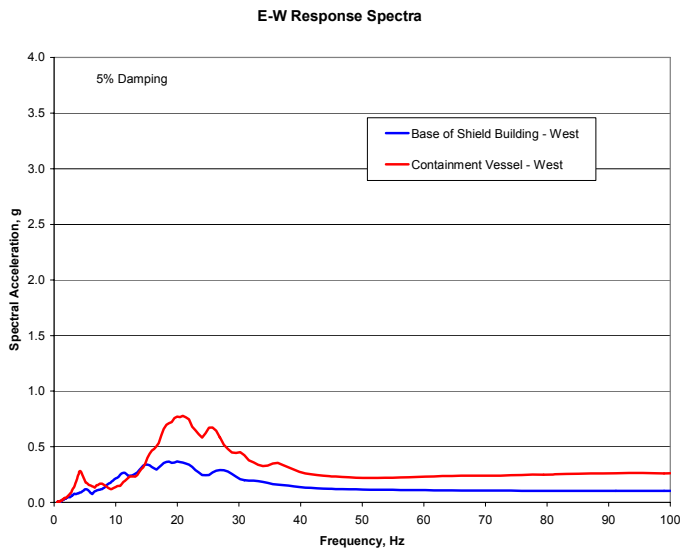


**Figure B.3-4**  
**Comparison of East-West Response Spectra**

Deleted: Effect of Embedment and Incoherence  
Deleted: Effect of Embedment and Incoherence  
Deleted: Effect of Embedment and Incoherence

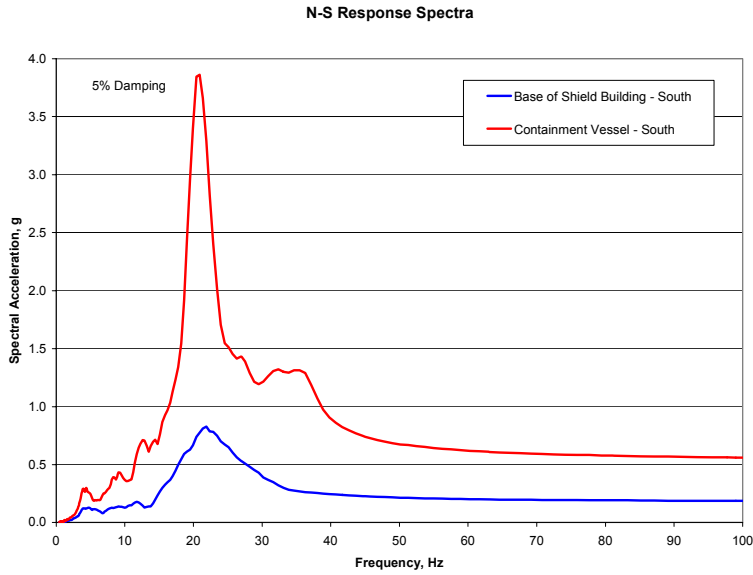


Figure B.3-5  
Comparison of North-South Response Spectra

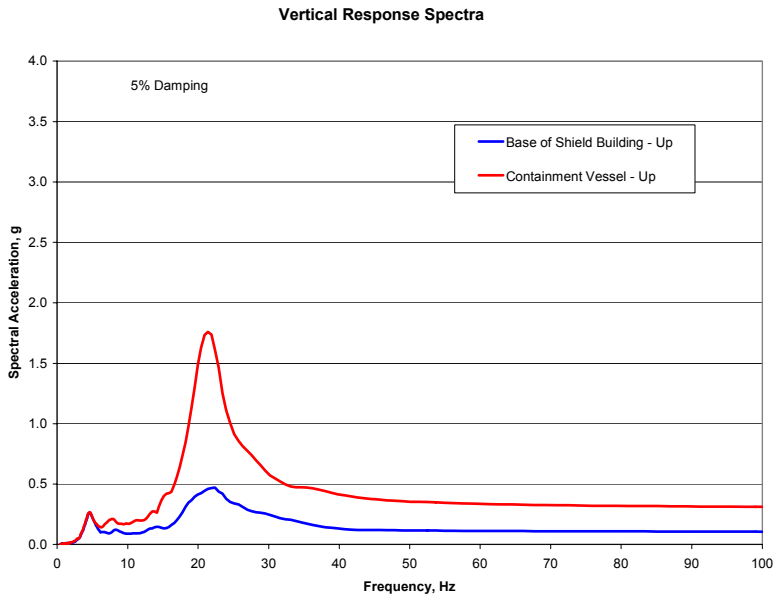


Figure B.3-6  
Comparison of Vertical Response Spectra

**Deleted:**  
*Effect of Embedment and Incoherence*

**Deleted:**  
*Effect of Embedment and Incoherence*

**Deleted:**  
*Effect of Embedment and Incoherence*

As can be noted in Figure B.3-1, the base mat instrument is placed at the outer diameter of the concrete shell Shield Building within a meter of the upper surface of the mat, and the Containment Vessel instrument is placed at a higher elevation on the outer diameter of the steel shell. If an overturning motion (i.e., rocking) of the base mat was present, this placement of instruments would result in coupled vertical and north-south translation records. Figures B.3-4 to B.3-7 suggest that both the vertical and translational motion of the base of Shield Building response is correlated to the structure response at the fundamental of approximately 5 Hz and at a higher mode frequency of approximately 20 Hz. Figure B.3-8 shows the Fourier spectra modulus,  $|F_{SB}[f]|$ , computed for the windowed (Hann-weighted) base of Shield building response. The presence of the same dominant frequencies (~5 Hz and ~20 Hz) in both the translational and vertical response is a clear indication that the horizontal response of both the Shield Building and Containment Vessel is inducing an overturning motion or uplift of the edge of the base mat.

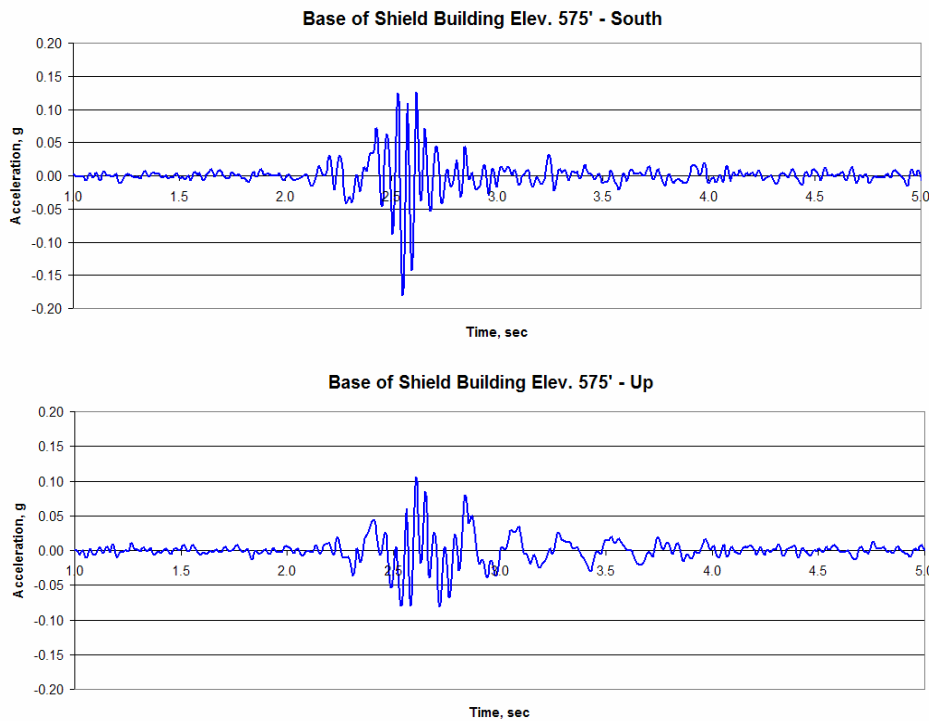


**Figure B.3-7**  
**North-South and Vertical Response Windows**

Both the plant AE (architect-engineer) and the USNRC (consultant) conducted analytical studies of the plant response. The AE used the design model which incorporated rock springs to simulate the interaction of the plant structures with the supporting media. The AE model indicated dominant modes at 4 and 19 Hz and the AE concluded that the observed response at 20 Hz was

Deleted: Effect of Embedment and Incoherence  
Deleted: Effect of Embedment and Incoherence  
Deleted: Effect of Embedment and Incoherence

to be expected as a result of the rock-structure system. The NRC assumed a fixed-base model (no rock interaction) and obtained dominant modes at 4.5 and 20 Hz. The NRC consultant concluded that base rocking was not significant but that a significant mode of response for the Containment Vessel occurs at approximately 20 Hz. The fixed-base model was then used, assuming that the recorded base motion was a free-field motion, to obtain estimate of the response spectra at containment shell location.

As can be noted in Figure B.3-1, the placement of the instruments would result in coupled vertical and north-south translational response. Figures B.3-4 to B.3-7 suggest that both the vertical and translational motion of the base of Shield Building response is correlated to the structure response at the fundamental and at approximately 20 Hz. Figure B.3-8 shows the Fourier spectra modulus,  $|F_{SB}[f]|$ , computed for the windowed (Hann weighted) base of Shield Building response. The presence of the filtered translational response in the vertical motion is a clear indication that rocking of the base mat is occurring.

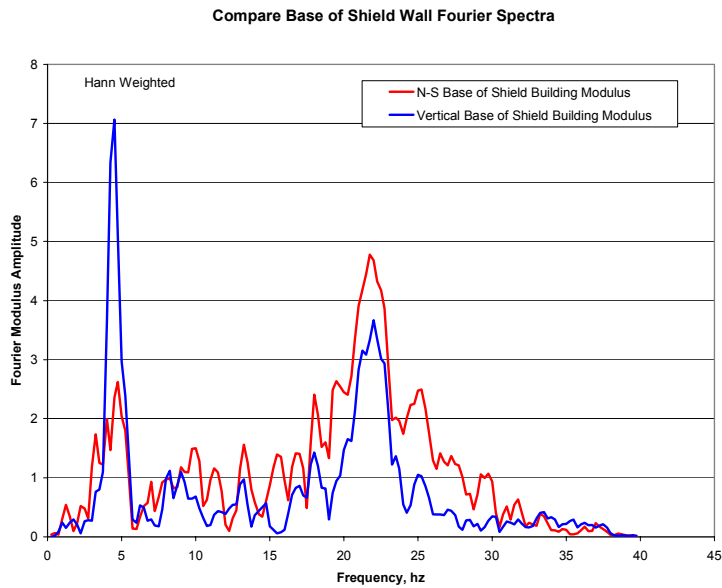
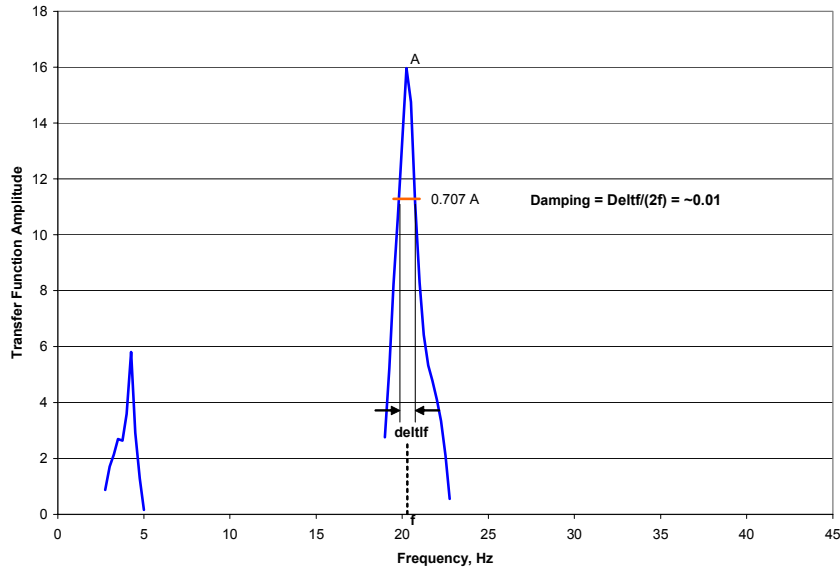


Figure B.3-8  
Fourier Modulus Spectra for Base of Shield Building

An estimate of the north-south transfer function for the translation response of containment vessel at the elevation of the operating floor may be provided by the ratio of the respective Fourier spectra moduli. Figure B.3-9 shows the ratio of Fourier spectra modulus,  $|F_{SB}[f]|/|F_{SB}[f]|$ , for the dominant frequency response regions. The bandwidth estimate of the Containment Vessel damping for the 20 Hz mode is approximately 1%.

Deleted:  
Effect of Embedment and IncoherenceDeleted:  
Effect of Embedment and IncoherenceDeleted:  
Effect of Embedment and Incoherence

**Figure B.3-9**  
**Estimated Transfer Function for Translational Response (North-South) of Containment Vessel**

Based on the above observations, it is concluded that the recorded motions of the Perry Nuclear Power Plant due to the 1986 Northeastern Ohio earthquake have extremely short duration, less than one second, and according to current evaluation criteria would be classified as non-damaging. The resulting stresses in the free-standing containment shell (1.5-in thick) would be very low and the estimated damping associated with the second mode response (~20 Hz) of the steel containment shell would be approximately 1% or less. The anchorage of the Shield Building into the base mat is accomplished by continuity of vertical reinforcement steel; however, the Containment Vessel is anchored into the base mat with a pattern of vertical straps cut from the steel shell (an unusual detail). Further, the annular space between the concrete Shield Building and Steel Containment Vessel has been filled with concrete and reinforcing in the lower 25-ft both structures. There was likely high-frequency content in the free-field rock motion, but the 20 Hz motion observed at the base of the Shield Building is likely due to both the feedback of the translational response of the structures causing base mat uplift or rocking and anchorage compliances between base mat and the Shield Building and the Containment Vessel (i.e., lack of fixed-base condition at the base mat interface). The amplified response observed for the Containment Vessel is an expected response of the structural system for low-level input motion with very low response damping. Since the motion duration was very short (less than 1 second), it is conjectured that the free-field motion was a vertically propagating single frequency pulse which would tend to be coherent over the base mat rock interface. Thus, the effects of foundation incoherence, which are associated with phasing effects of multi-frequency, longer duration motion, would not be present.

**Deleted:**

*Effect of Embedment and Incoherence*

**Deleted:**

*Effect of Embedment and Incoherence*

**Deleted:**

*Effect of Embedment and Incoherence*

The Perry Plant recordings are not felt to present a valid case of proving or disproving incoherency or high-frequency response amplification. The lack of a true free-field instrument inhibits any identification of base mat response averaging (i.e., the effect of incoherency) that may be present. The short duration and apparent single frequency of the motion would tend to suppress the development of incoherent motion. The location of the instruments coupled with a very low amplitude input motion (i.e., resulting in very low damping) causes the measured amplified vertical and horizontal response to be correlated.

#### **B.4 Conclusions Regarding the Validation of incoherency Effects Through Recorded Events**

The overall conclusion of this literature review of recorded seismic events reinforces the original premise of this research project that the effective input motion to structures is reduced from instrumental ground motion, particularly in the higher frequency parts of the response spectrum. This reduction is demonstrated (for large and relatively rigid foundations) within the 29 sites studied within the Kim and Stewart (2003) paper and from recordings at both the Diablo Canyon and the Perry nuclear power plants. Appendix B also highlights the difficulties inherent to a quantitative validation of the effects of incoherence of ground motion on nuclear power plant structures with data existing today. The key conclusions from the reviews described within this appendix include the following:

- General conclusions as to the existence of the phenomena and their effects on structures are validated.
- The phenomena of most interest to the nuclear power plant community are for frequencies greater than 10 Hz. For existing recorded motions, it is possible to draw general conclusions for this frequency range, but not specific quantitative conclusions.
- The existing data bases are for conventional structures and must be extrapolated to the situation of nuclear power plant type structures. This extrapolation is performed in general terms for validation purposes.
- An on-going difficulty in evaluating recorded data for soil-structure interaction is the separation of the various elements of the phenomena – kinematic vs. inertial interaction; kinematic interaction due to vertical spatial variation of ground motion for embedded foundations vs. horizontal spatial variation of ground motion; flexible vs. rigid foundation behavior. To further validation efforts in these regards, instrumentation plans need to be developed to isolate the aspects of SSI to be studied.
- The number of nuclear power plants, their locations in regions of low seismicity, and the small number of earthquakes recorded at these facilities has led to very limited data being recorded for validation of the various aspects of SSI. Further, the instrumentation schemes have not been developed for validation of the elements of SSI. Consequently, general behavior is validated, but not specifics. Two cases in point are the Diablo Canyon and Perry nuclear power plants discussed in sections B.2 and B.3. General information is derived from these situations, but not specific validation of elements of SSI.

**Deleted:**  
Effect of Embedment and Incoherence

**Deleted:**  
Effect of Embedment and Incoherence

**Deleted:**  
Effect of Embedment and Incoherence

In conclusion, the approach taken in the present study to account for incoherence of ground motion is compatible with that taken by Stewart and colleagues to evaluate recorded data and to implement the results into the seismic design process. Recorded data at Diablo Canyon and Perry nuclear power plants highlight the difficulties in using recorded data to validate specific elements of SSI. Carefully designed instrumentation schemes will be required in the future to validate these individual elements.

## B.5 References

- Abrahamson, N. (2006). *Spatial Coherency for Soil-Structure Interaction*, Electric Power Research Institute, Final Report 1014101, Palo Alto, CA. August (Draft).
- Abrahamson, N. (2005). *Spatial Coherency for Soil-Structure Interaction*, Electric Power Research Institute, Technical Update Report 1012968, Palo Alto, CA. December.
- Bechtel Power Corporation (1988). *Final Report on the Diablo Canyon Long Term Seismic Program, Soil-Structure Interaction Analysis*, prepared for Diablo Canyon Power Plant Long Term Seismic Program, PG&E Company, San Francisco, CA. July.
- Chang, C.-Y., M.S. Power, I.M. Idriss, P. Sommerville, W. Silva, and P.C. Chen (1985). *Engineering Characterization of Ground Motion, Task II: Observational Data on Spatial Variations of Earthquake Ground Motion*, NUREG/CR-3805, Vol. 3.
- EPRI (1997). *Soil-Structure Interaction Analysis Incorporating Spatial Incoherence of Ground Motions*, Electric Power Research Institute, Report TR-102631 2225, Palo Alto, CA. November.
- Ishii, K., T. Itoh, and J. Suhara (1984). *Kinematic Interaction of Soil-Structure System Based on Observed Data*, Proc. 8<sup>th</sup> World Conference on Earthquake Engineering, San Francisco, CA., Vol. 3, Earthquake Engineering Research Center, Berkeley, CA, pp. 1017-1024.
- Johnson, J.J. (2003). *Soil-Structure Interaction*, Earthquake Engineering Handbook, Chapter 10, W-F Chen, C. Scawthorn, eds., CRC Press, New York, NY.
- Kim, S. (2001). *Calibration of Simple Models for Seismic Soil-Structure Interaction from Field Performance Data*, PhD Dissertation, University of California, Los Angeles, CA.
- Kim, S. and J.P. Stewart (2003). *Kinematic Soil-Structure Interaction from Strong Motion Recordings*, J. Geotech. Geoenviron. Eng., Vol. 129, No. 4, pp. 323-335.
- Kohima, H., N. Fukuwa, and J. Tobita (2004). *Dynamic Response of Low and Medium-Rise Building Based on Detailed Observation Considering Soil-Structure Interaction*, Thirteenth World Conference on Earthquake Engineering, Vancouver, B.C., Canada, Paper No. 1243, August.
- Stewart, J.P., G.L. Fenves, and R.B. Seed (1999a). *Seismic Soil-Structure Interaction in Buildings I: Analytical Methods*, J. Geotech. Geoenviron. Eng., Vol. 125, No. 1, pp. 26-37.

Stewart, J.P., R.B. Seed, and G.L. Fenves, (1999b). *Seismic Soil-Structure Interaction in Buildings II: Empirical Findings*, J. Geotech. Geoenviron. Eng., Vol. 125, No. 1, pp. 38-48.

Veletsos, A.S., A.M. Prasad, and W.H. Wu (1997). *Transfer Functions for Rigid Rectangular Foundations*, Earthquake Eng. Str. Dyn., Vol. 26, No. 1, pp.5-17.

**Deleted:**  
Effect of Embedment and Incoherence

**Deleted:**  
Effect of Embedment and Incoherence

**Deleted:**  
Effect of Embedment and Incoherence

# C

## BENCHMARK PROBLEM COMPARISON

---

The direct approach for considering the effects of seismic wave incoherency has primarily been implemented using the CLASSI soil-structure interaction analysis program. However, in this appendix, the CLASSI approach is benchmarked against an alternate method using the SASSI soil-structure interaction analysis program. SASSI (modified for treatment of incoherency) allows the incorporation of general, three-dimensional (3-D) spatial coherency of free-field motions in the seismic input, thus allowing it to be used for seismic response analysis of structures with surface-supported or embedded foundations. This approach uses conventional “deterministic” time-history analysis approach rather than the “probabilistic” random vibrational analysis approach implemented using CLASSI.

By both CLASSI and SASSI, the characterization of spatial variations of free-field motions consists of frequency domain coherency functions as developed by Dr. Abrahamson. These coherency functions are parameterized in a form consistent with the assumption of a single coherent plane wave field of seismic input and have been employed for SSI analysis applications. With this form of coherency characterization, SASSI generates the incoherent ground motions which are compatible with the prescribed Abrahamson coherency functions for use as input to SSI analysis. The SASSI formulation makes use of the eigen properties of the coherency matrix derived from the prescribed coherency functions in generating the coherency-compatible incoherent free-field input and the conventional frequency-domain time history SSI analysis procedure.

The implementation of an incoherency model in SASSI follows the basic equations of motion for the SSI system for each frequency of analysis. Based on these equations, only the incoherent free-field load vector needs to be computed using the coherency function from Abrahamson. This vector is computed for each frequency and for the interaction nodes in contact with soil in the SSI model. To do so, the following steps are taken:

- For each frequency, the coherency function is used to construct the coherency matrix for all interaction nodes,  $i$ . The matrix can be readily constructed given the frequency of analysis,  $f$ , and the separation distance among the nodes,  $\xi_{ij}$ . This is a full matrix with off-diagonal terms reducing in absolute values as the separation distance among the nodes increases in accordance with the Abrahamson coherency function. A separate matrix for horizontal and vertical motion is constructed. Terms of the coherency matrix are obtained from Eq. (2-1).

The separation distance,  $\xi_{ij}$  is the radial distance from Node  $i$  to Node  $j$  projected to a horizontal plane and is obtained from the horizontal X- and Y-coordinates of the nodes. This matrix has dimensions of  $N \times N$ , with  $N$  being the total number of interaction nodes in the SASSI model. All diagonal terms of the matrix are unity. This matrix is a Hermitian matrix

**Deleted:** .  
*Effect of Embedment and Incoherence*

**Deleted:** .  
*Effect of Embedment and Incoherence*

**Deleted:** .  
*Effect of Embedment and Incoherence*

with real eigen values. It is also a normal matrix whose eigen vectors are orthogonal (the product of two different modes is zero) and the dot product of each mode by its transpose is unity.

- Each matrix is solved using complex eigen equation solver to obtain the eigen values and eigen vectors. Eigen vectors are used as mode shapes. Modal weights are the square root of the eigen values. All modes are considered in the analysis.
- The mode shapes and modal weights are combined linearly to develop the free-field vector. The free-field vector now includes the coherency functional relationship of Eq. (2-1) among the motions of the interaction nodes. Due to orthogonal properties of the mode shapes, it can be shown that the average free-field motion, averaged over all interaction nodes in the free-field for each frequency of analysis, is unity so that, on the average, the power spectral density of the input motion is preserved in the analysis.
- For embedded structures, the free-field vector is adjusted for amplitude reduction of free-field vector with depth just as it has been performed in the basic SASSI operation. The incoherency effects due to horizontal spacing among the nodes follows the same equation as those on the ground surface.
- The above steps are repeated for vertical and horizontal motions separately and corresponding free-field vectors are obtained for vertical and horizontal excitation.
- Once computation of the free-field vector is completed, SSI analysis follows the same steps as basic SASSI operation.

### **Rigid, Massless Foundation**

The development of incoherency transfer functions and spectral corrections for an example rigid, massless foundation has been validated by independent benchmark comparisons of results. For this purpose, the effect of incoherent ground motion has been evaluated by:

- Two different SSI computer programs; CLASSI and SASSI
- Two different algorithms; CLASSI-stochastic method and SASSI eigen decomposition method
- Two different analytical approaches; random vibration theory (RVT) by CLASSI and time history dynamic analyses by SASSI
- Two different organizations conducting the analyses; CLASSI by ARES and SASSI by Bechtel

Bechtel-SASSI results are from Ostadan, 2005. The problem considered for the benchmark comparison of the two approaches was to determine the incoherency transfer function and the response spectra for motion of a rigid, massless foundation founded on a rock half-space. Input earthquake excitation was the rock input motion for which the response spectra are shown in Figure 2-5. Other problem parameters included:

- 150 x 150-ft square foundation footprint

**Deleted:**  
*Effect of Embedment and Incoherence*

**Deleted:**  
*Effect of Embedment and Incoherence*

**Deleted:**  
*Effect of Embedment and Incoherence*

- 6300 fps rock shear wave velocity half-space
- Soil material damping of 1 percent

The comparison of incoherency transfer functions for both horizontal and vertical ground motion is presented in Figure C-1. CLASSI and SASSI generated incoherency transfer functions agree within 10 percent at all frequencies.

Horizontal foundation response spectra by CLASSI and SASSI are presented in Figure C-2 and vertical foundation response spectra by CLASSI and SASSI are presented in Figure C-3. These spectra also agree within 10 percent at all frequencies. Both computer programs and analytical approaches demonstrate significant reductions in the foundation motion as compared to the high-frequency free-field input response spectra.

The CLASSI and SASSI computer programs have been validated in accordance with the quality assurance program of each respective company. Software verification and validation have been performed by solving of example problems that exercise the features of the programs that are utilized in this study. Results are compared with results from alternative methods.

Excellent agreement is obtained for both incoherency transfer functions and spectra corrections on the foundation. Although the benchmark studies focused on translational responses rather than the combination of translations and rotations, the team is confident that when considering all effects, the benchmark comparison will meet engineering acceptability. The benchmark comparison is validation of the technical approach being employed in Task S2.1.

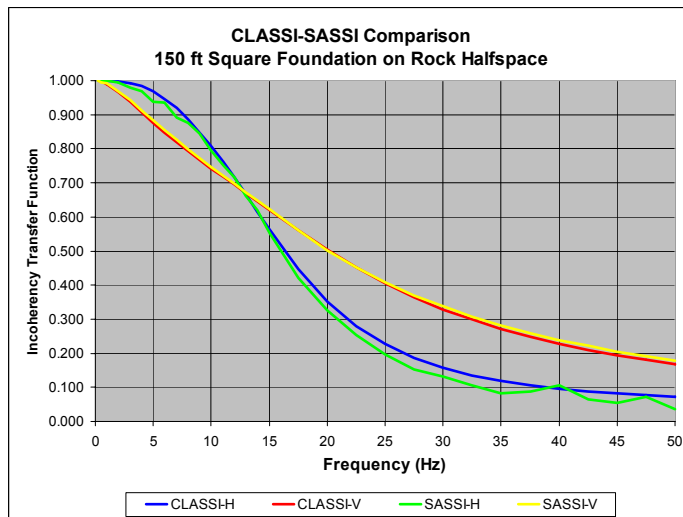


**Figure C-1**  
**CLASSI-SASSI Comparison of Incoherency Transfer Functions**

Deleted: Effect of Embedment and Incoherence  
Deleted: Effect of Embedment and Incoherence  
Deleted: Effect of Embedment and Incoherence

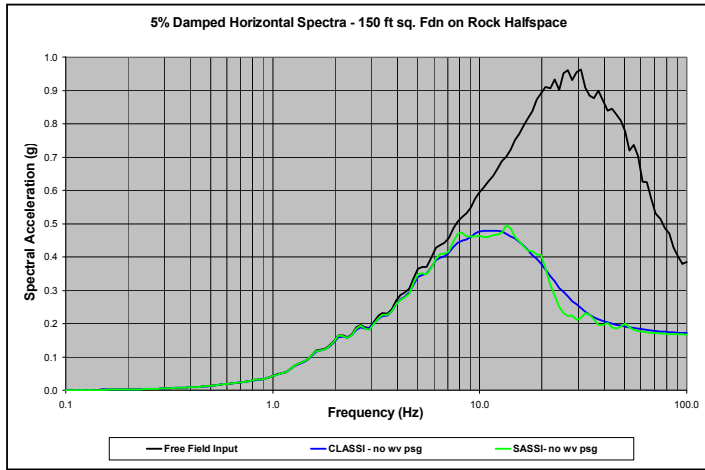


Figure C-2  
CLASSI-SASSI Comparison of Horizontal Foundation Response Spectra

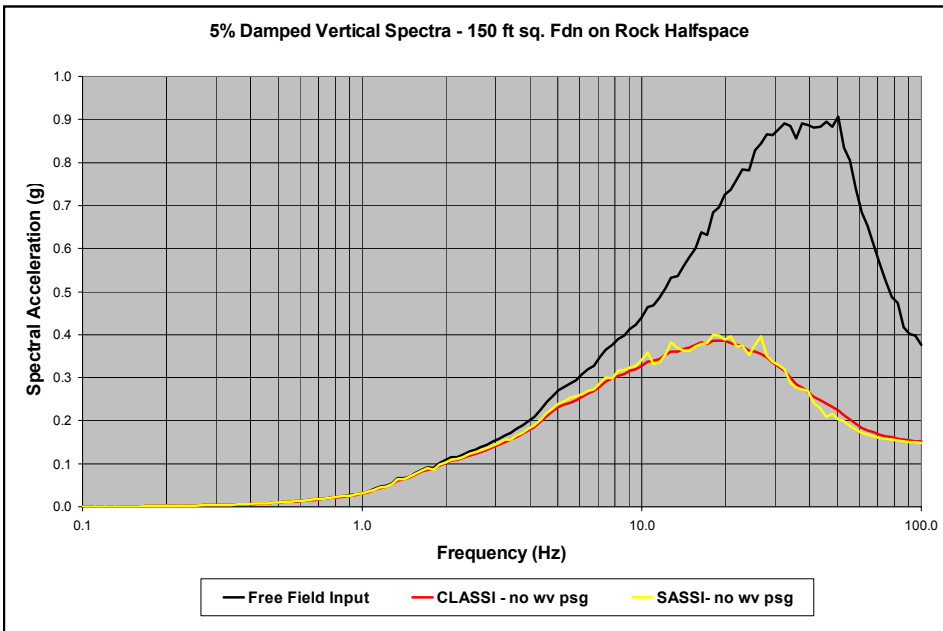


Figure C-3  
CLASSI-SASSI Comparison of Vertical Foundation Response Spectra

**Deleted:**  
*Effect of Embedment and Incoherence*

**Deleted:**  
*Effect of Embedment and Incoherence*

**Deleted:**  
*Effect of Embedment and Incoherence*

## SSI and Incoherency

The seismic analysis of structures including seismic wave incoherence and soil-structure interaction for an example nuclear power plant structure on a rigid, foundation has been validated by independent benchmark comparisons of results. For this purpose, the effect of incoherent ground motion has been evaluated by:

- Three different SSI computer programs; CLASSI, Bechtel SASSI, and ACS SASSI
- Two different algorithms; CLASSI-stochastic method and SASSI eigen decomposition method
- Two different analytical approaches; random vibration theory (RVT) by CLASSI and time history dynamic analyses by SASSI
- Two different organizations conducting the analyses; CLASSI by ARES, Bechtel SASSI by Bechtel, and ACS SASSI by ARES

Bechtel-SASSI results are from Ostadan, 2006. The problem considered for the benchmark comparison of the two approaches was to determine in-structure response spectra for the three stick AP1000-based model founded on the rock site profile and subjected to the associated high-frequency ground motion. The structural model, site profile, and input excitation were all described in Chapter 2. The foundation is the 150 x 150-ft square foundation footprint that is 15 foot thick as was used in the Chapter 5 analyses. It should be noted that for these benchmark comparisons the more simple model shown in Figure 2-8 was used. The model with outriggers and offset mass centers was not used for the analyses described in this appendix.

In-structure response spectra have been computed on the foundation and at the top of each of the three structure sticks. Recall from Chapter 2 that the model consists of three concentric sticks representing the Coupled Auxiliary and Shield Building (ASB), the Steel Containment Vessel (SCV), and the Containment Internal Structure (CIS). Three analyses have been performed for these benchmark comparisons.

- Fixed-base dynamic time history analyses
- Soil-structure interaction dynamic time history analyses with coherent ground motion
- Soil-structure interaction dynamic time history analyses with incoherent ground motion

Five percent damped in-structure response spectra determined by CLASSI, Bechtel SASSI, and ACS SASSI for fixed-base analyses are compared in Figures C-4 through C-15. 5% damped in-structure response spectra determined by CLASSI, Bechtel SASSI, and ACS SASSI for SSI coherent analyses are compared in Figures C-16 through C-27. 5% damped in-structure response spectra determined by CLASSI, Bechtel SASSI, and ACS SASSI for SSI incoherent analyses are compared in Figures C-28 through C-39. These spectra generally agree within 10 percent at all frequencies. There are a few locations where deviations are as large as 20 percent. For dynamic analyses including SSI by different programs and investigators, this level of agreement is considered excellent.

**Deleted:** .  
*Effect of Embedment and Incoherence*

**Deleted:** .  
*Effect of Embedment and Incoherence*

**Deleted:** .  
*Effect of Embedment and Incoherence*

The CLASSI and SASSI computer programs have been validated in accordance with the quality assurance program of each respective company. Software verification and validation have been performed by solving of example problems that exercise the features of the programs that are utilized in this study. Results are compared with results from alternative methods.

Excellent agreement is obtained for in-structure response spectra on the foundation and at the top of the structures. This benchmark comparison is further convincing validation of the technical approach being employed in Task S2.1.

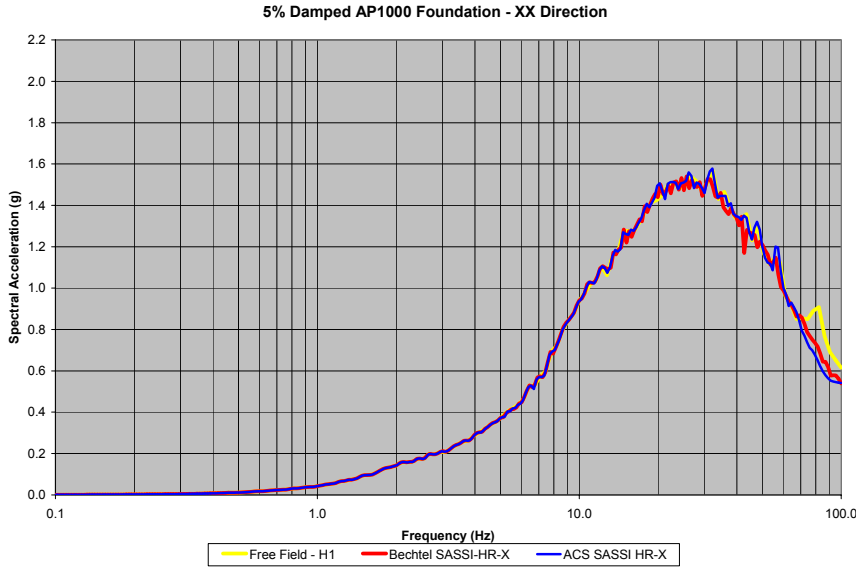


**Figure C-4**  
**Fixed-Base Analysis, Foundation Response Spectra – X Direction due to X Input –Free-Field Input, Bechtel SASSI, ACS SASSI (Node 1)**

**Deleted:**  
*Effect of Embedment and Incoherence*

**Deleted:**  
*Effect of Embedment and Incoherence*

**Deleted:**  
*Effect of Embedment and Incoherence*

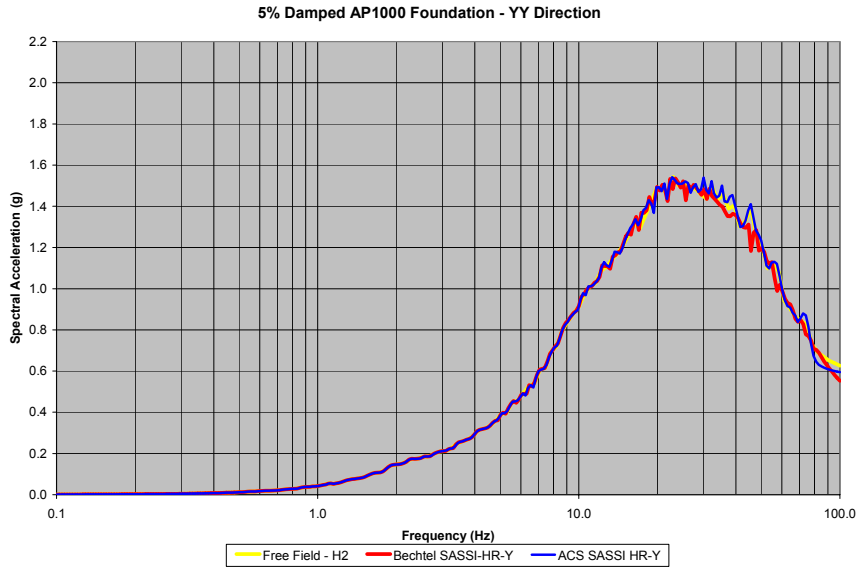


**Figure C-5**  
**Fixed-Base Analysis, Foundation Response Spectra – Y Direction due to Y Input –Free-Field Input, Bechtel SASSI, ACS SASSI (Node 1)**

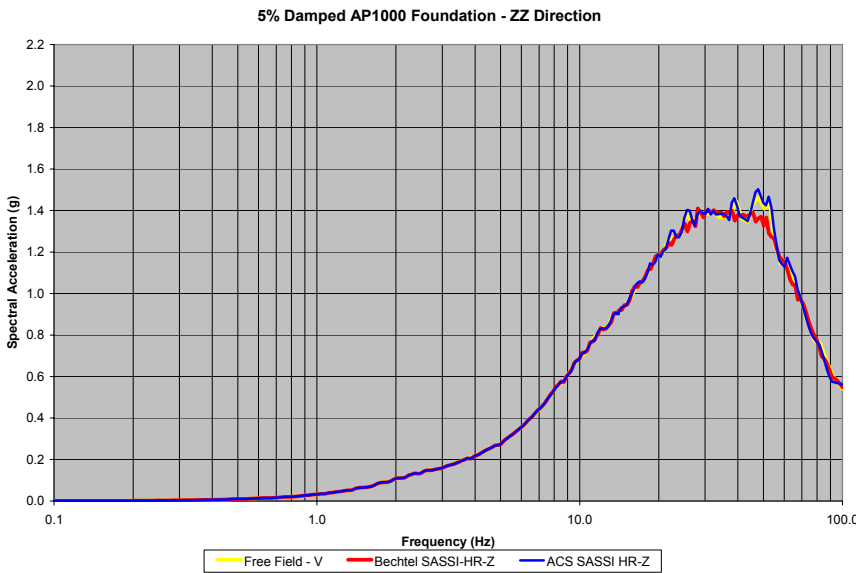


**Figure C-6**  
**Fixed-Base Analysis, Foundation Response Spectra – Z Direction due to Z Input –Free-Field Input, Bechtel SASSI, ACS SASSI (Node 1)**

Deleted: Effect of Embedment and Incoherence  
Deleted: Effect of Embedment and Incoherence  
Deleted: Effect of Embedment and Incoherence

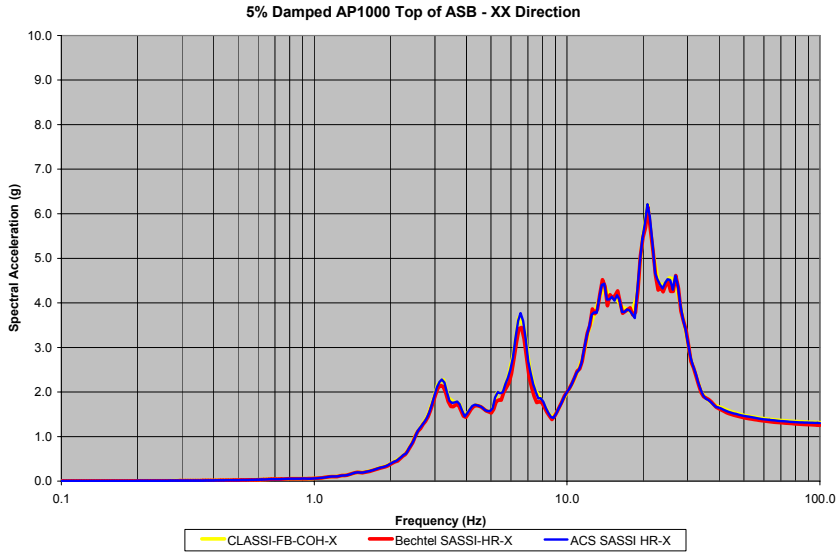


Figure C-7  
Fixed-Base Analysis, Top of Shield Building Response Spectra – X Direction due to X Input –Free-Field Input, Bechtel SASSI, ACS SASSI (Node 310)

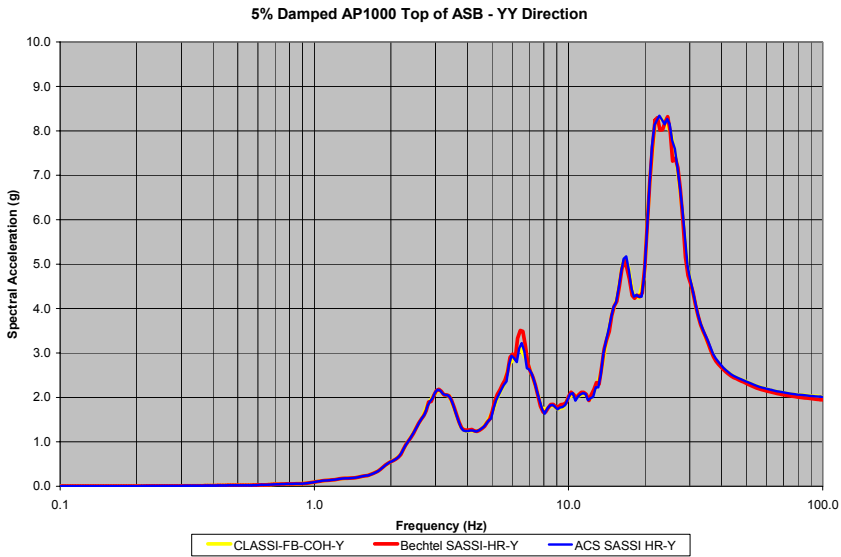
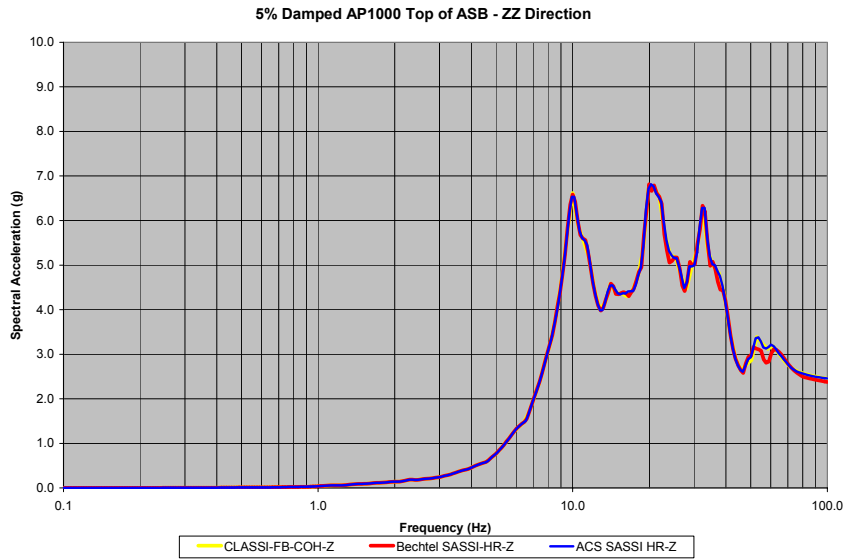


Figure C-8  
Fixed-Base Analysis, Top of Shield Building Response Spectra – Y Direction due to Y Input –Free-Field Input, Bechtel SASSI, ACS SASSI (Node 310)

**Deleted:**  
*Effect of Embedment and Incoherence*

**Deleted:**  
*Effect of Embedment and Incoherence*

**Deleted:**  
*Effect of Embedment and Incoherence*



**Figure C-9**  
Fixed-Base Analysis, Top of Shield Building Response Spectra – Z Direction due to Z Input –Free-Field Input, Bechtel SASSI, ACS SASSI (Node 310)

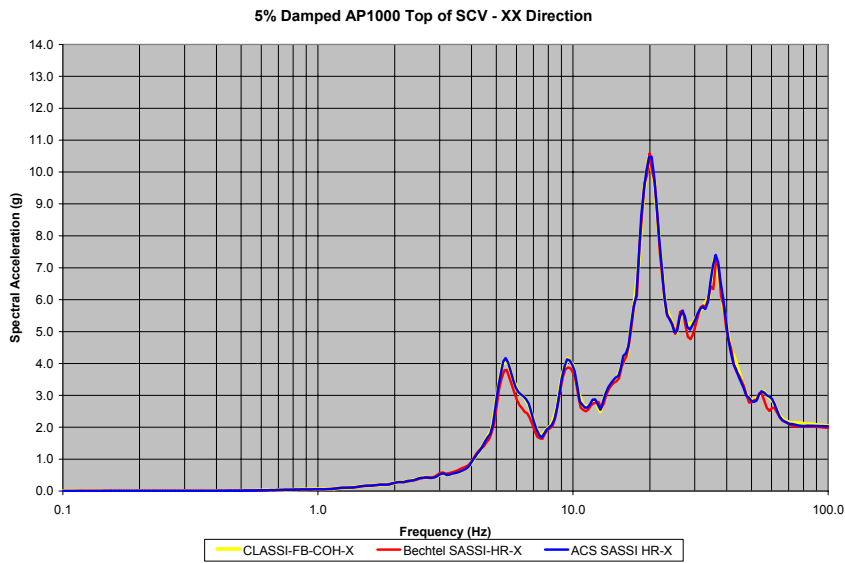


**Figure C-10**  
Fixed-Base Analysis, Top of SCV Response Spectra – X Direction due to X Input –Free-Field Input, Bechtel SASSI, ACS SASSI (Node 417)

Deleted: Effect of Embedment and Incoherence  
Deleted: Effect of Embedment and Incoherence  
Deleted: Effect of Embedment and Incoherence

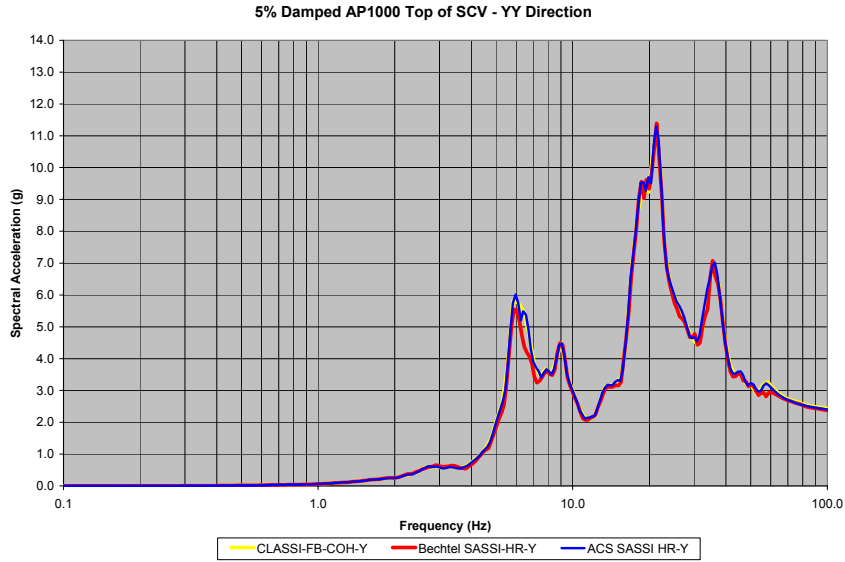


Figure C-11  
Fixed-Base Analysis, Top of SCV Response Spectra – Y Direction due to Y Input –Free-Field Input, Bechtel SASSI, ACS SASSI (Node 417)

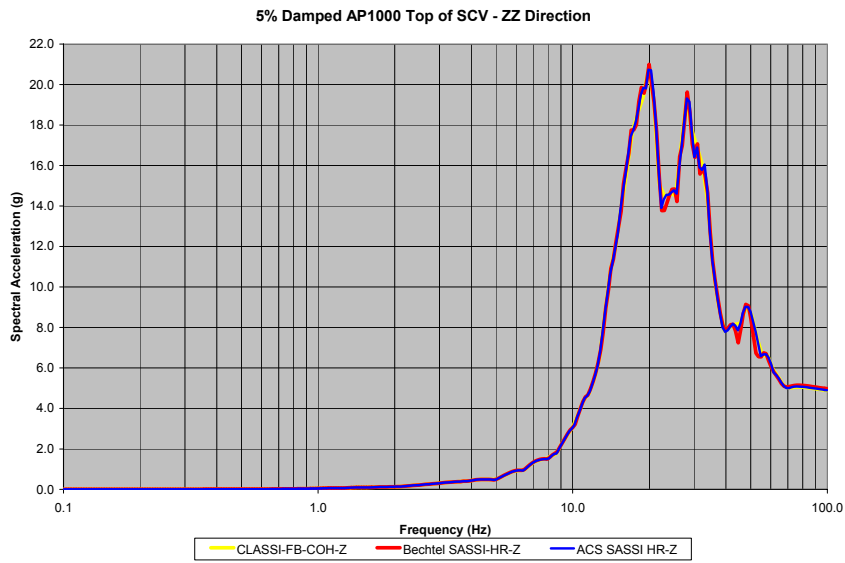
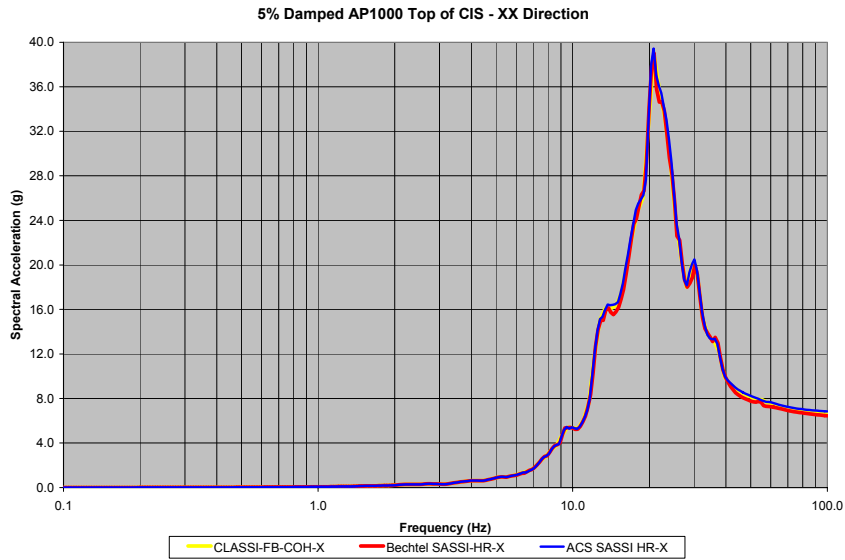


Figure C-12  
Fixed-Base Analysis, Top of SCV Response Spectra – Z Direction due to Z Input –Free-Field Input, Bechtel SASSI, ACS SASSI (Node 417)

**Deleted:**  
*Effect of Embedment and Incoherence*

**Deleted:**  
*Effect of Embedment and Incoherence*

**Deleted:**  
*Effect of Embedment and Incoherence*



**Figure C-13**  
Fixed-Base Analysis, Top of CIS Response Spectra – X Direction due to X Input –Free-Field Input, Bechtel SASSI, ACS SASSI (Node 538)

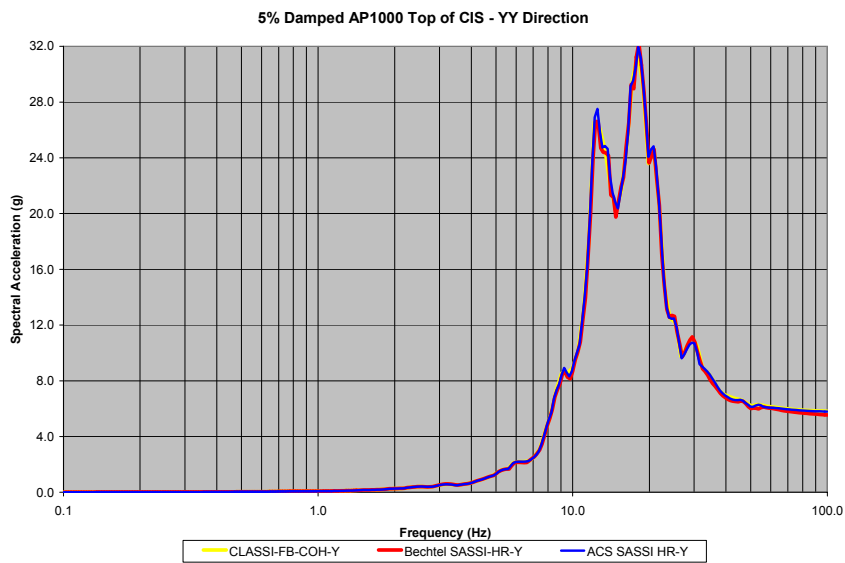


**Figure C-14**  
Fixed-Base Analysis, Top of CIS Response Spectra – Y Direction due to Y Input –Free-Field Input, Bechtel SASSI, ACS SASSI (Node 538)

Deleted: Effect of Embedment and Incoherence  
Deleted: Effect of Embedment and Incoherence  
Deleted: Effect of Embedment and Incoherence

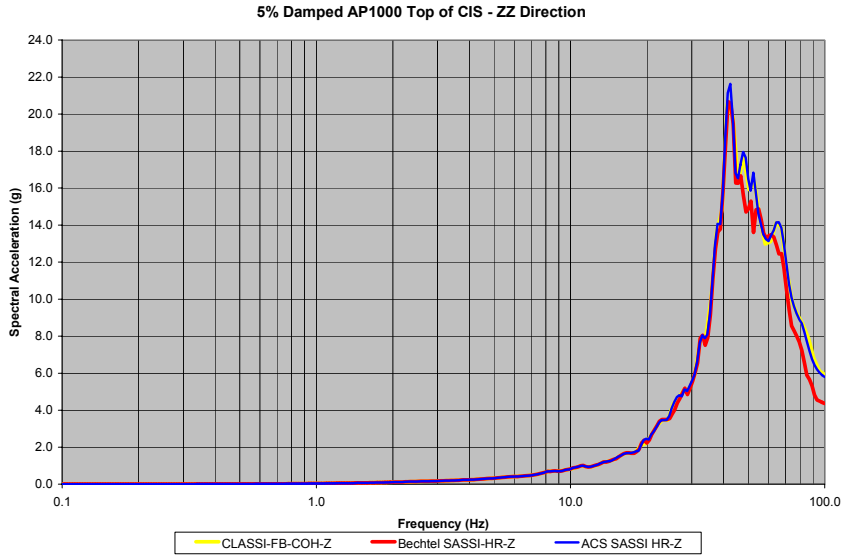


Figure C-15  
Fixed-Base Analysis, Top of CIS Response Spectra – Z Direction due to Z Input –Free-Field Input, Bechtel SASSI, ACS SASSI (Node 538)

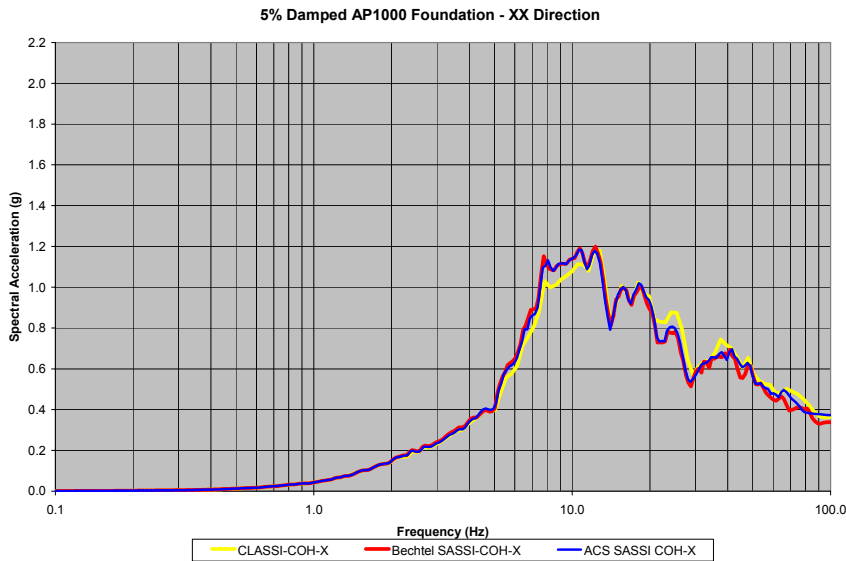
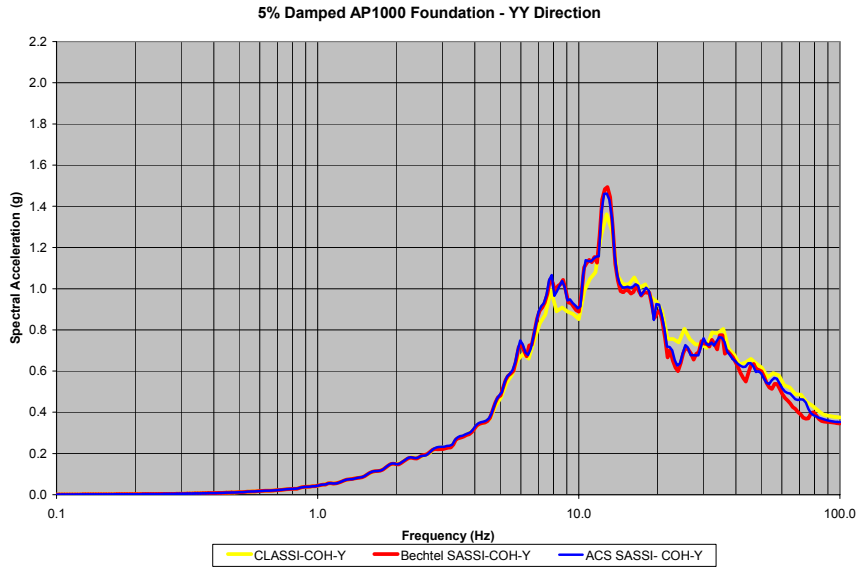


Figure C-16  
SSI Coherent Analysis, Foundation Response Spectra – X Direction due to X Input –Free-Field Input, Bechtel SASSI, ACS SASSI (Node 1)

**Deleted:**  
*Effect of Embedment and Incoherence*

**Deleted:**  
*Effect of Embedment and Incoherence*

**Deleted:**  
*Effect of Embedment and Incoherence*



**Figure C-17**  
SSI Coherent Analysis, Foundation Response Spectra – Y Direction due to Y Input –Free-Field Input, Bechtel SASSI, ACS SASSI (Node 1)

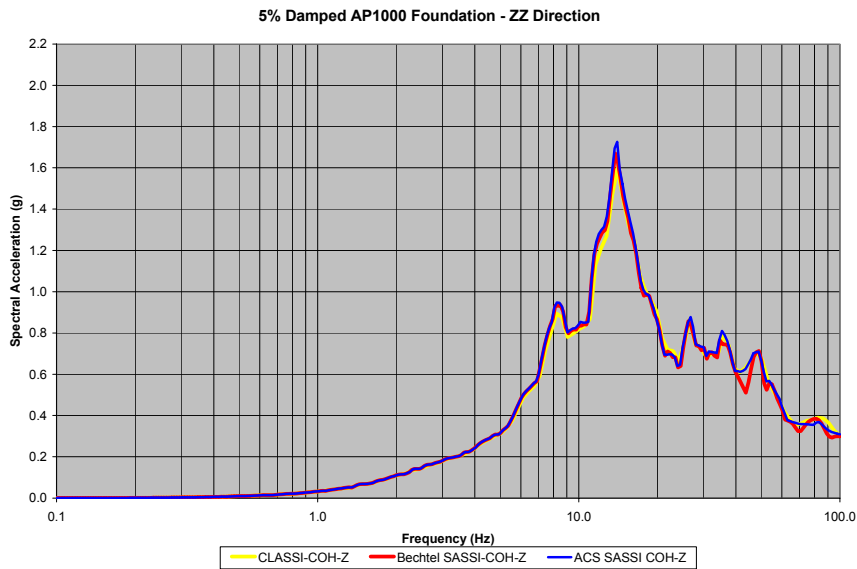


**Figure C-18**  
SSI Coherent Analysis, Foundation Response Spectra – Z Direction due to Z Input –Free-Field Input, Bechtel SASSI, ACS SASSI (Node 1)

**Deleted:** .  
*Effect of Embedment and Incoherence*

**Deleted:** .  
*Effect of Embedment and Incoherence*

**Deleted:** .  
*Effect of Embedment and Incoherence*

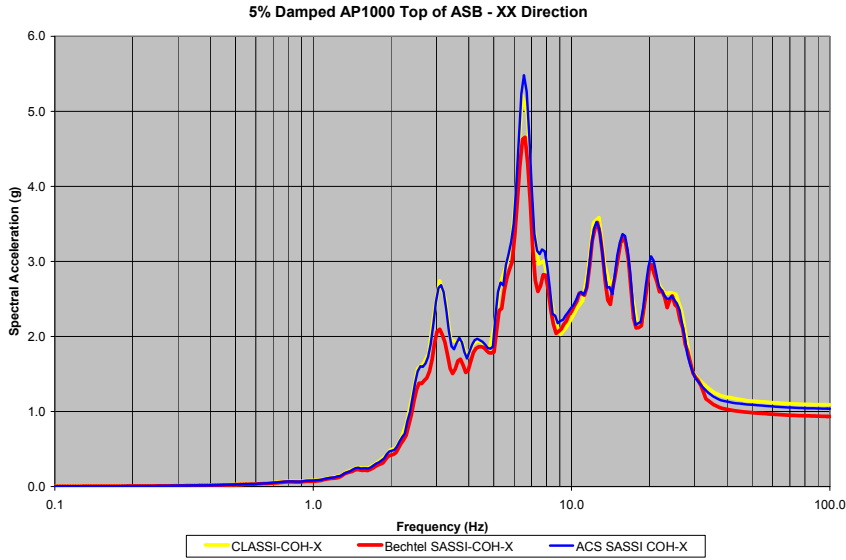


**Figure C-19**  
**SSI Coherent Analysis, Top of Shield Building Response Spectra – X Direction due to X Input –Free-Field Input, Bechtel SASSI, ACS SASSI (Node 310)**

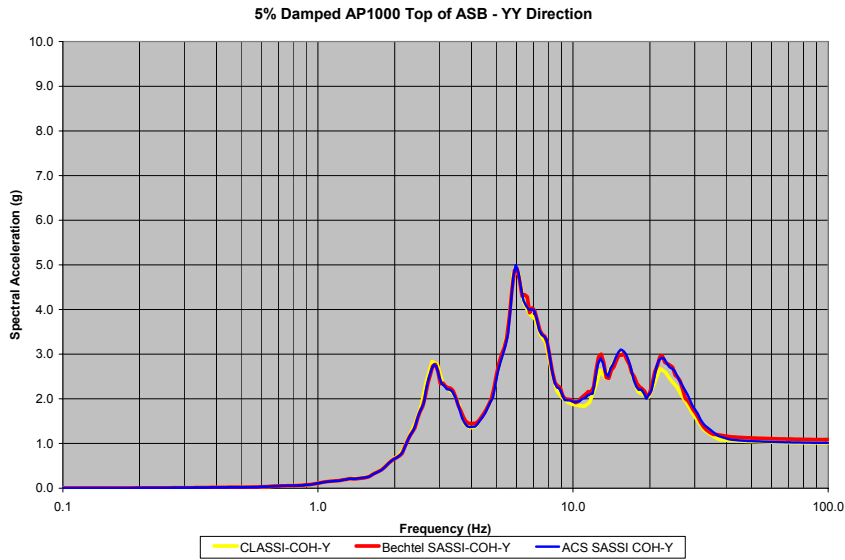


**Figure C-20**  
**SSI Coherent Analysis, Top of Shield Building Response Spectra – Y Direction due to Y Input –Free-Field Input, Bechtel SASSI, ACS SASSI (Node 310)**

**Deleted:**  
*Effect of Embedment and Incoherence*

**Deleted:**  
*Effect of Embedment and Incoherence*

**Deleted:**  
*Effect of Embedment and Incoherence*

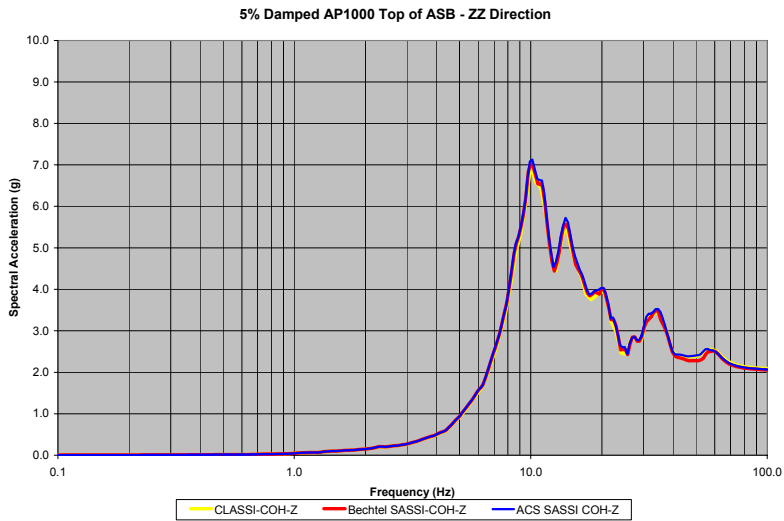


**Figure C-21**  
**SSI Coherent Analysis, Top of Shield Building Response Spectra – Z Direction due to Z Input –Free-Field Input, Bechtel SASSI, ACS SASSI (Node 310)**

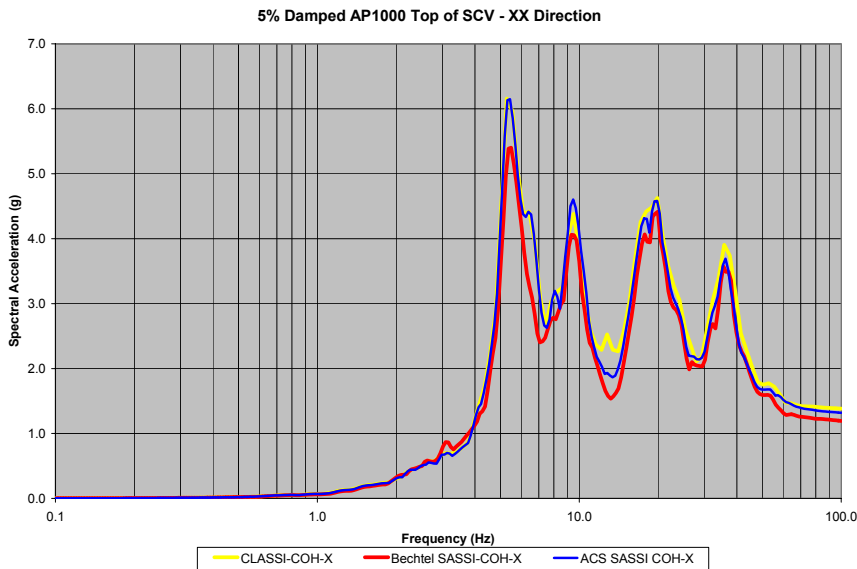


**Figure C-22**  
**SSI Coherent Analysis, Top of SCV Response Spectra – X Direction due to X Input –Free-Field Input, Bechtel SASSI, ACS SASSI (Node 417)**

**Deleted:** .  
*Effect of Embedment and Incoherence*

**Deleted:** .  
*Effect of Embedment and Incoherence*

**Deleted:** .  
*Effect of Embedment and Incoherence*

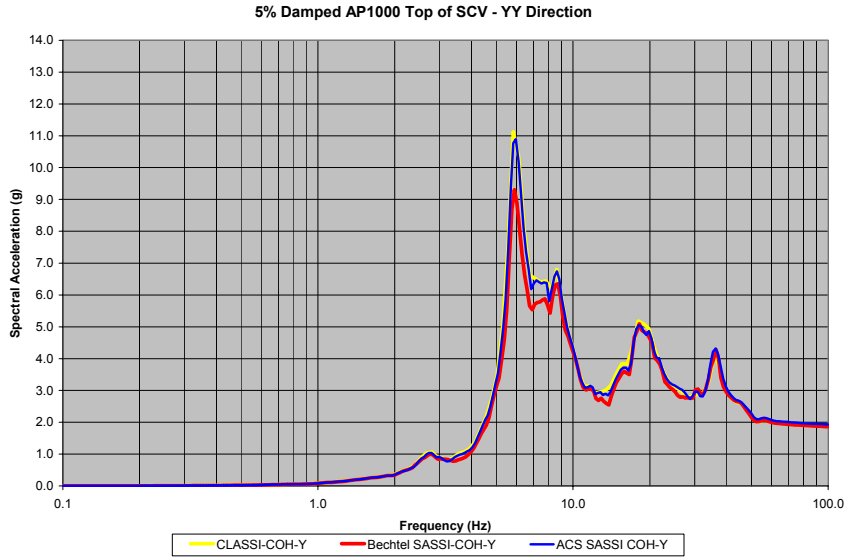


**Figure C-23**  
SSI Coherent Analysis, Top of SCV Response Spectra – Y Direction due to Y Input –Free-Field Input, Bechtel SASSI, ACS SASSI (Node 417)

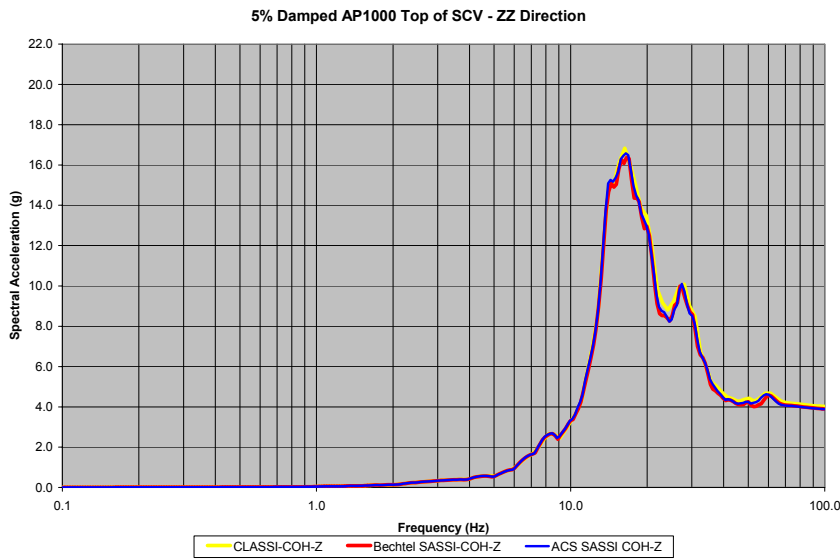


**Figure C-24**  
SSI Coherent Analysis, Top of SCV Response Spectra – Z Direction due to Z Input –Free-Field Input, Bechtel SASSI, ACS SASSI (Node 417)

**Deleted:**  
*Effect of Embedment and Incoherence*

**Deleted:**  
*Effect of Embedment and Incoherence*

**Deleted:**  
*Effect of Embedment and Incoherence*

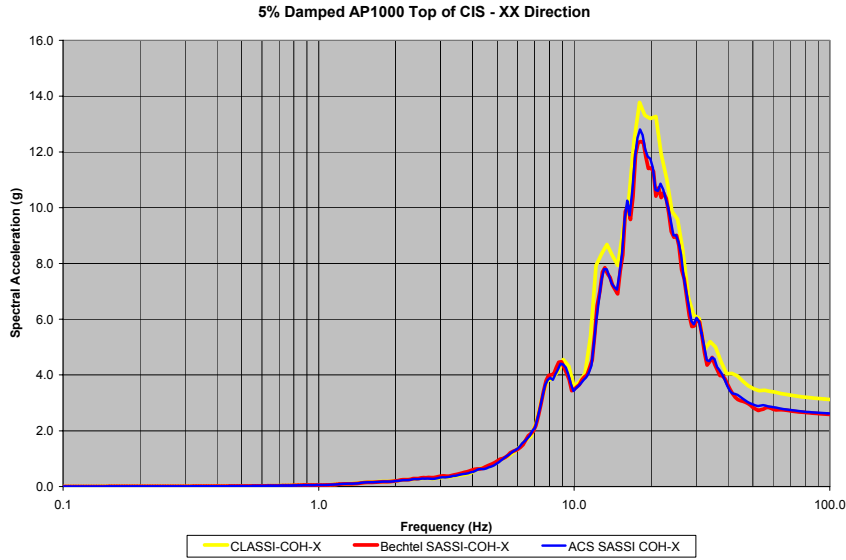


**Figure C-25**  
SSI Coherent Analysis, Top of CIS Response Spectra – X Direction due to X Input –Free-Field Input, Bechtel SASSI, ACS SASSI (Node 538)

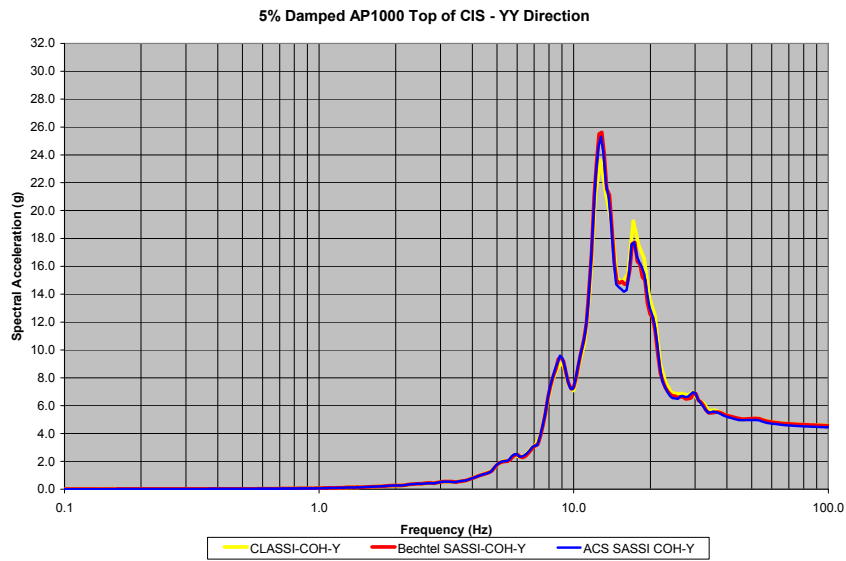


**Figure C-26**  
SSI Coherent Analysis, Top of CIS Response Spectra – Y Direction due to Y Input –Free-Field Input, Bechtel SASSI, ACS SASSI (Node 538)

**Deleted:** .  
*Effect of Embedment and Incoherence*

**Deleted:** .  
*Effect of Embedment and Incoherence*

**Deleted:** .  
*Effect of Embedment and Incoherence*

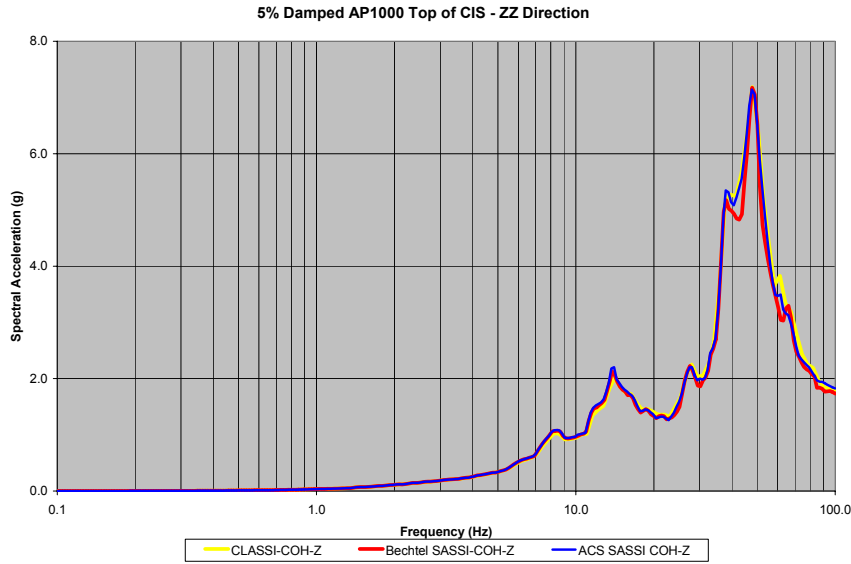


**Figure C-27**  
**SSI Coherent Analysis, Top of CIS Response Spectra – Z Direction due to Z Input –Free-Field Input, Bechtel SASSI, ACS SASSI (Node 538)**

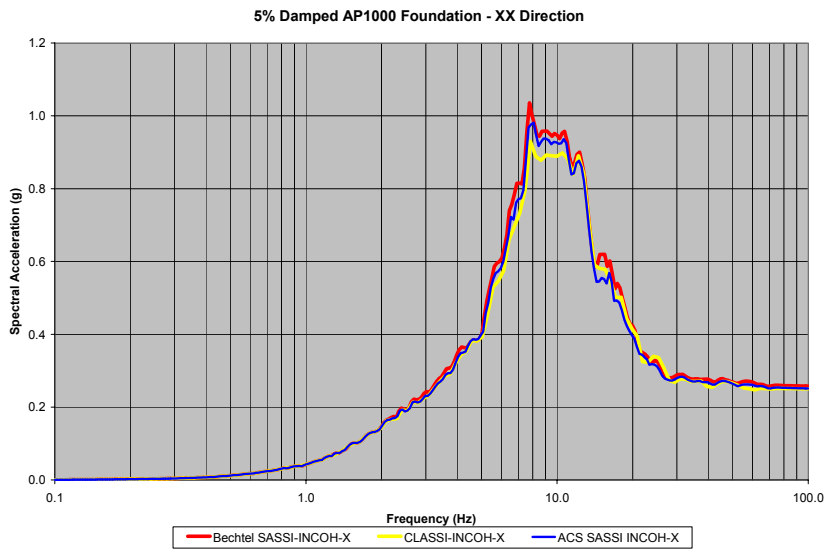


**Figure C-28**  
**SSI Incoherent Analysis, Foundation Response Spectra – X Direction due to X Input –Free-Field Input, Bechtel SASSI, ACS SASSI (Node 1)**

Deleted: Effect of Embedment and Incoherence

Deleted: Effect of Embedment and Incoherence

Deleted: Effect of Embedment and Incoherence

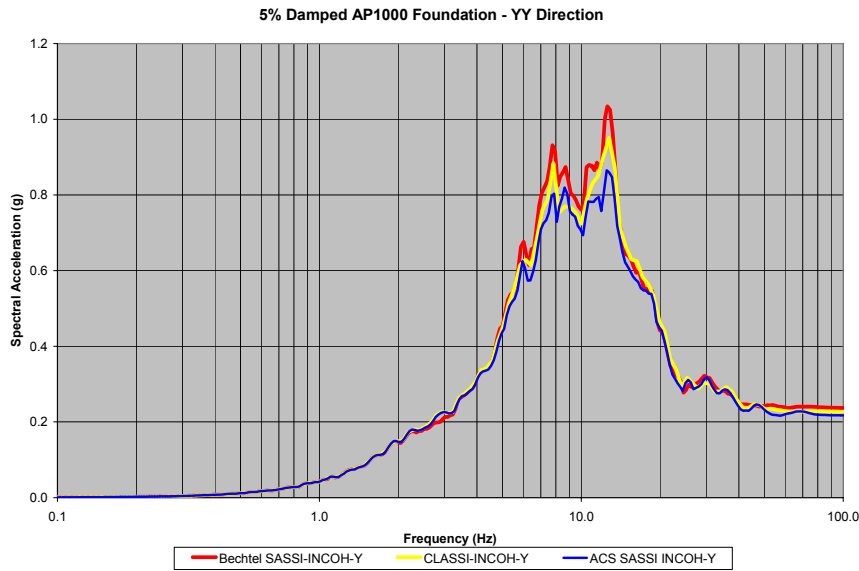


Figure C-29  
SSI Incoherent Analysis, Foundation Response Spectra – Y Direction due to Y Input –Free-Field Input, Bechtel SASSI, ACS SASSI (Node 1)

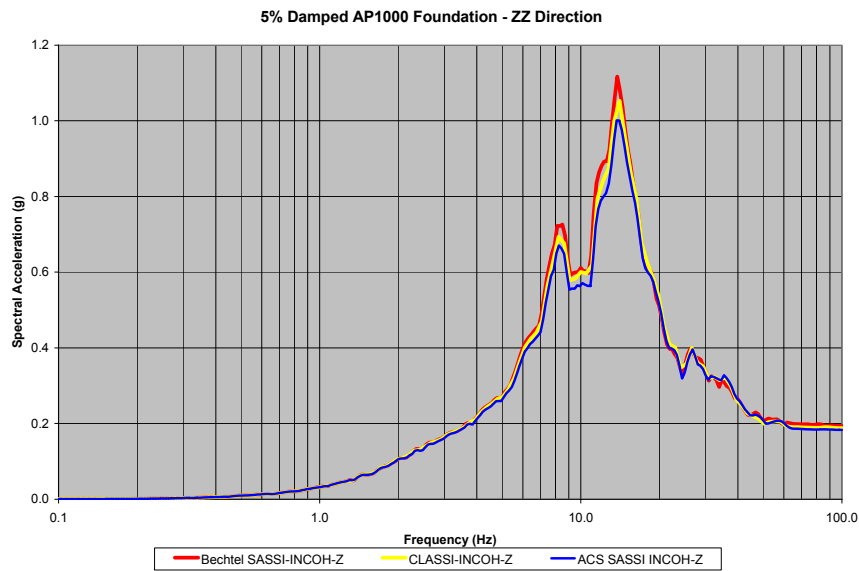


Figure C-30  
SSI Incoherent Analysis, Foundation Response Spectra – Z Direction due to Z Input –Free-Field Input, Bechtel SASSI, ACS SASSI (Node 1)

Deleted: Effect of Embedment and Incoherence  
Deleted: Effect of Embedment and Incoherence  
Deleted: Effect of Embedment and Incoherence

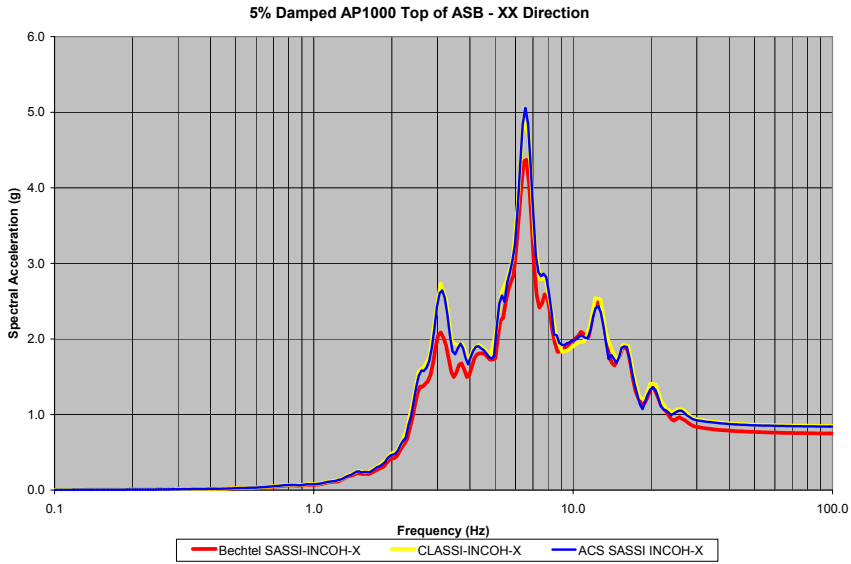


Figure C-31  
SSI Incoherent Analysis, Top of Shield Building Response Spectra – X Direction due to X Input –Free-Field Input, Bechtel SASSI, ACS SASSI (Node 310)

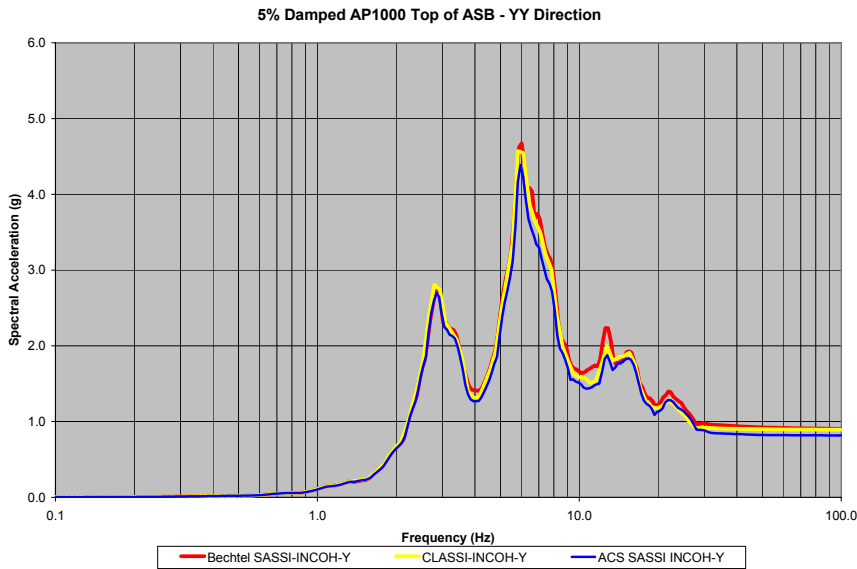
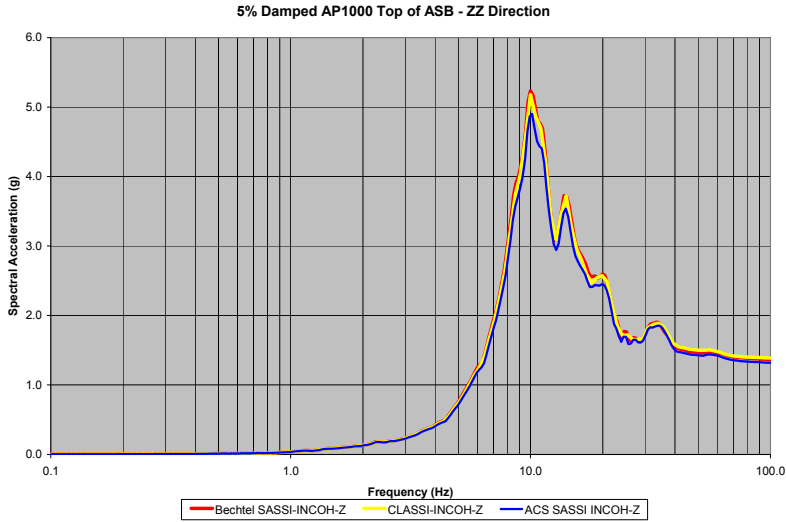


Figure C-32  
SSI Incoherent Analysis, Top of Shield Building Response Spectra – Y Direction due to Y Input –Free-Field Input, Bechtel SASSI, ACS SASSI (Node 310)

**Deleted:**  
*Effect of Embedment and Incoherence*

**Deleted:**  
*Effect of Embedment and Incoherence*

**Deleted:**  
*Effect of Embedment and Incoherence*



**Figure C-33**  
**SSI Incoherent Analysis, Top of Shield Building Response Spectra – Z Direction due to Z Input –Free-Field Input, Bechtel SASSI, ACS SASSI (Node 310)**

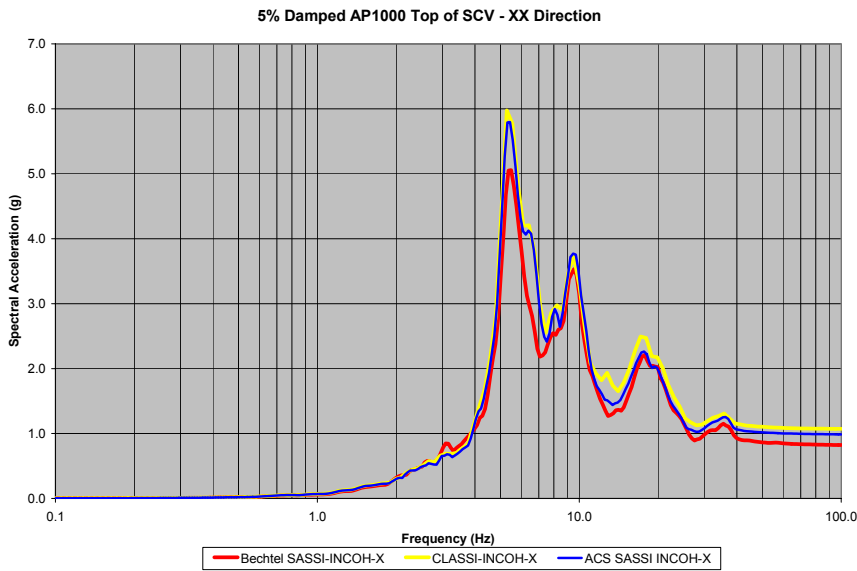


**Figure C-34**  
**SSI Incoherent Analysis, Top of SCV Response Spectra – X Direction due to X Input –Free-Field Input, Bechtel SASSI, ACS SASSI (Node 417)**

**Deleted:** .  
*Effect of Embedment and Incoherence*

**Deleted:** .  
*Effect of Embedment and Incoherence*

**Deleted:** .  
*Effect of Embedment and Incoherence*

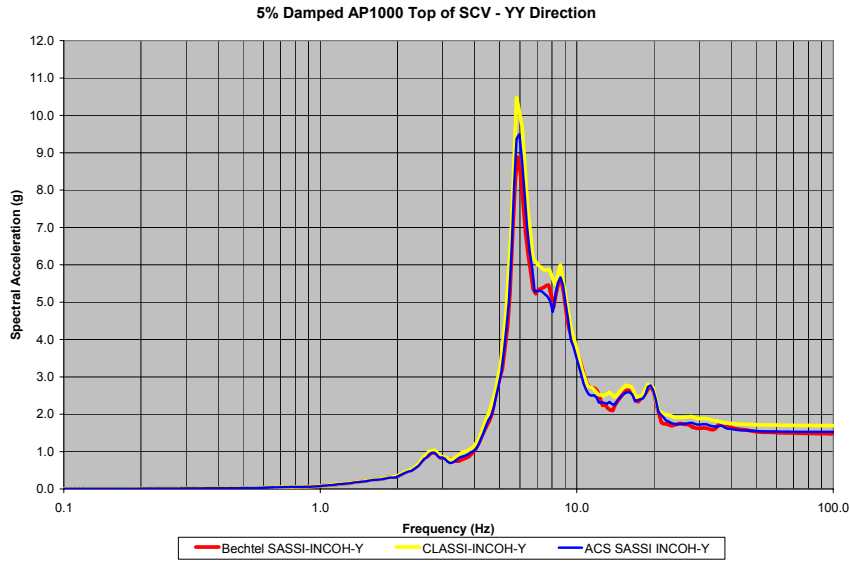


**Figure C-35**  
SSI Incoherent Analysis, Top of SCV Response Spectra – Y Direction due to Y Input –Free-Field Input, Bechtel SASSI, ACS SASSI (Node 417)

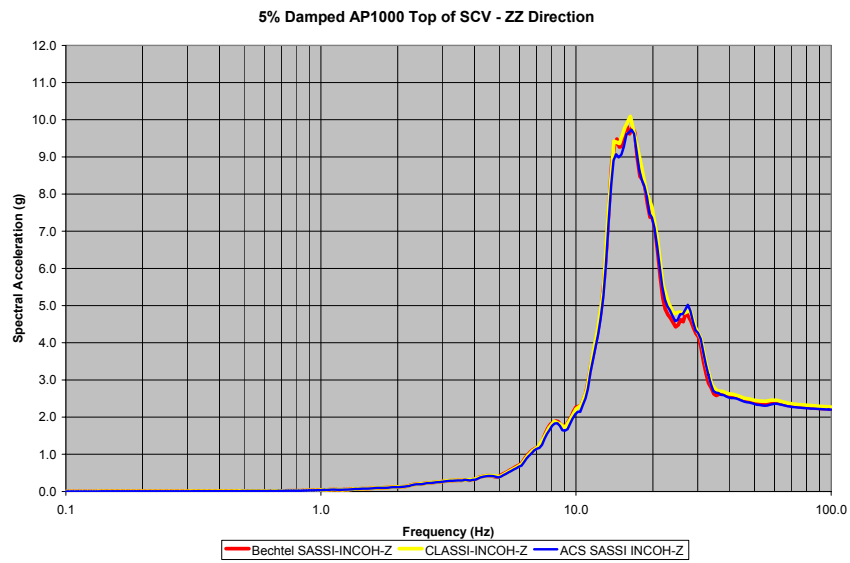


**Figure C-36**  
SSI Incoherent Analysis, Top of SCV Response Spectra – Z Direction due to Z Input –Free-Field Input, Bechtel SASSI, ACS SASSI (Node 417)

**Deleted:**  
*Effect of Embedment and Incoherence*

**Deleted:**  
*Effect of Embedment and Incoherence*

**Deleted:**  
*Effect of Embedment and Incoherence*

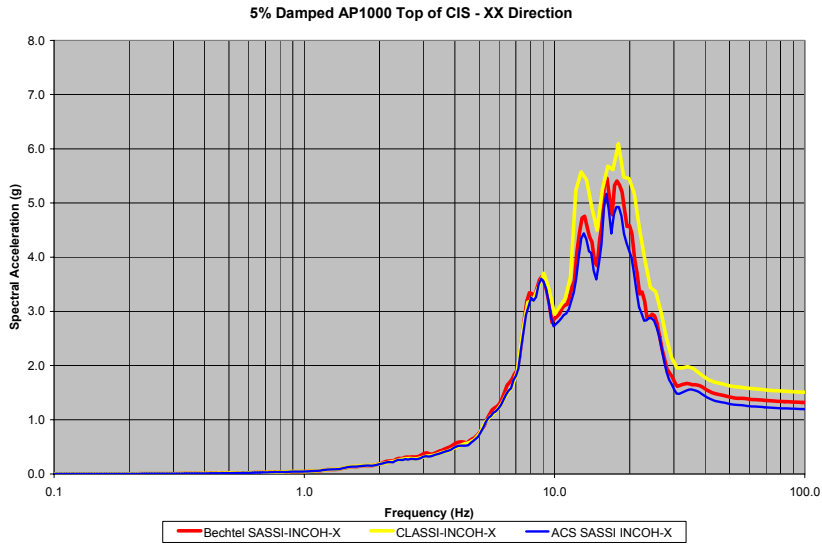


**Figure C-37**  
SSI Incoherent Analysis, Top of CIS Response Spectra – X Direction due to X Input –Free-Field Input, Bechtel SASSI, ACS SASSI (Node 538)

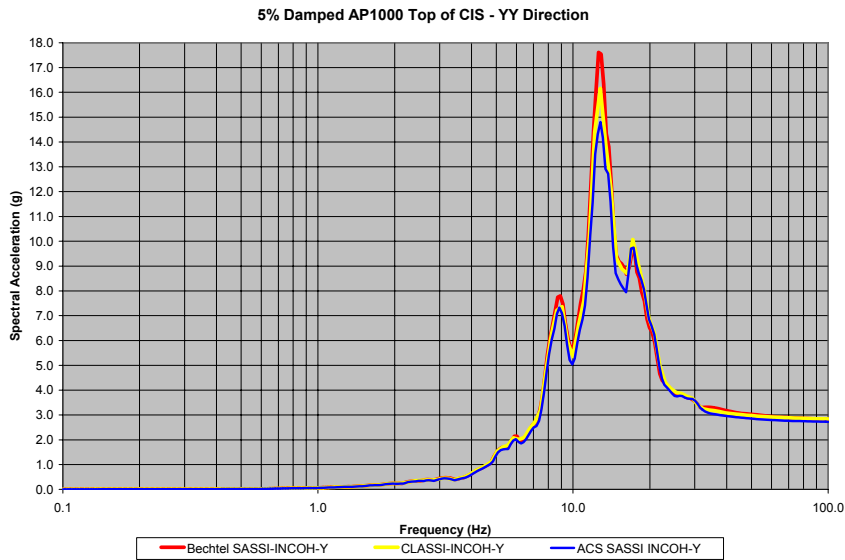


**Figure C-38**  
SSI Incoherent Analysis, Top of CIS Response Spectra – Y Direction due to Y Input –Free-Field Input, Bechtel SASSI, ACS SASSI (Node 538)

Deleted: Effect of Embedment and Incoherence  
Deleted: Effect of Embedment and Incoherence  
Deleted: Effect of Embedment and Incoherence

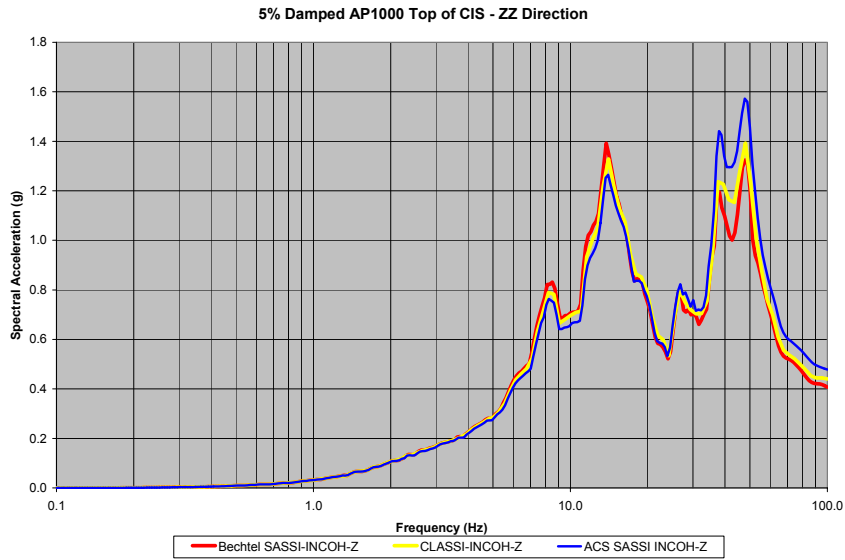


Figure C-39  
SSI Incoherent Analysis, Top of CIS Response Spectra – Z Direction due to Z Input –Free-Field Input, Bechtel SASSI, ACS SASSI (Node 538)

# D

## UNCERTAINTY EFFECTS ON INCOHERENCY FUNCTIONS

---

### Background

Chapter 2 presented the median coherency functions for horizontal and vertical ground motion as functions of frequency and distance between observation points, i.e., points on the foundation (Abrahamson, 2005a, 2006a). Equations 2-1, 2-2, and 2-3 and Table 2-1 specified the form and parameters of these functions. For this sensitivity study, Dr. Abrahamson provided an estimate of the variability in the coherency functions. The expression for the median coherency function (Equation 2-1) is reproduced here as Equation D-1. The corresponding variability in the coherency functions is defined in Equations D-2 and D-3.

The equation for median plane wave coherency is:

$$\gamma_{pw}(f, \xi) = \left[ 1 + \left( \frac{f \tanh(a_3 \xi)}{a_1 f_c} \right)^{n_1} \right]^{-1/2} \left[ 1 + \left( \frac{f \tanh(a_3 \xi)}{a_2 f_c} \right)^{n_2} \right]^{-1/2} \quad \text{(Equation D-1)}$$

where:  $f$  is frequency and  $\xi$  is separation distance between foundation locations and the constants  $a_1, a_2, a_3, n_1, n_2$ , and  $f_c$  are tabulated in Table 2-1.

Equations D-2 and D-3 (Abrahamson, 2005b) gives an expression for the 84<sup>th</sup> percentile plane wave coherency as the median value plus the sigma, where sigma is 0.4 for frequencies equal or greater than 20 Hz and smoothly varies to zero at zero frequency and at zero distance. Sigma is in Arctanh units.

$$\gamma_{pw,84}(f, \xi) = \tanh \left[ \tanh^{-1}(\gamma_{pw}(f, \xi)) + \sigma(f, \xi) \right] \quad \text{(Equation D-2)}$$

$$\sigma_H(f, \xi) = \begin{cases} 0.4 & \text{for } f > 20\text{Hz} \\ 0.4 + (f - 20)(-0.0065 - 1.9 \times 10^{-6} \xi^2) & \text{for } f \leq 20\text{Hz} \end{cases} \quad \text{(Equation D-3)}$$

Deleted: Effect of Embedment and Incoherence  
Deleted: Effect of Embedment and Incoherence  
Deleted: Effect of Embedment and Incoherence

## Objective of Sensitivity Study on Coherency Uncertainty

Perform a sensitivity study to establish a reasonable estimate of the effects of coherency uncertainty on the incoherency transfer functions. The focus is on the 84% non-exceedance probability (NEP) response of the rigid massless foundation (150-ft. square shape).

## Assumptions

The following assumptions were made to perform the analyses:

1. Coherency functions and incoherency transfer functions are assumed to be independent of frequency. Analyze each frequency of interest independently. These are common assumptions for SSI analysis in the frequency domain.
2. Point-to-point coherency functions are assumed to be independent. That is, no correlation of coherency functions for points equi-distant or for points within defined radii.

## Approach

The approach was to perform Monte Carlo simulations randomly varying the coherency functions and calculating the resulting incoherency transfer functions.

The steps in the analysis procedure were:

1. Define the normal distribution function for horizontal coherency over a sample of frequencies in the frequency range of interest (0 – 50 Hz) and over the point-to-point distances of the foundation discretization (approximately 5 ft. – 210 ft). The initial sample of frequencies was selected to be 10 Hz, 15 Hz, 20 Hz, and 25 Hz. The distances of interest are based on the discretization of the 150-ft square foundation mat – the center points of the 393 sub-regions of the foundation. The key elements of the coherency functions are given in Equations D-1, D-2, and D-3. For any cumulative probability,  $p$ , the coherency may be expressed as:

$$\gamma_{pw,p}(f, \xi) = \tanh\left[\tanh^{-1}(\gamma_{pw}(f, \xi)) + t_p * \sigma(f, \xi)\right] \quad \text{(Equation D-4)}$$

where  $t_p$  is the normal variate associated with cumulative probability,  $p$  (e.g.,  $t_p = 0$  for  $p = 0.50$ ,  $t_p = 1.0$  for  $p = 0.84$ , etc.). The resulting coherency,  $\gamma_{pw,p}$  was limited to be in the range of -1.0 to +1.0.

2. At each frequency of interest, generate a set of incoherency transfer function values by Monte Carlo simulation (1000 samples). The end result being the distribution of incoherency transfer function values conditional on each frequency of interest.
3. From the computed incoherency transfer function values at each frequency, evaluate the median and 84% NEP.

**Deleted:**  
Effect of Embedment and Incoherence

**Deleted:**  
Effect of Embedment and Incoherence

**Deleted:**  
Effect of Embedment and Incoherence

## Results

The sensitivity study was completed as described. All of the calculated incoherency transfer function values (1000 samples), at a given frequency, were very close to the median, i.e., the values shown in Figures 4-5 and 4-6 for the 150-ft square foundation on the rock site profile.

This led to a re-evaluation of the assumptions made. The assumption of randomly varying independent coherency function values between all points on the foundation leads to this end result. For example, given the foundation discretization of 393 sub-regions. This leads to 368 samples where the distance between center points of the sub-regions is 10.16m. Randomly sampling the coherency functions (Equation D-4) 368 times for this constant distance  $\xi$  effectively spans the distribution from minimum to maximum values, i.e., 184 of the samples are less than the median and 184 values are greater than the median as they should be. However, this leads to a median estimate of this contribution to the incoherency transfer functions and, consequently, in essence, median estimates of the resultant incoherency transfer functions.

Consultation with Dr. Abrahamson concerning these results led to concurrence that it should have been expected. Dr. Abrahamson performed a further evaluation of the recorded data to investigate whether there is correlation between coherency functions at pairs of observation points. Dr. Abrahamson's conclusion (Abrahamson, 2006b) is that the correlation is low, correlation coefficients less than 0.14 for frequencies 10 Hz and greater. The collective judgment of the Team is that incorporating this correlation into the uncertainty analysis will lead to only small variability in the incoherency transfer functions. There is no need to repeat the evaluation for these revised assumptions.

## References

Abrahamson, N. (2006a). *Spatial Coherency for Soil-Structure Interaction*, Electric Power Research Institute, Final Report 1014101, Palo Alto, CA. August (Draft).

Abrahamson, N. (2006b). Personal Communication, July 7.

Abrahamson, N. (2005a). *Spatial Coherency for Soil-Structure Interaction*, Electric Power Research Institute, Technical Update Report 1012968, Palo Alto, CA. December.

Abrahamson, N. (2005b). *Draft 84<sup>th</sup> Percentile Coherency Model*, Memo to G. Hardy, August 10.



# **E**

## **EFFECT OF EMBEDMENT AND INCOHERENCE**

---

All analyses conducted for this project as described in the main body of this report have considered surface foundations. However, many nuclear power plant structures have embedded foundations and partially embedded structures. A sensitivity study considering the effect of ground motion incoherence and embedded foundations is discussed in this Appendix. There are two objectives to this study:

1. Demonstrate the effects of combined incoherency and embedment on seismic response
2. Assess whether it is possible to consider incoherency and embedment effects separately in which incoherency is treated by modified free-field motion per the simplified approach and embedment is treated by conventional SSI analysis.

Embedment effects on SSI response of nuclear power plant structure are due to kinematic response and inertial response. Kinematic response effects are due to spatial variation of ground motion and the integrating effects of the embedded foundation and partially embedded walls. Two aspects of spatial variation of ground motion are to be considered: the variation of free-field ground motion with depth in the soil or rock over the embedded portion of the foundation/partially embedded structure; and the incoherency effects. The first has a significant effect on the foundation input motion generally reducing the translational motion of the foundation and increasing the rotational motion. This effect exists independent of incoherency. The second effect is that of incoherency, the subject of this project.

In order to evaluate the combined effects of spatially varying ground motion with depth and incoherency, the functional form of the coherency functions at depth in the rock/soil is required. Dr. Abrahamson notes that the coherency function presented in Chapter 2 is applicable at depth as well as on the surface of the soil or rock and is equally applicable to surface motion and motion at depths typical of embedded foundations/partially embedded structures. The question of validity of Abrahamson coherence functions at depth is addressed in detail within the EPRI Report 1014101.

A sensitivity study is conducted to investigate the combined effects of spatially varying ground motion with depth in the rock/soil due to foundation/structure embedment and incoherency of ground motion. Using the SSI analysis program ACS-SASSI, the two effects can be treated simultaneously. The sensitivity study utilizes a structure model representing a reactor building with an internal structure. Soil-structure interaction analyses are performed considering the reactor building to be surface founded and partially embedded. Incoherent-to-coherent spectral acceleration ratios are compared for

**DRAFT**

*Effect of Embedment and Incoherence*

the surface founded and embedded reactor building. In addition, incoherency transfer functions are computed by the approach described in Chapter 4, and for the surface founded and embedded reactor building.

The results of these efforts are documented in the following sections of this Appendix. The model of the structure and soil used is described in Section E.1. The soil-structure interaction analyses of the surface founded and embedded structures is described in Section E.2. The overall conclusions from these studies are contained in Section E.3. References are presented in Section E.4.

**Deleted:**  
*Effect of Embedment and Incoherence*

**Deleted:**  
*Effect of Embedment and Incoherence*

**Deleted:**  
*Effect of Embedment and Incoherence*

## E.1 Sensitivity Study Model

The Reactor Building model for the sensitivity studies consists of the cylindrical reinforced concrete containment shell with a hemispherical dome. A reinforced concrete internal structure is located inside the Reactor Building shell. The Reactor Building shell and internal structure are both supported by a common circular rigid concrete basemat. Significant dimensions of the reactor building model are listed below:

- Reactor Building shell radius = 84.63 feet
- Height of springline above basemat = 151.3 feet
- Wall thickness = 3.5 feet
- Basemat radius = 84.63 feet
- Basemat thickness = 10 feet

Note that the basemat radius of 84.63 feet is the same size as was used for analyses described in Chapter 4. This circular foundation has the same area as the 150 foot square foundation used in many analyses. As a result, the incoherency transfer function presented and discussed in Chapter 4 is appropriate for this model and can serve as a benchmark against which the results from this Appendix can be measured.

Material properties for the Reactor Building shell and basemat concrete are:

- Elastic modulus 519120 ksf
- Shear modulus 221850 ksf
- Weight density 0.150 kcf

The outer shell wall and dome as well as the basemat were modeled with three and four node shell elements. The material properties for the Reactor Building shell concrete were selected to produce a fundamental horizontal frequency of approximately 4 Hz, which was judged to be representative of existing cylindrical containment structures.

**Deleted:** .  
*Effect of Embedment and Incoherence*

**Deleted:** .  
*Effect of Embedment and Incoherence*

**Deleted:** .  
*Effect of Embedment and Incoherence*

The concrete internal structure was represented by an equivalent vertical stick model located at the center of the basemat. Properties of the internal structure model are summarized below. Note that elevation 0.0 ft represents the top of the basemat.

**Table E.1-1**  
**Reactor Building Internal Structure Nodes and Masses**

Node No.	Elevation (ft)	Nodal Mass (k-sec <sup>2</sup> /ft)
814	0	0
815	8	86.96
816	13	77.95
817	22	195.34
818	33.5	116.77
819	49	265.22
820	61	37.89
821	93	25.47

The internal structure beam element connectivities and element stiffnesses are summarized below.

**Table E.1-2**  
**Reactor Building Internal Structure Beam Elements**

Elem No.	I node	J node	A (ft <sup>2</sup> )	Av (ft <sup>2</sup> )	I (ft <sup>4</sup> )
2	814	815	2000	1320	1.1 x 10 <sup>6</sup>
3	815	816	2560	1560	1.2 x 10 <sup>6</sup>
4	816	817	2210	1460	1.2 x 10 <sup>6</sup>
5	817	818	1960	730	1.3 x 10 <sup>6</sup>
6	818	819	1740	600	0.9 x 10 <sup>6</sup>
7	819	820	780	360	0.2 x 10 <sup>6</sup>
8	820	821	190	70	4000

Material properties for the internal structure concrete are:

- Elastic modulus 690000 ksf
- Shear Modulus 270000 ksf
- Weight density 0 ksf

Figures E.1-1 and E.1-2 show the configuration of the containment shell model and the internal structure.

**Deleted:** .  
*Effect of Embedment and Incoherence*

**Deleted:** .  
*Effect of Embedment and Incoherence*

**Deleted:** .  
*Effect of Embedment and Incoherence*

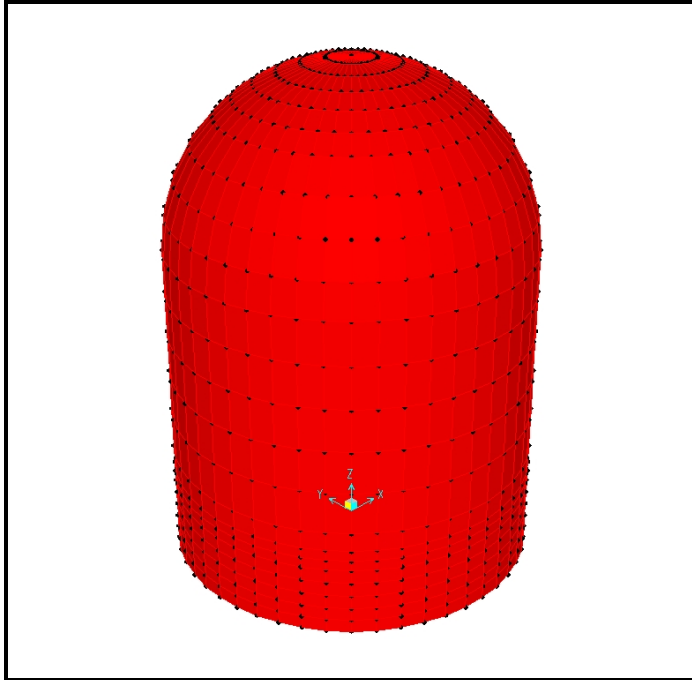


**Figure E.1-1**  
**Reactor Building Shell Finite Element Model**

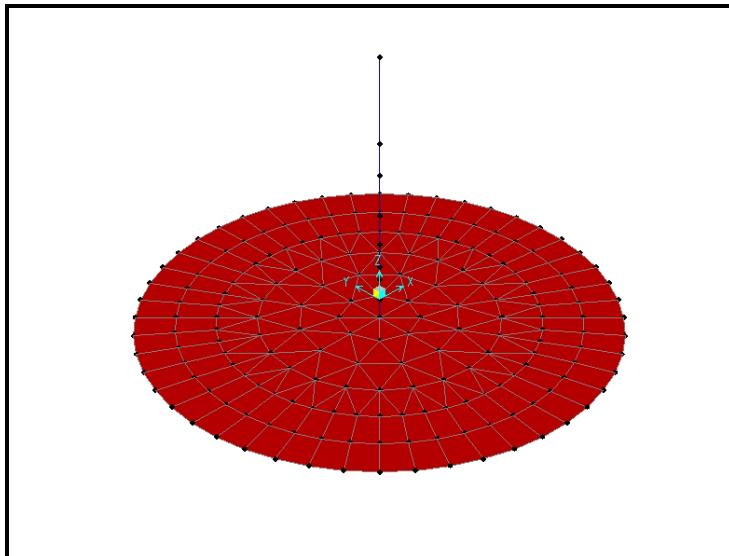


**Figure E.1-2**  
**Basemat and Internal Structure Finite Element Model**

**Deleted:** .  
*Effect of Embedment and Incoherence*

**Deleted:** .  
*Effect of Embedment and Incoherence*

**Deleted:** .  
*Effect of Embedment and Incoherence*

Fixed-base modal analysis was performed using SAP2000 to determine the natural frequencies of the reactor building containment shell and internal structure. Significant frequencies of the structure are shown below.

- Reactor Building shell horizontal frequencies: 3.91 Hz, 11.30 Hz
- Reactor Building shell vertical frequencies: 10.49 Hz, 17.42 Hz
- Internal Structure horizontal frequencies: 11.96 Hz, 17.49 Hz, 46.52 Hz
- Internal Structure vertical frequency: 39.35 Hz

The fixed-base modal frequencies were used as a guide to identify significant frequencies to be evaluated in the soil-structure interaction analyses.

## **E.2 Soil-Structure Interaction Analyses**

Soil-structure interaction analyses were performed using ACS SASSI. This program has the capability to analyze both surface founded and embedded structures considering ground motion incoherency. In the sensitivity studies, two conditions were considered for the Reactor Building model: (1) surface founded and (2) partially embedded. In the embedded case, the Reactor Building was embedded 42.3 feet such that the embedment-to-radius ( $e/R$ ) ratio was 0.5.

The rock site profile identified in Table 2-2 was used to define the site conditions. For the sensitivity study, the seismic response analyses considered horizontal input in one direction only. The input ground motion used was based on the rock site ground response spectrum as shown in Figure 2-5. The spectrum compatible horizontal acceleration time history as described in Chapter 2 was applied as the control motion at the ground surface.

Four cases were evaluated:

- Surface founded, coherent ground motion
- Surface founded, incoherent ground motion
- Embedded, coherent ground motion
- Embedded, incoherent ground motion

The surface founded structure was analyzed considering coherent and incoherent ground motion to establish a baseline to demonstrate the effects of ground motion incoherency on the seismic response of the Reactor Building. In-structure response spectra (ISRS) were calculated at selected locations in the structure. The results were summarized in terms of incoherent-to-coherent spectral acceleration ratios as a function of frequency. In addition, an incoherency transfer function was computed as the ratio of the incoherent to coherent transfer functions (ITFs) as computed in ACS SASSI. The embedded case was similarly analyzed considering coherent and incoherent ground motion. Comparison of

the embedded structure results with the surface founded results then can be used to assess the effect of embedment combined with incoherency of the ground motion.

Note that in Chapter 4, ITFs are derived from the square root of the diagonal terms of the cross power spectral density matrix given input motion defined by unity power spectral density following random vibration theory. In this Appendix, ITFs are evaluated from the ratio of SASSI generated transfer functions for incoherent motion to that for coherent motion. The SASSI generated transfer functions relate response at structure/foundation locations to the free-field ground motion in the frequency domain. ITFs computed in the latter matter isolate the effects of incoherency from the effects of inertial interaction and vertical spatial variation of motion due to embedment. As a result, it is concluded that the Chapter 4 random vibration theory ITFs are equivalent to the incoherent to coherent transfer function ratios computed in the Appendix.

The in-structure response spectra were evaluated at the following locations:

- Center of the foundation mat, node 1
- Top of the Reactor Building dome, node 831
- Quarter point (0.24H) of the Internal Structure, node 817
- Mid-height (0.53H) of the Internal Structure, node 819
- Top of the Internal Structure, node 821

Figures E.2-1 through E.2-10 show comparisons of the in-structure response spectra (ISRS) at the above locations for the surface founded and embedded cases.

Review of Figures E.2-1 through E.2-10 indicates similar trends as observed previously for the AP1000 SSI analyses. The ISRS show significant reductions at frequencies greater than 10 Hz, when ground motion incoherency is considered for both the surface founded and embedded structure configurations.

Reductions of ISRS due to incoherency are:

- Foundation peak near 30 Hz
  - Factor of about 4 reduction for surface case
  - Factor of 3 to 5 reduction for embedded case
- Top of reactor building dome peak near 12 Hz
  - Factor of about 1.3 reduction for surface case
  - Factor of about 1.8 reduction for embedded case
- Top of internal structure peak near 12 Hz
  - Factor of about 1.6 reduction for surface case
  - Factor of about 1.25 reduction for embedded case

**Deleted:**  
*Effect of Embedment and Incoherence*

**Deleted:**  
*Effect of Embedment and Incoherence*

**Deleted:**  
*Effect of Embedment and Incoherence*

**Deleted:** .  
*Effect of Embedment and Incoherence*

**Deleted:** .  
*Effect of Embedment and Incoherence*

**Deleted:** .  
*Effect of Embedment and Incoherence*

- Internal structure mid-height peak near 18 Hz
  - Factor of about 2 reduction for surface case
  - Factor of about 1.7 reduction for embedded case

Embedment results in increased containment structure frequencies as the foundation/structure is stiffened by the below ground constraining soil/rock. Frequencies of the internal structure are not significantly affected by embedment. Embedment generally results in reduced response due to the vertical spatial variation of the free-field ground motion with depth in the rock resulting in basemat motion less than the free-field motion at the ground surface.

Due to frequency shifts from embedment, it is possible to get embedded response greater than surface response. Such a case is the top of the reactor building dome as shown in Figures E.2-3 and E.2-4, where the second fixed-base mode is at 11.3 Hz. For this location, the second SSI mode for the surface case is about 11 Hz and for the embedded case is about 13 Hz. In this frequency range, the input ground motion is increasing as from 10 to 25 Hz and, as a result, the response for this peak of the ISRS is larger for the embedded case than for the surface case. However, in general, embedment produces reduced ISRS and for some locations and some frequencies the reductions are very significant as demonstrated below:

Changes to ISRS due to embedment are:

- Foundation peak near 12 Hz
  - Factor of about 1.7 reduction for the coherent case
  - Factor of about 1.5 reduction for the incoherent case
- Foundation peak near 25 Hz
  - Factor of about 1.5 reduction for the coherent case
  - Factor of about 1.6 reduction for the incoherent case
- Top of reactor building dome peak near 4 Hz
  - Factor of about 1.1 reduction for both surface and embedded cases
- Top of reactor building dome peak near 12 Hz
  - Factor of about 1.25 increase for surface case
  - Factor of about 1.2 reduction for embedded case
- Top of internal structure peak near 12 Hz
  - Factor of about 1.9 reduction for surface case
  - Factor of about 1.5 reduction for embedded case
- Internal structure mid-height peak near 18 Hz

- Factor of about 2 reduction for surface case
- Factor of about 1.6 reduction for embedded case

**Deleted:**  
Effect of Embedment and Incoherence

**Deleted:**  
Effect of Embedment and Incoherence

**Deleted:**  
Effect of Embedment and Incoherence

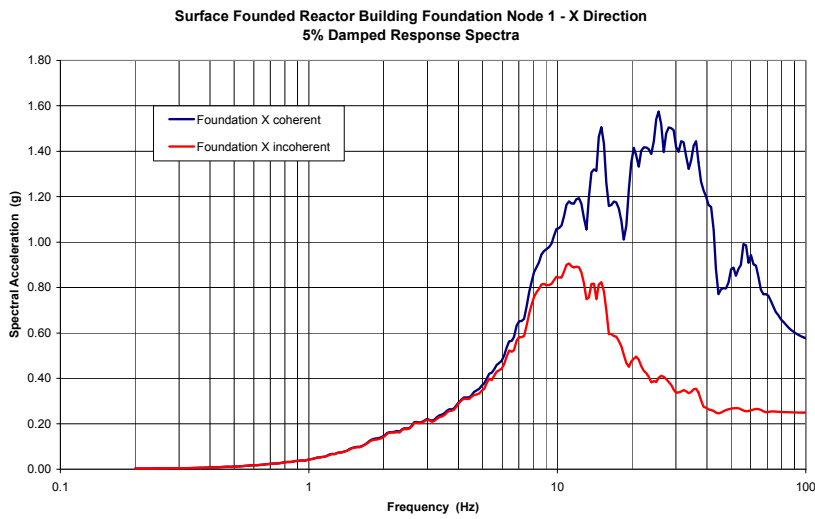


**Figure E.2-1**  
**Comparison of ISRS at the Center of the Foundation of the Surface Founded Building for the Coherent and Incoherent Ground Motion**

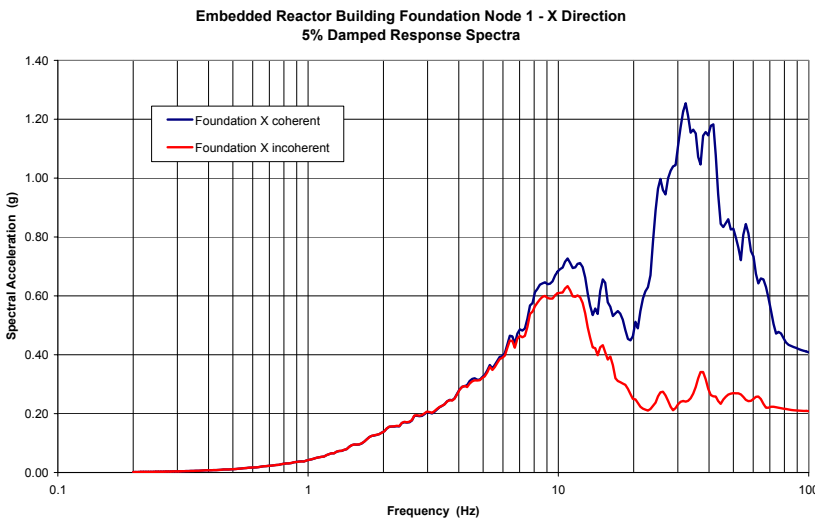


**Figure E.2-2**  
**Comparison of ISRS at the Center of the Foundation of the Embedded Building for the Coherent and Incoherent Ground Motion**

**Deleted:**  
*Effect of Embedment and Incoherence*

**Deleted:**  
*Effect of Embedment and Incoherence*

**Deleted:**  
*Effect of Embedment and Incoherence*

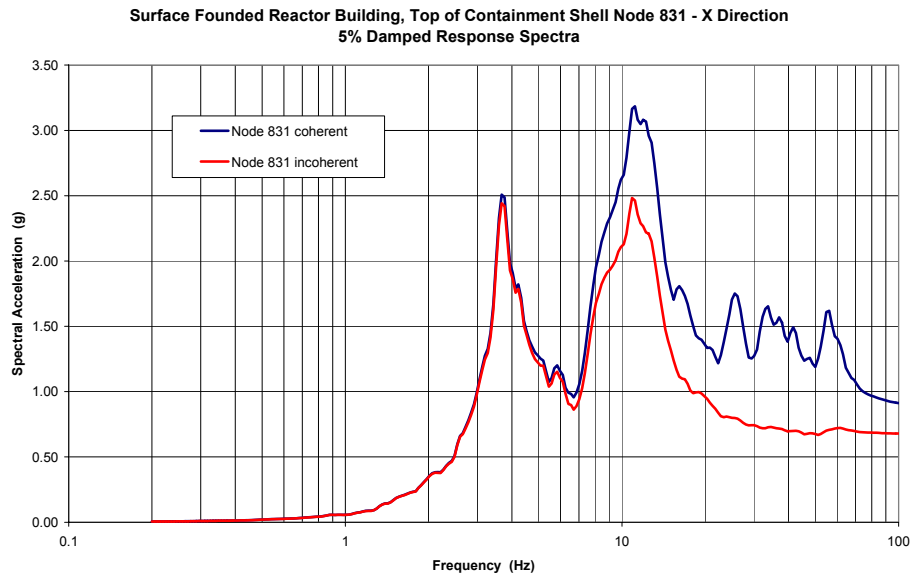


**Figure E.2-3**  
**Comparison of ISRS at Top of the Containment Dome of the Surface Founded Building for the Coherent and Incoherent Ground Motion**

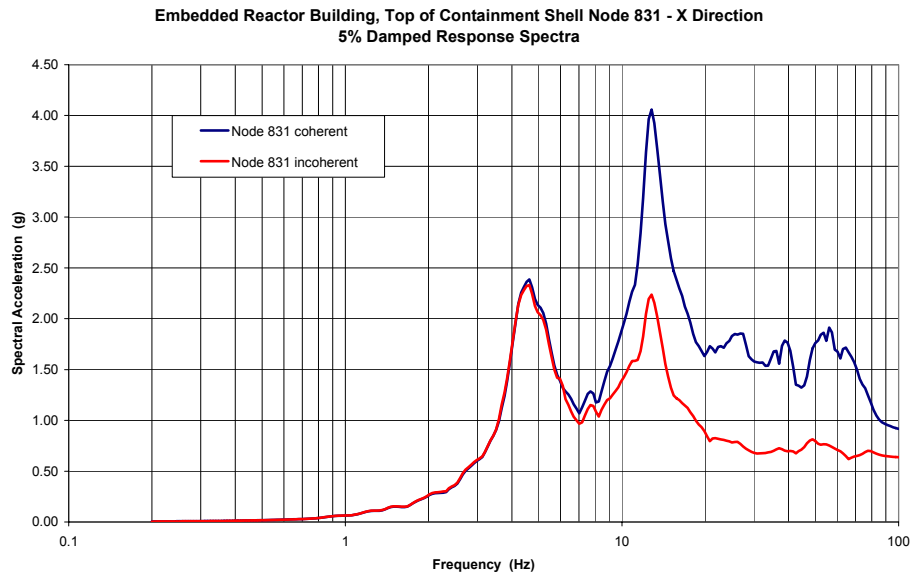


**Figure E.2-4**  
**Comparison of ISRS at the Top of the Containment Dome of the Embedded Building for the Coherent and Incoherent Ground Motion**

Deleted: Effect of Embedment and Incoherence

Deleted: Effect of Embedment and Incoherence

Deleted: Effect of Embedment and Incoherence

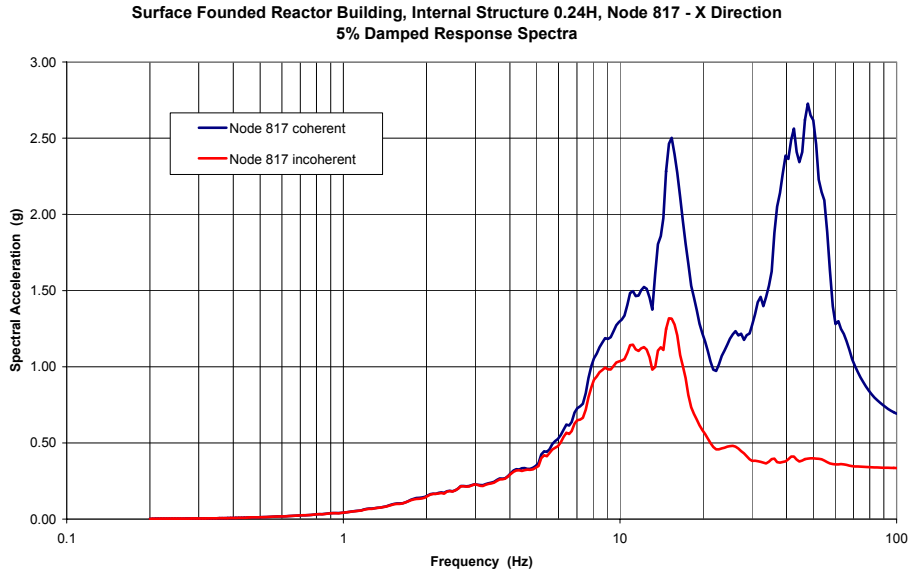


Figure E.2-5  
Comparison of ISRS at Quarter Height of the Internal Structure of the Surface  
Founded Building for the Coherent and Incoherent Ground Motion

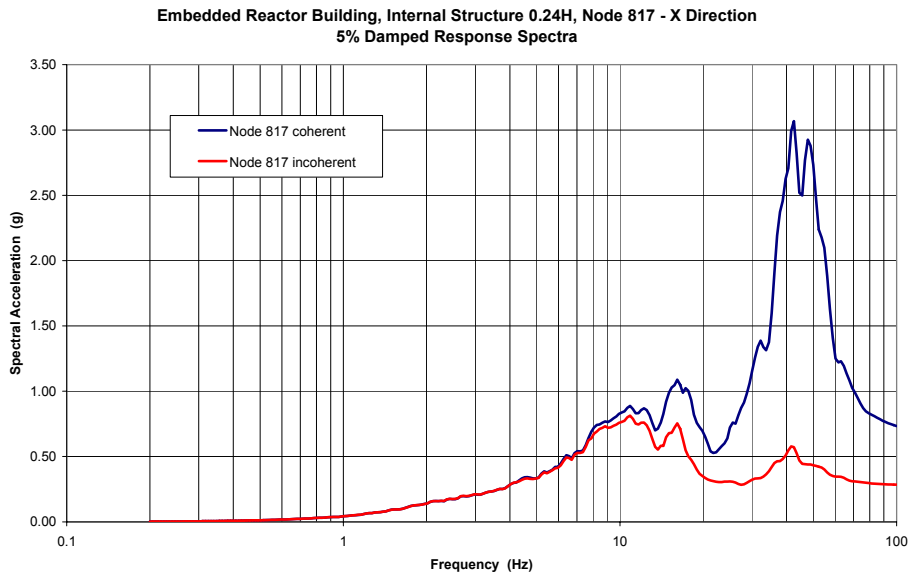
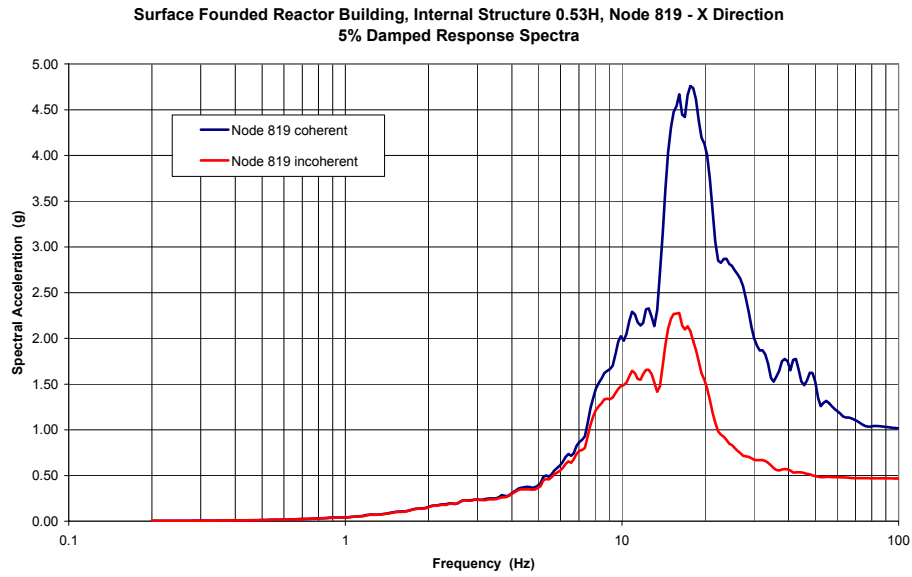


Figure E.2-6  
Comparison of ISRS at Quarter Height of the Internal Structure of the Embedded  
Building for the Coherent and Incoherent Ground Motion

Deleted: Effect of Embedment and Incoherence

Deleted: Effect of Embedment and Incoherence

Deleted: Effect of Embedment and Incoherence



**Figure E.2-7**  
Comparison of ISRS at Mid-Height of the Internal Structure of the Surface Founded Building for the Coherent and Incoherent Ground Motion

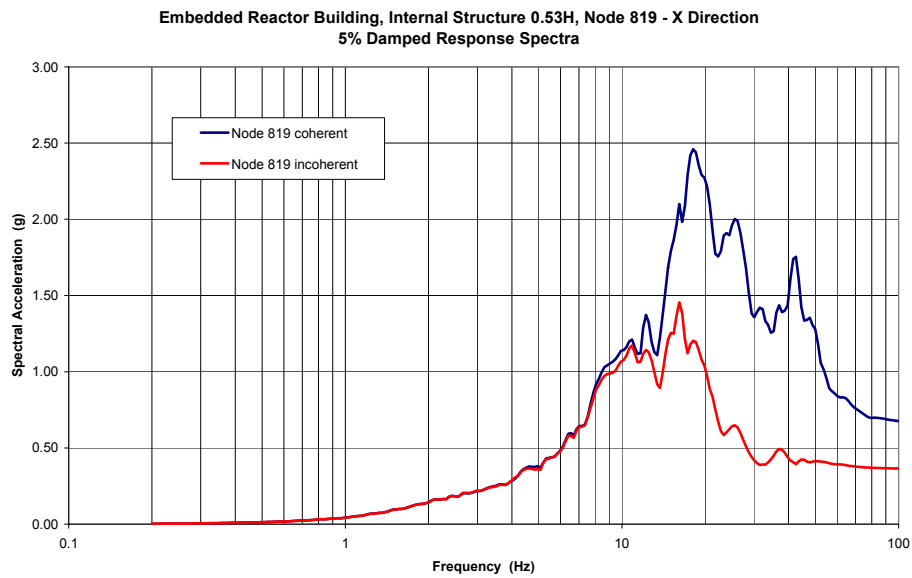


**Figure E.2-8**  
Comparison of ISRS at Mid-Height of the Internal Structure of the Embedded Building for the Coherent and Incoherent Ground Motion

Deleted: Effect of Embedment and Incoherence

Deleted: Effect of Embedment and Incoherence

Deleted: Effect of Embedment and Incoherence

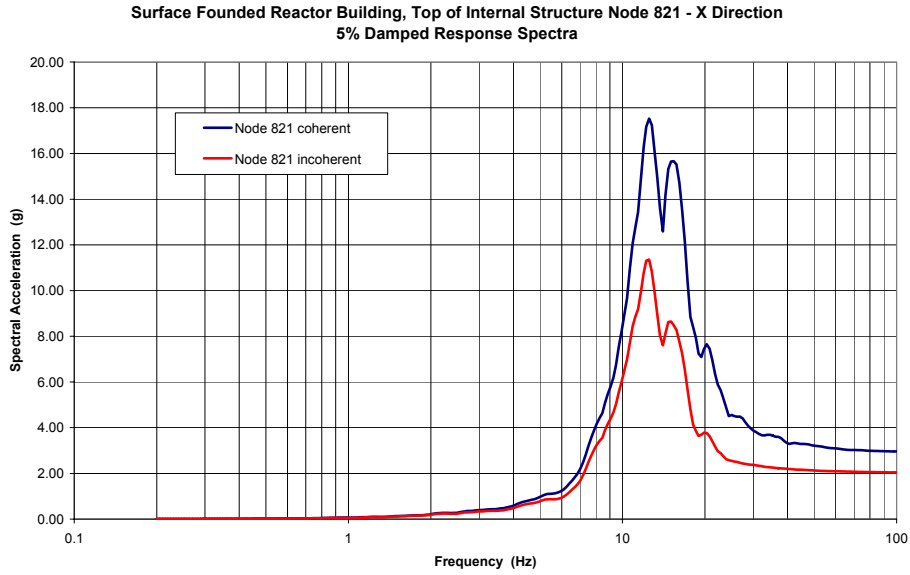


Figure E.2-9  
Comparison of ISRS at Top of the Internal Structure of the Surface Founded Building for the Coherent and Incoherent Ground Motion

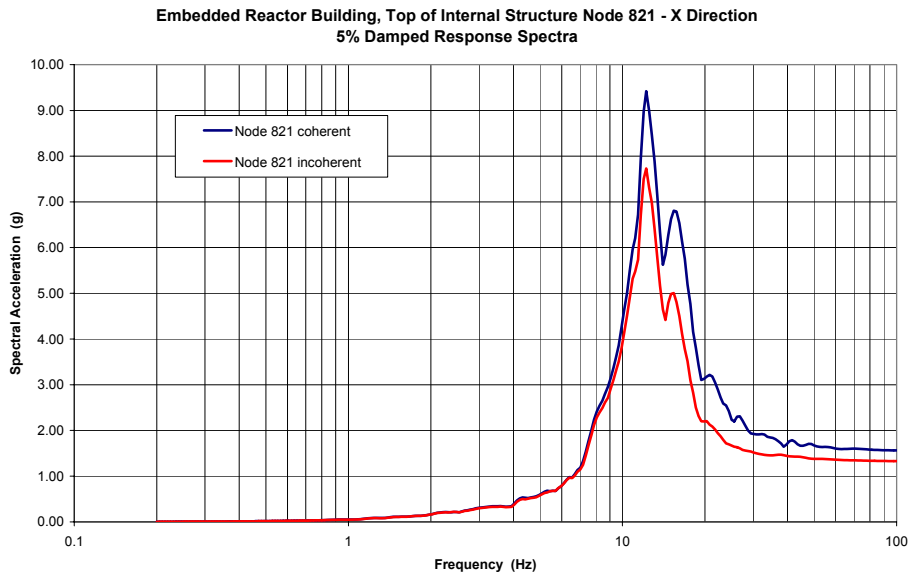


Figure E.2-10  
Comparison of ISRS at the Top of the Internal Structure of the Embedded Building for the Coherent and Incoherent Ground Motion

**Deleted:** .  
Effect of Embedment and Incoherence

**Deleted:** .  
Effect of Embedment and Incoherence

**Deleted:** .  
Effect of Embedment and Incoherence

To better demonstrate comparisons of the surface founded and embedded results, the relationship between the ISRS with and without incoherency is expressed in terms of a spectral ratio. This spectral ratio (SR) is defined to be the ratio of the spectral acceleration with incoherency ( $S_{a \text{ incoherent}}$ ) to the spectral acceleration with coherent input ( $S_{a \text{ coherent}}$ ).

$$SR = \frac{S_{a \text{ incoherent}}}{S_{a \text{ coherent}}}$$

To provide a comparison of surface founded and embedded response completely in the frequency domain, the transfer functions computed by ACS SASSI during the course of conducting soil-structure interaction analyses are utilized. ACS SASSI seismic analyses are performed in the frequency domain and transfer functions relate the response at any structure or foundation location to the free-field input motion as a function of frequency. Unlike response spectra where spectral values at one frequency can be affected by response at other frequencies, the transfer function describes the response amplification or attenuation at each frequency independent of all other frequencies. By the SASSI approach, the coherency function defines the relation between motion at interaction nodes as a function of the horizontal projected distance between the nodes and as a function of frequency. This coherency function is used with eigen-decomposition to define coherency function-compatible incoherent free-field input to be used in conventional SASSI SSI analyses. Transfer functions differ between the incoherent and coherent cases because the input motion is revised due to incoherency.

For coherent motion analyses, the transfer function includes the effects of soil-structure interaction consisting of both inertial interaction and kinematic interaction. For incoherent motion analyses, the transfer function includes the above effects plus the effects of incoherency. By taking the ratio of the transfer function (TF) for incoherent motion to the transfer function for coherent motion, the incoherency transfer function (ITF) can be isolated.

$$ITF = \frac{TF_{\text{incoherent}}}{TF_{\text{coherent}}}$$

Figures E.2-11 through E.2-20 show comparisons of the incoherent-to-coherent spectral ratios and incoherency transfer functions for the surface founded and embedded structures and for the same foundation and structure locations for which ISRS were presented. At each location, the ratio of incoherent to coherent spectral acceleration is presented for both the surface founded and embedded structure analyses. Also at each location, the incoherency transfer function evaluated from both the surface founded and embedded structure analyses is presented. In addition, the incoherency transfer function evaluated by random vibration theory (RVT) for this foundation area as presented in Chapter 4 is included in the comparison figures.

Deleted: Effect of Embedment and Incoherence

Deleted: Effect of Embedment and Incoherence

Deleted: Effect of Embedment and Incoherence

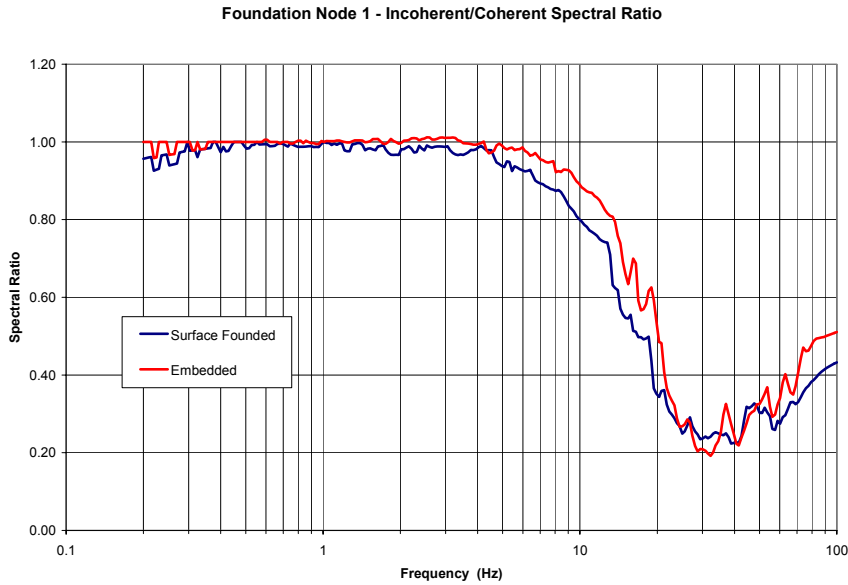


Figure E.2-11 Comparison of the Spectral Ratios at the Center of the Foundation for the Surface Founded and Embedded Cases

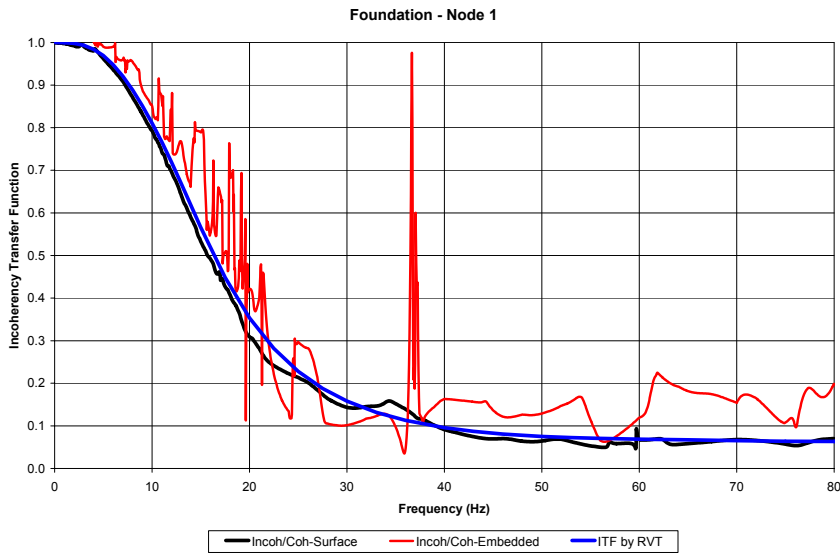
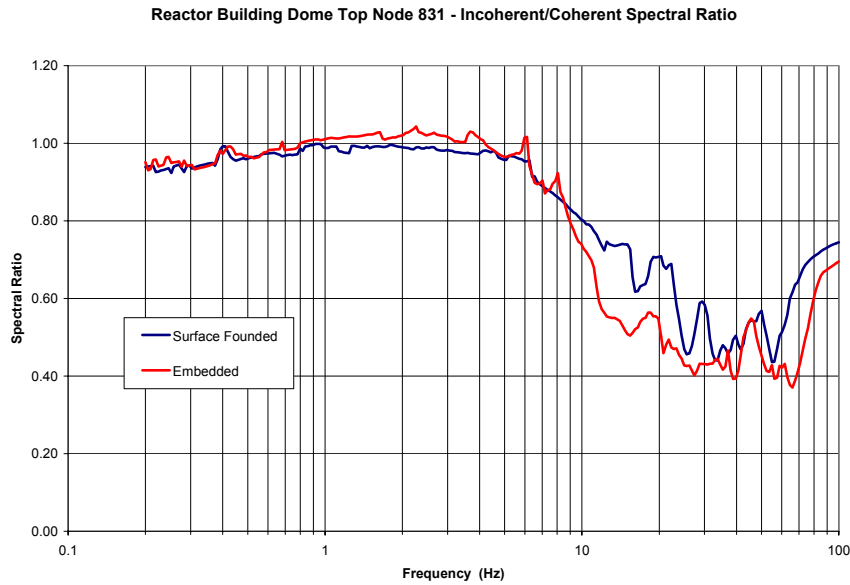


Figure E.2-12 Incoherency Transfer Function at the Center of the Foundation for the Surface Founded and Embedded Cases

**Deleted:** .  
*Effect of Embedment and Incoherence*

**Deleted:** .  
*Effect of Embedment and Incoherence*

**Deleted:** .  
*Effect of Embedment and Incoherence*



**Figure E.2-13**  
**Comparison of the Spectral Ratios at the Top of the Reactor Building Dome for the Surface Founded and Embedded Cases**

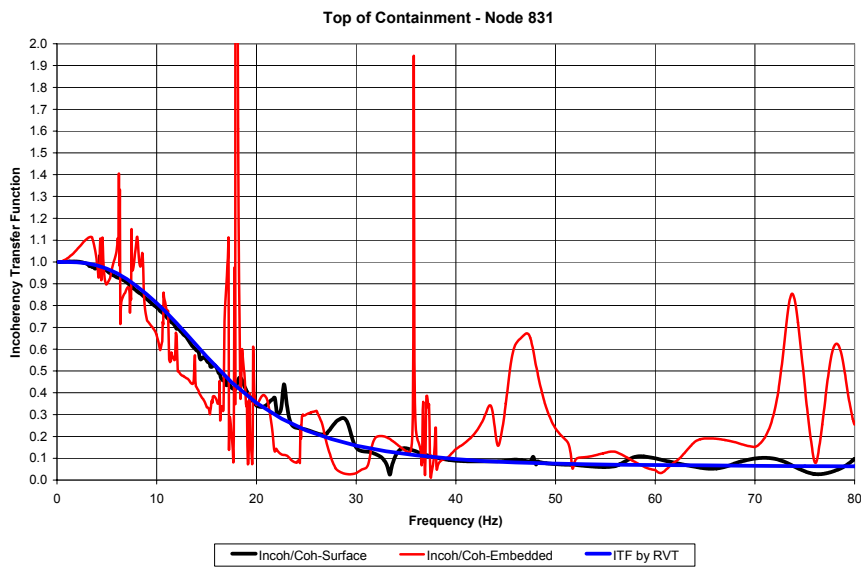


**Figure E.2-14**  
**Incoherency Transfer Function at the Top of the Reactor Building Dome for the Surface Founded and Embedded Cases**

Deleted: Effect of Embedment and Incoherence

Deleted: Effect of Embedment and Incoherence

Deleted: Effect of Embedment and Incoherence

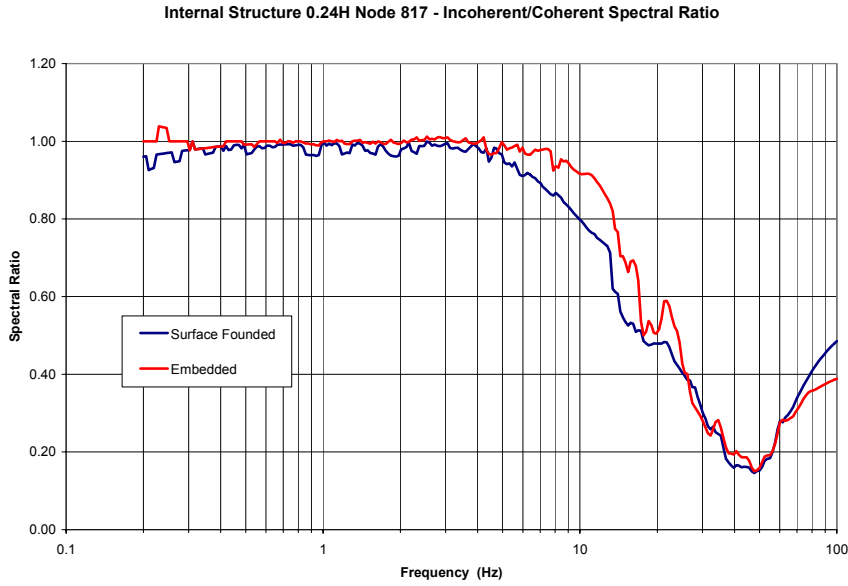


Figure E.2-15 Comparison of the Spectral Ratios at Quarter-Height of the Internal Structure for the Surface Founded and Embedded Cases

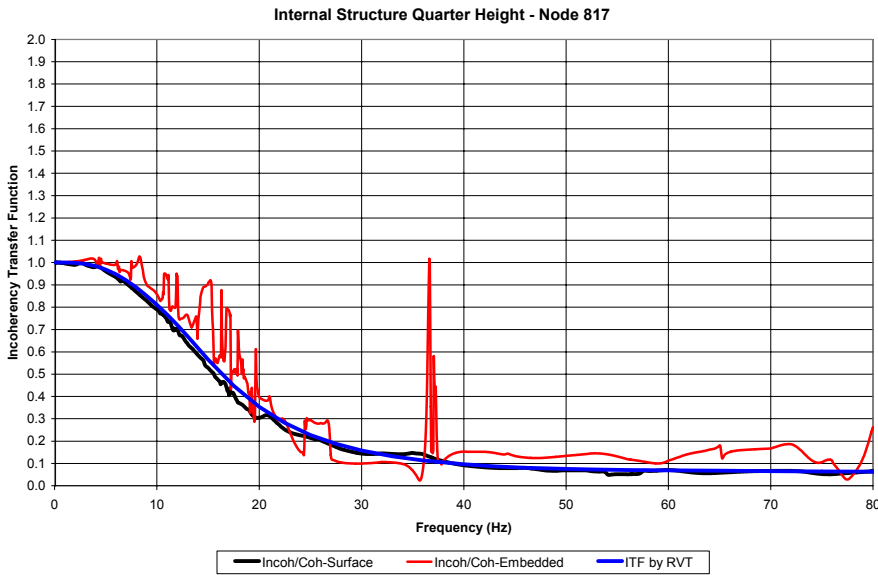
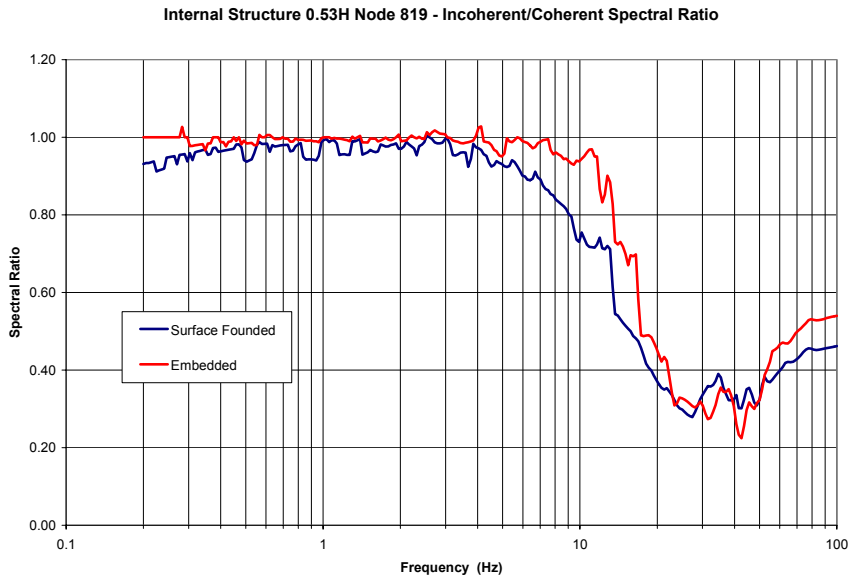


Figure E.2-16 Incoherence Transfer Function at Quarter-Height of the Internal Structure for the Surface Founded and Embedded Cases

**Deleted:** .  
*Effect of Embedment and Incoherence*

**Deleted:** .  
*Effect of Embedment and Incoherence*

**Deleted:** .  
*Effect of Embedment and Incoherence*



**Figure E.2-17**  
**Comparison of the Spectral Ratios at Mid-Height of the Internal Structure for the Surface Founded and Embedded Cases**

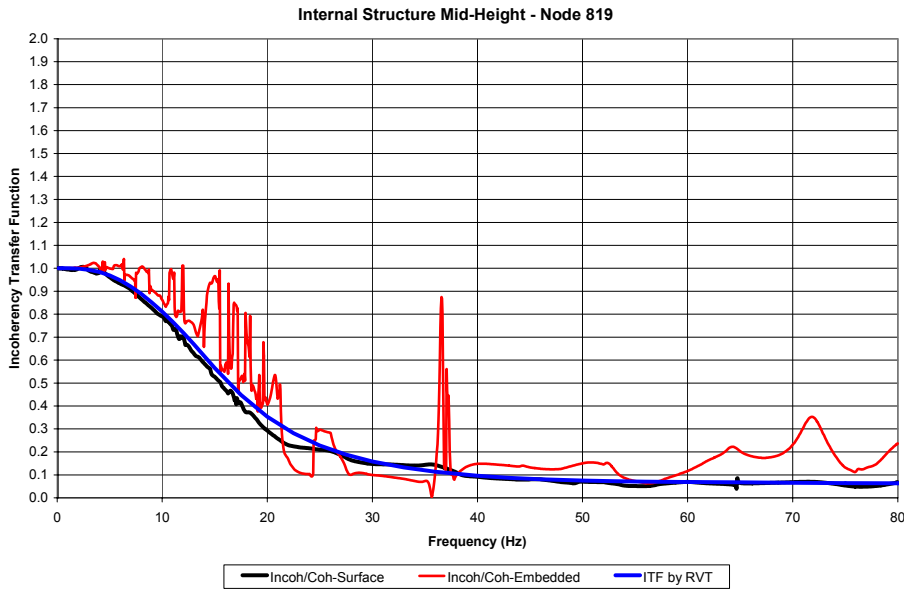


**Figure E.2-18**  
**Incoherency Transfer Function at Mid-Height of the Internal Structure for the Surface Founded and Embedded Cases**

Deleted: Effect of Embedment and Incoherence

Deleted: Effect of Embedment and Incoherence

Deleted: Effect of Embedment and Incoherence

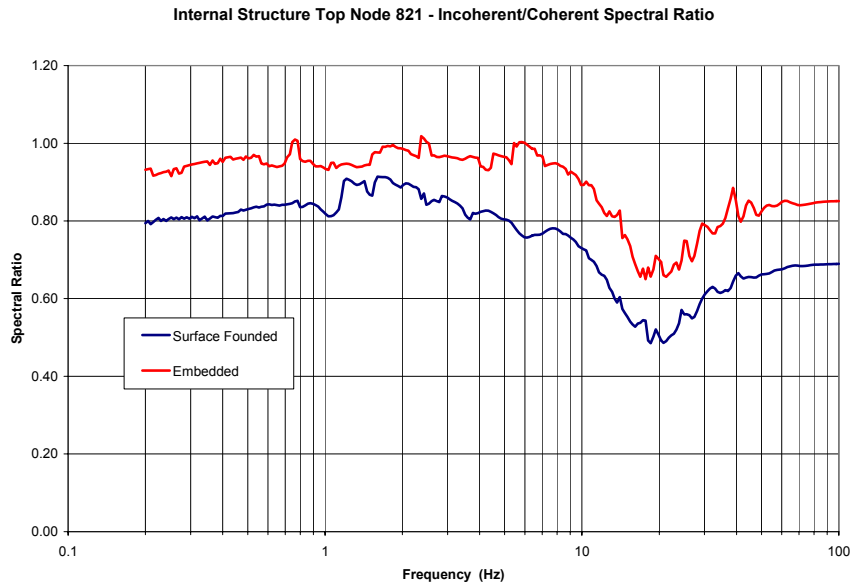


Figure E.2-19 Comparison of the Spectral Ratios at the Top of the Internal Structure for the Surface Founded and Embedded Cases

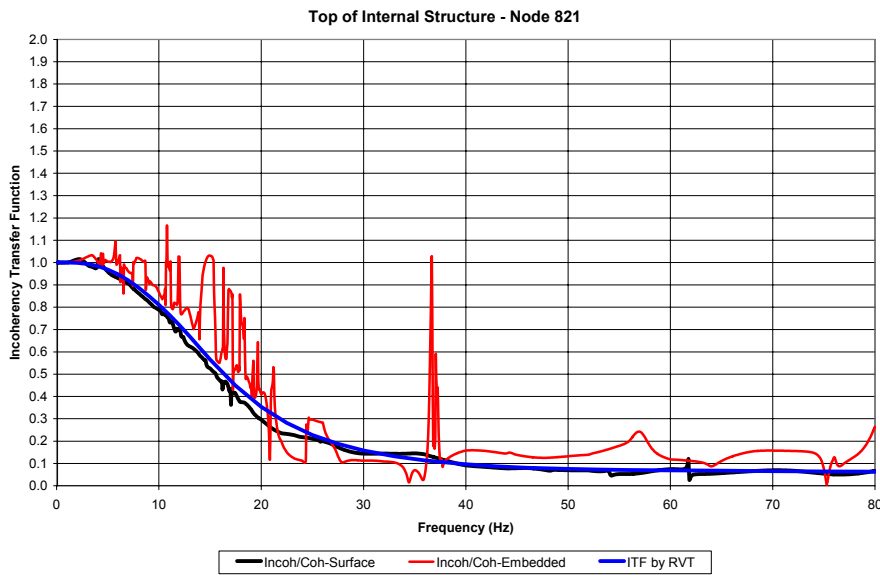


Figure E.2-20 Incoherence Transfer Function at the Top of the Internal Structure for the Surface Founded and Embedded Cases

Deleted: .  
Effect of Embedment and Incoherence

Deleted: .  
Effect of Embedment and Incoherence

Deleted: .  
Effect of Embedment and Incoherence

Review of Figures E.2-11, E.2-13, E.2-15, E.2-17, and E.2-19 indicates that spectral ratios generally are similar for the surface founded and embedded cases. In most cases, the spectral ratio curves follow each other over the complete frequency range of the ISRS. This suggests that the effect of incoherence is generally independent of the effect of embedment (i.e., spatially varying ground motion with depth).

At the foundation, the embedded spectral ratio is about 10 percent greater than the surface founded spectral ratio from 4.5 to 22 Hz. They are about equal below 4.5 Hz and from 22 to 60 Hz, with the embedded ratio being larger above 60 Hz. At the top of the reactor building dome, the surface spectral ratio is as much as 30 percent greater than the surface founded spectral ratio from 9 to 30 Hz. They are about equal below 9 Hz and from 30 to 60 Hz, with the surface ratio being larger above 60 Hz.

At the top of the internal structure, the embedded spectral ratio is between 10 and 20 percent greater than the surface founded spectral ratio at all frequencies. At mid-height on the internal structure, the embedded spectral ratio by as much as 30 percent greater than the surface founded spectral ratio from 5 to 22 Hz. They are about equal below 5 Hz and from 22 to 50 Hz, with the embedded ratio being larger above 50 Hz. At the quarter height on the internal structure, the embedded spectral ratio by about 15 percent greater than the surface founded spectral ratio from 5 to 18 Hz. They are about equal below 5 Hz and from 18 to 70 Hz, with the surface ratio being larger above 70 Hz.

Review of Figures E.2-12, E.2-14, E.2-16, E.2-18, and E.2-20 indicates that the incoherency transfer functions generally are similar for the surface founded and embedded cases. The incoherency transfer function (ITF) for coherent motion closely follows the incoherency transfer function from random vibration theory per Chapter 4. It is interesting to note that the incoherency transfer function for the surface founded structure is the same at locations in the structure as it is at the foundation. The difference between the embedded and surface ITF is similar to the difference in spectra ratios. In the frequency range from 5 to 20 Hz, the embedded ITF differs from the surface incoherency function from 10 to 30 percent. Of the five locations for which ITFs were computed, the embedded ITF is greater than the surface ITF at four locations and less than the surface ITF at one location.

As expected, the embedded ITF is not a smooth curve like the surface ITF. For the foundation response, the individual transfer functions that were used to compute ITFs are shown in Figures E.2-21 and E.2-22 for the surface founded and embedded cases, respectively. These figures demonstrate the reductions in response due to incoherency for both the surface founded and embedded cases. The figures do not indicate why the embedded ITF has so many jagged peaks as compared to the relatively smooth surface founded ITF. It is not likely a characteristic of the complex behavior of embedded structures. For the embedded case, there is a spike or apparent singularity at about 37 Hz. It is believed that this is a characteristic of the interaction of motion of the excavated soil and rotation of the embedded structure within that excavated soil. Note that all transfer functions, as those shown in Figures E.2-21 and E.2-22, were computed with 100 frequencies and no errors due to interpolation between frequencies is expected. All peaks

and valleys in the transfer functions were well represented with actual calculated frequencies.

Deleted: Effect of Embedment and Incoherence

Deleted: Effect of Embedment and Incoherence

Deleted: Effect of Embedment and Incoherence

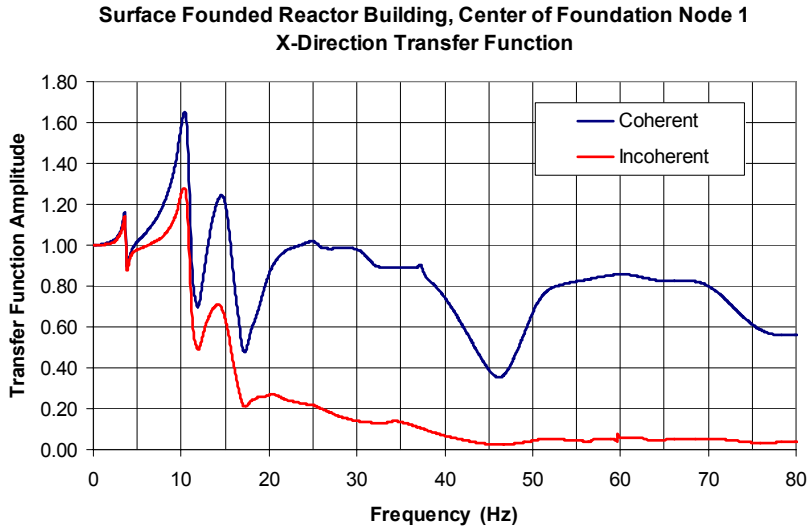


Figure E.2-21 Comparison of the Coherent and Incoherent Transfer Functions at the Center of the Foundation for the Surface Founded Case

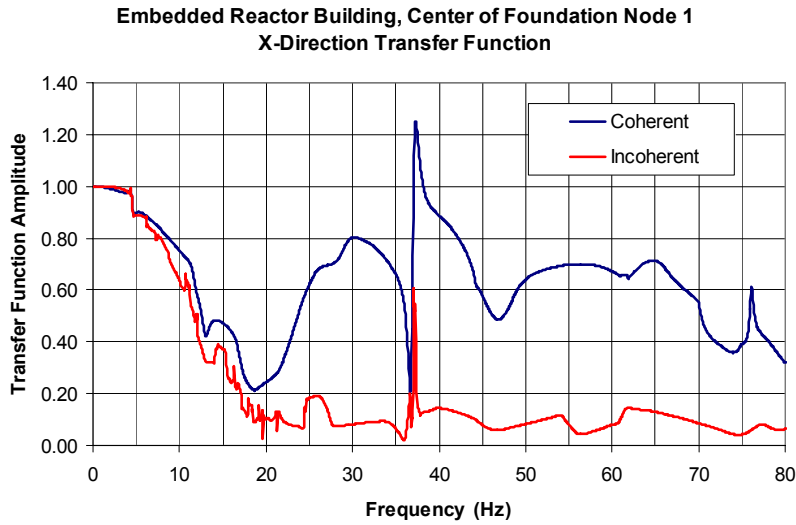


Figure E.2-22 Comparison of the Coherent and Incoherent Transfer Functions at the Center of the Foundation for the Embedded Case

Deleted: Effect of Embedment and Incoherence

Deleted: Effect of Embedment and Incoherence

Deleted: Effect of Embedment and Incoherence

### E.3 Conclusions

Appendix E summarizes the sensitivity study to investigate the combined effects of spatial variation of ground motion with depth due to embedment and incoherency. General conclusions and observations from the sensitivity study are as follows.

- The effects of incoherency are generally similar for the surface founded structure and the embedded structure. Incoherent to coherent spectral ratios are computed as a general indicator of the effect of incoherency in this Appendix. The best indication of incoherency effects is the incoherency transfer function as these values were also provided in this Appendix. In terms of incoherent to coherent spectra ratios of incoherent vs. coherent response and incoherency transfer functions for surface founded and embedded cases, differences are no larger than about 30 percent. Also, there does not seem to be a systematic difference between surface-founded and embedded cases as at some locations one is larger and at other locations the other is larger.
- The general trends observed for the surface-founded case also appear in the embedded case. Namely, the ground motion incoherency leads to reductions in the in-structure response spectra at frequencies higher than about 10 Hz.
- For both the surface founded and the embedded case, the largest reductions in spectral accelerations occur at locations with multi-mode responses at higher frequencies. For example, the lowest spectral ratio values are observed at the foundation, the quarter-point and mid-point of the internal structure. Review of the ISRS for these locations indicates multiple peaks at frequencies above 10 Hz for the coherent ground motion input.
- The incoherency transfer function for the surface-founded structure as computed from ACS SASSI seismic analyses agrees closely with the incoherency transfer function from random vibration theory as described in Chapter 4. The incoherency transfer function for the embedded structure is not a smooth curve as a function of frequency as is the surface founded incoherency transfer function. This is an indication of the complex nature of evaluating seismic response of embedded structures.

This sensitivity study demonstrates significant reduction of high-frequency response for both surface founded and embedded structures. The results show relatively small differences between incoherency effects for the surface-founded and embedded cases. However, the differences have no systematic bias such that it is concluded that incoherency effects are independent of structure embedment. This is an indication that the effect of spatial variation of ground motion with depth can be treated independently from the effects of ground motion incoherency.

**DRAFT**

*Effect of Embedment and Incoherence*

#### **E.4 References**

Ghiocel Predictive Technologies, Inc. (2006). ACS-SASSI, An Advanced Computational Software for 3D Dynamic Analysis Including Soil-Structure Interaction, Version 2.1, Pittsford, New York.

Abrahamson, N. (2006). *Spatial Coherency for Soil-Structure Interaction*, Electric Power Research Institute, Final Report 1014101, Palo Alto, CA. August (Draft).

**Deleted:**  
*Effect of Embedment and Incoherence*

**Deleted:**  
*Effect of Embedment and Incoherence*

**Deleted:**  
*Effect of Embedment and Incoherence*

**Export Control Restrictions**

Access to and use of EPRI Intellectual Property is granted with the specific understanding and requirement that responsibility for ensuring full compliance with all applicable U.S. and foreign export laws and regulations is being undertaken by you and your company. This includes an obligation to ensure that any individual receiving access hereunder who is not a U.S. citizen or permanent U.S. resident is permitted access under applicable U.S. and foreign export laws and regulations. In the event you are uncertain whether you or your company may lawfully obtain access to this EPRI Intellectual Property, you acknowledge that it is your obligation to consult with your company's legal counsel to determine whether this access is lawful. Although EPRI may make available on a case-by-case basis an informal assessment of the applicable U.S. export classification for specific EPRI Intellectual Property, you and your company acknowledge that this assessment is solely for informational purposes and not for reliance purposes. You and your company acknowledge that it is still the obligation of you and your company to make your own assessment of the applicable U.S. export classification and ensure compliance accordingly. You and your company understand and acknowledge your obligations to make a prompt report to EPRI and the appropriate authorities regarding any access to or use of EPRI Intellectual Property hereunder that may be in violation of applicable U.S. or foreign export laws or regulations.

**The Electric Power Research Institute (EPRI)**

The Electric Power Research Institute (EPRI), with major locations in Palo Alto, California, and Charlotte, North Carolina, was established in 1973 as an independent, nonprofit center for public interest energy and environmental research. EPRI brings together members, participants, the Institute's scientists and engineers, and other leading experts to work collaboratively on solutions to the challenges of electric power. These solutions span nearly every area of electricity generation, delivery, and use, including health, safety, and environment. EPRI's members represent over 90% of the electricity generated in the United States. International participation represents nearly 15% of EPRI's total research, development, and demonstration program.

Together...Shaping the Future of Electricity

---

**ELECTRIC POWER RESEARCH INSTITUTE**